

Magnetic Resonance Spectroscopy as applied to epilepsy

Robert Simister, MRCP

Department of Clinical and Experimental Epilepsy,
Institute of Neurology,
University College London (UCL),
Queen Square,
London
WC1N 3BG

Thesis submitted to University College London for the Degree of Doctor in
Philosophy, 2010

Table of Contents:

Abstract	p.003
Statement of involvement	p.007
Acknowledgements	p.008
List of Tables	p.009
List of Figures	p.010
Published articles and presentations	p.012
Main Index	p.015
List of Abbreviations	p.020
Introduction and Background	p.024
Methods	p.125
Results	p.143
3.1	p.144
3.2	p.168
3.3	p.188
3.4	p.205
3.5	p.224
3.6	p.234
3.7	p.252
Thesis Conclusions and Further Work	p.267
Bibliography	p.273

ABSTRACT

Epilepsy is the most common serious disease of the brain. Magnetic Resonance Spectroscopy (MRS) is a novel imaging technique that offers the opportunity for co-localising biochemical information relating to metabolites specific to the study of epilepsy with high resolution MRI.

Aims:

The work included in this thesis was undertaken with two fundamental aims. The first was to apply a standardised MRS methodology in order to gain reproducible semi-quantitative information about the variation of relevant neuro-metabolites such as gamma amino butyric acid (GABA), glutamate (as glutamate plus glutamine [GLX]), N acetyl aspartate (NAA), myo-inositol (Ins) and creatine plus phosphocreatine (Cr) within epilepsy syndromes or pathological groups. The second main aim was to test a series of hypotheses relating to the regulation of the concentrations of these metabolites in the region of epileptic seizures, immediately following seizures and associated with particular medical and surgical treatment interventions.

Methods:

Seven experiments were performed in this thesis. In all seven studies the findings in the patient groups were compared against results from an acquired control group made up of healthy volunteers.

In the first experiment [3.1] twenty patients with temporal lobe epilepsy, with (10), and without hippocampal sclerosis were studied using multi voxel magnetic resonance spectroscopic imaging (MRSI) sequences in order to examine for differences in the obtained metabolites N acetyl aspartate (NAA), creatine plus phosphocreatine (Cr), choline containing compounds (Cho), GLX and myo-inositol (Ins) across the pathological groups and against a control population.

In experiments [3.2], [3.3], [3.4] and [3.6] an MRS protocol that incorporated a double quantum filter acquisition sequence was applied in order to allow measurement of GABA+ (a combined measure of GABA plus homocarnosine) in addition to measurement of the metabolites examined in [3.1]. Studies were

performed in the occipital lobes in patients with idiopathic generalised epilepsy (IGE) (n = 10) or occipital lobe epilepsy (n = 10) [3.2], in the frontal lobes in patients with IGE (n = 21) and within regions of the MRI visible pathology in patients with large focal malformations of cortical development (MCD, n = 10) [3.4]. In the last experiment using this technique patients with hippocampal sclerosis and temporal lobe epilepsy (n = 16) were studied in the ipsilateral and also in the contralateral temporal lobes and following temporal lobe surgery (n = 10) [3.6].

In experiment [3.5] ten patients were examined whilst taking and when not taking sodium valproate in order to further examine for an effect of this medication on the measured metabolite concentrations.

In experiment [3.7] ten patients were studied immediately after an epileptic seizure and then again during a subsequent inter-ictal period in order to examine for an influence of the recent seizure on the measured concentrations of the main metabolites.

Results:

MRSI in the temporal lobes in patients with temporal lobe epilepsy identified low NAA in the anterior hippocampus that was most severe in those patients with hippocampal sclerosis. GLX elevation was a feature in the patients without hippocampal sclerosis. Metabolic abnormality was most marked in the anterior compared to the posterior hippocampal regions.

GABA⁺ levels were elevated in patients with MCD and in the ipsilateral temporal lobe in temporal lobe epilepsy associated with hippocampal sclerosis but levels were not altered in patients with IGE or OLE. GLX was also elevated in MCD in the region of MRI visible abnormality and in IGE patients when measured in the frontal lobes. Low NAA was a feature of TLE and MCD. Patients with IGE showed normal NAA levels in the occipital lobes but reduced frontal lobe concentrations.

Cr concentrations were abnormal in the immediate post ictal period but normalised within 120 minutes. NAA was not altered and no significant change in lactate concentrations was observed.

Finally sodium valproate treatment was associated with a reduction in the levels of Ins and with unchanged NAA and GLX levels.

Main Conclusions:

MRS techniques demonstrate metabolite abnormalities in epileptic patients. NAA is the most sensitive metabolite marker of chronic pathology but levels are insensitive to recent seizure history. These findings repeat earlier observations of the usefulness of NAA measurement in the assessment of chronic epilepsy whilst illustrating ongoing uncertainty as to the correct patho-physiological interpretation of reduced NAA levels.

Measurable changes in the combined Cr signal are detectable whilst elevated lactate is not reliably observed following brief epileptic seizures at 1.5T. This finding indicates a potential role for MRS in functional activation studies.

Malformations of cortical development have abnormal levels of both GABA+ and GLX and MCD sub-types may well demonstrate different metabolite profiles. This finding suggests that MRS could be a useful tool in the MRI classification of MCD and in the pre-surgical assessment of patients with focal malformations.

Following successful temporal lobe surgery levels of NAA remain unchanged but NAA/Cr levels appear to normalise in the contralateral temporal lobe.

NAA and GLX/NAA levels were altered in the frontal lobes but not in the occipital lobes in Idiopathic Generalised Epilepsy. This finding provides imaging support for frontal lobe dysfunction as a cause or consequence of IGE.

Metabolite levels are affected by administered antiepileptic drugs. Sodium valproate reduces the levels of MRS visible Ins levels whilst topiramate and gabapentin appear

to be associated with higher GABA+ levels. These findings may be of major importance in the assessment of treatment effect or in the investigation of patients with possible drug resistance. The effect of valproate on Ins levels may become particularly interesting in the light of a growing understanding of the role of astrocyte dysfunction in a range of neurological conditions which include migraine, epilepsy, Alzheimer's disease, motor neurone disease and in ischaemic lesions.

Statement of Involvement:

Experimental design was decided by myself for experiments [3.2] to [3.7]) and by Friedrich Woermann (experiment [3.1]) following discussion with the other members of the NSE MRS group (Mary McLean, John Duncan and Gareth Barker).

I was responsible for patient recruitment for experiments [3.2] to [3.7]. Experiment [3.1] was commenced by and all subjects were recruited by Friedrich Woermann.

I was responsible for the data analysis and interpretation in all experiments

Acknowledgements:

I would like to take the opportunity to particularly thank my supervisors Mary McLean and John Duncan for their support and guidance throughout the period of this research. They will remember how many drafts and revisions they have very patiently reviewed before the completion of the work presented in this thesis.

I would also like to thank:

Gareth Barker who has also played a major role in guiding and reviewing this work.

Friedrich Woermann who generously passed over to me the work that he had started on the first experiment in this thesis.

Tuuli Salmenpera who helped to identify, recruit and often transport patients to the scanner in the post-ictal series.

My contemporaries at the MRI Unit at The National Society for Epilepsy from February 2000 to March 2004 and particularly Sofia Eriksson, Maxime Guye, Rebecca Liu, Martin Merschenke, Tejal Mitchell, Robert Powell, Fergus Rugg-Gunn, Afraim Salek-Haddadi and Tuuli Salmenpera for their time (often as control subjects) and friendship.

The MRI Unit Radiography Department who regularly organised scans for me and usually at short notice on busy days.

Finally and most importantly I have benefited from the generosity of more than 150 patients with epilepsy who allowed me to recruit them into my studies.

List of Tables:

- 1.6.1** Natural abundance, nuclear spin and resonant frequency for several commonly studied nuclei
- 1.7.1** Chemical shifts and coupling constants for GABA
- 3.1.1** Demographics of subject groups in MRSI TLE study (MRSI in TLE)
- 3.1.2** Metabolite concentrations across temporal lobes (MRSI in TLE)
- 3.2.1** Demographics of subject groups (OLE/IGE study)
- 3.2.2** Metabolite concentrations across groups (OLE/IGE study)
- 3.2.3** Correlation coefficients between metabolites (OLE/IGE study)
- 3.3.1** Demographics of subject groups (frontal GABA+ in IGE study)
- 3.3.2** Metabolic concentrations across groups (frontal GABA+ in IGE study)
- 3.4.1** Demographics of subject groups (GABA+ in MCD study)
- 3.4.2** Metabolite concentrations across groups (GABA+ in MCD study)
- 3.4.3** Individual patient metabolite concentrations (GABA+ in MCD study)
- 3.5.1** Demographics of subject groups (Effect of VPA study)
- 3.6.1** Demographics of subject groups (GABA+ in TLE study)
- 3.6.2** Temporal lobe metabolite concentrations (GABA+ in TLE study)
- 3.6.3** Contralateral temporal lobe concentrations in surgical group (GABA+ in TLE study)
- 3.7.1** Demographics of subject groups (Post ictal study)
- 3.7.2** Metabolite concentrations across groups (Post ictal study)

List of Figures:

- 1.2.1 The GABA_A receptor
- 1.7.1 Typical short TE ¹H MRS spectrum
- 1.7.2 Chemical structure of GABA
- 1.7.3 The PRESS localisation sequence
- 1.7.4 Typical MRSI pulse sequence
- 1.7.5 ¹H MRS spectrum for GABA
- 1.7.5 ¹H MRS spectrum for myo-Inositol
- 2.2.1 The PRESS localisation sequence
- 2.2.2 LCModel Output
- 2.3.1 ROI placement using LCModel Interactive
- 2.3.2 Typical MRSI pulse sequence
- 2.4.1 DQF GABA+ pulse sequence
- 2.4.2 DQF GABA+ spectrum
- 3.1.1 VOI and sample spectra (MRSI in TLE)
- 3.1.2 95% error bars for metabolites and ratios across groups (MRSI in TLE)
- 3.2.1 VOI and sample spectra (OLE/IGE study)
- 3.2.2 Box plots for metabolites and ratios across groups (OLE/IGE group)
- 3.3.1 VOI and sample spectra (frontal GABA+ in IGE)
- 3.3.2 Error bar plots for metabolites and ratios across groups (frontal GABA+ in IGE study)
- 3.3.3 Plots of GLX and NAAt against seizure history (frontal GABA+ in IGE study)
- 3.4.1 VOI in patients and controls in GABA+ in MCD study
- 3.4.2 Representative spectra (GABA+ in MCD study)
- 3.4.3 Metabolite concentrations across groups (GABA+ in MCD study)
- 3.4.4 Effect of valproate and topiramate in patient group (GABA+ in MCD study)
- 3.5.1 VOI and representative spectra (Effect of VPA study)
- 3.5.2 Error bar plots of inter-scan difference (effect of VPA study)
- 3.6.1 VOI and representative spectra (GABA+ in MCD study)

- 3.6.2** Error bar plots of metabolite concentrations across subject groups (GABA+ in TLE study)
- 3.6.3** Error bar plots of longitudinal change in metabolite concentrations post surgery (GABA+ in TLE study)
- 3.7.1** VOI and representative spectra (Post ictal study)
- 3.7.2** Inter scan change in metabolite concentrations (Post ictal study)
- 3.7.3** Time line plots for recovery of A) Cr_{144}/Cr_{30} and B) $NAAt_{144}/Cr_{144}$ (Post ictal study)

List of published work and presentations arising from this work:**Original Papers:**

Proton MR Spectroscopy of Metabolite Concentrations in Temporal Lobe Epilepsy and Effect of Temporal Lobe Resection. *Epilepsy Res.* 2009; 83: 168-76. **Simister RJ**, McLean MA, Barker GJ, Duncan JS.

The effect of epileptic seizures on proton MRS visible neurochemical concentrations. *Epilepsy Res.* 2007 74, 215—219. **Simister RJ**, McLean MA, Salmenpera TM, Barker GJ, Duncan JS.

The effect of sodium valproate on proton MRS visible neurochemical concentrations. *Epilepsy Res.* 2007;74:215-9. **Simister RJ**, McLean MA, Barker GJ, Duncan JS.

Proton magnetic resonance spectroscopy of malformations of cortical development causing epilepsy. *Epilepsy Res.* 2007;74(2-3):107-15. **Simister RJ**, McLean MA, Barker GJ, Duncan JS

Discrimination between neurochemicals and macromolecular signals in human frontal lobes using short echo time proton magnetic resonance spectroscopy. *Faraday Discuss* 2004; 126:93-105 Mclean M, **Simister R**, Barker G, Duncan J.

Proton Magnetic Resonance Spectroscopy Reveals Frontal Lobe Metabolite Abnormalities in Idiopathic Generalised Epilepsy. *Neurology* 2003;61:897-902 **Simister R**, McLean M, Barker G, Duncan J

A proton magnetic resonance spectroscopy study of metabolites in the occipital lobes in epilepsy *Epilepsia* 2003; 44: 550-558 **Simister R**, McLean M, Barker G, Duncan J

In vivo GABA+ measurement at 1.5T using a PRESS-localized double quantum filter. *Magn Reson Med* 2002; 48: 233-241 McLean M, Busza A, Wald L, **Simister R**, Barker G, Williams S

A short-echo-time proton magnetic resonance spectroscopic imaging study of temporal lobe epilepsy. *Epilepsia* 2002; 43: 1021-1031 **Simister R**, Woermann F, McLean M, Bartlett P, Barker G, Duncan J

In vivo short echo time ¹H-magnetic resonance spectroscopic imaging (MRSI) of the temporal lobes. *Neuroimage* 2001; 14: 501-509 McLean M, Woermann F, **Simister R**, Barker G, Duncan J

Abstracts:

Cerebral metabolite and neurotransmitter concentrations in idiopathic generalised epilepsy measured with short echo time proton MR spectroscopy. *Proceedings of the ABN. JNNP* 2002 73: 219. **Simister R**, Mclean M, Barker G, Duncan J

A comparison of metabolite concentrations in primary generalised epilepsy and partial epilepsy using short echo time proton spectroscopy and a double quantum GABA filter. *Proc 10th ISMRM* 2002; 420. **Simister R**, McLean M, Barker G, Duncan J

Metabolite nulling improves reliability of LCModel analysis of short echo time spectroscopy *Proc 10th ISMRM* 2002; 529. McLean M, **Simister R**, Barker G, Duncan J

A short echo time proton magnetic resonance spectroscopic imaging study of metabolites in temporal lobe epilepsy *Proc 9th ISMRM* 2001; 387. **Simister R**, Woermann F, McLean M, Barker G, Duncan J

In vivo GABA measurement using a PRESS-localised double quantum filter in patients with malformations of cortical development and epilepsy *Proc 9th ISMRM* 2001; 420. McLean M, **Simister R**, Barker G, Duncan J

Oral Presentations:

“A 1H magnetic resonance spectroscopy study of metabolites in idiopathic generalised epilepsy” Association of British Neurologists Meeting April 2002

Simister R, McLean M, Barker G, Duncan J

“A short echo time proton magnetic resonance spectroscopy imaging in temporal lobe epilepsy” 9th ISMRM (International Society for Magnetic Resonance Imaging in Medicine) Glasgow, 2001. **Simister R**, Woermann F, McLean M, Barker G, Duncan J

“A short echo time MRS study of metabolites in the occipital lobes in epilepsy” 10th ISMRM, Hawaii, USA 2002 **Simister R**, McLean M, Barker G, Duncan J

Poster presentations:

“Idiopathic generalised epilepsy is associated with disturbance in frontal lobe neurochemical concentrations” American Epilepsy Society, Seattle, USA 2002

Simister R, McLean M, Barker G, Duncan J

“A short echo time MRS study of metabolites in the temporal lobe in temporal lobe epilepsy” 3rd International Magnetic Resonance Imaging in Epilepsy conference, Alabama, USA 2000. **Simister R**, Woermann F, McLean M, Barker G, Duncan J

Chapter 1: Introduction

1.1 Introduction and background

p. 024

1.1.1 The epilepsies

1.1.1.1 Classification of epileptic seizures and syndromes

1.2 Neurotransmission

p. 028

1.2.1 Introduction

1.2.2 Energetics of neurotransmission

1.2.3 Glutamate metabolism

1.2.4 Glutamate receptor function

1.2.4.1 AMPA receptors

1.2.4.2 Kainate Receptors

1.2.4.3 NMDA Receptors

1.2.5 Glutamate and epilepsy

1.2.6 GABA metabolism

1.2.7 GABA receptors

1.2.7.1 GABA_A receptors

1.2.7.2 GABA_B receptors

1.2.8 GABA and Epilepsy

1.3 Idiopathic Generalised Epilepsies

p. 045

1.3.1 Introduction

1.3.2 Pathophysiology of generalised spike wave discharges

1.3.3 Genetics of Idiopathic Generalised Epilepsy

1.3.4 Imaging of Idiopathic Generalised Epilepsy

1.3.5 Idiopathic Generalised Epilepsy Sub-syndrome description

1.3.5.1 Childhood Absence Epilepsy

1.3.5.2 Juvenile Absence Epilepsy

1.3.5.3 Juvenile Myoclonic Epilepsy

1.3.5.4 Idiopathic Generalised Epilepsy with Generalised Tonic Clonic Seizures only

1.3.6 Epileptic syndromes associated with photosensitivity

1.4 Localisation Related Epilepsies

p. 054

1.4.1 Introduction

1.4.2 Temporal Lobe Epilepsy (TLE)

1.4.2.1 Pathology and pathophysiology in TLE

1.4.2.2 Clinical features of mesial TLE

1.4.2.3 EEG features of mesial TLE

1.4.2.4 Imaging features of mesial TLE

1.4.2.5 Clinical features of neo-cortical TLE

1.4.2.6 EEG features of neo-cortical TLE

1.4.2.7 Imaging features of neocortical TLE

1.4.3 Occipital lobe epilepsy

1.5 Malformations of cortical development (MCD)

p. 061

1.5.1 Introduction

1.5.2 Normal brain development

1.5.2.1 Normal microscopic development of the neocortex

1.5.2.2 Normal microscopic development of the archi-cortex

1.5.3 Abnormal cortical development resulting in MCD.

1.5.3.1 Proliferation and differentiation

1.5.3.1.1 Focal Cortical Dysplasia (FCD)

1.5.3.2 Neuronal migration

1.5.3.2.1 Lissencephaly

1.5.3.2.2 Subependymal nodular heterotopia (SEH)

1.5.3.2.3 Subcortical heterotopia (SCH)

1.5.3.2.3 Band Heterotopia (BH)

1.5.3.3 Post-migrational cortical organisation

1.5.3.3.1 Polymicrogyria (PMG)

1.5.3.3.2 Schizencephaly (SHZ)

1.5.3.4 Other relevant MCD sub-types

1.5.3.4.1 Microdysgenesis

1.6 Magnetic Resonance Imaging

- 1.6.1 Introduction
- 1.6.2 MR physics
 - 1.6.2.1 T₁ Relaxation
 - 1.6.2.2 T₂ relaxation / decay
 - 1.6.2.3 Repetition Time (TR)
 - 1.6.2.4 The Spin-Echo Sequence
 - 1.6.2.5 The Gradient Echo Sequence
 - 1.6.2.6 The Inversion Recovery Sequence
- 1.6.3 Clinical application of MRI
 - 1.6.3.1 Structural Magnetic Resonance Imaging (MRI)
 - 1.6.3.2 Quantitative MRI
 - 1.6.3.3 Diffusion weighted MRI
 - 1.6.3.4 Magnetisation transfer MRI
- 1.6.4 Other non-MRI imaging modalities (PET, SPECT)

1.7 ¹H Magnetic Resonance Spectroscopy

p. 083

- 1.7.1 Introduction
- 1.7.2 MRS Physics
 - 1.7.2.1 Chemical Shift
 - 1.7.2.2 Free Induction Decay
 - 1.7.2.3 Spin-spin coupling
 - 1.7.2.4 T₂ and visibility
- 1.7.3 Basic acquisition and processing techniques
 - 1.7.3.1 Shimming
 - 1.7.3.2 Water suppression
 - 1.7.3.3 Choice of Echo Time (TE)
 - 1.7.3.4 Localisation techniques
 - 1.7.3.5 T₁ and T₂ correction
 - 1.7.3.6 Referencing to a standard solution
 - 1.7.3.7 Signal to noise ratio and signal averaging
- 1.7.4 Advanced acquisition and processing techniques
 - 1.7.4.1 Two dimensional (2D) NMR spectroscopy techniques

- 1.7.4.2 Spectral Editing techniques
- 1.7.4.3 Higher Magnetic Field Strengths
- 1.7.4.4 Magnetisation Transfer Spectroscopy
- 1.7.5 Biological Significance of Metabolite Peaks
 - 1.7.5.1 N-Acetyl Aspartate
 - 1.7.5.2 Creatine plus phosphocreatine
 - 1.7.5.3 Choline containing compounds
 - 1.7.5.4 GABA, glutamate and glutamine
 - 1.7.5.5 Myo-inositol
 - 1.7.5.6 Lactate
- 1.7.6 MRS in Healthy Adults

1.8 Application of ^1H MRS to the investigation of epilepsy **p. 106**

- 1.8.1 Introduction
- 1.8.2 Ex vivo MRS of epileptic tissue
- 1.8.3 Findings in temporal lobe epilepsy
- 1.8.4 Findings in extra-temporal lobe epilepsy
- 1.8.5 Findings in malformations of cortical development
- 1.8.6 Association of MRS findings with seizure history
- 1.8.7 Effect of antiepileptic drugs on MRS metabolites
- 1.8.8 ^{31}P and ^{13}C MRS findings in epilepsy
- 1.8.9 Correlation of MRS findings with other imaging modalities

Chapter 2 Common Methodology **p. 125**

2.1 Introduction **p. 126**

2.2 Common Methods **p. 126**

- 2.2.1 Subject recruitment
- 2.2.2 Volumetric data acquisition and analysis
- 2.2.3 MRS data acquisition
- 2.2.4 MRS data processing
 - 2.2.4.1 LCModel
- 2.2.5 MRS data analysis

2.3	Magnetic Resonance Spectroscopic Imaging (MRSI)	p. 132
2.4	Double Quantum Filter (DQF) measurement of GABA	p. 134
2.5	Metabolite nulled measurement of glutamate and glutamine	p. 139
2.6	Post-ictal MRS	p. 141
 Chapter 3: Results		p. 143
3.1	Multi-voxel MRSI in TLE	p. 144
3.2	MRS in the Occipital lobes in IGE and OLE	p. 168
3.3	MRS in the Frontal lobes in IGE	p. 188
3.4	MRS in Malformations of Cortical Development	p. 205
3.5	The effect of Sodium Valproate on MRS measured metabolites	p. 224
3.6	MRS in TLE post Temporal Lobe Surgery	p. 234
3.7	MRS in the immediate post ictal period	p. 252
 Chapter 4: Thesis Conclusions and Further Work		p. 267
Bibliography		p. 273

List of Abbreviations:

AED(s)	antiepileptic drug(s)
AMPA	alpha-amino-3-hydroxy-5-methyl-4-isoxazole proprionate
ANLSH	astrocyte neuronal lactate shuttle hypothesis
ADP	adenosine diphosphate
ATP	adenosine triphosphate
BH	band heterotopia
CAE	childhood absence epilepsy
CBF	cerebral blood flow
Cho	choline containing compounds
CK	creatine kinase
Cl ⁻	chloride ion
CNS	central nervous system
CO ₂	carbon dioxide
CA	cornu ammonis
Cr	creatine plus phosphocreatine
CPS	complex partial seizure(s)
Creat	creatine
CSF	cerebrospinal fluid
CSI	chemical shift imaging
CT	(X-ray) computed tomography
DNA	deoxyribonucleic acid
DNET	dysembryoplastic neuro-epithelial tumour
DQF	double quantum filter
DTI	Diffusion Tensor Imaging
DWI	Diffusion-Weighted Imaging
ECF	extracellular fluid
EEG	electroencephalogram
EGTCA	epilepsy with generalised tonic clonic seizures on awakening
FC	febrile convulsion(s)
FCD	focal cortical dysplasia
FDG	[¹⁸ F]-fluorodeoxyglucose

FID	free induction decay
FLAIR	fluid attenuation inversion recovery
fMRI	functional Magnetic Resonance Imaging
FOV	field of view
FWHM	full width at half maximum
GABA	gamma-amino butyric acid
GABA+	combined GABA signal from GABA + homocarnosine
GAD	glutamic acid decarboxylase
GE	General Electric
GFAP	glial fibrillary acidic protein
GLUT	glucose transporter
GLX	glutamate plus glutamine
GM	grey matter
GSWD	generalised spike wave discharge
GTCS	generalised tonic-clonic seizure(s)
HS	hippocampal sclerosis
Hz	hertz
IGE	idiopathic generalised epilepsy
ILAE	International League Against Epilepsy
Ins	myo-inositol
IQ	intelligence quotient
IPS	intermittent photic stimulation
IR	inversion recovery
ISIS	image selective in-vivo spectroscopy
JAE	juvenile absence epilepsy
JME	Juvenile Myoclonic Epilepsy
Ka	kainate
LDH	lactate dehydrogenase
MAO-B	monoamine oxidase type B
MCD	malformation(s) of cortical development
MQC	multiple quantum coherence
MRI	Magnetic Resonance Imaging
mRNA	messenger ribonucleic acid

MRS	Magnetic Resonance Spectroscopy
MWP	molecular water pump
mTLE	mesial temporal lobe epilepsy
NAA	N acetyl aspartate
NAAG	N acetyl aspartyl-glutamate
NAA _t	N acetyl aspartate + N acetyl aspartyl-glutamate
N-CAM	Neural Cell Adhesion Molecule
NEX	number of excitations
NMDA	N-methyl-D-aspartate
NSE	National Society for Epilepsy
OLE	occipital lobe epilepsy
p.	page
PET	Positron Emission Tomography
PCreat	phosphocreatine
Pi	inorganic phosphate
PI	phosphoinositol
PMG	polymicrogyria
PNH	periventricular nodular heterotopia
PPR	photo-paroxysmal response
PRESS	point resolved spectroscopy
RF	radiofrequency
ROI	region of interest
SCH	sub-cortical heterotopia
SD	standard deviation
SEH	sub-ependymal heterotopia
SMIT	sodium myo-inositol co-transporter
SHZ	schizencephaly
SNR	signal to noise ratio
SPECT	Single Photon Emission Computed Tomography
SPM	statistical parametric mapping
SPS	simple partial seizure(s)
SWD	spike wave discharge
STEAM	stimulated echo acquisition mode

TCA	tricarboxylic acid
TE	echo time
TMS	tetramethyl silane
TR	repetition time
UK	United Kingdom
VBM	voxel-based morphometry
VOI	volume of interest
WM	white matter
xTLE	extra-temporal lobe epilepsy

AED abbreviations:

CBZ	carbamazepine
CLB	clobazam
CLN	clonazepam
DZP	diazepam
ETH	ethosuximide
GBP	gabapentin
LEV	levetiracetam
LTG	lamotrigine
OXC	oxcarbazepine
PHT	phenytoin
PB	phenobarbitone
PRM	primidone
TIA	tiagabine
TPM	topiramate
VPA	sodium valproate

1.1 Introduction and Background

1.1.1 Background

This thesis investigates the application of an MRI technology, Magnetic Resonance Spectroscopy (MRS), to the study of epilepsy. Prior to the period during which this work was undertaken several groups had reported MRS findings in patients with epilepsy. These studies, which had generally reported on only the major visible metabolites and which had used metabolite ratios rather than individual metabolite concentrations, had indicated that MRS may be a sensitive tool for the in vivo assessment of biochemical disturbance associated with epilepsy [for a summary of the available evidence prior to the period of this thesis see (Duncan, 1996; Kuzniecky, 1999)]. This thesis builds on that preliminary evidence and takes advantage of developments in scanner hardware and pulse sequences which allowed the semi-quantification of neuro-metabolites such as glutamate and γ -amino butyric acid (GABA) that are of fundamental importance to understanding epilepsy.

The work included in this thesis was undertaken based upon several hypotheses. Namely that:

I Cortical excitability in idiopathic generalised epilepsy (IGE) is associated with reduced concentrations of GABA and / or raised concentrations of glutamate and glutamine in the cerebral cortex.

II In patients with focal seizures, there will be a disturbance in GABA and / or glutamate levels in the region of the epileptic focus compared to healthy controls measured in the same anatomical region.

III There will be measurable metabolite abnormalities in epileptogenic malformations of cortical development as a consequence of the abnormal development of this tissue.

IV There will be a measurable disturbance of brain metabolites at the site of interictal epileptiform activity that will help to characterise the epileptic focus.

V Immediately following focal seizures there will be a transient disturbance in those measurable metabolites relevant to cell energetics and neurotransmission such as lactate, GABA, glutamate and glutamine and phosphocreatine.

In order to evaluate these hypotheses the work has necessarily covered a wide range of epilepsy syndromes and seizure types which are briefly introduced in this Introduction. Other sections of this chapter are intended to introduce the underlying principles and techniques of MRS relevant to my work and to present the published work from other experimenters in the field that sets the foundation on which this work has been based.

MRS is potentially a uniquely important imaging tool: an MRS experiment can provide simultaneous in vivo data relating to neuronal function and / or cell loss, glial function, and neurotransmitter cycling in regions of interest mapped directly upon structural MR volumetric images. MRS measured metabolite concentrations also appear to be sensitive to exogenous factors such as concomitant antiepileptic medications and endogenous factors such as recent seizure history. The Results and Discussion Chapters of this thesis consider these themes further while the key measured metabolites and some fundamental considerations relating to cell energetics and neurotransmitter cycling in the human brain are briefly introduced first in this Introduction.

Finally, this work is an investigation of epilepsy and epileptic syndromes and for this to be informative a clear understanding of the classification of epileptic seizures and syndromes is necessary from the outset.

1.1.2 Classification of epileptic seizures and syndromes

Epilepsy is a condition characterised by the occurrence of recurrent epileptic seizures of primary cerebral origin. Epileptic seizures consist of a paroxysmal dysfunction of cerebral neuro-physiological function and, in general, have a correlate on the electroencephalogram (EEG).

The International League Against Epilepsy (ILAE) first introduced a classification of the epilepsies in 1970(Merlis, 1970) with subsequent revisions occurring in 1985 and in 1989(The International League Against Epilepsy, 1989). Classification of

seizure type was revised in 1981. In 2001 the ILAE published a proposed new diagnostic scheme for people with epileptic seizures and epilepsy(Engel, Jr., 2001)which described an approach to classification based upon five components or axes: ictal phenomenology, seizure type, syndrome, aetiology and impairment. Seizure type was divided into self-limited seizures (incorporating generalised seizures and focal onset seizures); continuous seizure types incorporating focal and generalised status epilepticus; and precipitating stimuli for reflex seizures. In 2006 the ILAE decided to defer introduction of a new classification system but recognised that the 1989 classification system was imperfect(Engel, Jr., 2006). In this system an epilepsy syndrome is a complex of signs and symptoms that define a unique epilepsy condition and is more than just the seizure type (e.g. Idiopathic Generalised Epilepsy is an epilepsy syndrome characterised by a cluster of signs and symptoms occurring together). An epilepsy disease is a pathological condition with a single specific well defined aetiology (e.g. Unverricht-Lundborg)

In 2009 the ILAE organised for consultation on a revised terminology for the organisation of the epilepsies(ILAE Commission on Classification and Terminology, 2009). The revised terminology will make a number of changes to the above classification system. Amongst these changes is the recognition that generalised seizures may originate at some location but rapidly engage bilaterally distributed networks whilst focal seizures may be discretely localised or more widely distributed in networks limited to one hemisphere but will have onset that is consistent from one seizure to another. The use of the term “syndrome” will be restricted to a group of clinical entities that are reliably identified by a cluster of electro-clinical characteristics. Underlying aetiology will be grouped as Genetic, Structural / Metabolic and Unknown.

Seizure classification will also change with a new structure for the description of generalised seizures

GENERALIZED SEIZURES

Tonic Clonic (in any combination)

Absence:

- Typical
- Atypical
- Absence with special features
 - Myoclonic absence
 - Eyelid myoclonia

Myoclonic

- Myoclonic
- Myoclonic atonic
- Myoclonic tonic

Clonic

Tonic

Atonic

The description of focal seizures will also change so that the current concepts of “simple” and “complex” partial seizures and secondarily generalised seizures will be revised to reflect the often difficult distinction between strictly “simple” and “complex” seizures.

The old concept of an “epileptic disease” will be lost and syndromic classification as “electroclinical” syndromes will be tighter and will represent distinctive disorders identifiable on the basis of a typical age onset, specific EEG characteristics, seizure types, and often other features which, when taken together, permit a specific diagnosis. Other common entities which will represent electro-clinical syndromes but which do represent common clinical entities such as mesial temporal lobe epilepsy will be referred to as Constellations. Epilepsies secondary to specific structural or metabolic lesions or conditions and Epilepsies of Unknown Cause will represent the remaining two classification groups. The terminology “Idiopathic Generalised Epilepsy” for the cluster of epilepsy syndromes described in Section 1.3 will remain for the time being but with the recognition that the term “idiopathic” is now inaccurate and out-dated.

1.2 Neurotransmission

1.2.1 Introduction

1.2.2 Energetics of neurotransmission

1.2.3 Glutamate metabolism

1.2.4 Glutamate receptor function

1.2.4.1 AMPA receptors

1.2.4.2 Kainate Receptors

1.2.4.3 NMDA Receptors

1.2.5 Glutamate and epilepsy

1.2.6 GABA metabolism

1.2.7 GABA receptors

1.2.7.1 GABA_A receptors

1.2.7.2 GABA_B receptors

1.2.7.3 GABA_C receptors

1.2.8 GABA and Epilepsy

1.2.1 Introduction

Several of the neuro-metabolites that are visible to MRS play an important role in the fundamental processes of brain cells, including energy balance and signalling. These metabolites include glutamate, glutamine, γ -amino butyric acid (GABA), lactate and creatine (Creat) plus phosphocreatine (PCreat). Glutamate and GABA are respectively the principal excitatory and inhibitory neurotransmitters in the brain and the study of both is fundamental to an understanding of epilepsy.

1.2.2 Energetics of neurotransmission

Brain metabolism accounts for 20% of the body's resting metabolism (Leonard et al., 2007). MRS studies have shown that glucose utilisation is closely linked to the rate of brain glutamate – glutamine cycling between neuronal and glial compartments and indicate that up to 75% of total energy expenditure in grey matter is devoted to cell to cell signalling (Pellerin et al., 1998; Sibson et al., 1998a; Sibson et al., 1998b; Rothman et al., 1999; Attwell and Laughlin, 2001).

Under normal conditions the brain derives almost all of its energy from the oxidation of glucose (Simpson et al., 1978). For this it needs a continuous supply of glucose and oxygen delivered by the blood supply through a rich network of vessels. Maintenance of bio-energetic homeostasis requires that the metabolic rate varies rapidly in response to abrupt changes in cell energy demand. Glycolysis is the series of enzyme catalysed reactions in the cytosol responsible for the breakdown of glucose with the formation of two molecules of ATP and pyruvate. In the presence of oxygen the pyruvate so formed would normally enter the Krebs cycle (tricarboxylic acid cycle [TCA]) and undergo oxidative phosphorylation.

Glucose is transported into neurones and astrocytes by several members of the GLUT family of membrane spanning proteins. In the brain the important transporters are GLUT1 (present on astrocyte cell membranes) and GLUT3 (present on neuronal cell membranes) (Maher et al., 1994). They show maximum transport rates several orders of magnitude higher than seen with non-brain located glucose transporters so glucose transport is not usually a rate limiting step for glycolysis (Maher et al., 1994). Astrocytes are ideally positioned to sense increases in synaptic activity and increase glucose uptake. These cells cover the surface of the intra-parenchymal capillaries with specialised processes called astrocytic end feet

and GLUT1 are expressed on these feet (Morgello et al., 1995) suggesting that astrocytes may be a likely site of prevalent glucose uptake. Other astrocyte processes wrapped around synaptic contacts possess receptors and reuptake sites for neurotransmitters.

The conventional view that brain energy metabolism is almost exclusively aerobic was challenged by the observation of a decoupling of O₂ consumption from glucose utilisation in activated brain tissue (Fox and Raichle, 1986; Villringer and Dirnagl, 1995). Further support for these observations was obtained from MRS work in humans (Frahm et al., 1996; Prichard et al., 1991; Sappey-Marinier et al., 1992), and in animals (Fellows et al., 1993; Hu and Wilson, 1997b), showing an increase in tissue or extracellular lactate during cerebral activation and in turn this has led to a detailed discussion as to the potential role of lactate as a neuronal fuel in activated brain tissue. Most discussion has centred around a proposal by Pellerin and Magistretti and referred to as the astrocyte–neuron lactate shuttle (ANLS) hypothesis (Pellerin and Magistretti, 1994, 2003) which has sought to link export of astrocyte produced lactate via aerobic glycolysis (i.e. glycolysis derived lactate despite the presence of oxygen) to neurons with glutamate–glutamine cycling between these two cell compartments.

This hypothesis was based in large part on work performed using ¹³C MRS by Sibson and others where rates of total glutamate to glutamine cycling were measured against neuronal glucose oxidation rates in anaesthetised rats and at different levels of electrical activity and which found a linear relationship above electrical baseline with a slope of 1 indicating a 1:1 relationship (Sibson et al., 1997; Sibson et al., 1998a; Sibson et al., 1998b; Rothman et al., 1999). This was combined with glial culture studies performed which described glial glutamate uptake (Flott and Seifert, 1991), co-transport with Na⁺ stimulated glial glycolysis (Kimmelberg et al., 1989) and lactate production (Ercinska and Silver, 1987). In this theory the two ATP equivalents produced per glucose molecule were in principle sufficient to maintain active glutamate clearance from the extracellular space and recycling to the neurone (one used for pumping of Na⁺/K⁺ ions and one for glutamine synthesis).

Lactate normally represents a metabolic dead end unless it is converted back to pyruvate. This can only be accomplished with the enzyme lactate dehydrogenase

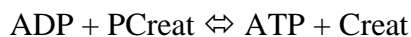
(LDH) which has several isoforms each representing a tetrameric combination of two different polypeptide chains. LDH5 is found in tissues producing lactate while tissues containing predominantly the LDH1 isoform are more oxidative and consume lactate by favouring conversion to pyruvate. These properties have significance for cell physiology. Increase in brain adenosine diphosphate (ADP) concentration stimulates glycolysis by activation of the regulatory enzyme phosphofructokinase. When maximally stimulated the rate of formation of pyruvate can rise to close to the maximum rate at which it can enter the tricarboxylic acid (TCA) cycle. The increase stimulates pyruvate conversion into lactate as well as its transport into the mitochondrial matrix and export into the circulation. The greater the equilibrium lactate/pyruvate ratio the more slowly this rise occurs. For cells with a greater proportion of LDH5 isoforms than LDH1 there is a much higher rate of increase of conversion into lactate. There is evidence that mRNA for LDH1 alone is expressed in neurones while astrocytes appear to express both LDH1 and LDH5 and their corresponding mRNA (van Hall G., 2000).

The ANLS hypothesis has been the subject of an intense debate during the last decade [for example: (Magistretti et al., 1993; Magistretti and Pellerin, 1997; Pellerin et al., 1998; Magistretti and Pellerin, 1999; Magistretti et al., 1999; Magistretti and Pellerin, 2000; Pellerin et al., 2001; Chih et al., 2001; Dienel and Hertz, 2001; Pellerin and Magistretti, 2003; Mangia et al., 2003a; Mangia et al., 2003b; Hertz, 2004; Pellerin et al., 2007; Simpson et al., 2007; Mangia et al., 2009). Several of these authors have disputed the validity of the ANLSH (Chih et al., 2001; Gruetter, 2002; Hertz and Hertz, 2003; Mangia et al., 2009) and in particular the requirement of the hypothesis that neurones preferentially utilise astrocyte derived lactate ahead of glucose in oxidative metabolism and the assumption that astrocytic oxidative phosphorylation does not play a part in these energy transactions. However there remains general agreement that there is a link between the rate of glutamate-glutamine cycling and the TCA flux of the neuron even if this relationship does not fit the 1:1 association necessary for the ANLSH.

The energy currency of cells, adenosine triphosphate (ATP), is the link between energy utilising and energy producing processes. Brain energy metabolism normally maintains constant concentration of ATP as the processes that restore this metabolite are sensitive to increased ATP utilisation. Observations in heart and brain suggest

that even a tenfold increase in cellular work output can be sustained with minimal ATP concentration fluctuation(Petroff et al., 1984;Young et al., 1985). Both short term and longer term regulatory mechanisms are used to maintain a constant concentration of ATP. One important short term mechanism for maintaining ATP concentration is by hydrolysis of PCreat(Fedosov, 1994;Friedman and Roberts, 1994;Wallimann et al., 1998;Brustovetsky et al., 2001;Neumann et al., 2003). More sustained increases in rates of ATP utilisation are balanced by increases in rates of glycolysis and oxidative phosphorylation.

The enzyme creatine kinase (CK) catalyses the inter-conversion of ADP and PCreat with ATP and Creat according to the reaction:



Only after PCreat is reduced by 70 - 80% is ATP concentration lowered, in parallel with the accumulation of ADP and, later on, AMP(Hilberman et al., 1984). The transfer of energy from the mitochondrial matrix to the cytoplasm is achieved via a creatine phosphate energy shuttle system(Bessman and Geiger, 1981). CK isoforms are present both within mitochondria and also within the cytosol. Intracellular compartmentation of these enzymes helps to establish a buffering system for cellular energy stores and a shuttle for high-energy phosphates from the mitochondria to the cytosol. At the outer surface of the inner mitochondrial membrane a mitochondrial isoform of CK (MtCK) is coupled both structurally and functionally to the adenine nucleotide translocator(Jacobus and Lehninger, 1973;Moreadith and Jacobus, 1982). As ATP derived from oxidative phosphorylation enters the inter membranous space of mitochondria MtCK preferentially transfers the gamma phosphoryl to creatine and ADP is recycled back to the matrix(Wallimann et al., 1998) whilst cytosol located CK isoforms (BCK) can both utilise PCreat to convert ADP to ATP and convert ATP to PCreat for energy storage(Fedosov, 1994). In most regions of the brain BCK is concentrated in synaptic regions indicating the importance of the shuttle in the metabolic support of synaptic transmission(Friedman and Roberts, 1994).

1.2.3 Glutamate metabolism

The amino acid L-glutamate is the major mediator of excitatory signals in mammalian central nervous system. Glutamate and γ -amino butyric acid (GABA), its conjugate inhibitory neurotransmitter, constitute the principal transmitters in more than 90% of cortical neurons in the adult mammalian brain (Nicholls, 1989, 1993) and glutamate is probably involved in most aspects of normal brain function including cognition, memory and learning (Fonnum, 1984; Collingridge and Lester, 1989; Headley and Grillner, 1990). Most neurons, and some glial cells have glutamate receptors in their plasma membranes but receptor concentration differs greatly in these cell types; glutamatergic neurons possess ~80%, whereas GABAergic neurons contain between 2% to 10% and astrocytes ~10% of total tissue glutamate (Storm-Mathisen et al, 1983; Ottersen and Storm-Mathisen, 1984; Korf and Venema, 1983; Van den Berg and Garfinkel, 1971; Patel et al, 1974; Ottersen et al, 1992; Lebon et al, 2002).

The brain contains huge amounts of glutamate, about 5–15 mmol per kg wet weight (Schousboe, 1981), but only a tiny fraction of this glutamate is normally present in the extracellular compartment. The concentrations in the extracellular fluid, which represents 13–22% of brain tissue volume, and in the cerebrospinal fluid (CSF) are normally around 3–4 μ M and around 10 μ M, respectively (Lehmann et al., 1983; Hamberger and Nystrom, 1984). Consequently, the concentration gradient of glutamate across the plasma membranes is several thousand-fold. The highest concentrations are found inside nerve terminals (Ottersen et al., 1992; Storm-Mathisen et al., 1992).

The distribution of glutamate is in a dynamic equilibrium which is highly sensitive to changes in the energy supply. Glutamate is continuously being released from cells and removed from the extracellular fluid. Synaptically released glutamate is taken up mainly by astrocytes, driven by the co-transport with each glutamate of 3 Na^+ and 1 H^+ and the counter transport of 1 K^+ (Levy et al., 1998). Approximately one third of the glutamate so taken up by the neighbouring astrocytes is converted into glutamine (de Barry J. et al., 1983) in a process requiring 1 ATP per glutamate. One quarter of the glutamate remains as glutamate, 1/5 is converted to alpha-ketoglutarate by GAD and the other 1/5 may be transaminated by aspartate.

Glutamine may leave the astrocyte and enter neurons without consuming energy. In the neuron the glutamine may be converted into glutamate and repackaged in synaptic vesicles. This packaging is powered by vesicular H^+ -ATPase. At least one H^+ is pumped to accumulate a glutamate anion. This requires hydrolysis of 1/3 ATP molecule. An extra 1.14 ATP/glutamate may be hydrolysed to counteract leakage from the vesicle. For the average 4,000 glutamate molecules per vesicle, 11,000 ATP are required. Other energy requirements are due to activation of post synaptic receptors in the post-synaptic neuron, pre-synaptic Ca^{2+} fluxes and the vesicular release mechanism, the energy need to maintain action potentials and the energy expended on the resting potential. In total the energy expended per vesicle of glutamate released is 1.64×10^5 ATP molecules (Attwell and Laughlin, 2001).

This trafficking of glutamate and glutamine between astrocytes and neurons has been proposed to be a major pathway by which transmitter glutamate is recycled. It is commonly referred to as the glutamine–glutamate cycle. The concept of a compartmentation of glutamate into two pools was introduced in the early seventies based on ^{14}C tracer studies (van den Berg and Garfinkel, 1971) and the notion of a predominantly glial synthesis of glutamine a little later when glutamine synthetase was shown immunocytochemically to be a glial enzyme (Martinez-Hernandez et al., 1977; Erecinska and Silver, 1990) (Westergaard et al., 1995). Glutamine is normally present in the extracellular fluid at around 200–500 μM (Gjessing et al., 1972; Hamberger and Nystrom, 1984). This does not compromise neurotransmission because glutamine does not activate glutamate receptors.

Following the release of glutamate from a pre-synaptic nerve terminal, glutamate will diffuse into the synaptic cleft and interact with glutamate binding proteins (transporters and receptors) present there, e.g. AMPA and NMDA receptors. The diffusion will continue out of the cleft and glutamate may interact with metabotropic glutamate receptors along the spine and nerve terminal membranes and come within reach of glial glutamate transporters.

Metabotropic glutamate receptors located pre-synaptically on glutamatergic and on some GABAergic nerve terminals modulate the release of the transmitter (Sanchez-Prieto et al., 1996; Scanziani et al., 1997; Vogt and Nicoll, 1999). This implies that glutamate transporters are indirectly involved in the control of transmitter release

because they control the amount of glutamate that reaches the pre-synaptic receptors. In line with this, inhibition of glutamate uptake has been reported to cause decreased synaptic release of glutamate and GABA (Maki et al., 1994; Semyanov and Kullmann, 2000) (Maki et al., 1994) due to increased activation of these receptors.

The concentrations of glutamate transporter molecules in brain tissue are very high. It has been shown that 15,000 and 21,000 glial glutamate transporter molecules are present per μm^3 tissue in the striatum radiatum of hippocampus CA1 and the molecular layer of cerebellum, respectively (Lehre and Danbolt, 1998).

The glutamate concentration profile within the synaptic cleft depends on the amount of glutamate released into the cleft, on the speed with which it is released and on how fast it is removed from the cleft. The removal depends on uptake and on diffusion which again depends on the water concentration, the tortuosity of the extracellular space and the interaction with glutamate binding sites. Regulation of this activity can be modulated at many levels, e.g. DNA transcription, mRNA splicing, protein synthesis, protein targeting, and actual amino acid transport and associated ion channel activities (Gegelashvili and Schousboe, 1998; Sims and Robinson, 1999).

Failure of regulation may lead to the 'deleterious network hypothesis' (Ying, 1998) in which high extracellular glutamate can activate glutamate receptors causing further glutamate release. Glutamate receptor activation increases energy consumption and free radical production which may in turn impair energy production and glutamate uptake and possibly even reverse the transporter direction leading to an escalating positive feedback of glutamate release. The influx of ions may cause oedema (Kimelberg et al., 1995) and ischaemia and the formation of highly reactive compounds such as the superoxide anion radical (O^{2-}), hydroxyl radicals, H_2O_2 and peroxynitrite (for review, see (Fridovich, 1997; Koppenol, 1998) leading to neuronal injury or death (Gotz et al., 1994; Dawson and Dawson, 1996; Delanty and Dichter, 1998). Regulation failure secondary to down-regulation of glial glutamate transporters has been described in a variety of situations, e.g. after transient ischemia, in amyotrophic lateral sclerosis, and after traumatic brain injury.

1.2.4 Glutamate receptor function

Glutamate exerts its effects by action on glutamatergic receptors of which there are ionotropic and metabotropic receptor subtypes. Each of the two main families of glutamate receptors comprises three functionally defined groups of receptor. These are made up of numerous individual subunits, each encoded by a different gene. Ionotropic sub-types include three classes originally named after selective agonists: N-methyl-D-aspartate (NMDA), α -amino-3-hydroxy-5-methyl-4-isoxazole propionic acid (AMPA) and kainate (Ka). As many as ten distinct subfamilies of ionotropic glutamate receptor genes have been identified, based on evidence from molecular biology experiments.

1.2.4.1 AMPA receptors

AMPA receptors are the receptors responsible for most rapid excitatory transmission within the vertebrate CNS. The associated channels are rapidly activated and inactivated, and appear to be present on all neurons within the CNS. AMPA receptors can be activated following the binding of L-glutamate and other agonists, such as quisqualate and domoic acid, as well as AMPA. The affinity of AMPA receptors for L-glutamate, the endogenous amino acid that represents the most likely candidate in mediating neurotransmission at these receptors, is much lower than is the affinity at NMDA receptors.

Four glutamate receptors (GluR 1 to GluR 4) have been cloned and identified as subunits which have the electrophysiology and pharmacology of the AMPA receptor. AMPA receptors are widely present throughout the brain, although there are regional differences in the relative amounts of each receptor.

1.2.4.2 Kainate Receptors

The distinguishing hallmark of the electrophysiology of kainate receptors is that, in general, for vertebrate CNS neurons, there is no agonist-induced desensitization. However, like the AMPA receptor subfamily, the kainate receptors are coupled to ion channels that are permeable to monovalent cations and have reversal potentials near 0 mV. Often, these receptors are considered, along with AMPA receptors, to be simply non-NMDA receptors, as both types have overlapping pharmacologic and electrophysiological profiles.

In situ hybridization studies have led to the discovery of different distributions throughout the brain for mRNA encoding the glutamate receptors GluR 5, 6, and 7 respectively. In contrast to GluR5 and GluR6, GluR7 receptors are not present in high numbers in the hippocampus, although they have been found in the granule cells of the dentate gyrus. Messenger RNA for both GluR6 and GluR7 is present in high abundance in brain regions that have been found to be profoundly sensitive to destruction following kainic acid treatment. These areas include the hippocampus, cortex, cerebellum, and reticular thalamic regions. KA1 is expressed at high levels in only CA3 pyramidal cells and dentate granule cells, whereas KA2 is found in virtually all brain regions. There is evidence to support the hypothesis that the KA2 receptor is co-expressed in some areas with GluR6 and GluR5, and that KA1 may be co-expressed with GluR6 in the hippocampus.

1.2.4.3 NMDA Receptors

Agonists at the NMDA receptor include N-methyl-D-aspartate, glutamate, and a variety of other excitatory amino acids. As with the non-NMDA receptor, the NMDA receptor possesses two agonist-binding sites. The NMDA receptor is also distinguished by the fact that it has an absolute requirement for a co-agonist, glycine. If the glycine site on the receptor is blocked or unoccupied, binding of glutamate to the receptor will not result in the channel opening. In addition to its co-agonist requirement, the NMDA receptor has been shown to be modulated by Mg^{2+} , H^+ , Zn^{2+} , polyamines and steroids.

The behaviour of the activated NMDA receptor-channel complex differs dramatically from that of the non-NMDA receptor. Activation of the channel is much slower, with the time to the peak current being often tens of milliseconds. Desensitization at NMDA receptors during exogenous application of agonist takes several hundred milliseconds to develop, whereas desensitization at AMPA receptors occurs within 5–10 ms.

Another difference between non-NMDA and NMDA receptors is the voltage-sensitive block of Mg^{2+} at the NMDA receptor. In addition, single-channel experiments have revealed that once agonist has bound to the NMDA receptor, the

channel can open and close repeatedly for up to several hundred milliseconds, resulting in long-lasting currents.

1.2.4.4 Metabotropic receptors (mGluR)

These receptors, unlike their ionotropic counterparts, are not comprised of subunits that form an integral ion channel; instead, they are comprised of polypeptides that have a trans-membrane spanning domain with a large extracellular NH₂ terminal region. When an agonist binds to the mGluR, activation of a variety of G-proteins occurs. This G-protein coupled activation then results in a diverse biochemical cascade that can result in the modulation of a variety of cellular functions, such as current flow through voltage-gated ion channels. To date, within the three groups of receptors, eight subtypes of the mGluR have been cloned and correspond to a novel gene family of G-protein coupled receptors. Activation of this class of glutamate receptors has been implicated in a variety of CNS functions, including different forms of synaptic plasticity and excitotoxicity.

1.2.5 Glutamate and epilepsy

Elevated glutamate concentrations have been observed in most (Perry et al., 1975; Sherwin et al., 1988; Petroff et al., 1989) but not all (Peeling and Sutherland, 1993; van Gelder and Sherwin, 2003) ex-vivo studies of resected epileptic tissue.

In patients with refractory complex partial seizures requiring depth electrode insertion for further electrographic investigation, During and Spencer were able to implant micro-dialysis probes bilaterally along the hippocampi. Their measurements of glutamate and GABA concentrations in relation to the electrographic onset of spontaneous seizures showed a significant increase in glutamate concentration directly before seizure onset on the epileptogenic side. The non-epileptogenic side showed a smaller increase in glutamate concentration beginning after seizure onset and an associated rise in GABA concentration. (During and Spencer, 1993). During and Spencer were also able to report the observation that the glutamate levels fell slower indicating impaired removal from the extra cellular space

Other groups have found similar. Wilson (Wilson et al 1996 add) found elevated glutamate, aspartate and GABA in the epileptogenic hippocampus whilst Thomas and Philips found similar with spontaneously vigorous hippocampal epileptiform

activity increased by more than 23 fold, 19 fold and 10 fold compared to cases with minimal hippocampal activity.

Glutamate acting on AMPA, NMDA and probably also mGluR1 receptors is thought to play an important role in cell death subsequent to status epilepticus. The primary mechanism involved is ionic disequilibrium related to the excessive entry into the cell of Na^+ and Ca^{2+} through ligand gated voltage sensitive channels. Raised intracellular Ca^{2+} activates various enzymes (e.g. proteases, phospholipases, nitric oxide synthesis or endonucleases) that contribute to cell death (Meldrum, 2000).

Agonists acting at GluR are pro-convulsant following intra-cerebral or systemic injection. Antibodies to GluR3, as found in sera of subjects with Rasmussen's encephalitis, enhance neuronal excitability and are associated with seizures. Kainate and domoate, which are synthesised by marine plants, induce limbic seizures apparently by acting at high-affinity kainate receptors in the CA3 subfield of the hippocampus. Pre-synaptically they inhibit GABA release; post-synaptically they are depolarising. Seizures can also be induced by agonists acting on the NMDA receptors and type 1 metabotropic receptors whilst NMDA and AMPA receptor antagonists are powerful anticonvulsants in a range of animal models (Meldrum and Chapman, 1999).

For these reasons precise regulation of glutamate is crucial in healthy tissue and likely to be impaired in epileptogenic tissue. MRS allows the in vivo study of glutamate (in this thesis as the combined signal of glutamate plus glutamine [GLX]) and measurement of GLX in different epileptic disorders is an important part of this thesis.

1.2.6 GABA metabolism

The role of GABA as an inhibitory neurotransmitter in the mammalian brain was firmly established by the mid-1970s. It is estimated that between 17% and 50% of all synapses in the brain are GABAergic (Bloom and Iversen, 1971; Mody et al., 1994). GABA exerts its effect through GABA_A , GABA_B and GABA_C receptors (see below). The clinical importance of the GABAergic system is reflected in the wide range of drugs modifying GABAergic transmission (mainly GABA_A receptors), including anticonvulsants (benzodiazepines and barbiturates), steroids, anaesthetics,

and anxiolytics. The paramount importance of GABA metabolism is reflected in the multiple roles attributed to GABAergic transmission including the modulation of cortical excitability, anxiety levels, feeding and drinking behaviour, circadian rhythms, cognition, vigilance, memory and learning [reviewed by (Sieghart et al., 1999)]. In the developing brain, however, it is now established that GABA-mediated signalling can be excitatory and has been implicated in the regulation of several phases of brain development from cell proliferation to circuit refinement (Ben Ari, 2001; Ben Ari, 2002; Ben Ari et al., 2004). GABAergic transmission may also sometimes become excitatory in adults, for example in patients with mesial temporal lobe epilepsy (mTLE) (Fujiwara-Tsukamoto et al., 2003; Ben-Ari, 2006). In microdialysis experiments of epileptogenic hippocampi epileptic seizures were associated with large increases in glutamate but also with elevation of GABA indicating ictal activation of GABAergic pathways.

The evidence for the role of GABA as an important inhibitory neurotransmitter began to accumulate when GABA was localised to mammalian nerve terminals and antibodies raised to GABAergic enzymes were shown to localise to inhibitory nerve terminals [for recent review of GABA metabolism and mechanisms of action see (Schousboe and Waagepetersen, 2007)]. Glucose is the principal precursor for GABA production in vivo although pyruvate and other amino acids also can act as precursors. GABA is formed in vivo by a metabolic pathway referred to as the GABA shunt. The shunt is a closed loop process with the dual purpose of producing and conserving the supply of GABA. The first step in the synthesis of GABA from tricarboxylic acid intermediates is the transamination of alpha ketoglutarate to glutamic acid by GABA-Transaminase (GABA-T). Glutamic acid is then decarboxylated to form GABA by glutamic acid decarboxylase (GAD). GAD appears only to be expressed in GABAergic cells. Two forms of GAD have been identified – GAD65 and GAD67. GABA is metabolised by GABA-T to form succinic semialdehyde in a process that results in the transfer of an amino group from GABA to alpha ketoglutarate thereby reforming glutamic acid.

GABA formed in this process is concentrated within synaptic vesicles by action of a vesicular neurotransmitter transporter (VGAT) and vesicle release at the pre-synaptic terminal occurs by calcium-dependent exocytosis although non-vesicular GABA release has also been demonstrated. After release into the synaptic cleft,

extracellular GABA is removed (and the GABA signal terminated) by re-uptake into neurons and uptake into glia by plasma-membrane GABA transporters. These transport systems are both temperature and ion dependent processes. The transporters are capable of bidirectional neurotransmitter transport. They have an absolute requirement for extracellular Na^+ and an additional dependence on Cl^- ions. The ability of the reuptake system to transport GABA against a concentration gradient had been demonstrated using synaptosomes. The driving force for this reuptake process is supplied by the movement of Na^+ down its concentration gradient. GABA taken back up into the neuron is available for re-release but GABA taken up by glial cells is metabolised to succinic semialdehyde and cannot be resynthesised in this compartment due to lack of GAD. GABA is returned to the neuronal pool following transfer of glial glutamine and conversion by glutaminase to glutamate and re-entry to the GABA shunt.

In the neocortex, most GABA-containing neurons are local interneurons which vary according to morphology, intrinsic membrane properties and synaptic connectivity. GABA synapses are present in all neocortical layers and are observed most frequently on cell somata, proximal dendrites and axon initial segments but also on distal dendrites and dendritic spines.

1.2.7 GABA receptors

The actions of GABA are mediated through GABA_A , GABA_B and GABA_C receptors.

1.2.7.1 GABA_A receptors

The GABA_A receptor is a multi-subunit, heteromeric ion channel directly activated by the transmitter, GABA. There are usually five subunits, although a minority may have four subunits only. The exact subunit composition determines the physiological and pharmacological properties of the receptor (Barnard et al., 1998). Ligand binding is followed by conformational change in the channel protein that allows a net inward or outward flow of ions through the membrane-spanning pore of the channel. The directionality of flow depends on the electrochemical gradient of the particular permanent ion. Most GABA_A receptors carry primarily chloride ions and there is now evidence that these receptors undergo a switch during development with respect

to their response to GABA signalling consequent upon intracellular chloride concentrations. With maturation neuronal $[Cl^-]$ decreases and the $GABA_A$ reversal potential becomes more negative allowing the effect of GABA to become progressively more inhibitory (Ben Ari, 2002). Consistent with this finding is the observation that cation-chloride co-transporters are expressed differentially in the cortex as development continues. In the embryonic brain a $Na^+K^+Cl^-$ co-transporter (NKCC1) is dominantly expressed and acts to increase intracellular Cl^- , whilst with maturity an outwardly directed co-transporter (KCC2) plays an increased role. Consequently in immature brain tissue (and tissue demonstrating impaired neuronal development such as may be found in some types of malformations of cortical development) or within areas of epileptic tissue associated with structural reorganisation the response to GABA stimulation may not be inhibitory. This interaction between altered GABAergic signalling and the interneuron connectivity of GABA releasing neurons has been shown in hippocampal slices to support pathological synchronisation of aberrant discharges (Cohen et al., 2003).

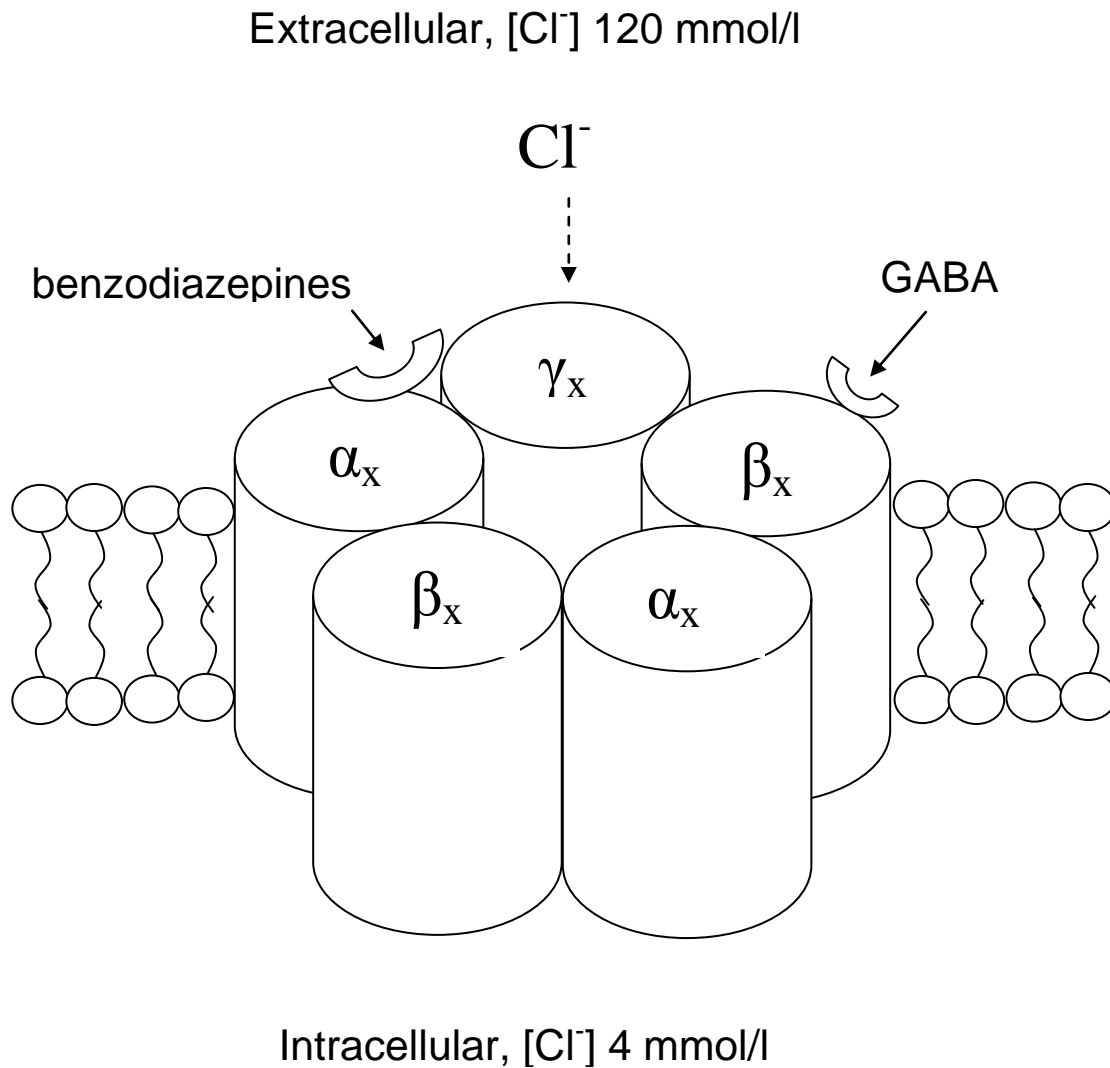


Figure 1.2.1 Sub-unit stoichiometry, arrangement, membrane position and binding sites of the GABA_A receptor

1.2.7.2 GABA_B receptors

GABA_B receptors are less numerous than GABA_A receptors but are still widely distributed in the brain. In contrast to GABA_A receptors, they are metabotropic (Sivilotti and Nistri, 1991) and are thought to have pre-synaptic locations where they impair release of both excitatory and inhibitory neurotransmitter from vesicles.

1.2.7.2 GABA_C receptors

GABA_C receptors are ionotropic and composed of ρ sub units (Cutting *et al.*, 1991). These subunits can form homo- or hetero-oligomeric channels with other ρ subunits but do not seem to combine with GABA_A receptor subunits.

1.2.8 GABA and Epilepsy

It has long been known that enhancing central nervous system GABA levels with GABA transaminase inhibitors or succinic semi-aldehyde inhibitors has an anti-convulsant effect and also that lowering these levels produces seizures. In 1995 During and Spencer performed micro-dialysis experiments which demonstrated reduced GABA/glutamate ratios in the ictal temporal lobe (During and Spencer, 1993) and Petroff and co-workers have authored a number of MRS studies over several years that report low levels of GABA in patients with epilepsy (Petroff *et al.*, 1996b; Petroff *et al.*, 1999a; Petroff *et al.*, 2000) and increasing GABA levels with improved seizure control or GABAergic antiepileptic medications such as topiramate or vigabatrin (Petroff *et al.*, 1996a; Petroff *et al.*, 1996b; Petroff *et al.*, 1999c; Petroff *et al.*, 2000).

Several antiepileptic drugs in widespread use have actions mediated by an alteration of the GABA receptor system. Post-synaptic GABA_A receptor currents are enhanced by barbiturates and benzodiazepines. Pre-synaptic GABA release is likely modified by the antiepileptic drug vigabatrin. The uptake of GABA has been shown to be modified by compounds such as tiagabine. Valproic acid has been suggested either to enhance the release of GABA or to enhance postsynaptic GABA responses whilst topiramate may increase GABA mediated Cl⁻ influx.

This complex role of GABA in guiding brain development, regulating synchronous cell discharge and blocking excitatory pathways would indicate that simple reduction in GABA concentrations is probably an inadequate explanation for many epileptic disorders. However GABA metabolism is clearly extremely important to the regulation of cell signalling and the measurement of GABA levels in several epileptic disorders is one of the main aims of this thesis.

1.3 Idiopathic Generalised Epilepsies

1.3.1 Introduction

1.3.2 Pathophysiology of generalised spike wave discharges

1.3.3 Genetics of IGE

1.3.4 Pathology of IGE

1.3.5 Imaging of IGE

1.3.6 Idiopathic Generalised Epilepsy Sub-syndrome description

1.3.6.1 Childhood Absence Epilepsy

1.3.6.2 Juvenile Absence Epilepsy

1.3.6.3 Juvenile Myoclonic Epilepsy

1.3.6.4 Idiopathic Generalised Epilepsy with Generalised Tonic Clonic Seizures only

1.3.7 Epileptic syndromes associated with photosensitivity

1.3.1 Introduction

The Commission on Classification of the International League Against Epilepsy currently describes Idiopathic Generalised Epilepsy as follows:

“Idiopathic generalised epilepsies are forms of generalised epilepsies in which all seizures are initially generalised (absences, myoclonic jerks and generalised tonic clonic seizures), with an EEG expression that is a generalised bilateral, synchronous, symmetrical discharge ... The patient usually has a normal inter-ictal state, without neurological or neuro-radiological signs. In general, inter-ictal EEGs show normal background activity and generalised discharges, such as spikes, polyspike spike-wave, and polyspike-wave > 3 Hz... No aetiology can be found other than a genetic predisposition towards these disorders.”(The International League Against Epilepsy, 1989)

The seizures of IGE are typical absences, myoclonic jerks and generalised tonic clonic seizures.

Typical absence seizures are brief (lasting for seconds) generalised epileptic seizures of abrupt onset and abrupt termination. They manifest clinically with impairment of consciousness (absence) and EEG with generalised 3-4 Hz spike and slow wave discharges. Impairment of consciousness is variable and automatisms may be seen. Typical absence seizures are easily precipitated by hyperventilation in untreated patients. Absences may remit with increasing age or be life-long.

Myoclonic jerks are shock like irregular and often arrhythmic clonic-twitching movements that may be singular or repetitive of variable amplitude and force. The myoclonic jerks of IGE mainly occur on awakening and are precipitated by sleep deprivation fatigue, excitement or distress. They may also often be precipitated by photic stimulation. The patient is fully aware of myoclonic jerks except when these occur during absence seizures.

Generalised tonic clonic seizures (GTCS) in IGE are generalised from onset. They are the same irrespective of epilepsy type. They are never preceded by the focal subjective symptoms (aura) of focal onset seizures. The occurrence of GTCS in IGE

does not have diagnostic significance but does influence the morbidity and mortality.

The 2001 ILAE Task Force on Classification recognises the following IGE sub-syndromes(Engel, Jr., 2001):

Benign Myoclonic Epilepsy in Infancy

Epilepsy with myoclonic-astatic seizures

Childhood absence epilepsy

Epilepsy with myoclonic absences

Idiopathic Generalised Epilepsies with variable phenotypes

 Juvenile absence epilepsy

 Juvenile myoclonic epilepsy

 Epilepsy with generalised tonic-clonic seizures only

Generalised epilepsy with febrile seizures plus (syndrome in development)

This classification system has been controversial. Revised systems for Childhood Absence Epilepsy (CAE)(Loiseau and Panayiotopoulos, 2005) and for Juvenile Absence Epilepsy (JAE)(Wolf, 1999) have been proposed. The argument for tighter classification is that this will improve prognostication in patients fulfilling the criteria at the expense of a higher number of unclassifiable cases. In the revised classification system the occurrence of myoclonus other than prior to or during the active stage of the absence is a contraindication to the diagnosis of CAE. All the patients included in the current work were classified according to the 1989 ILAE Classification.

1.3.2 Pathophysiology of Generalised Spike Wave Discharges (SWD)

There has been historical debate as to the origin of SWD. Following the initial analysis of EEG in patients with absence seizures by Jasper and Kershman in 1941(Jasper HH and Kershman J, 1941) and the observation of abrupt onset of EEG spike and wave discharge in both hemispheres a sub-cortical origin of the seizure activity was proposed and formalised in the centrencephalic theory by Penfield in 1952(Penfield W, 1952). In 1968 Gloor proposed the cortico-reticular hypothesis of SWD generation (namely that SWD result from an abnormal interaction of ascending inputs from midbrain and midline thalamic reticular systems and a

diffusely hyper excitable cortex)(Gloor, 1968). Buzsaki later updated the earlier centrencephalic theory of Penfield to suggest a “thalamic clock” trigger to seizure onset based on experimental observations of the development of high voltage spindle field potentials in the thalamic reticular nucleus which preceded the EEG changes of typical absence seizures(Buzsaki, 1991).

Since then a number of neurobiological studies of the neuronal activity behind the ictal EEG manifestation of absence epilepsy have been reported. Meeren and co-workers have reported a series of experiments performed on Wistar Albino Glaxo / Rijswijk (WAG/Rij) rats (reviewed (Meeren et al., 2002) finding that typical absence seizures appear to require both an intact thalamus and in particular reticular thalamic nucleus; a functionally intact cortex; and that seizures appeared to have reliable onset in the somatosensory cortex before spreading to other cortical regions and to the thalamus, so initiating a cascade within the thalamocortical network which transforms the spike into a spike wave complex – the “cortical focus theory”(Meeren et al., 2005).

Blumenfeld has recently reviewed the current evidence and considers that the spike-wave discharge should be considered a final common output resulting from intrinsic brain circuit oscillation between excitation and inhibition and triggered by a range of causes. The author asserts the requirement for an intact cortex, thalamus and thalamo-cortical interconnection for the occurrence of spontaneous discharges but finds no evidence to support a requirement in all cases for onset to arise in cortex or thalamus(Blumenfeld, 2005).

1.3.3 Genetics of IGE

The majority of individuals with IGE have a complex genetic etiology(Ottman, 2005) for which the underlying genetic alterations remain largely unknown. Heritability estimates are >80% and risk for first-degree relatives can be as high as 9%(Helbig et al., 2008). Twenty percent of children of parents with IGE manifest GSWD activity in their EEG, and multiple spike-and-wave (“polyspike”) activity occurs in 15% of family members with myoclonic seizures. Numerous genes have now been identified that are linked to various patterns of epilepsy. All the genes identified so far for monogenic epilepsy syndromes cause disorders of ion channels

giving rise to the opinion that IGE could represent a channelopathy(Kaneko et al., 2002;Hirose et al., 2005;Reid et al., 2009).

Interest has recently focussed on a microdeletion syndrome associated with generalised epilepsy, learning difficulties and schizophrenia. The microdeletion site is in the region 15q13.3 which contains several genes including the CHRNA7 gene encoding for the alpha7 sub-unit of the nicotinic acetylcholine receptor which may be a candidate gene for the epilepsy phenotype. CHRNA7 is highly expressed in the thalamus potentially indicating a role in modulating thalamocortical activity. The deletion is very uncommon in the general population but occurred fifty fold more frequently in individuals with IGE in a study by Helbig and colleagues(Helbig et al., 2009) a result which was later confirmed in an independent IGE sample(Dibbens et al., 2009). Further screening for possible microdeletion “hot-spots” by Kovel and colleagues has shown additional sites at 15q11.2 and 16p13.11(de Kovel et al., 2010).

Cloning of epilepsy genes in large families with monogenic inheritance has further identified several rare gene variants including mutations in CACNA1H(Chen et al., 2003) which impair calcium channel function. CACNA1H is associated with CAE in the Chinese Hans. Cumulative evidence from studies using both human and animal subjects suggests that thalamic T-channels are necessary for the regulation of spike-and-wave discharges(Kim et al., 2001) and disruption of this function might predispose to generalised discharges. Functional variants of the CACNA1H cause different IGE types(Heron et al., 2007)

Genetic loci for JME have been mapped at 5q12-q14(Kapoor et al., 2007), 5q34 (Cossette et al., 2002), 6p21.2-p11(Liu et al., 1995) and 15q14(Elmslie et al., 1997) and individual genes that have been identified for JME are: GABRA1 (gamma-amino butyric acid A receptor, alpha 1) at 5q34(Cossette et al., 2002), and EFHC1 (EF-hand domain containing 1) at 6p12-p11(Suzuki et al., 2004). In addition, genetic associations have been observed between JME and gene polymorphisms at BRD2 (bromodomain containing 2) at 6p21.3(Pal et al., 2003) and CX36 (connexin-36) at 15q14(Mas et al., 2004).

1.3.4 Pathology of IGE

The concept that IGE may be associated with microscopic abnormality in cortical grey matter and / or adjacent white matter continues to be debated following reports by Janz and colleagues of cortical and sub-cortical dystopic neurones (“microdysgenesis”) in a large percentage of a limited number of pathological specimens from patients with IGE (Meencke and Janz, 1984; Meencke and Janz, 1985). Lyon and Gastaut have considered that these reported findings can also occur in neurologically normal controls (Lyon G and Gastaut H, 1985) whilst a controlled and blinded histological study did not replicate earlier findings of microdysgenesis and increased frontal neuronal density (Opeskin et al., 2000).

1.3.5 Imaging in Idiopathic Generalised Epilepsy

Despite grossly normal structural MRI on visual assessment the evidence from quantitative MRI, PET, SPECT, functional MRI (fMRI) and from MRS is that IGE is associated with imaging abnormalities that often involve frontal and thalamic regions and which provides support for current thalamocortical models (Blumenfeld, 2005) of generalised spike wave discharges. (For a review of this literature see Duncan (Duncan, 2005).)

Quantitative MRI has shown increased grey matter content in studies of patients with IGE. Woermann and colleagues found abnormal cerebral grey matter in 8 out of 20 patients with juvenile myoclonic epilepsy (JME), 1 of 10 patients with childhood absence epilepsy (CAE), 4 of 10 patients with juvenile absence epilepsy (JAE), and 2 out of 5 patients with GTCS on awakening, but in none of the 30 control subjects (Woermann et al., 1998b). Voxel based morphology (VBM) methods have shown increased grey matter in the medial frontal regions in patients with JME (Woermann et al., 1999a; Woermann et al., 1999b; Kim et al., 2007) and superior mesiofrontal regions in Absence Epilepsy patients (Betting et al., 2006) and decreased thalamic grey matter bilaterally (Kim et al., 2007) in patients with JME. Thalamic atrophy was found in a group of CAE patients (Chan et al., 2006) and in a mixed population of IGE patients (Helms et al., 2006).

PET imaging of ^{11}C flumazenil binding has shown diffuse reduction of cortical binding in a mixed group with generalised epilepsy (Savic et al., 1990) and decreased binding in the thalami (Savic et al., 1994). Regional increase in thalamic blood

flow(Prevett et al., 1995a) and unchanged flumazenil binding(Prevett et al., 1995b) is described during absence seizures. Studies of opioid receptor binding using ^{11}C diprenorphine has indicated a faster elimination of ^{11}C diprenorphine from association areas of neocortex but not thalamus, basal ganglia, or cerebellum following hyperventilation-induced serial absences in IGE(Bartenstein et al., 1993).

Most recently the consistent finding of decreased cortical BOLD signal and a corresponding increased thalamic BOLD signal has been widely reported using continuous EEG-correlated fMRI during generalised SWD(Salek-Haddadi et al., 2003;Aghakhani et al., 2004;Hamandi et al., 2006;Hamandi et al., 2008) with some evidence that these changes precede the generalised SWD and may commence in the thalamus(Moeller et al., 2008). Shmuel and colleagues have inferred from fMRI experiments performed in the visual cortex that the negative BOLD reaction occurs as a consequence of reduced synaptic activity rather than spiking activity thereby indicating cortical deactivation with generalised SWD and increased activity in the thalamus (Shmuel et al., 2006).

Magnetic Resonance Spectroscopy has also shown a thalamocortical pattern of abnormality in IGE patients. Savic and colleagues reported a 10% reduction in frontal NAA in patients with JME compared to controls (Savic et al., 2000a) while Mory and colleagues have reported low NAA/Cr in the thalamus also in JME patients (Mory et al., 2003). Petroff has reported low occipital GABA in JME patients but did not measure levels in thalamus or in frontal regions(Petroff et al., 2001a).

1.3.6 Idiopathic Generalised Epilepsy Sub-syndrome description

1.3.6.1 Childhood Absence Epilepsy (CAE)

CAE has peak age of onset at 6–7 years. It is characterised by very frequent (several to many per day) absences. During adolescence GTCS may occur but otherwise there is remission or rarely persistence of absences as the only seizure type. The absences of CAE are easily precipitated by hyperventilation. During a typical absence the impairment of consciousness is severe. Automatisms occur in two thirds of the seizures but are not stereotyped. The duration of absences in CAE is short, typically 10-12 seconds. The interictal EEG is normal whilst the ictal EEG shows generalized, spike and slow wave complexes at 3 Hz.

1.3.6.2 Juvenile Absence Epilepsy

The first manifestation occurs around puberty whilst the absences usually occur sporadically in comparison to CAE. GTCS precede the absence manifestations more often than in CAE and occur more frequently. Occasionally myoclonic jerks are seen. As with CAE there is usually severe impairment of consciousness but the absences last longer than for CAE (approximately 16 seconds). The EEG features are similar to those observed in CAE. Remission with increasing age is uncommon.

1.3.6.3 Juvenile Myoclonic Epilepsy (JME)

JME (Janz Syndrome) appears around puberty and is characterized by seizures with bilateral, single or repetitive arrhythmic, irregular, myoclonic jerks. GTCS may occur but absences are infrequent and usually associated with mild reduction in level of consciousness. Seizures are most common shortly after awakening and are often precipitated by sleep deprivation. The background EEG activity is usually normal. The characteristic ictal EEG pattern is one of a bilateral symmetric polyspike-wave complex with fronto-central accentuation. The spikes have a frequency of 10–16 Hz. Up to 40% of JME patients may display photosensitivity. It is accepted that relapse occurs in up to 100% of patients if the antiepileptic drug treatment is discontinued, even after many years of complete seizure control.

1.3.6.4 Idiopathic Generalised Epilepsy with Generalised Tonic Clonic Seizures only

Epilepsy with Grand Tonic Seizures on Awakening has a wide range of onset between 17 and 31 years and is characterised by GTCS occurring exclusively or predominantly shortly after awakening, regardless of the time of day. If other seizures occur, they are mostly absence or myoclonic, as in juvenile myoclonic epilepsy. Seizures may be precipitated by sleep deprivation. Patients are often photosensitive. EEG shows generalised discharges of spike / multiple spike slow waves in approximately half of patients studied.

1.3.7 Epileptic syndromes associated with photosensitivity

Photosensitivity or photoparoxysmal response (PPR) is an abnormal, highly hereditary electroencephalographic (EEG) trait characterized by the occurrence of spikes or spike-wave discharges in response to visual stimulation (Fisher et al., 2005). Although PPR has been found rarely in subjects without epilepsy it is a more

common feature of idiopathic generalised epilepsies (IGE), in which a PPR may be observed in 40–90% of the patients (Wolf and Goosses, 1986; Appleton et al., 2000; Lu et al., 2008). Functional imaging studies performed by Moeller and colleagues has shown that intermittent photic stimulation causing photoparoxysmal response is associated with activation in the parietal cortex adjacent to the intraparietal sulcus in five subjects and in the premotor cortex in all 6 subjects occurring 3 seconds prior to the SWD and deactivation in all areas at the time of SWD. These results were considered to suggest that PPR is a cortical phenomenon with involvement of the parietal and frontal cortices (Moeller et al., 2009).

Photosensitivity is best demonstrated with EEG with appropriate intermittent photic stimulation (IPS) eliciting an abnormal PPR. PPR broadly are broadly categorised as:

- 1 A generalised spike / spike-wave response that is highly associated with clinical seizures, particularly if the response outlasts the stimulus, and may be associated with clinical events such as brief myoclonic jerks.
- 2 Spike / polyspike discharges induced in posterior regions of the EEG only. Approximately 50% of subjects with this result will have epileptic seizures.

1.4 Focal Epilepsies

1.4.1 Introduction

1.4.2 Temporal Lobe Epilepsy (TLE)

1.4.2.1 Pathology and pathophysiology in TLE

1.4.2.2 Clinical features of mesial TLE

1.4.2.3 EEG features of mesial TLE

1.4.2.4 Imaging features of mesial TLE

1.4.2.5 Clinical features of neo-cortical TLE

1.4.2.6 EEG features of neo-cortical TLE

1.4.2.7 Imaging features of neocortical TLE

1.4.3 Occipital lobe epilepsy

1.4.1 Introduction

Focal epilepsies may be symptomatic, cryptogenic or idiopathic. Ictal symptoms, particularly at outset are determined by localisation and not by aetiology. Focal epilepsies account for up to 70% of all epilepsies and half of these arise from the temporal lobes. High resolution MRI and advanced MR sequences that include MRS are often directed to the investigation of subjects with focal epilepsy, particularly if initially labelled 'MRI negative', because these investigations may yield the underlying aetiology and perhaps 'surgical cure'. Focal epilepsy with ictal onset within the frontal or parietal lobes was not specifically studied in this thesis and therefore not covered in this Introduction.

1.4.2 Temporal Lobe Epilepsy (TLE)

TLE is the most common form of focal epilepsy. Mesial temporal lobe epilepsy (mTLE) is a specific form of epilepsy which is usually associated with hippocampal sclerosis (HS) although dual pathology can often be identified in resected surgical specimen (Spencer and Huh, 2008). Patients with mTLE typically have medically refractory seizures but a good outcome following anterior temporal lobe resections, with some 53-84% of patients reporting seizure freedom for at least 1 year after anteromesial temporal lobe resection (recently reviewed by Spencer and Huh (Spencer and Huh, 2008).

1.4.2.1 Pathology and pathophysiology in TLE

HS is typically unilateral and diffuse (Quigg et al., 1997a) but more localised damage may occur (Woermann et al., 1998a). Bilateral damage is seen but is usually asymmetrical with the greater degree of atrophy on the epileptogenic side (Quigg et al., 1997b). HS is described histo-pathologically by the presence of neuronal loss and gliosis which is usually most severe in the CA (cornu ammonis) and sector CA1 (Sommer W, 1880) and to a lesser extent in CA3 and CA4. CA2 pyramidal cells are typically resistant to damage (Spielmeyer, 1925). A discrete form of HS is end folium sclerosis in which hippocampal damage is centred on the hilus and dentate gyrus. End folium sclerosis is undetectable on low field strength MRI scans. There is evidence that HS can follow prolonged febrile convulsions in infancy, early childhood or possibly status epilepticus in older individuals (Falconer et al.,

1964; Kuks et al., 1993; Nohria et al., 1994; Wieshmann et al., 1997). Progressive atrophy with continued seizures is reported in some (Van Paesschen W. et al., 1997a; Briellmann et al., 2002; Fuerst et al., 2003) but not all studies (Liu et al., 2005)

The mechanism for the development of HS is probably related to toxic release of excitatory amino acid neurotransmitters (glutamate, aspartate) and calcium-mediated neuronal death (Sloviter and Dempster, 1985) with particular damage recorded in the vulnerable CA3 pyramidal cells and dentate hilar neurons (Sloviter, 1996). CA2 might be relatively resistant due to a higher abundance of calcium binding proteins in its pyramidal cells (Sloviter et al., 1991). This process may well occur in the context of pre-existing abnormalities either acquired during prolonged febrile convulsion or as a consequence of underlying congenital malformation of neural development (Baulac et al., 1998; Fernandez et al., 1998).

Following an initial insult abnormal mossy fibre sprouting leads to the formation of aberrant excitatory pathways. Mossy fibres are the axons of the excitatory granule cells in the dentate gyrus. They terminate at the dendrites of the pyramidal neurons of the neighbouring fields CA3 and CA4. Sprouting of the mossy fibres results in additional aberrant innervation of other granule cells in the dentate gyrus and of pyramidal neurons in CA1 and CA2, resulting in abnormal feedback and feed-forward excitation (Babb et al., 1992; Mathern et al., 1995).

Other pathological processes are also important. Sloviter *et al.* have proposed the "dormant basket cell" hypothesis, stating that loss of excitatory input to GABAergic interneurons causes a net disinhibition of granule cells resulting in increased excitability of these cells (Sloviter et al., 1991).

1.4.2.2 Clinical features of mesial TLE

Although the majority of children who suffer from febrile convulsions will not develop epilepsy there is a strong association of history of febrile convulsion in patients with mTLE secondary to HS particularly if the convulsion was prolonged (Cendes, 2004; Huang and Chang, 2009; Dube et al., 2009). Seizure onset is typically in the second half of the first decade of life. There may then be a seizure-

free period of several years with antiepileptic drugs before seizures return and the epilepsy becomes refractory.

Typical seizures associated with mTLE are briefly described as follows. Patients may experience auras (simple partial seizures) in isolation or which evolve to altered awareness as complex partial seizures (CPS) or secondarily generalised seizures. Seizures are generally longer in duration than frontal lobe seizures; usually lasting more than 2 minutes, have a more gradual onset and offset, and a slower evolution.

Typical auras comprise visceral, cephalic, gustatory, dysmnestic, affective, perceptual or autonomic symptoms. Ascending epigastric sensations are particularly common. Autonomic symptoms include changes in skin colour, blood pressure, heart rate, and pupil size. There is usually no or only severely reduced speech, but occasionally repetitive vocalisation with formed words may occur if the seizure originates in the non-dominant temporal lobe. An intense sense of fear may arise without an obvious trigger. Other affective symptoms occurring in TLE include depression, anger and irritability and, more rarely, elation, erotic thoughts, serenity or exhilaration.

Motor arrest, or a 'motionless stare' is a prominent feature of the progression of the SPS to a CPS. When the aura is short, unreported or absent, this is often the first manifestation of a seizure noticed by eyewitnesses. Automatisms may then be observed. Automatisms which are defined as 'a more or less coordinated involuntary motor activity occurring during the state of clouding of consciousness either in the course of, or after, an epileptic seizure, usually followed by amnesia of the event' are usually oro-alimentary or gestural. The former include lip-smacking, chewing and swallowing and the latter include fumbling, fidgeting, repetitive motor actions, undressing, walking, and sexually-directed actions. They can sometimes be prolonged or semi-purposeful, e.g. rearranging items on a desk. Limb automatisms are usually ipsilateral to the focus, with contralateral dystonic posturing. Vocalisation of identifiable words suggests a non-dominant seizure focus. Secondary generalisation is much less common than in extra-temporal lobe epilepsy.

1.4.2.3 EEG features of mesial TLE

The EEG in mTLE typically shows anterior or mid-temporal spikes. These are best shown on superficial sphenoidal or zygomatic electrodes. Intermittent or persistent slow activity may be present over the temporal lobes. The EEG abnormalities can be unilateral or bilateral, but are usually more marked ipsilateral to the focus.

1.4.2.4 MRI features of mesial TLE

MRI will frequently reveal the cause of the mTLE. HS is the most commonly identified pathology. It is demonstrated by a reduced hippocampal volume (on T₁ weighted images) and an increased signal on T₂-weighted MRI scans (Jackson et al., 1990; Van Paesschen W. et al., 1997b; Jackson and Connelly, 1999). The hippocampus is a curved structure with its concave surface facing the brainstem and with its longitudinal axis at approximately 35° to the traditionally used axial imaging plane for MRI, the orbito-meatal line. Imaging sensitivity for abnormality is improved by acquiring the coronal images perpendicular to the long axis of the hippocampus. In equivocal cases sensitivity can be further increased if hippocampal volume and T₂ relaxation times are quantified using established protocols (Free et al., 1995; Duncan et al., 1996).

1.4.2.5 Clinical features of neo-cortical TLE

In neocortical TLE, there is usually a detectable structural pathology, for example glioma, angioma, hamartoma, dysembryoplastic neuroepithelial tumour (DNET), malformations of cortical development or post-traumatic change. In contrast to mTLE, there is no association with a history of febrile convulsions. Clinically, consciousness may be preserved for longer than in a typical mesial temporal lobe seizure. Simple auditory phenomena such as humming, buzzing or hissing may be reported in seizures arising in the superior temporal gyrus whilst seizures arising from the Sylvian region can start with olfactory hallucinations which are usually unpleasant in quality. More complex hallucinatory or illusionary states occur with phenomenology related to their origin with association areas and may include distortion of size or shape, complex visual or auditory disturbance. Affective, visceral or psychic auras may occur but are less common than in mTLE. The automatisms can be unilateral and have more prominent motor manifestations than in mTLE.

1.4.2.6 EEG features of neo-cortical TLE

The interictal EEG in neocortical TLE often shows spikes over the temporal region, maximal over the lateral convexity rather than infero-mesial electrodes.

1.4.2.7 Imaging features of neocortical TLE

Standard MRI sequences may demonstrate extra-hippocampal structural lesions responsible for the epilepsy if they are present. Hippocampal volumes and T2 measurements on MRI may be normal but can show subtle abnormality with advanced imaging modalities.

1.4.3 Occipital lobe epilepsy (OLE)

Occipital onset seizures account for approximately 10% of epilepsies but are less prevalent in neurosurgical series. Seizures may arise spontaneously from an epileptic focus or be triggered by external visual stimuli. Occipital epilepsies may be idiopathic or symptomatic. Idiopathic occipital seizures usually start in late childhood whilst symptomatic seizures may start at any age. Typical clinical manifestations are mainly visual or oculomotor.

Idiopathic photosensitive occipital epilepsy (IPOE) is an uncommon focal epilepsy beginning in late childhood or adolescence and marked by seizures that are triggered by environmental photic stimulation such as the television (Guerrini et al., 1995; Yalcin et al., 2000). These seizures are usually diurnal, last minutes to hours and rarely secondarily generalize (Yalcin et al., 2000). Electro-clinical overlap between IPOE and JME is described in four families by Taylor and colleagues (Taylor et al., 2004).

Malformations of cortical development are relatively common causes of symptomatic occipital lobe epilepsy whilst a number of processes including eclampsia, malignant hypertension, mitochondrial cytopathies and progressive myoclonic epilepsies such as Lafora disease are all preferentially associated with occipital onset seizures.

Visual symptoms include elementary and occasionally complex visual hallucinations, blindness, visual illusions and palinopsia. Elementary visual hallucinations are the most common manifestation of occipital lobe seizures. They usually take the form of small multi-coloured patterns that appear in the periphery of

the temporal visual field, become larger as the seizure progresses, and may move across the visual field. They are brief, lasting typically less than 3 minutes. They do not have the linear, zigzag, achromatic or black and white characteristics of visual aura associated with migraine. More complex visual hallucinations may occur from the outset of the seizure but more typically follow from elementary symptoms. “Blurring” of vision may be a common initial seizure manifestation. Ocular symptoms include tonic deviation of the eyes, oculoclonic or nystagmoid movements and repetitive eyelid closure or eyelid fluttering are all reported. Secondary generalisation may occur.

1.4.3.1 EEG in Occipital lobe epilepsy

In symptomatic cases the EEG is often abnormal with posterior lateralised slow waves. Unilateral occipital spikes and occasional occipital paroxysmal bursts may occur and there may be a positive photoparoxysmal response. Ictal EEG usually manifests with paroxysmal fast activity that is localised to the occipital regions with occasional anterior spreading and generalisation.

1.4.3.2 Imaging features in occipital lobe epilepsy

High resolution MRI is mandatory as this may detect a structural lesion that itself requires treatment. Additionally, research MRI sequences that may be more sensitive for pathology than conventional MRI are often also performed for subjects with “MRI Negative” focal epilepsy.

1.5 Malformations of cortical development (MCD)

1.5.1 Introduction

1.5.2 Normal brain development

1.5.2.1 Normal microscopic development of the neocortex

1.5.2.2 Normal microscopic development of the archicortex

1.5.3 Abnormal cortical development resulting in MCD.

1.5.3.1 Proliferation and differentiation

1.5.3.1.1 Focal Cortical Dysplasia (FCD)

1.5.3.2 Neuronal migration

1.5.3.2.1 Lissencephaly

1.5.3.2.2 Subependymal nodular heterotopia (SEH)

1.5.3.2.3 Subcortical heterotopia (SCH)

1.5.3.2.3 Band Heterotopia (BH)

1.5.3.3 Post-migrational cortical organisation

1.5.3.3.1 Polymicrogyria (PMG)

1.5.3.3.2 Schizencephaly (SHZ)

1.5.3.4 Other relevant MCD sub-types

1.5.3.4.1 Microdysgenesis

1.5.1 Introduction

The favoured term of “malformation of cortical development” (MCD) encompasses many disorders that differ in their clinical presentation, associated pathology and genetic basis. MCD may be the consequence of a variety of inherited or acquired insults. Several sub-types of MCD are well described and MCD in general are associated closely with refractory epilepsy and learning disability. MCD are otherwise rare in the general population. Focal cortical dysplasia (FCD) is probably the most common of the recognised MCD although in all sub-groups the true prevalence is not known.

In contrast to surgical treatment of refractory focal epilepsy associated with hippocampal sclerosis where excellent seizure outcome might occur in a high proportion of cases, surgical treatment of MCD is often unsuccessful. Sisodiya has reviewed the available literature and has found that seizure freedom (Engel class I) at 2 years occurred in approximately 40% of surgically treated MCD patients. This compares to figure of between 70-80% for mesial temporal lobe epilepsy associated with hippocampal sclerosis(Sisodiya, 2000).

An explanation for the poor surgical outcome in these patients is likely to be a consequence of functional cortical abnormality in subjects with MCD that extends outside the area of visible structural abnormality. Indeed EEG is often non-localising in patients with MCD(Palmini et al., 1991a;Palmini et al., 1991b;Raymond et al., 1995;Dubeau et al., 1998;Sisodiya, 2000) whilst PET studies(Hammers et al., 2001), MRS studies(Woermann et al., 2001b) and volumetric MRI or DWI(Eriksson et al., 2001) have all identified abnormal signal outside the area of MR visible abnormality.

A further limitation when contemplating surgical treatment of MCD is that the region of the visible MCD may still have some residual level of “normal” biological function. For example Leblanc showed that electro-stimulation of a posterior temporal lobe dysgenetic region caused interference with speech(Leblanc et al., 1995).

The classification of MCD is based upon the concept that cerebral cortical development consists of three major processes: cell proliferation and apoptosis; neuronal migration; and cortical organisation.

1.5.2 Normal brain development

The nervous system develops from a thickening of the ectoderm, the neural plate, which appears at day 13 post conception and gradually expands towards the primitive streak. By the end of the 3rd week post conception the lateral edges of the neural plate become elevated and approach each other in the midline to form the neural tube the rostral end of which will ultimately develop into the brain.

Around day 28, three primary brain vesicles appear: prosencephalon, mesencephalon and rhombencephalon. By about day 35, the first and third of these vesicles have both grown into two vesicles. The resulting five secondary brain vesicles are:

1. Telencephalon (ultimately forming the cortex, striatum and olfactory system)
2. Diencephalon (ultimately forming thalamus, hypothalamus and sub thalamus)
3. Mesencephalon (ultimately forming the midbrain)
4. Metencephalon (ultimately forming the pons and cerebellum)
5. Myelencephalon (ultimately forming the medulla oblongata).

1.5.2.1 Normal microscopic development of the neocortex

Most of the cells destined to eventually become cortical neurones or glial cells are derived by proliferation of neuroepithelial cells in the cortical ventricular or sub-ventricular zone (germinal matrix). The highest rate of cell division occurs in the second trimester of gestation. The number of cells created is far larger than the final number of neurons in the adult brain. Many cells undergo programmed (apoptotic) cell death, particularly if appropriate synaptic contacts have not been formed.

Four anatomical migratory pathways have classically been described: via the corpus pontobulbare to the pontine and medullary nuclei; via the corpus gangliothalamicum to the basal ganglia and thalamus; to the cerebellum; and centrifugal migration from the cortical ventricular zone to the cerebral cortex. Errors in the development of cells involved in this latter pathway result in the most commonly observed MCD.

Neurons that are generated in the ventricular zone migrate along radial glial fibres towards the pial surface. The earliest neurons form the pre-plate at embryonic weeks 8 to 9. Through weeks 10-18 accumulation of newly migrated cells forms the cortical plate within the pre-plate and dividing it into the outer marginal zone and the inner sub-plate. Neurons arriving subsequently in the cortical plate penetrate both the sub-plate and the previously deposited cortical plate neurons in an “inside-out” formation. Pyramidal cells and neuroglial cells form via this process. Cells that will eventually become non-pyramidal GABAergic cortical inhibitory inter-neurons are generated from a distinct proliferative zone in the ganglionic eminence of the ventral telencephalon. In contrast to the radial migration of pyramidal cells these non-pyramidal cells use tangential migratory pathways. They first appear in the marginal zone in the form of Cajal-Retzius cells. These cells release signalling compounds such as Reelin that are important in facilitating the migration of neurons to the cortical plate.

1.5.2.2 Normal microscopic development of the archicortex

Neuroblasts that will form the hippocampus are also generated in the ventricular zone. They migrate to the cortical plate which in this area is designated the "ammonic plate" [(Stanfield and Cowan, 1988), reviewed by (Raymond et al., 1995)]. In contrast to the development of the neocortex, the migrating neurons dissociate themselves earlier from the radial glial fibres and accumulate in the deeper aspects of the ammonic plate. During a subsequent phase, these neurons are reorganised to more superficial positions so that the formation of Ammon's Horn follows an inside-out gradient similar to that of the neocortex, to form the archicortex. The development of the dentate gyrus is different in many ways. Neurogenesis occurs initially in the ventricular zone, but a second, sub-pial germinal centre develops at a later stage and appears to become the dominant germinal centre (Schlessinger et al., 1975). Another difference is the assembly of the laminar architecture which follows an outside-in pattern, with neurons arriving later being added to the deeper layers. Tangential migration may be more important than radial migration. During maturation of the archicortex, the dentate granule cell layers and the hippocampal pyramidal cell layers which are originally in continuity become separated, probably in the course of the complex folding of the hippocampus (Duvernoy, 1998; Klingler, 1948; Stanfield and Cowan, 1988). Unlike neocortical

development, granule cell generation continues well into postnatal life, with the peak of neurogenesis in the early postnatal period (Schlessinger et al., 1975).

1.5.3 Abnormal cortical development resulting in MCD.

MCD are classified according to the scheme proposed by Barkovich and colleagues. This classification broadly categorises MCD according to failure at different stages of cortical development - neuronal proliferation and eventual apoptosis of selected cells; neuronal migration; and cortical organisation (Barkovich et al., 2001).

1.5.3.1 Proliferation and differentiation

1.5.3.1.1 Focal Cortical Dysplasia (FCD)

FCD describes a localised MCD with characteristic histological appearance (Taylor et al., 1971). FCD are likely to represent the most common form of focal developmental disorder associated with intractable epilepsy (Kuzniecky and Barkovich, 2001) but the true prevalence is not known. Sisodiya found FCD to be the most common form of MCD in surgical series (Sisodiya, 2000) although this will have been influenced by selection bias. FCD seems to be rare in persons without epilepsy and absent in 500 controls in one series (Wolf et al., 1995) and not seen in 170 controls in the National Society for Epilepsy MRI study (Everitt et al., 1998).

Macroscopically FCD have smooth cortex with lack of sulci, coarse gyri and blurring of the grey-white matter junction (Thom, 2001). Histology (Norman et al., 1995d; Prayson and Estes, 1995; Taylor et al., 1971) shows, beneath a molecular layer that is usually normal, cortical laminar architectural disorganisation with hypercellular cortex, possibly with persistent columnar alignment. Clusters of atypical neurons and glia can occur within the cortex, and heterotopic nerve cells may also be present in increased numbers in the underlying juxtacortical white matter.

Cytology (Norman et al., 1995d; Thom, 2001) shows aberrant differentiation of nerve cells which are described as bizarre and cytomegalic and scattered in all cortical layers. They maintain an overall pyramidal shape and are usually greater than 20 microns. These nerve cells often appear randomly orientated, with loss of the normal vertical polarity of the apical dendrites. In a large proportion of cases, abnormal and enlarged astrocytic cells of up to 50µm in diameter are present. These

are mostly called "balloon cells", but other terms include "balloon cell glia", "grotesque cells", "dysplastic glial cells" or "uncommitted cells". Their appearance is intermediate between nerve cell and astrocyte. Glassy cytoplasm is abundant, nuclei are large and sometimes multiple. They are preferentially located in the deeper regions of the cortex or in the juxtacortical white matter. They resemble similar cells seen in cortical tubers in tuberous sclerosis and subependymal giant cell astrocytoma. A frequently used classification system is based on the absence (FCD type I) or presence (FCD type II) of these balloon cells (Kuzniecky and Barkovich, 2001).

Other lesions may coexist with FCD. Tumours have been reported [e.g. (Daumas-Duport et al., 1988; Prayson and Estes, 1995; Prayson et al., 1993)]. Hippocampal sclerosis is relatively frequently found, in 9% (Prayson and Estes, 1995) and 12% (Wolf et al., 1995) respectively in two series.

FCD may have a genetic inheritance, particularly when diffuse lesions are seen, as suggested by a case report of two brothers (Kuzniecky, 1994). Histological similarities with the cortical tubers of tuberous sclerosis and FCD have been noted, and FCD has been suggested to be a "forme fruste" of tuberous sclerosis (Palmini et al., 1991b). However the common presentation of FCD without evident family history suggests that environmental factors are usually a factor.

The onset of epilepsy in patients with FCD is usually in the first decade. Seizures are often refractory despite treatment with antiepileptic drugs (Kuzniecky and Barkovich, 2001). MRI features are blurring of the grey-white matter interface, focal thickening of the cortex, gyral thickening and abnormal T₂ signal, particularly in the underlying white matter (Kuzniecky and Barkovich, 2001).

1.5.3.2 Neuronal migration

Disorders of neuronal migration can occur and can be genetically determined. Filamin 1 is a large actin-binding / cross linking protein whose gene is located on chromosome Xq28. It plays an important role in migration. Defects may be inherited or due to sporadic mutations, and lead to migrational defects in females, while affected males foetuses generally do not survive to term. Other factors such as integrins, Ra1A and presenilin 1 may be involved in the initiation of migration

(reviewed by (Gleeson and Walsh, 2000)). Insight into the mechanisms of migration between the ventricular zone and the cortical plate comes from two disorders where migration is arrested part way between source and target, Lissencephaly type I and band heterotopia (BH).

1.5.3.2.1 Lissencephaly

Lissencephaly can be caused by mutations in at least two genes. The LIS1 gene is located on chromosome 17p13.3 (Cardoso et al., 2002; Dobyns et al., 1991). Its autosomal mode of inheritance causes haplo-insufficiency in affected individuals and the Lissencephaly phenotype (severe mental retardation and intractable epilepsy), suggesting that two wild type copies of the gene are necessary for normal cortical development. LIS1 probably exercises its role in migration through interaction with the microtubule cytoskeleton (Morris et al., 1998).

In males, a second Lissencephaly locus on the X chromosome, termed DCX gene, leads to a phenotype that is similar to the one caused by the LIS1 mutation. Affected females, however, retain a working copy of the gene and have a band heterotopia together with a milder phenotype.

Lissencephaly type II (cobblestone Lissencephaly) in humans, the related Fukuyama disease (Kobayashi et al., 1998) and Walker-Warburg syndrome (Kanoff et al., 1998) all produce disruptions of the architecture of the developing cerebral wall and severe disorders of neuronal migration. The pial limiting membrane is defective, and neurons migrate out of the CNS and into the meninges [reviews by (Gleeson and Walsh, 2000; Golden, 2001)].

1.5.3.2.2 Subependymal nodular heterotopia (SEH)

Grey matter accumulation between the ependyma lining the lateral ventricles and the cortex is described as heterotopic, as compared to the normotopic overlying cortical grey matter. SEH are characterised by periventricular (subependymal) collections of neurons which form nodules.

The nodules measure typically 2-10mm in diameter (Eksioglu et al., 1996), but may merge to form an irregular band of overlapping nodules (Raymond et al., 1994b). They may be unilateral or bilateral, and in published series comprising 7

(Huttenlocher et al., 1994), 8 (Barkovich and Kjos, 1992a), 13 (Raymond et al., 1994b), 20 (Raymond et al., 1995) and 33 patients (Dubeau et al., 1995), respectively, they were seen bilaterally in 40-100%. While the whole length of the ventricles may be involved, the trigones and occipital horns are more commonly involved (Raymond et al., 1995). Frontal and temporal horns are less frequently involved, and the third and fourth ventricles are spared.

SEH are among the more common forms of MCD encountered in adult epilepsy patients, accounting for 20/100 patients with MCD in the National Hospital series (Raymond et al., 1995), but again the true prevalence is not known. SEH has occasionally been seen in people undergoing MRI as “healthy controls” (Raymond et al., 1995) (Dubeau et al., 1995). There is a female preponderance. The gene, FLN1 (named after its gene product, filamin), has been linked to Xq28, and affected hemizygous males in typical pedigrees do not appear to survive gestation.

SEH can be associated with other CNS malformations, for example Chiari Type II malformations or agenesis of the corpus callosum, and metabolic disorders such as Zellweger’s syndrome or neonatal adrenoleukodystrophy [reviewed by (Kuzniecky and Barkovich, 2001)]. In Dubeau's series of 33 patients with SEH, 13 also had sub-cortical nodular heterotopia (Dubeau et al., 1995), and this combination was present in 2 of 20 patients in Raymond's series as well (Raymond et al., 1995). These cases were mostly unilateral, and abnormalities of the overlying cortex were frequently seen. Hippocampal sclerosis is described in association with SEH (Dubeau et al., 1995; Raymond et al., 1994b).

The heterotopia are composed of islands of relatively mature cells which resemble cortical neurons rather than the neurons of deep grey nuclei, in keeping with their likely provenance. They contain multiple neuronal types but no dysplastic nerve cells, and calcifications are not seen. Synaptophysin immunohistochemistry has shown dense pre-synaptic terminals around the heterotopic cells (Eksioglu et al., 1996) but the origin of these afferents is not established. A study of nodular heterotopia in four children using dye tracing methods has shown limited connectivity of neurons between nodules (Hannan et al., 1999), for which there is indirect evidence through functional imaging studies that show task-induced activation in heterotopic gray matter (Pinard et al., 2000; Richardson et al., 1998a;

Spreer et al., 2001). The detailed autopsy study in children (Hannan et al., 1999) showed abnormal calretinin-positive neurons in the nodules and far less arborisation of dendritic trees. The interneurons in the nodules appeared generally immature.

Epilepsy is common (Raymond et al., 1995). As the onset of seizures is typically in the second decade of life, relatively later than in other forms of MCD, the prevalence of epilepsy may be underestimated in series including young patients. Learning difficulties may not be present in milder cases (Raymond et al., 1995) but become more likely with bilateral and more extensive SEH (Kuzniecky and Barkovich, 2001).

Focal, multifocal and generalized seizures can occur and at the severe end of the spectrum, infantile spasms and Lennox-Gastaut syndrome are seen (Golden, 2001). Epileptic phenomena are frequently discordant or contralateral to the side or location of the lesion (Raymond et al., 1995). There is direct evidence for epileptogenicity of heterotopic neuronal clusters (Francione et al., 1994; Kothare et al., 1998; Mattia et al., 1995; Palmieri et al., 1995; Sisodiya et al., 1999a).

On MRI, the isolated or confluent nodules are seen as isointense to normotopic grey matter on all standard MR sequences but are most readily seen on T1 weighted images (Raymond et al., 1995). Coexisting hippocampal sclerosis (dual pathology) is relatively frequent (Cendes et al., 1995; Raymond et al., 1995).

1.5.3.2.3 Subcortical heterotopia (SCH)

SCH are characterised by collections of neurons in the hemispheric white matter. These are separated from both the ventricles and the cortex through white matter. SCH are rare, accounting for only 3/100 malformations in the National Hospital series (Raymond et al., 1995).

The nodules are of widely varying size, from less than 5mm to 20 or more mm in diameter. Abnormalities of the overlying cortex may be present [e.g. (Battaglia et al., 1996; Guerrini et al., 1996)]. Histology shows unlayered neurons which may look normal on inspection (Battaglia et al., 1996), but closer study suggests an imbalance between excitation and inhibition within the heterotopia (Hannan et al.,

1999). SCH are often sporadic, indicating that somatic rather than germ line mutations may be involved (Kuzniecky and Barkovich, 2001).

Epilepsy is common and usually develops early in life (Kuzniecky and Barkovich, 2001). Patients with small unilateral subcortical heterotopia may be neurologically normal (Barkovich and Kjos, 1992a), whereas patients with extensive unilateral heterotopia are likely to present with hemi-plegia. At the severe end of the spectrum, patients with bilateral, large or spatially extended lesions may present with moderate to severe developmental delay and neurological deficits (Kuzniecky and Barkovich, 2001). Heterotopic grey matter (Francione et al., 1994; Kothare et al., 1998; Sisodiya et al., 1999a) may be intrinsically epileptogenic.

On MRI, the subcortical nodules are seen as isointense to normotopic grey matter (Raymond et al., 1995). The overlying cortex may look normal but may also be thin with small gyri and shallow sulci. Coexisting abnormalities are frequent, Kuzniecky and Barkovich claim that an agenetic or hypogenetic corpus callosum is present in approximately 70% of affected brains (Kuzniecky and Barkovich, 2001), and other malformations, particularly SEH, are frequently seen (Cendes et al., 1995; Raymond et al., 1995).

1.5.3.2.3 Band Heterotopia (BH)

BH usually affects the fronto-central and/or parieto-occipital areas with sparing of the temporal, inferior frontal and cingulate/medial frontal cortices. They are rare in adult epilepsy patients, accounting for 8/100 patients with MCD in the National Hospital series (Raymond et al., 1995).

The bands are composed of differentiated, randomly orientated neurons of all types, accompanied by glial cells. In most cases, the overlying cortex shows the normal six-layered architecture, but layers V and VI may be poorly delineated and merge with the subcortical white matter and the lateral parts of the bands.

A developmental link between Lissencephaly and BH was reported in a study of two families. Females had BH and hemizygous male offspring had Lissencephaly (Pinard et al., 1994). Subsequently, mutations of the gene, named DCX after its gene product, doublecortin, or XLIS after the mode of transmission, have been identified

on the X chromosome (Des Portes et al., 1998). Mutations have also been seen in some sporadic cases where DCX mutations account for some 85% of cases, whereas mutations have been found in 11 of 11 pedigrees with X-linked transmission of laminar heterotopia [reviewed by (Ross and Walsh, 2001)]. Doublecortin is a microtubule-associated protein expressed by migrating neurons (Gleeson et al., 1999). While its precise function is unknown, it is thought to play a role in regulation of the microtubule cytoskeleton (Gleeson and Walsh, 2000).

Most if not all subjects with BH develop epilepsy within the first two decades. A variety of seizure types is seen, including infantile spasms, Lennox-Gastaut syndrome, or other forms of secondary generalized, focal or multifocal epilepsy. On MRI, the BH are usually bilateral and approximately symmetrical. As with the other heterotopia, they are isointense to normotopic grey matter on all sequences. Typically, the medial border of the lamina is smooth, whereas the lateral border follows the white matter into the crowns of the gyri. The cortex overlying the laminae may appear macrogyric. Patients with the DCX/XLIS mutation show an anterior>posterior gradient of severity which is in contrast to that seen in LIS1 patients.

1.5.3.3 Abnormal post-migrational cortical organisation

1.5.3.3.1 Polymicrogyria (PMG)

PMG arises when neurons move out to the cortical surface but organise abnormally to produce multiple small gyri. It may be focal but is often bilateral, occurring predominantly in perisylvian, frontal, parieto-occipital or mesial occipital areas (Kuzniecky and Barkovich, 2001).

PMG is characterised by many small microgyri separated by shallow sulci, abnormally thin cortex which appears thickened through the juxtaposition of the tightly packed microgyri, neuronal heterotopia and often enlarged ventricles (Kuzniecky and Barkovich, 2001). Two patterns are recognised, four-layered polymicrogyria, in which there is a molecular layer, an organised outer layer, a cell sparse layer and a disorganised inner layer, and an unlayered (disorganised) form. These two forms likely reflect the timing of the causative insult during corticogenesis (Norman et al., 1995c). Associated MCD may be present, including neural and glial leptomeningeal ectopia, areas resembling FCD, clefts, and

calcification. There is an excess of reelin immunopositive Cajal-Retzius cells in the region of the malformation which may be part of the malformation or may represent a reaction to an area of cortical injury (Eriksson et al., 2001b). Bilateral perisylvian polymicrogyria is relatively frequent and considered a discrete congenital syndrome by some (Kuzniecky et al., 1993a) but not others (Raymond et al., 1995).

PMG is generally considered to be due to environmental insults rather than genetic causes, and diffuse PMG has been associated with intrauterine cytomegalovirus (CMV) infection (Barkovich, 1995), toxoplasmosis, syphilis, or maternal hypoxia. The environmental hypothesis is further strengthened by the rat freeze model where a focal freezing injury leads to the formation of microgyri (Dvorák and Feit, 1977; Jacobs et al., 1999a) and epilepsy through hyperexcitability caused by reorganisation of neural networks in perilesional areas (Jacobs et al., 1999b; Jacobs et al., 1999c). Lesion experiments suggest mechanisms that interfere with radial glial function, but this need not be the mechanism in all cases (Ross and Walsh, 2001).

However familial cases do occur and several genes have been implicated (Ferrie et al., 1995)(Barkovich et al., 1999). An autosomal recessive inheritance is possible in purely frontal polymicrogyria. Genetic heterogeneity has also been indicated in kindreds with perisylvian polymicrogyria, with both X-linked (Cardoso et al., 2000; Guerreiro et al., 2000; Leventer et al., 2000; Yoshimura et al., 1998) and autosomal (dominant with incomplete penetrance, or recessive) patterns (Borgatti et al., 1999; Leventer et al., 2000). The genetic locus for bilateral perisylvian polymicrogyria has recently been mapped to Xq28 by linkage analysis in five families (Villard et al., 2002). No inheritance pattern was discernible in nine individuals with parieto-occipital polymicrogyria (Guerrini et al., 1997).

Epilepsy associated with learning difficulties is common. Neurological signs are more likely to occur when the abnormality is located in or near eloquent cortex (Raymond et al., 1995). The polymicrogyria may be visible on high resolution MRI or be indistinguishable from macrogyria / pachygyria (Raymond et al., 1995).

1.5.3.3.2 Schizencephaly (SHZ)

SHZ describes full-thickness clefts of the cerebral hemisphere lined by grey matter which may appear normal or be polymicrogyric. SHZ may be "closed-lipped" (type I) when the edges of the cleft are in apposition to each other or "open-lipped" (type II) when the appearance is that of a wide cleft. It may be unilateral or bilateral.

SHZ is thought to be among the rarer forms of MCD (Sisodiya, 2000). Only two patients out of 100 with MCD in the National Hospital series fulfilled the criteria for true SHZ (Raymond et al., 1995).

Apart from the cleft, the neuropathological appearance corresponds to polymicrogyria and indeed SHZ has been suggested to be an extreme form of polymicrogyria (Barkovich and Kjos, 1992c) and similar aetiological factors seem likely. Other areas of the brain, outside the SHZ, may be histologically abnormal (Packard et al., 1997).

While most cases are sporadic, a minority of cases of open-lipped (type II) severe SHZ are due to germ line mutations in *EMX2* (Brunelli et al., 1996), a homeobox gene involved in cell fate determination [reviewed by (Ross and Walsh, 2001)].

Neurological signs are common, and may be accompanied by learning difficulties, the severity of which is usually related to the type of defect, with open-lipped (type II) defects and bilateral clefts leading to more severe clinical pictures (Barkovich and Kjos, 1992c; Kuzniecky and Barkovich, 2001). Epilepsy seems to be the rule and is often intractable. MRI may be able to clearly show the polymicrogyric nature of the thickened grey matter lining the clefts (Raymond et al., 1995).

1.5.3.4 Other relevant MCD sub-types

1.5.3.4.1 Microdysgenesis

Sometimes histological examination identifies abnormal cortical formation despite normal prior neuro-imaging studies and normal macroscopic pathological examination. Whether these microscopic abnormalities represent a distinct pathological process or part of the normal continuum is often debated, but a combination of abnormal histological features has been described in pathological tissue from subjects with epilepsy and labelled as microdysgenesis.

The original description was based upon the study of eight autopsy specimens from patients with IGE (Meencke and Janz, 1984). Seven of the eight showed similar qualitative histopathological abnormalities that included an excess of nerve cells in the subpial region and the molecular layer of the cortex, increased numbers of heterotopic nerve cells in the adjacent white matter and blurring of the cortical laminae 1 and 2 (Meencke and Janz, 1984). Meencke later used a morphometric method to study neuronal densities in the molecular layer of frontal cortical specimens from epilepsy patients and found increased neuronal densities compared to age-matched controls. Further studies have also reported increased white matter neuronal densities in subjects with epilepsy (Emery et al., 1997) or abnormal clustering of cortical neurones in layers II-IV in specimens from temporal lobe epilepsy patients with poor post-operative outcome following temporal lobe surgery. In contrast, some authors have argued against the presence of microdysgenesis in patients with epilepsy (Palmini et al., 1995; Opeskin et al., 2000).

Increased numbers of heterotopic nerve cells described in microdysgenesis might represent arrested migration of nerve cells destined for the cortex or neurones that failed to undergo programmed cell death. By definition, microdysgenesis is not observable using conventional MRI sequences. Research morphometric imaging methods have shown increased grey matter volumes in subjects with IGE compared to controls (Woermann et al., 1999b) which would be consistent with the initial observations of microdysgenesis in this population by Meencke and Janz. Features commonly accepted to represent subtle MCD include neuronal clustering, mislamination, abnormal cortical myelinated fibres, and an excess of neurons in cortical layer I and the subcortical white matter (Sisodiya, 2004).

1.6 Magnetic Resonance Imaging

1.6.1 Introduction

1.6.2 Basic NMR physics

1.6.2.1 T_1 Relaxation

1.6.2.2 T_2 relaxation / decay

1.6.2.3 Repetition Time (TR)

1.6.2.4 The Spin-Echo Sequence

1.6.2.5 The Gradient Echo Sequence

1.6.2.6 The Inversion Recovery Sequence

1.6.3 Advanced Magnetic Resonance Imaging (MRI) applications

1.6.1 Introduction

Magnetic resonance imaging (MRI) involves the application of alternating magnetic fields and radiofrequency (RF) electromagnetic waves. It was first developed in 1946 independently by Bloch and co-workers at Stanford and by Purcell at Harvard. In 1967 Jackson produced the first signals from a live animal.

This Section and the following Section describing the underlying concepts of MRS (1.7) are intended to contain sufficient physics to allow an appreciation of the methodologies used in this thesis. A more complete description of the physics of MR imaging techniques may be found by reference to dedicated texts (for example see(Tofts, 2003))

1.6.2 Physics of nuclear magnetic resonance imaging (MRI)

A fundamental property of protons and neutrons is that they possess an angular momentum, which is often referred to as spin. Not all nuclei have a net spin. Specifically any nucleus with an even atomic number and an even charge number has no spin. If a nucleus does have net spin, the fact that it carries a positive charge results in a non-zero nuclear magnetic moment and an associated resonant frequency dependent on the strength of the external magnetic field. Table 1.6.1 shows the natural abundance, nuclear spin and resonant frequency at 1 Tesla for several such nuclei.

Table 1.6.1 Natural abundance, nuclear spin and resonant frequency at 1 Tesla for several nuclei commonly studied in vivo.

Nucleus	Natural Abundance (%)	Spin (I)	Resonant Frequency
¹ H (hydrogen)	99.9	½	42.6 MHz
¹³ C (carbon)	1.1	½	10.7 MHz
³¹ P (phosphorus)	100	½	17.25 MHz

Hydrogen has the highest resonant frequency because it has the strongest magnetic moment. It is also naturally abundant and these properties make it the ideal nucleus for MRI techniques.

Magnetic field theory dictates that a nucleus with a magnetic moment can occupy $(2I + 1)$ energy levels, where I is the spin number of the nucleus. For the nuclei in the table above $I = \frac{1}{2}$ and the energy level diagram will therefore consist of two levels. In the lower energy state the nuclear moment lies parallel to the external field while the higher energy state has a moment that lies anti-parallel to the external field. Within a sample subjected to an external field at physiological temperatures there is only a small imbalance between the population of nuclei that occupies the lower energy state and the population that occupies the higher state. If the sample is then excited by an additional radiofrequency (RF) magnetic field providing *precisely the difference* in energy between the two levels, energy transitions between the two levels can be induced that perturb the net magnetisation so that a signal can be produced. The relationship between the frequency of the resulting signal and the static external field is given by the Larmor equation as follows:

$$\nu = (\gamma/2\pi)B_0 \quad \text{[Eqn 1.6.1]}$$

where B_0 is external magnetic field strength in Tesla, and $\gamma/2\pi$ is the gyro-magnetic ratio in MHz /Tesla for the spin under consideration. ν is the resonant frequency of the material studied and is shown by this relationship to be dependent on the applied external field.

The application of an RF pulse that causes resonance to occur is termed excitation. This absorption of energy causes an increase in the “spin-down” hydrogen nuclei population (that is the population of nuclei that occupy the higher energy spin state with net moment anti-parallel to the applied field), as a proportion of the “spin-up” (the population in the lower energy state with moment parallel to the applied field) nuclei transition to the higher energy state.

The RF pulse generally used for MR imaging is in the form of a rotating magnetic field, denoted by \mathbf{B}_1 , which is applied for a short time in the plane perpendicular to the main field (\mathbf{B}_0). To tip the net nuclear magnetisation (\mathbf{M}), this \mathbf{B}_1 field must rotate precisely at the precession frequency of the protons. The first result of resonance is that the net magnetisation moves out of alignment away from \mathbf{B}_0 . The angle to which the magnetisation moves out of alignment is called the flip angle. The magnitude of the flip angle depends on the magnitude and duration of the RF

pulse. Usually the flip angle chosen is 90 degrees, i.e. the magnetisation is given enough energy by the RF pulse to move through 90 degrees relative to \mathbf{B}_0 . \mathbf{B}_0 is aligned along the longitudinal axis and the plane at 90 degrees to the longitudinal axis \mathbf{B}_0 is termed the transverse plane.

Immediately following excitation the magnetic moments of the hydrogen nuclei within the transverse plane move in phase with each other: their precessional paths around \mathbf{B}_0 are aligned.

The most basic MR experiment is to perturb the nuclear magnetic moment into the transverse plane using a brief RF pulse (\mathbf{B}_1), and then to observe the signal induced by Faraday's law of induction in a receiver coil. An oscillating signal is induced in the coil that decays under an exponential envelope (the free induction decay). The detected signal can be analysed for its frequency components by means of Fourier transform.

1.6.2.1 T_1 Relaxation

RF stimulation causes a proportion of the exposed nuclei to absorb energy, lifting them to the excited state. The nuclei in this state can return to the ground state only by dissipating their excess energy. Spin lattice relaxation (T_1 relaxation) depends on energy transfer to the surrounding environment (i.e. when a stimulated proton encounters another magnetic field nearby). Relaxation recovery is an exponential process with the T_1 time being the recovery time constant.

1.6.2.2 T_2 relaxation / decay

T_2 relaxation is also called spin-spin relaxation. T_2 relaxation results from any intrinsic process that causes the spins to lose their phase coherence in the transverse plane. Most frequently it results from static or slowly fluctuating local magnetic field variations within the tissue itself. As with the T_1 recovery this rate of transverse signal decay is exponential and by convention has time constant T_2 .

In biological tissues the main contribution to T_2 relaxation is from the relatively static magnetic field from neighbouring protons. In rigid molecules such as membrane phospholipids, where molecular motions are extremely slow, T_2 relaxation is very rapid and the transverse magnetisation may decay so rapidly that

signal is not detected by the receiver coil. Alternatively, when molecules are moving rapidly, any short local field inhomogeneity experienced by an excited proton will average to zero over a short time and the T_2 relaxation times are correspondingly much longer.

1.6.2.3 Repetition Time (TR)

The time between repeated RF excitation pulses is called the repetition time (TR). The TR determines the amount of relaxation that is allowed to occur between the end of one RF pulse and the application of the next. Longer repetition times allow more T_1 relaxation and this property can be used to exploit the contrast between tissues with different T_1 .

1.6.2.4 The Spin-Echo Sequence

In practice the net transverse magnetisation shrinks more rapidly than expected from T_2 relaxation alone and is characterised by time constant T_2^* where T_2 can be thought of as the natural or true spin-spin relaxation of the tissue and T_2^* as the “observed” relaxation due to both spin-spin relaxation effects as well as other causes of spin dephasing (principally due to inhomogeneities in the main magnetic field). However, a 180 degree RF pulse applied at time T after the 90 degree excitation pulse can re-establish phase coherence at time 2T as a spin echo. The amplitude of the transverse magnetisation at the echo peak depends on TE and T_2 of the tissue. In a spin echo this amplitude is proportional to e^{-TE/T_2} . If TE equals T_2 the transverse magnetisation has decayed to 37% of its initial amplitude. As TE is lengthened, the transverse magnetisation becomes weaker. As for TR, the TE can be chosen to exploit biological variation in T_2 to provide image contrast.

1.6.2.5 The Gradient Echo Sequence

Gradient echo imaging techniques provide methods of accumulating images in much shorter total times than conventional pulse sequences. The gradient echo pulse sequence uses a rapidly reversing RF gradient instead of the relatively time consuming refocusing 180 degree pulse sequence that is used to form a spin echo. In spin echo imaging the 180 degree pulse reverses the direction of all transverse magnetisation making the relaxation that occurs between the initial 90 degree RF pulse and signal echo immune to *fixed* magnetic field inhomogeneities. These

magnetic field inhomogeneities may be static magnetic field non uniformities, any un-reversed gradients applied during the time interval TE, or magnetic susceptibility inhomogeneities. As a result the transverse relaxation measured in SE sequences is related entirely to “true” T_2 relaxation effects. In gradient echo imaging, formation of an echo by gradient reversal does not eliminate the dephasing effects of magnetic field inhomogeneities. Therefore the signal decay between the initial 90 degree pulse and the gradient echo depends on true T_2 relaxation plus relaxation caused by magnetic field inhomogeneities and is governed by T_2^* , which is shorter than T_2 . In extremely homogeneous magnetic fields and in tissue regions without magnetic susceptibility inhomogeneities, T_2^* values approach T_2 times. In voxels where there are inhomogeneities T_2^* can be very much shorter than T_2 .

Gradient echo sequences are used in the majority of fast scan MRI techniques. Typical measuring times for a single two dimensional image are seconds. These scan times compare favourably with the time constants of most physiological motion in humans and can provide access to functional information such as blood flow.

1.6.2.6 The Inversion Recovery Sequence

In this sequence, an 180° pulse is applied before the net magnetisation is tipped into the transverse plane. The effect of this pulse is to reverse the direction of the initial magnetisation. As spin-lattice relaxation occurs and the net-magnetisation starts to return toward its equilibrium position aligned along the external magnetic field it will reach a point where there is zero net longitudinal magnetisation. If a 90 degree pulse is applied at this inversion time (TI) no transverse magnetisation will be produced. This sequence is applied to study tissue containing several components with differing T_1 times. By correct choice of the TI signal from one or more of the tissue components can be minimised. This forms the basis of the Fluid Attenuated Inversion Recovery (FLAIR) sequence and also the metabolite nulling sequence described in section 2.5.

1.6.3 Advanced Magnetic Resonance Imaging (MRI) applications

MRI is superior to computed tomography (CT) in the detection of the pathology underlying focal epilepsies in both adults and children (Kuzniecky *et al.*, 1993b; Sperling *et al.*, 1986; Theodore *et al.*, 1986a). The most commonly identified abnormalities are hippocampal sclerosis, malformations of cortical development,

vascular malformations, tumours, and acquired cortical damage. Due to the rapid advances in MRI techniques, abnormalities are not infrequently identified in patients who were previously regarded as being 'MRI-negative', and it has become important to describe the MRI sequences, MRI field strengths and the criteria by which patients are considered 'MRI-negative'.

More advanced MRI techniques such as MRS, diffusion weighted imaging (DWI), magnetisation transfer, volumetric analysis and functional imaging (fMRI) may also be indicated to characterise the epileptogenic focus and are often applied to the assessment of potential surgical candidates. Other modalities such as PET and/or SPECT may also be helpful in some subjects.

3D T1-weighted MRI produces images with high anatomical definition which form the basis of several quantitative volumetric techniques useful in diagnosing and characterising epilepsy. The techniques for reliable detection of hippocampal sclerosis by MRI are well established (Jackson et al., 1990; Cook et al., 1992; Duncan et al., 1996; Duncan, 1997; Van Paesschen W. et al., 1997a). Hippocampal atrophy identified by MRI correlates well with hippocampal loss, particularly in the CA1 sub-region (Van Paesschen W. et al., 1997b). Amygdala volumes may be similarly determined (Cendes et al., 1993). Measures may also be derived of cerebral hemisphere grey matter and sub-cortical volumes (Sisodiya et al., 1995). Further, the distributions of grey and white matter may be compared between groups of subjects, between a single subject and a control group using regional measures (Sisodiya et al., 1995) and / or voxel based morphometry (Richardson et al., 1997; Woermann et al., 1999a).

1.7 ¹H Magnetic Resonance Spectroscopy

1.7.1 Introduction

1.7.2 MRS Physics

1.7.2.1 Chemical Shift

1.7.2.2 Free Induction Decay

1.7.2.3 Spin-spin coupling

1.7.2.4 T₂ and MR visibility

1.7.3 Basic acquisition and processing techniques

1.7.3.1 Shimming

1.7.3.2 Water suppression

1.7.3.3 Choice of Echo Time (TE)

1.7.3.4 Localisation techniques

1.7.3.5 T₁ and T₂ correction

1.7.3.6 Referencing to a standard solution

1.7.3.7 Signal to noise ratio and signal averaging

1.7.4 Advanced acquisition and processing techniques

1.7.5 MRS at higher field strengths

1.7.6 Biological Significance of Metabolite Peaks

1.7.6.1 N-Acetyl Aspartate

1.7.6.2 Creatine plus phosphocreatine

1.7.6.3 Choline containing compounds

1.7.6.4 GABA, glutamate and glutamine

1.7.6.5 Myo-inositol

1.7.6.6 Lactate

1.7.7 MRS in Healthy Adults

1.7.1 Introduction

This section introduces the basic physics behind MRS and practical aspects of performing a MRS experiment. The most commonly studied metabolite peaks in ^1H MRS experiments are introduced but their relevance to the investigation of epilepsy is outlined in more detail in Section 1.8. The metabolism of GABA, glutamate, glutamine and lactate has already been discussed in Section 1.2 and is not repeated in depth here.

1.7.2 MRS Physics

In MRI it is generally acceptable to consider that the resonant frequency of any particular nucleus depends only on the applied magnetic field (\mathbf{B}_0). In fact the stimulated nuclei are also subject to the local environment. Nearby electrons and other nuclei have small but significant effects on the net field to which the nucleus is exposed. From the Larmor equation this will alter the frequency at which that nucleus will resonate. MRS experiments aim to separate and measure different metabolites on the basis of this variation in resonant frequency or chemical shift. Most biomedical MRS experiments are performed with ^1H , ^{13}C or ^{31}P .

Both ^1H and ^{31}P are naturally abundant isotopes (99.98% and 100%, respectively) and are present in sufficiently high concentrations in the brain in biologically important compounds. These characteristics have resulted in the widespread use of ^1H and ^{31}P for the study of metabolites in vivo. However, the MR sensitivity of ^{31}P is only 7% that of ^1H , so larger volumes of tissue need to be examined for ^{31}P MRS than for ^1H MRS, leading to a loss of spatial resolution. For the case of carbon only 1.1% of the total carbon population consists of the magnetically active isotope ^{13}C . This factor together with a smaller gyro-magnetic ratio than for ^1H means that the relative sensitivity of ^{13}C is 60 times less than that of ^1H . However the relatively small endogenous ^{13}C signal can be used to advantage when using ^{13}C enriched media where the vast majority of the recorded signal will derive from labelled ^{13}C .

In practice the poor spatial resolution with ^{31}P and ^{13}C MRS limits the clinical usefulness of such studies although they remain important research tools. The remainder of this section will deal with predominantly ^1H MRS.

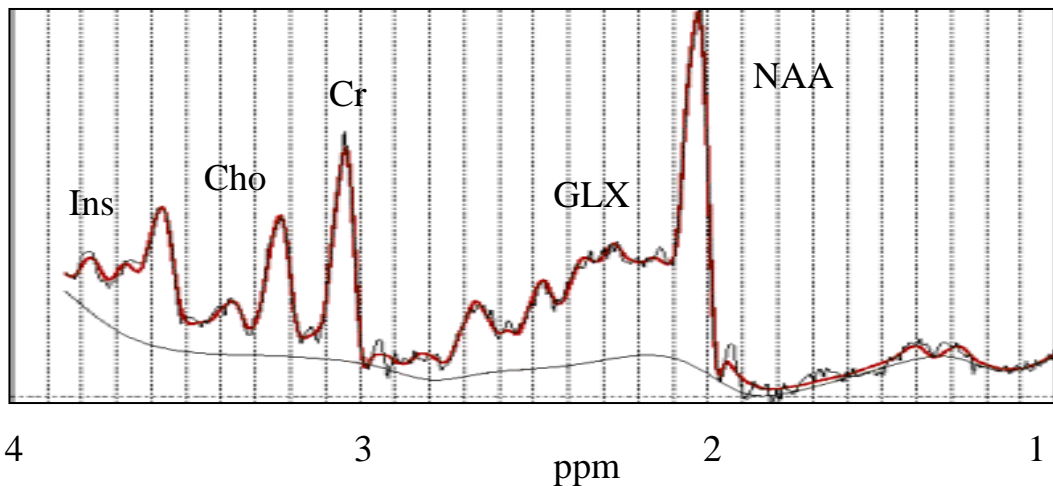


Figure 1.7.1 Typical short TE ^1H MRS spectrum obtained in a healthy volunteer studied in the frontal lobes. NAA = N Acetyl aspartate, GLX = glutamate plus glutamine, Cr = creatine plus phosphocreatine, Cho = choline containing compounds and Ins = myo-Inositol

1.7.2.1 Chemical Shift

A proton (or any other resonating atomic nucleus) has a resonant frequency proportional to the magnetic field it experiences. This is the sum of the large external applied field and the small local field produced by the electrons moving around the nucleus. This local field opposes the main applied field, slightly shielding the nucleus from the external field B_0 such that the effective field experienced by the proton is given by:

$$B = B_0 (1 - \sigma) \quad [\text{Eqn 1.7.1}]$$

where σ is the shielding constant. The modified Larmor equation is then given by:

$$\nu = \gamma/2\pi(1 - \sigma)B_0 \quad [\text{Eqn 1.7.2}]$$

The shielding electrons are therefore said to result in a chemical shift of the resonant frequency of the nucleus. The magnitude of the shielding effect and hence the magnitude of the chemical shift varies. For example the ^1H nuclei in water molecules (H_2O) generally experience less shielding than ^1H in lipid molecules. They therefore experience a larger net magnetic field resulting in a higher resonant frequency for the same applied external field. Usually the X-axes of MR spectra are displayed in units of chemical shift, defined as the frequency of resonance relative to the resonant frequency of a reference chemical. Chemical shift (δ) is usually stated in parts per million (ppm) according to:

$$\delta = 10^6 (v_{\text{sample}} - v_{\text{reference}}) / v_{\text{reference}} \quad [\text{Eqn. 1.7.3}]$$

By convention the reference used in proton MRS is the resonant frequency of the equivalent ^1H nuclei in tetramethyl silane (TMS), which by definition resonate at 0 ppm. TMS is an appropriate reference because the shielding of protons in this compound is greater than in other organic compounds. Consequently MR signals of most relevant molecules are shifted in the same direction downfield from TMS and have chemical shifts between 0 and 10 ppm. Water has a chemical shift of 4.7 ppm whilst aliphatic lipids have chemical shifts of about 1.2 ppm. By convention spectra are displayed with chemical shift increasing along the horizontal axis from right to left so that the water peak is to the left of the lipid peak. Chemical shift measured in ppm is independent of the B_0 field and this allows comparison of spectra acquired on different scanners and at different field strengths. The area under the peaks is proportional to the number of protons in each environment and with the same chemical structure.

1.7.2.2 Free Induction Decay

In MRS a strong RF pulse is applied that will cause all the nuclear species under investigation to resonate. The signal recorded, defined as the free induction decay (FID) is a convolution of these individual metabolite resonant frequencies decaying exponentially with time.

1.7.2.3 Spin-spin (J) coupling

It is not only the surrounding electron cloud that has an effect on the resonant frequency of a particular nucleus. The obtained spectra may also display the effect of line splitting due to field interaction of two nuclear spins on the same molecule. For example if a proton (H_A) is near another non-equivalent proton (H_B) (i.e. H_B has different chemical shift), in half of the molecules the H_A proton will be adjacent to an H_B aligned with the field and in the other half the H_A proton will be adjacent to an H_B aligned against the field. Thus, half the H_A protons in the sample will feel a slightly larger magnetic field than they would in the absence of H_B and half will feel a slightly smaller magnetic field and resultant peak will be split into 2 equal halves. Such “spin-spin” coupling is independent of the intensity of the external field B_0 . The distance between the split peaks (in Hz) is called the “coupling constant” and is

usually represented by the symbol J. Provided the coupling effect is weak (the coupling constant is small compared to the difference in the chemical shifts between the coupled nuclei) the final spectrum will be determined by the spin and the number of interacting nuclei to produce $(2nI + 1)$ lines (for first order coupling, where I is the spin of the adjoining nuclei and assuming n equivalent interacting nuclei) and the relative intensities of the multiplet will be given as follows.

e.g. for ^1H where $I = \frac{1}{2}$.

n = 0			1				
n = 1			1		1		
n = 2		1		2		1	
n = 3	1		3		3		1
..							

The GABA molecule is shown together with the J values for the interacting H nuclei (Fig. 1.7.2). The GABA peaks at 3.01, 2.28 and 1.89 ppm are all heavily overlapped in the standard spectrum acquired at short TE and therefore GABA cannot be easily measured. For this reason techniques have been developed which make use of the J modulation to simplify the spectrum and allow GABA peak measurement. The double quantum filter technique used in this thesis to measure GABA concentration is one such technique. The filter is described in more detail in Chapter 2. Further description of the techniques used to simplify the spectrum using J-coupling effects is provided in Section 1.7.4.

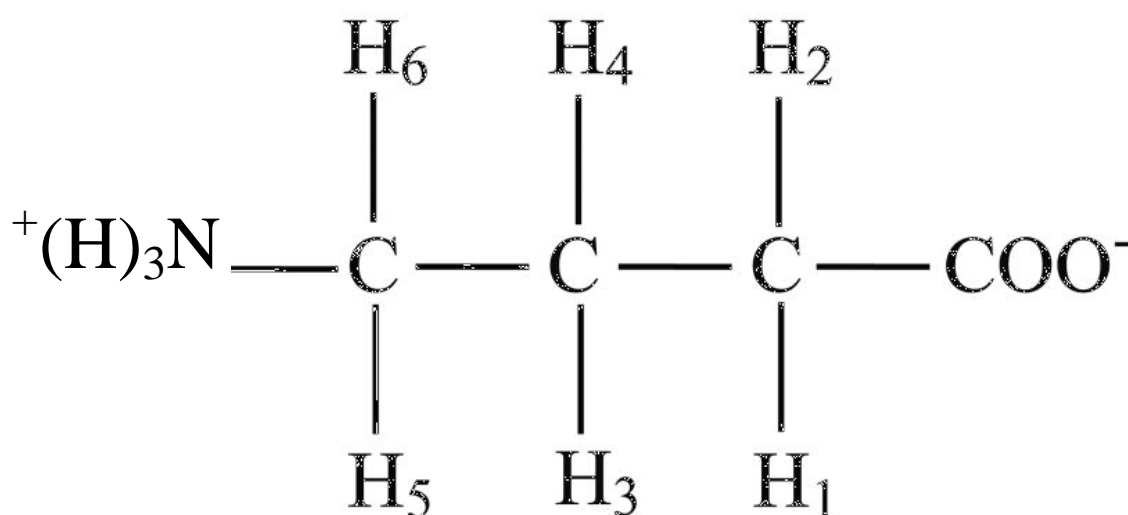


Figure 1.7.2 Gamma amino butyric acid. The three pairs of ^1H : H₁ and H₂, H₃ and H₄, H₅ and H₆ interact with their adjacent pairs as shown in the table below:

Resonance	Chemical Shift (ppm)	J-Coupling (Hz)
H ₁	3.0128	H ₁ – H ₃ (5.37) H ₁ – H ₄ (7.13)
H ₂	3.0128	H ₂ – H ₃ (10.58) H ₂ – H ₄ (6.98)
H ₃	1.8890	H ₃ – H ₅ (7.76) H ₃ – H ₆ (7.43)
H ₄	1.8890	H ₄ – H ₅ (6.17) H ₄ – H ₆ (7.93)
H ₅	2.2840	
H ₆	2.2840	

Table 1.7.1: Chemical shifts and coupling constants for GABA(Govindaraju et al., 2000)

1.7.2.4 T₂ and MR visibility

MRS studies performed at short TE (< 60 ms) will still include some components from partially mobile macromolecules and lipids or metabolites with short T₂. Studies performed at longer TE will not show these compounds. In practice the aims of the MRS study will dictate the acquisition TE. Short TE studies can measure a greater range of compounds and are less susceptible to changes in T₂ in pathological tissue. However analysis is more complicated at short TE because the baseline contains a series of broad peaks from macromolecules and lipids. Long TE studies benefit from the fact that as the TE lengthens there is diminishing presence of these broad baseline resonances and direct, “by eye”, qualitative assessment of the ratios of the main visible metabolite peaks is possible.

1.7.3 Basic acquisition and processing techniques

1.7.3.1 Shimming

The magnetic field inside an ideal magnet will be highly homogeneous. For simple solenoids this requires an infinitely long magnet length compared to the diameter of the coil in order to minimise the effect of the strong divergence of the field lines at the ends of the coil. To compensate for this divergence and to generate a reasonably homogeneous field in a bore of an acceptable length that can be incorporated into currently available MRI scanners, the coil segments are wound with a smaller radius or more turns at the end of the coil than at the centre. Further fine adjustment of field homogeneity at the site of interest is called shimming. MRS experiments which depend upon detecting the small differences in resonant frequencies corresponding to small variations in the local field experienced by each resonating hydrogen nucleus are particularly sensitive to field inhomogeneity and shimming procedures will usually be applied prior to the commencement of MRS acquisitions from prescribed regions of interest.

The field homogeneity is improved by passing current through appropriate gradient coils, which generate small magnetic field gradients superimposed on the main B₀ field. These gradients add to, or subtract from, the field at desired points along its axis or transverse to it, smoothing out the field non-homogeneities.

1.7.3.2 Water suppression

The water peak dominates the unsuppressed ^1H MRS spectrum because of the high concentration of water in the human brain. Without water suppression the other metabolite peaks are hard to measure and the baseline is massively distorted by the dominant water peak. In order to visualise the other non-water metabolites it is necessary to suppress the signal from the water hydrogen nuclei. A practical measure to overcome this is to suppress the water signal immediately prior to the time of acquisition. Although suppression of the water signal may be achieved via a number of different methods a convenient method entails the prescription of a series of chemical shift selective pulses adjusted to the resonant frequency of water that transfer the water signal to the transverse plane and are followed by “crusher” gradients in the transverse plane that dephase the transverse magnetism before a spatially localised spectrum is acquired (see Chapter 2 for pulse sequences used in this thesis).

1.7.3.3 Choice of Echo Time (TE)

Early in-vivo work was generally carried out at long TE. A value of TE = 135 ms was often chosen because at this TE the lactate peak is inverted and easily identified. Longer TE acquisitions are technically less demanding and produce well defined main peaks and a flat baseline. However, as noted above, T_2 losses are large and can constitute a problem, both because of reduction in the signal to noise ratio (SNR) and also because the resulting signal has to be corrected for these losses as part of the quantification procedure. More recent work has made use of improvements in gradient switching times and the shielding of eddy currents to perform short TE studies. Such studies suffer fewer T_2 losses and result in higher signal to noise ratio. More metabolites are visible at shorter TE but the baseline is now complex and irregular as a consequence of broad macromolecule peaks and this has to be modelled before quantification of metabolite concentrations is possible.

1.7.3.4 Localisation techniques

For a detailed review of the developmental history of these techniques please see a review by Keevil (Keevil, 2006). In order to allow for a meaningful interpretation of MRS results, localisation techniques are employed to acquire spectra from a limited pre-defined volume of interest (VOI) only. A number of localisation methods have

been developed but for the majority of studies localised spectra are now obtained by applying one of the following four methods:

The STimulated-Echo Acquisition Mode (STEAM) was first demonstrated as a viable localisation method for proton spectroscopy of the human brain by Frahm and was rapidly taken up by other groups (Frahm et al., 1989). The sequence consists of three 90 degree selective pulses, each applied in the presence of an orthogonal gradient to excite a slice. Because these are 90 degree pulses, gradient refocusing lobes must be used. The resulting signal is from the VOI defined by the intersection of the orthogonal slices. Although the STEAM sequence is both simple and robust it suffers from the fact that the final stimulated echo yields at best only half of the possible signal from the VOI. Also, although it can be used advantageously for short TE studies it is not well suited for the study of nuclei with very short T_2 values (e.g. phosphorus) because of the time required for application of the gradient refocusing lobes.

The Point RESolved Spectroscopy (PRESS) localisation experiment (Bottomley, 1987) consists of a 90-180-180 degree pulse sequence with each pulse applied in the presence of an orthogonal gradient so that the final echo comes from the intersection of the planes as depicted in Figure 1.7.3. Unlike STEAM the PRESS sequence retains the full signal. A disadvantage of PRESS is that the longer sequence preparation time makes it less suitable for acquisitions at very short TE.

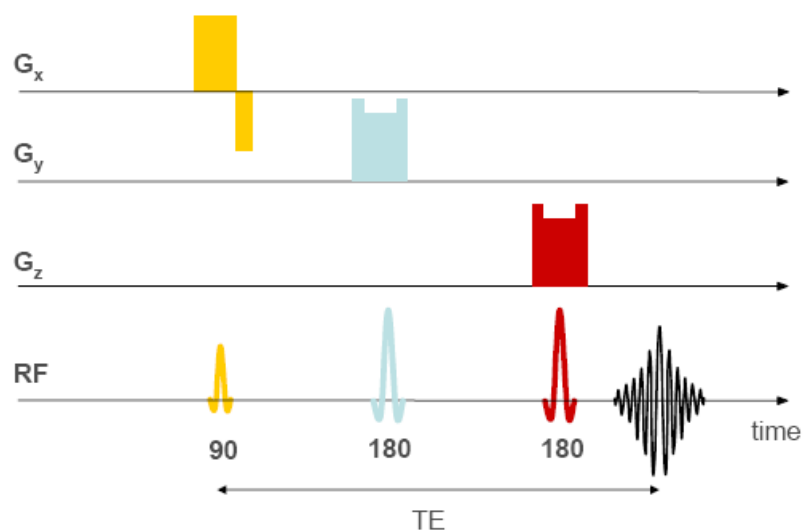


Figure 1.7.3 The PRESS Sequence. For simplicity, the initial water suppression, outer volume suppression are not shown

The Image Selected In vivo Spectroscopy (ISIS) experiment also uses frequency selective pulses in the presence of orthogonal gradients (Ordidge et al., 1988). However the selective pulses are inversion pulses and a fourth non-selective pulse is applied for observation of the signal. A series of eight acquisitions with different combinations of inversion pulses is required to achieve the localisation of the VOI defined by the intersection of the orthogonal slices. Because the signal is received immediately after the final RF pulse there is minimal loss from T_2 relaxation, and ISIS has proved to be a particularly effective localisation experiment for observation of nuclei with short T_2 values such as ^{31}P . The availability of frequency selective pulses with immunity to B_1 inhomogeneity has made ISIS an important localisation experiment for use with surface coil experiments where the B_1 field is inherently inhomogeneous.

Magnetic Resonance Spectroscopic Imaging (MRSI) (alternatively known as Chemical Shift Imaging or CSI) techniques involve spatial encoding by switched gradients (Bottomley et al., 1988). The number of encodings required is equal to the desired number of pixels in the final spectroscopic image. The spatial encoding in spectroscopic imaging is accomplished by phase encoding gradient steps as used in conventional MRI methods (Fig. 1.7.4). However to preserve the chemical shift information, the data in spectroscopic imaging methods are collected in the absence of a readout gradient; this is in contrast to MRI methods in which a readout gradient is used to obtain spatial information in one of the dimensions. MRSI methodology is discussed in more detail in Chapter 2.

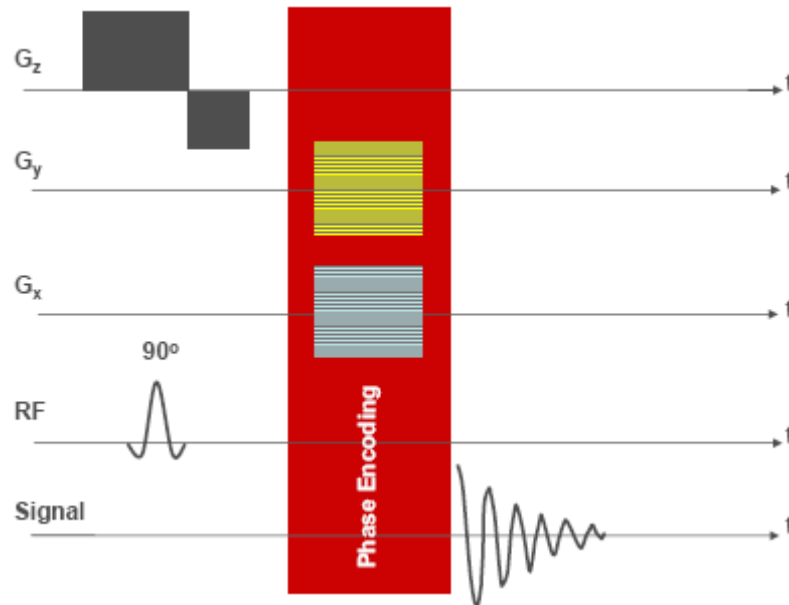


Figure 1.7.4 Typical 2D MRSI pulse sequence. Again for simplicity the initial water suppression, outer volume suppression, and associated slice-selective crusher gradients are not shown

1.7.3.5 T_1 and T_2 correction

Nuclear concentration is only proportional to peak area under two conditions. First, the longitudinal magnetisation must have had time to fully recover after any previous pulses, i.e. it must be fully relaxed ($TR \gg T_1$). Second the transverse magnetisation must be fully intact at the time of signal acquisition, with no transverse magnetisation decay ($TE \ll T_2$). The first condition is sometimes achieved, although data collection times can become very long. The second condition is rarely achieved in 1H MRS since an echo is required for the spatial localisation schemes. Thus a correction is often made for T_1 and T_2 decay. This can be kept as small as possible, by using long TR and short TE so that small errors in the T_1 and T_2 values used in the corrections do not have a large effect on the estimate of concentration. Relaxation times can change in disease, thus corrections which assume standard values can be inaccurate. The alternative of measuring T_1 for each subject is time consuming. T_2 measurements may be more desirable when correcting long echo time spectra (e.g. $TE = 135ms$).

1.7.3.6 Referencing to a standard solution

Although the concentration of a metabolite is proportional to its spectroscopic peak area, the determination of the constant of proportionality is not trivial. The

calculation depends on the receiver gain, the coil loading (which depends on the subject or sample), the voxel size and the temperature.

Internal water referencing has been advocated. It is easy to collect a rapid brain spectrum that includes water as an internal standard. If the water concentration is known, this then calibrates the gain of the spectrometer, establishing the link between proton concentration and peak area. Non-uniformity in the receiver sensitivity is the same for water and metabolites and therefore need not be corrected for. The water signal has a high signal to noise therefore only a few averages are required. The difficulty is that the water concentration is usually not known exactly. It depends on the proportions of white matter, grey matter and CSF in the voxel, and is often increased in disease. It must be measured separately, or some assumption made about its value.

For this reason external referencing is frequently used to quantify the metabolite signal. The signal from water, or a metabolite of known concentration, can be measured in a separate acquisition from a phantom (test object). This overcomes the problem of the incomplete information about the water concentration. A “same time” external standard can be measured in the same sequence as the subject of interest. “Same-place” external standard measurement can also be used. This requires that the phantom is measured in the same position within the magnetic field as would be occupied by the specimen of interest, for example the centre of the brain in a volunteer undergoing a Head MRS study (thus overcoming the major problems of spatial non-uniformity). “Same place” scanning must clearly be performed at a different time point to the acquisition of the volunteer scan. It is therefore vulnerable to changes in coil sensitivity (brought about by the change from loading by a head to loading by a phantom), and to receiver instability (whether caused by explicit gain changes or unexpected drift). Corrections for RF non-uniformity across the different regions in the brain are still needed in principle, although they may be minimal in a relatively uniform coil.

An alternative to the above techniques which try to reference the obtained metabolite signal to a known internal or external concentration is to choose a stable metabolite peak from the produced spectrum; and then to use this peak value as an internal standard by reporting the other acquired peaks with reference to this

“standard”. This is helpful where one metabolite is known not to vary in concentration. In most cases there is no such standard metabolite and the biological interpretation of any change in a peak ratio can become very difficult. This last method was employed in the majority of the early MRS studies of subjects with epilepsy. The creatine plus phosphocreatine (Cr) peak was considered to be relatively invariant across brain regions and between pathologies and was used as the “standard” peak. However, as discussed in Chapter 3 of this thesis, this use of ratios can lead to loss of information as to the true trend to change in metabolite concentrations in regions of pathology.

1.7.3.7 Signal to noise ratio and signal averaging

Metabolite concentrations are usually too low to obtain a satisfactory signal-to-noise ratio (SNR) in the spectrum from a single FID or echo signal. By adding together many signals before Fourier transformation, the SNR is improved. Signal averaging enables the noise to be decreased (since it is random), relative to the signal.

The SNR is given approximately by:

$$\text{SNR} = \text{SNR}_0 * \text{NEX}^{1/2} * \text{VOI} \quad [\text{Eqn. 1.7.4}]$$

Where SNR_0 is the SNR for 1cc of tissue in a single acquisition, NEX is the number of excitations (averages), and VOI is the volume from which the spectrum is being collected (i.e. the total number of protons excited). Thus, from (1.7.5), SNR increases rapidly with increasing VOI, and more slowly with increasing NEX (as $\text{NEX}^{1/2}$). To achieve a given SNR, more NEX (and therefore a longer exam time) is required as VOI is reduced. An acceptable SNR can be achieved in about 10 minutes for a 2ml voxel at 1.5 Tesla (using short TE PRESS).

1.7.4 Advanced acquisition and processing techniques

Advanced MRS sequences may be applied to filter or simplify the spectrum to allow the identification of a particular peak. In Chapter 2 a Double Quantum Filter technique is described. The technique has been employed extensively in this thesis and GABA measurement in several different epilepsy syndromes is reported in Chapter 3 ([3.2], [3.3], [3.4], and [3.6]).

Another technique employed to simplify GABA measurement is the technique of spectral editing. This technique has been widely applied by Rothman and co-workers in order to measure GABA concentrations in a number of studies of subjects with epilepsy and the findings of this group are referred to frequently in the discussion sections of this thesis. It is therefore instructive at this point to briefly describe Rothman and co-workers' methodology of GABA signal detection by spectral editing techniques.

As shown below the ^1H spectrum of GABA consists of three multiplets at circa. 1.9, 2.5 and 3.0ppm respectively. Each multiplet is heavily overlapped by other metabolite peaks. The C4 GABA resonance at 3.0 ppm (H1 and H2) is a triplet arising from J-coupling with the protons bonded to the C3 carbon (protons H3 and H4 which resonate at 1.9 ppm). The major overlapping resonance at 3.0 ppm is the Cr peak which is a singlet.

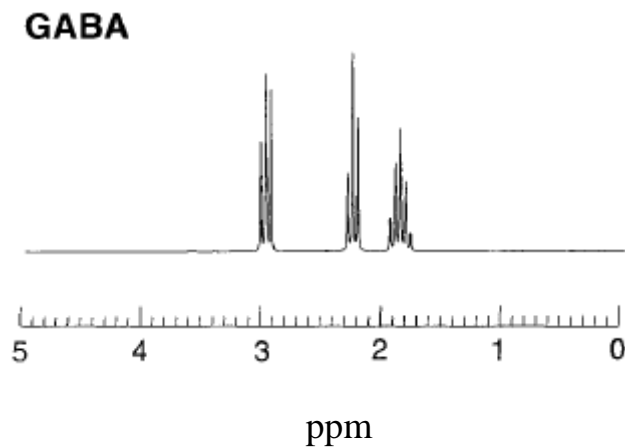


Figure 1.7.5 ^1H MRS spectrum for GABA[from (Govindaraju et al., 2000)]

In spectral editing, a semi-selective refocusing pulse is applied in the first instance placed at the C3 GABA resonance at 1.9 ppm. Next, to selectively induce J-modulation a tailored excitation pulse train is applied to invert the C3 GABA resonance and cause the outer sidebands of the C4 GABA triplet to invert. Subtraction of a spectrum obtained with this sequence from a spectrum obtained without the sequence eliminates signals that are not J-coupled to resonances at 1.9 ppm and gives an edited GABA spectrum at 3.0 ppm. Specifically, the major overlapping Cr peak, which does not exhibit J-coupling, is subtracted out from the

final spectrum. Since only the outer two peaks of the triplet are detected the maximum yield is 50%.

The double quantum filter (DQF) used in this thesis to measure GABA concentrations also uses J-coupling effects to remove the overlapping Cr peak at 3.0 ppm and is described fully in Chapter 2. Each of these techniques which filter or edit the obtained spectra from a volume of interest result in reduced signal to noise in the finally obtained spectrum. Whilst equation [1.7.5] demonstrates that this reduction in signal can be countered by increasing scan times or by increasing the studied volume of interest the final scan sequences applied at conventional magnet field strengths will usually require some compromise between signal quality and acceptable scan duration and / or spatial resolution.

1.7.5 MRS at Higher Magnetic Field Strengths

An alternative mechanism to improve the resolution of the separate metabolite peaks is to apply a higher external magnetic field. Returning to the Larmor equation (1.7.3) it can be seen that increasing the magnetic field B_0 will increase the separation of the individual metabolites along the frequency axis. High static field MRI scanners are now becoming available and several studies have reported good separation of overlapping peaks (Gruetter et al., 1998a; Gruetter et al., 1998b; Tkac et al., 2003). Increasing B_0 will also improve the separation of metabolite peaks by directly increasing the SNR.

1.7.6 Biological Significance of Metabolite Peaks

Several brain metabolites are reliably measured using ^1H MRS. Three dominant signals are visible at both short and long TE. These three metabolites are N-acetyl aspartate (NAA), creatine plus phospho-creatine (Cr) and Choline containing compounds (Cho). Other brain metabolites are visible only at short TE. These short TE visible metabolites include GLX, the complex signal of glutamate plus glutamine, GABA and myo-inositol (Ins). Finally lactate is visible at low concentration at both short and long TE in some healthy control subjects and is visibly elevated in some pathological conditions. A reference library of the spectral peaks of some 35 metabolites visible to ^1H MRS has been compiled by Govindaraju (Govindaraju et al., 2000).

1.7.6.1 Principal metabolites: NAA, Cr, Cho

1.7.6.1.1 NAA

NAA is a non-essential amino acid and is the most visible metabolite peak of the ^1H MRS spectrum. Within the brain NAA is synthesised primarily in neurons being present in concentrations of up to 20mM and representing about 7% of neuronal osmolarity. The majority of MRS studies published to date have found NAA to be the most sensitive MRS visible metabolite marker of pathological states. The role of N-acetyl aspartate in brain tissue, however, has been unclear and although reduced level of NAA is commonly referred to as a marker of “neuronal loss or dysfunction” the biological explanation for this reduction has also been absent. However, evidence has begun to accumulate that NAA synthesis is linked with mitochondrial function(Heales et al., 1995;Bates et al., 1996) and that NAA has an important and dynamic role in removing neuronal water produced as a consequence of increased metabolic activity. NAAG appears to act as a specific transmitter signalling to adjacent astrocyte foot processes to increase regional blood flow and uptake of glucose. [For more detailed discussion of NAA metabolism see (Baslow, 2000;Moreno et al., 2001;Barker, 2001;Baslow et al., 2003;Baslow, 2003b;Baslow et al., 2007;Baslow and Guilfoyle, 2009)]

NAA metabolism appears to span three metabolically linked compartments. Using a combined method of ^{13}C MRS and labelled glucose infusion in humans in vivo, it has been demonstrated that NAA synthesis is directly coupled to glucose metabolism(Moreno et al., 2001). Neurons synthesise NAA in mitochondria and it is calculated that 1mol of NAA is synthesized for every 40 mol of glucose oxidized in the brain. NAAG is formed from NAA and glutamate. However neither NAA nor NAAG can be catabolised within the neuron and must be released to the extra-cellular fluid (ECF). In this space NAAG interacts with astrocyte foot process surface NAAG peptidase producing NAA and glutamate whilst NAA reacts with oligodendrocyte surface membrane aspartoacylase which converts it to acetate and aspartate. The glutamate formed at the astrocyte surface is thought to provide specific signalling to increase blood flow and increase supply of glucose.

Investigations of NAA export from stimulated neurons have estimated that each NAA molecule transports with it 32 molecules of obligated water. This can be achieved using the NAA system at the relatively low energy cost of about 1% of the

brain's daily energy budget(Baslow and Resnik, 1997). The water removal process from the brain would most likely involve diffusion of liberated water down its gradient via aquaporin-4 (AQP4), the predominant water channel protein that is heavily expressed in astrocytes but not in neurons or oligodendrocytes.

This has led to the theory that NAA probably functions as a molecular water pump (MWP)(Baslow, 2003a) to transport neuronal metabolic water to ECF for its removal from the brain via aquaporin 4 (AQP4) channels present on the surfaces of astrocytes and vascular endothelial cells(Verkman et al., 2006). MWPs are recently discovered entities that can actively pump water against its gradient(Meinild et al., 1998;Zeuthen, 2000;MacAulay et al., 2001). MWP appear to be highly efficient, with 1 molecule of MWP solute able to transport as many as 500 water molecules during its passage.

Baslow has suggested that the metabolism of NAA is via an inter-compartmental shuttle(Baslow, 2002). In humans, NAA turnover in the brain is very rapid, and the efflux of NAA is 0.55 $\mu\text{M/g/h}$ from the neuronal compartment into the extra cellular space. For equilibrium NAA must be removed from the ECS at the same rate. The role of the oligodendrocyte localised amidohydrolase II is to participate in this process by hydrolyzing NAA that has been liberated from neurons(Bhakoo et al., 2001). It follows that the products of NAA hydrolysis, aspartate and acetate, must also be removed, at the same rate as NAA hydrolysis, or the action of this hydrolytic enzyme would also be compromised. NAA-derived acetate is metabolised by oligodendrocytes or astrocytes, and incorporated into many lipid components and thus lost from the NAA cycle. The NAA-derived aspartate diffuses towards the neuron surface, where it is taken up to complete the shuttle action. Aspartate does not easily pass into the brain across the blood-brain barrier, and this conservative step ensures a sufficient supply of aspartate for neuron use in the continuous and rapid formation and inter-compartmental release of NAA. Conservation of acetate is not essential in the brain because it easily passes across the blood brain barrier at about the same rate as glucose.

These findings would propose that NAA function is linked with neuronal metabolic activity both by providing a mechanism for the removal of waste water of metabolism as well as a specific signalling pathway to the astrocyte end processes

leading to increased glucose uptake. Such proposals seem to be supported by the results of functional magnetic resonance spectroscopy (fMRS) studies of the human visual cortex in response to visual stimulation (Baslow et al., 2007) which showed 13% NAA reduction after intense visual activity with complete recovery after a subsequent “rest period” and which represents export of preformed NAA with activation and recovery following re-synthesis during a period of reduced metabolic activity.

The astrocytic surface metabotropic glutamate receptor 3, (GRM3) activation of which initiates intracellular calcium transients (Hashemi et al., 2008) and secondary astrocyte–astrocyte and astrocyte–vascular system signals that increase focal blood flow (Baslow and Guilfoyle, 2007), is the likely target for NAAG (Baslow, 2008; Baslow, 2009)

Disorders of NAA metabolism are known and are associated with significant pathology. Canavan disease is a rare recessive genetic neurodegenerative brain disorder associated with many different mutations in the gene encoding aspartoacylase and leading to accumulation of NAA and the development of a spongiform leukodystrophy. There is also a single human case of apparent lack of NAA (Martin et al., 2001) and relatively preserved neurological function and this observation of apparently normal function without NAA has yet to be assimilated into the theories developed above.

1.7.6.1.2 Creatine plus phosphocreatine (Cr)

Cr is the second major visible metabolite peak in the ^1H MRS spectrum at 3.0 ppm. It is the combined peak of Creatine (Creat) and phosphocreatine (PCreat) which together provide an important buffer system of intracellular ATP levels (see section 1.2.2).

1.7.6.1.3 Choline containing compounds

Choline containing compounds (single peak at ~3.22 ppm) include choline, phosphocholine and glycerophosphocholine. In adult human controls choline concentration does not appear to vary in concentration between grey matter and white matter in adult human control frontal and parietal lobes (McLean et al., 2000). In early development Cho is high whilst NAA levels are low. With increasing maturity Cho falls whilst NAA increases (Tkac et al., 2003). The early high levels of

Cho are presumed to be a consequence of rapid cell membrane development (Kreis et al., 1993; Kreis et al., 2002; Kok et al., 2002; Girard et al., 2006a; Girard et al., 2006b).

Elevated Cho levels are now widely recognised as a general marker for neoplastic tissue in the brain as well as in other tissues. Again, the elevation is likely to be due to cell membrane synthesis in rapidly dividing cells (Ross and Michaelis, 1994; Swanson et al., 2001; Yeung et al., 2002; Mueller-Lisse and Scherr, 2007; Papanagiotou et al., 2007). Multiple sclerosis brain lesions are associated with abnormal Cho levels both in acute lesions and in normal appearing white matter (Husted et al., 1994; Rooney et al., 1997) secondary to fluctuations in membrane turnover rates due to inflammatory / demyelinating processes (Arnold et al., 1990).

Cho levels have also been shown to be elevated in malformations of cortical development associated with epilepsy in some studies (Kuzniecky et al., 1997b) although normal findings were observed by other groups (Widjaja et al., 2003). Elevated Cho in the regions of the primitive brain tissue of MCD may be expected from the literature of MRS examinations acquired during early development.

1.7.6.2 Glutamine, glutamate, Myo-inositol

Early proton MRS studies generally reported only the three principal metabolites. Studies performed at shorter TE provide the opportunity to measure additional metabolites relevant to the investigation of brain metabolism. Glutamate and glutamine (resolved at 1.5 Tesla as the combined signal GLX) and myo-inositol (Ins) may be measured using short TE sequences whilst GABA can be measured with advanced pulse sequences that make use of J-modulation effects. As magnet B_0 field strengths and scanner hardware generally improve these metabolites will be measured with increasing reliability and further compounds will also become resolvable.

1.7.6.2.1 GABA, glutamate and glutamine

The metabolism of GABA, glutamate and glutamine has been discussed in a previous section (Section 1.2). All are visible to ^1H MRS performed at short TE, although visualisation of the spectral peaks is made more complicated by overlap with other more dominant peaks and with each other and most researchers have been

obliged to report the combined signal of glutamate plus glutamine (GLX) or to employ more sophisticated methodologies such as spectral editing or J-resolved experiments to measure them directly. There are so far very few reports of the separate measurement of glutamate and glutamine in humans although Petroff has reported separate measurement in the occipital lobes of human volunteers using spectral editing (Petroff et al., 2000) and Garcia has reported separate values in human patients with epilepsy taking valproate examined on a 3T system (Garcia et al., 2009). Several groups have reported on measurement of GABA. Petroff, Rothman and co-workers have published extensively using a spectral editing sequence. The findings of this group are considered in Section 1.8.

1.7.6.2.2 Myo-inositol

Myo-Inositol (Ins) [(cis-1,2,3,5-trans-4,6-cyclohexanehexol)], is a carbocyclic polyol that is the core component of the increasingly important phosphoinositide family of phospholipids. Phosphoinositides act as substrates for the generation of potent intracellular second messengers and as activators of other signalling proteins (for review see (Hammond and Schiavo, 2007)). The central nervous system possesses relatively high concentrations of myo-inositol as well as the means to synthesize it from glucose 6 phosphate. Myo-Inositol serves not only as a precursor molecule for inositol lipid synthesis, but also as a physiologically important osmolyte.

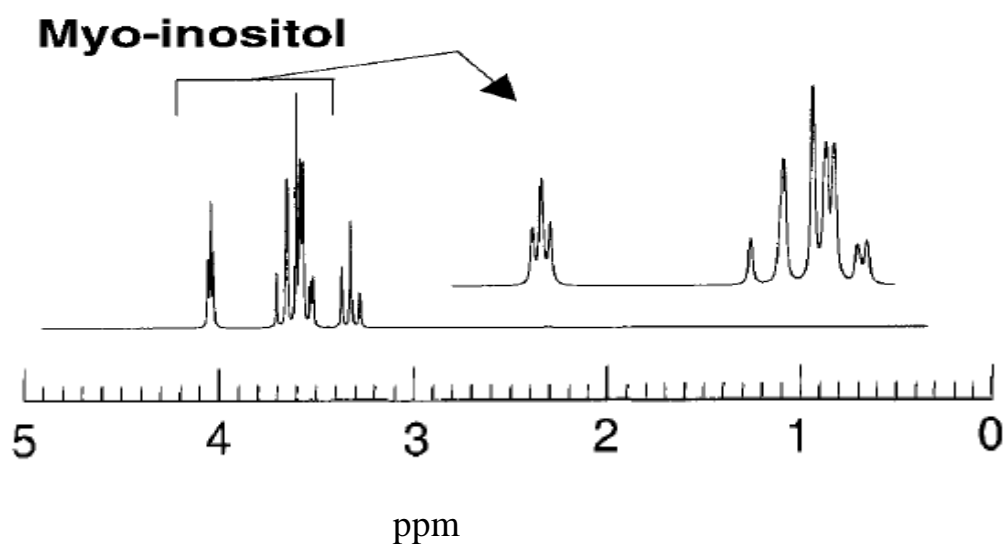


Figure 1.7.6 1H MRS spectrum for myo-Inositol [from (Govindaraju et al., 2000)]

In the first stage of phosphoinositide synthesis Ins is combined with diacylglycerol to form phosphatidyl inositol (PI) with later phosphorylation at the 3, 4 or 5 position

of the inositol ring. The major phosphoinositide in many of the above activities is phosphatidylinositol 4,5-bisphosphate (PI(4,5)P₂). PI(4,5)P₂ is hydrolysed by PI(4,5)P₂ specific phospholipase C (PLC) to yield Ins(1,4,5)P₃ (IP₃) and diacylglycerol (DAG). IP₃ acts as a second messenger to mobilize Ca²⁺ from intracellular Ca²⁺ stores, whereas DAG activates C1-domain-containing proteins, such as protein kinase C (PKC) and MUNC-13 which plays a pivotal role in controlling synaptic vesicle formation (Brose and Rosenmund, 2002; Irvine, 2003). Furthermore, PI(4,5)P₂ is also phosphorylated at position 3 to yield PI(3,4,5)P₃, another important second messenger (Vanhaesebroeck et al., 2001).

Over the past decade a large number of membrane transport proteins have been shown to be sensitive to the action of phosphoinositides in the plasma membrane. These proteins include voltage-gated potassium and calcium channels, ion channels that mediate sensory and nociceptive responses, epithelial transport proteins and ionic exchangers. Each of the regulatory lipids is also under multifaceted regulatory control (Hammond and Schiavo, 2007). Phosphoinositide modulation of membrane proteins in neurons often has a dramatic effect on neuronal excitability and synaptic transmitter release. In astrocytes phosphoinositides have been implicated in the generation of intracellular [Ca²⁺] oscillations and inter cellular signalling (Nedergaard et al., 2003; Nahorski et al., 2003).

The PI system has been the subject of much speculation in parallel with the development of a new understanding of the role of astrocytes in nervous system tissue (Nedergaard et al., 2003; Oberheim et al., 2006). Glial cells have been shown to form non-overlapping domains bordered by small blood vessels. The glial foot processes overlap these blood vessels and also the synaptic terminals of neurons included within the functional domain. This anatomy places the astrocyte at the centre of the interaction between glia, neurons and the blood brain barrier. In this position astrocytes have been shown to modulate synaptic activity, take up and recycle neurotransmitter compounds released at the synaptic terminal, and to regulate the flow of molecules such as water and perhaps glucose through their close association with the blood brain barrier. Current understanding of this functional unit has encouraged speculation that astrocyte function (and dysfunction) may explain a wide range of neurological conditions (De Keyser J. et al., 2008). In particular the phenomenon of cortical spreading depression may be explainable in

terms of astrocytic Ca^{2+} activation with associated synaptic terminal inhibition and this observation together with the release of cyclo-oxygenase by activated astrocytes across the blood brain barrier causing a reactive hyperaemia may neatly explain many of the manifestations of migraine. Epilepsy associated with K^+ channel disorders would also be a potential consequence of primarily astrocytic dysfunction.

Myo-inositol is visible to proton MRS at magnetic field strengths of 1.5T as a single peak at ~3.5 ppm. Early experiments have indicated that this signal is predominantly derived from Ins within the glial pool (Brand et al., 1993) although inositol concentrations in some neuronal populations may equal or exceed those observed for glia.

Interest in the measurement of Ins in humans developed in the field of psychiatry in the late 1980s with the observation that lithium administration is associated with reduction in measurable Ins levels leading to the proposal of an “inositol depletion” theory as a suggested mechanism for the therapeutic effect of lithium (Berridge et al., 1982; Berridge and Irvine, 1989; Berridge et al., 1989). Lithium reduces Ins levels by acting as an uncompetitive inhibitor of inositol monophosphatase (IMPase) resulting in an accumulation of inositol monophosphates and a reduction in Ins concentrations. Subsequent MRS experiments in vivo revealed that Ins decreases following lithium treatment (Moore et al., 1999) and that bipolar patients may have elevated pre-treatment levels of Ins (Davanzo et al., 2001). Later work by O'Donnell (O'Donnell et al., 2003) in rats and in vitro work by Williams (Williams et al., 2002) showed that both lithium and sodium valproate decrease the concentration of Ins, despite the fact that valproate is not known to have any effect on the IMPase enzyme. Ding and Greenberg later reported a study of the effects of valproate and lithium in *saccharoyces cerevisiae* yeast. They found that the addition of either of these agents brought about a decrease in PI synthesis and to a lesser but still significant degree, the steady state relative PI composition (Ding and Greenberg, 2003).

Other work has focussed on the role of Ins as an osmolyte in glial cells. Ins is taken up against a steep concentration gradient (Biden and Wollheim, 1986) via the high affinity sodium myoinositol co-transporter (SMIT) which appears to be highly expressed in astrocytes (Kwon et al., 1992). Chronic exposure to various cell types to

hypertonicity leads to up regulation of SMIT(Ibsen and Strange, 1996). This effect protects the cell since it increases the intracellular Ins concentrations and thus osmolarity without disrupting cellular functioning. Both the activity of SMIT and the expression of its mRNA in astrocytes are down regulated in astrocytes with chronic ingestion of lithium over a period of 8 days (which is similar to the time required for efficacy of the drug).

1.7.6.2.3 Lactate

Lactate metabolism has also been discussed in Section 1.2. Lactate signal is visible to ^1H MRS. The spin-spin coupling of lactate means that the lactate doublet is in phase at TEs of 270ms and mostly in phase at TE less than about 60ms but inverted at TE = 135ms. This characteristic pattern has been utilised in a number of studies that have reported the presence of visible elevation of lactate in ischemia, status epilepticus and mitochondrial encephalopathy(Fazekas et al., 1995;Saunders, 2000;McKnight, 2004;Bianchi et al., 2007). Elevation in lactate has also been reported in healthy volunteers following functional activation(Sappey-Marinier et al., 1992). As noted above for glutamate, glutamine and GABA, two dimensional acquisition techniques are sometimes used to better visualise the lactate peak.

1.7.7 MRS in Healthy Adults

Quantitative in vivo single voxel measurements from occipital grey matter and parietal white matter(Kreis et al., 1993) identified differences between grey and white matter contents of Cr, NAA and Cho. These reports were subsequently confirmed in spectroscopic imaging studies in which volumetric image segmentation techniques allowed separate determination of metabolite content in white matter and grey matter(Hetherington et al., 1996;McLean et al., 2000). McLean measured the differences in metabolite concentrations between grey and white matter in normal volunteers (n = 13). A positive correlation was found between metabolite concentration and grey matter content for most metabolites studied. The estimated ratios of metabolite concentration in grey versus white matter were: N-acetyl aspartate + N-acetyl aspartyl glutamate (NAAt) = 1.16 +/- 0.11; Cr = 1.7 +/- 0.3; glutamate + glutamine = 2.4 +/- 0.5; myo-inositol = 1.6 +/- 0.3; choline = 0.9 +/- 0.2. The ratio of NAAt/Cr was negatively correlated with grey matter content: grey/white = 0.69 +/- 0.08. As well as unequal metabolite distribution between grey matter and white matter there is also some MRS evidence for spatial distribution of the

metabolites through the brain. Pouwels and Frahm(Pouwels and Frahm, 1998) found that N acetyl aspartyl glutamate (a metabolite of NAA) was elevated and Cho reduced in the occipital lobes compared to the frontal lobes in 34 healthy volunteers.

Based upon these findings it is clear that tissue heterogeneity in spectroscopic volumes of interest will impact on the obtained voxel metabolite concentrations. Specifically, due to the lower total Cr content in white matter as opposed to grey matter, inclusions of significant amounts of white matter in predominantly grey matter voxels would lower Cr content and increase NAA/Cr ratio, thereby mimicking more healthy tissue and resulting in false negatives. Similarly, volumes with substantial grey matter, due to higher Cr content, would artificially bias the NAA/Cr downwards, giving the appearance of greater damage.

A number of methodologies have been developed to try to limit the effects of tissue heterogeneity. Linear regression analyses have been developed to obtain metabolite concentration plots for “pure” grey and “pure” white matter content and ratios of the two(Chu et al., 2000). Alternatively volumetric images are acquired and segmented using statistical parametric methods to obtain estimates of the relative proportions of grey matter, white matter and CSF present in each voxel to allow correction to be made for CSF which is considered to return negligible metabolite information and evaluation of the obtained metabolite concentrations in the context of known information relating to the grey matter: white matter ratio in the volume studied(Woermann et al., 1999c;McLean et al., 2000).

1.8 Application of ^1H MRS to the investigation of epilepsy

1.8.1 Introduction

1.8.2 Ex vivo MRS of epileptic tissue

1.8.3 Findings in temporal lobe epilepsy

1.8.4 Findings in extra-temporal lobe epilepsy

1.8.5 Findings in malformations of cortical development

1.8.6 Association of MRS findings with seizure history

1.8.7 Effect of antiepileptic drugs on MRS metabolites

1.8.8 ^{31}P and ^{13}C MRS findings in epilepsy

1.8.9 Correlation of MRS findings with other imaging modalities

1.8.1 Introduction

Most early studies ^1H MRS studies of epilepsy reported on only the three main metabolites NAA, Cr and Cho expressed as ratios and measured at longer TE(NAA/Cr; NAA/(Cr + Cho), NAA/Cho) (see (Duncan, 1996;Kuzniecky, 1999). Later investigators performed MRS experiments at shorter TE which provided additional information on metabolites such as Ins and GLX that are visible only at short TE(Woermann et al., 1999c;Savic et al., 2000a;Savic et al., 2000b;Wellard et al., 2003). From this work a number of common findings have emerged although the wide range in subject selection criteria, acquisition techniques, acquisition parameters and statistical analysis methodology makes integration of these results difficult.

1.8.2 Ex vivo MRS of epileptic tissue

^1H MRS has been successfully applied to the ex vivo investigation of epileptic tissue. Measured at very high magnetic field strength the resulting spectrum allows the discrimination of metabolite peaks that are heavily overlapped at lower field strengths. When such studies have been combined with histopathological techniques direct comparison of the observed metabolite concentrations with measurements of cell content has been possible.

Petroff and co-workers have studied ex vivo epileptic tissue obtained at surgery for medically refractory epilepsy(Petroff et al., 1989;Petroff et al., 1995;Petroff et al., 2002b;Petroff et al., 2003). They found that glutamate content and GABA content were elevated while NAA content was reduced in ex vivo epileptic cortex compared with in vivo measurements in healthy volunteers. After separating the tissue into synaptosomes, neuronal cell bodies and glial cell fractions they reported that the neuronal fractions were enriched in glutamate whilst the glial cell fractions were higher in lactate, glutamine and Ins. MRS of ex vivo hippocampal tissue was combined with histopathological examination(Petroff et al., 2002b;Petroff et al., 2003). Sixteen of 20 hippocampi were abnormal on pre-operative MRI while four had had normal MRI. MRS investigation of the tissue showed reduced NAA compared to reference levels for healthy volunteers with lowest values obtained for those abnormal on MRI. However when NAA, glutamate and Cr concentrations were separately correlated with hippocampal neuron loss no relationship was

observed suggesting that metabolite concentrations do not simply reflect neuronal numbers. There were similarly no correlations between Cr or NAA and glial cell density. Comparisons of NAA versus glutamate and NAA versus Cr showed high correlation coefficients. The authors concluded that the findings appeared to support the proposal that NAA is directly linked with energy metabolism in the neuron.

Vielhaber and co-workers have applied very high field MRS at 14 T to ex-vivo tissue slices from three hippocampal subfields (CA1, CA3, dentate gyrus) in patients with mTLE. The authors again found a large variance in NAA concentrations in the individual regions but particularly noted that in the subfield CA3 there was marked reduction in NAA and elevated lactate despite otherwise moderate preservation of cell densities. The authors conclude that this indicated that reduced NAA is not directly a measure of neuronal cell loss and support the proposal that NAA is linked with mitochondrial function (Vielhaber et al., 2008). This is in agreement with work by Hammen and colleagues who performed an analysis of in-vivo metabolite concentrations according to hippocampal sub-field histopathological findings (Hammen et al., 2008). They also found that cell loss in CA1, CA3 and the dentate gyrus was associated with reduced NAA and further reported that Ins levels were positively correlated with astroglial glial fibrillary acidic protein (GFAP) expression.

There is a very limited literature concerning *ex vivo* MRS of MCD. In a study by Aasly and co-workers histopathological examination identified mild cortical dysplasia in four subjects with associated gliosis in three and MRS examination showed reduced NAA and increased Cho (and GABA) (Aasly et al., 1999).

1.8.3 Findings in temporal lobe epilepsy

A number of excellent reviews of the MRS literature in temporal lobe epilepsy are available [(Duncan, 1996; Duncan, 1997; Antel et al., 2002; Hetherington et al., 2002; Willmann et al., 2006)]. The focus of most studies has been to investigate the role of MRS in the surgical pre-assessment of patients with refractory temporal lobe epilepsy. The data to date appear to suggest that whilst MRS may be useful as an adjunct to other surgical assessments the technique has not become established as a primary assessment tool.

Other imaging tools such as PET and diffusion weighted MRI have also been much investigated in this group of patients. Several authors have compared relative merits of these different techniques in the pre-operative assessment of patients with epilepsy (see Section 1.8.9) but generally these new techniques have yet to become core assessments in pre-surgical assessment protocols.

Prior to widespread ^1H MRS availability phosphorus MRS was applied to the study of these patients. Weiner and colleagues (Laxer et al., 1992) evaluated the use of ^{31}P spectroscopy for the lateralization of epileptogenic regions. In these initial studies at 2.0T, significant alterations in inorganic phosphate (Pi) (73% increase in Pi) and brain pH (0.17 unit increase) were reported. Although subsequent studies at 1.5T and 4.1T failed to reproduce the reported changes in pH, significant alterations in bioenergetic parameters were reported (Kuzniecky et al., 1992; Chu et al., 1996; Chu et al., 1998).

At 1.5T, Kuzniecky reported that PCreat/Pi was reduced by 50% in the ipsilateral temporal lobe, whereas it was reduced by 24% in the contralateral lobe (Kuzniecky et al., 1992). At 4.1T, Chu later reported that PCreat/Pi was significantly decreased in both the ipsilateral (32%) and contralateral lobes (19%). Within this group, 73% of the patients were correctly lateralized using the PCreat/Pi ratio (Chu et al., 1998). Despite the controversy regarding pH changes, bio-energetic impairment (increased Pi and decreased PCreat/Pi) was reported by both groups. Since patients with recent seizures were excluded these effects could reflect a chronic impairment of energy metabolism.

Hetherington and colleagues, using a sophisticated multi-compartment model in order to minimise extraneous signal inclusion, showed that the largest decrements in PCreat/ATP were found overlying the ipsilateral hippocampus (Hetherington et al., 2001) and Simor and colleagues have shown that the pre-surgical abnormalities seen in the contralateral hippocampus are reversible following successful surgery (Simor et al., 1997).

Reduced PCreat/ATP in epileptic tissue which has also been reported in ex-vivo studies of epileptic (Williamson et al., 1995) tissue has been explained by description of the role of the creatine - phosphocreatine equilibrium in maintaining stability of ATP levels by buffering the balance between cellular demand and

production(Williamson et al., 2005). As a result, the ratio of PCreat/ATP determined inter-ictally has been suggested by some authors to represent a “steady-state” energy balance (review Pan(Pan et al., 2008)).

¹H MRS has been used extensively to assess patients with temporal lobe epilepsy. Several groups have attempted to correlate in-vivo MRS findings with histopathological examination performed on resected epileptic temporal lobe tissue(Tokumitsu et al., 1997;Kuzniecky et al., 2001;Cohen-Gadol et al., 2004;Hammen et al., 2008). Tokumitsu and colleagues used an animal model of temporal lobe epilepsy to show reduced NAA and Cr in the presence of neuronal loss and gliosis(Tokumitsu et al., 1997). Hammen also found reduced NAA particularly in the CA1 hippocampal subfield and the dentate gyrus and found correlation of Ins levels with expression of Glial Fibrillary Activated Protein (GFAP)(Hammen et al., 2008). Cohen-Gadol and co-workers found no relationship between NAA/Cr and neuronal cell loss or frequency or duration of seizures(Cohen-Gadol et al., 2004). A similar finding was earlier reported by the same group(Kuzniecky et al., 2001).

Almost all human in-vivo studies have reported on the three main metabolite peaks, have performed investigations at longer TEs and have generally reported metabolite peak ratios. Some investigators have considered that a side-to-side asymmetry in metabolite ratios can reflect significant pathology whilst other groups have reported only on reduced ratios as compared to a control population. The relatively large voxel sizes of MRS experiments has resulted in further methodological variance amongst experimenters as regions of interest have varied in size, location in tissue composition. Findings have generally been concordant but no standard methodology, metabolite peak or metabolite ratio has been uniformly agreed. It is for these reasons that whilst MRS has been generally informative in the work up of patients with TLE the technique has not superceded other imaging modalities or EEG in pre-surgical assessment protocols.

Reduction in NAA and NAA / Cr has been consistently reported in the epileptic temporal lobe in TLE by most groups using either single voxel or multi-voxel techniques and at short and long TE [for example as reported by (Cendes et al., 1994;Connelly et al., 1994;Gadian et al., 1994;Cendes et al., 1995;Hetherington et

al., 1995a;Cendes et al., 1997b;Woermann et al., 1999c;Riederer et al., 2006)]. Most reporters have observed that even in subjects with well lateralised epilepsy on clinical and electrophysiological grounds and concordant unilateral MRI abnormality MRS identifies bilateral reductions in NAA or NAA/Cr in between 20 and 54% of subjects studied(Connelly et al., 1994;Cross et al., 1996;Achten et al., 1997;Cendes et al., 1997b;Woermann et al., 1999c). In those studies that have compared findings in different regions of the mesial temporal lobe a greater sensitivity for abnormality is generally reported in the regions including the anterior structures of the hippocampus compared to the more posterior structures(Vermathen et al., 2000). This is consistent with MRI evidence that hippocampal sclerosis is typically more marked anteriorly(Woermann et al., 1998a). Although most studies have been performed on epileptic subjects with mesial TLE secondary to HS a small number of studies(Connelly et al., 1998;Woermann et al., 1999c;Hammen et al., 2006) have studied patients with normal conventional imaging and found reduction in NAA or NAA/Cr in between 30 to 60% of cases. Patients with bilateral EEG abnormalities seem to have more bilateral 1H MRS abnormalities (Cendes et al., 1997a) and there is some limited evidence to suggest that the more unilateral the EEG finding, the more asymmetric the MRS finding (Cendes et al., 1997b).

Several studies have investigated whether MRS performed prior to temporal lobe surgery will provide prognostic information about post-operative seizure control. Knowlton found that prognosis depended on the presence or absence of ipsilateral hippocampal atrophy but was not influenced by pre-operative MRSI or FDG-PET findings(Knowlton et al., 1997). Antel and co workers reviewed 81 patients selected for temporal lobe surgery that had had preoperative MRI and MRSI (TE / TR 270/2000 ms) and constructed Bayesian predictors of seizure outcome. They found that the asymmetry index of NAA/Cr in the mid temporal region together with the ipsilateral hippocampal volume and hippocampal asymmetry were predictors of “worthwhile” improvement (in 60/63 who had worthwhile improvement)(Antel et al., 2002).

Willmann(Willmann et al., 2006) performed a meta-analysis of patients considered for surgery in published reports between 1992 and 2003 and included 22 studies (Hugg et al., 1993;Cendes et al., 1994;Connelly et al., 1994;Constantinidis et al., 1996;Knowlton et al., 1997;Achten et al., 1997;Ende et al., 1997;Cendes et al.,

1997a;Cendes et al., 1997b;Duc et al., 1998;Thompson et al., 1998;Achten et al., 1998;Kuzniecky et al., 1999;Eberhardt et al., 2000;Li et al., 2000b;Park et al., 2001;Huijin et al., 2001;Stefan et al., 2001b;Kantarci et al., 2002;Antel et al., 2002;Suhy et al., 2002) (Vikhoff-Baaz et al., 2001) in adult patients describing over 600 patients who had in the vast majority of cases MRI evidence of unilateral HS. Even within this carefully selected meta-analysis there was substantial variance in methodology. Across these studies the post operative interval range was from 3 months to 78 months whilst age ranged from three years to 66 years. Chemical shift imaging techniques were used in 15 studies whilst 7 used single voxel techniques. The TE ranged from 50 to 272ms and the repetition time from 1.5 to 6s. Field strengths ranged from 1.5 to 4.1T and the reporting of abnormality differed between sites – usually ratios or asymmetry indexes involving NAA/Cho +Cr, NAA/Cr, NAA/Cho, Cr/NAA and occasionally NAA alone. Voxel placement protocols were not standardised and in general no attempt was made in these studies to make correction for variation in tissue composition within each region of interest. Despite this substantial inter-study heterogeneity Willmann and colleagues were able to make some statements about the performance of MRS in the assessment of patients undergoing surgical resection for TLE. They found that in sixty-four percent of the assessed surgical candidates MRS showed a correctly lateralized decrease ipsilateral to the side of final surgical decision. They calculated that the positive predictive value for good outcome with an ipsilateral reduction in NAA/Cr was 82% and calculated an odds ratio of 4.89 in favour of post operative freedom from seizures with unilateral compared to bilateral metabolite reductions. Few MRI negative studies were included and the authors identified that the data in this group was conflicting. Li and co workers (Li et al., 2000b) reported that in a study of 21 patients with bilateral hippocampal atrophy at MRI temporal lobe NAA/Cr reduction was concordant to the side of major EEG abnormality and surgery in 11 of 16 patients with good outcome. None of the five patients with non-concordant MRS temporal NAA/Cr reduction had a good outcome. The importance of pre-operative normal contralateral temporal lobe NAA/Cr levels has also been noted by other authors (Kuzniecky et al., 1999;Eberhardt et al., 1999;Stefan et al., 2001a). In contrast, successful surgical outcome for a small number of patients with bilateral abnormalities has been reported (Knowlton et al., 1997;Achten et al., 1997). However, since the majority of these studies were performed in patients already carefully assessed with EEG and MRI the added value offered by MRS has been

difficult to quantify(Wallimann et al., 1998). One paper however has indicated that MRS might be more sensitive for the detection of subtle MRI negative cortical malformations(Stefan et al., 2001b) although higher field strength MRI can be expected to now identify more abnormalities in patients with previously labelled MRI-negative MCD.

Post-operative normalisation of the NAA/Cr values in the ipsilateral temporal lobe after surgery for seizure-free patients and post-operative persistence of abnormally low contralateral NAA/Cr values for non seizure free patients has been noticed(Cendes et al., 1997a). Non-significant contralateral NAA recovery and increases of Cho and Cr after surgery in eight seizure-free and two improved patients have been also reported(Vermathen et al., 2002). More abnormal contralateral values were observed post-operatively as compared to pre-operatively by MRS in another five patients whose seizure control worsened after surgery(Eberhardt et al., 1999). Cendes has also reported lower pre-operative NAA/Cr value in the temporal lobe contralateral to surgery for well-assessed patients who continued to have seizures after surgery as compared to patients who became seizure-free(Cendes et al., 1997a).

The value of MRS in predicting medical outcome has been less well studied although there is some evidence from work by Briellmann and colleagues that factors influencing the response to medical treatment may be the degree of reduction in ipsilateral NAA/Cr together with the presence of T2 signal abnormality outside the hippocampus(Briellmann et al., 2005).

The argument for the reporting of metabolite ratios had conventionally been that any inhomogeneity effects would be expected to affect the numerator and the denominator equally. Most ratios involve Cr in accord with the early belief that Cr levels were stable across brain regions. However Cr levels in any region of interest may well vary according to the inclusion of pathological tissue and may be decreased (Ende et al., 1997;Duc et al., 1998) or increased(Connelly et al., 1994) in hippocampal sclerosis. Cr levels will certainly also vary with differing tissue composition between voxels(McLean et al., 2000). Ex vivo findings(Petroff et al., 2003) might predict unchanged or reduced Cr concentrations rather than elevation.

Concentrations of Cho have rarely been reported in these studies but many investigators have used the ratio NAA/(Cr + Cho) to report on metabolite disturbances. Choline containing compound (Cho) concentrations also vary across brain regions (Noworolski et al., 1999) and according to tissue composition of the voxel of interest (McLean et al., 2000). Some groups have reported on Cho levels and suggest that concentrations are increased in TLE associated with hippocampal sclerosis (Connelly et al., 1994; Hammen et al., 2006). Stefan and colleagues have found a high prevalence of co-existence of subtle malformation of cortical development and hippocampal sclerosis in surgical specimens from patient undergoing temporal lobe surgery for mesial TLE (occurring in 13 or 25) (Stefan et al., 2001b) which might explain the elevated Cho since Cho levels appear to be increased in MCD (Kuzniecky et al., 1997b; Aasly et al., 1999).

Few investigators have reported on in vivo concentrations of the metabolites GLX (glutamate plus glutamine) or Ins. Woermann and co-workers observed elevation in GLX concentrations in subjects with TLE and normal MRI but not in subjects with HS (Woermann et al., 1999c) while Savic reported that the ratio GLX/NAA was sensitive for identifying abnormality in the sclerotic temporal lobe (Savic et al., 2000b). Increase in Ins has been reported in the sclerotic hippocampus (Woermann et al., 1999c; Wellard et al., 2003) and has been correlated with increased expression of GFAP (Hammen et al., 2008).

Pan and colleagues have developed a spectral editing sequence at high field strength that can measure hippocampal glutamate concentrations with MRS. This sequence performed in a small number of cases showed higher concentrations of glutamate in hippocampus and temporal lobe cortex compared to temporal white matter and higher glutamate levels in MRI negative patients compared to patients with hippocampal sclerosis (Pan et al., 2006). No studies have reported on MRS measured GABA concentrations in-vivo in TLE.

Several MRS studies have examined for evidence of metabolic disturbance outside the region of seizure localisation (Li et al., 2000a; Mueller et al., 2002; Wellard et al., 2003). Mueller and colleagues used multi-slice MRSI (1.5T, TE/TR 135 / 1800 ms, TI = 170 ms) in patients with unilateral TLE to measure metabolite concentrations in frontal grey and white matter and non-frontal grey and white matter. Volumetric

images were segmented to determine the tissue composition of the spectroscopic voxels. A modest reduction in NAA was identified in the patient group that was bilateral and diffuse (observed in frontal grey matter and non-frontal white matter regions). Li measured 51 patients with focal epilepsy of whom 21 had TLE, 20 had extra temporal lobe epilepsy and 10 had a multi-lobar epilepsy and found reduction in NAA / Cr in more than 40 % that extended beyond the epileptogenic zone defined by clinico-EEG criteria or the structural abnormality defined by MRI. Vermathen has also reported the investigation of 11 subjects with unilateral mesial TLE using MRSI. Metabolite concentrations in 13 extra-hippocampal regions were measured and diffuse reduction in NAA/(Cr + Cho) observed in the regions of interest ipsilateral to seizure onset. A less marked reduction in the metabolite ratio was observed in the contralateral hemisphere(Vermathen et al., 2003). Similar changes have also been described by Hetherington et al who found reduced NAA/Cr in both the ipsilateral and contralateral thalami as well as the contralateral hippocampus(Hetherington et al., 2007).

Memory decline and reduced language skills are associated features of TLE. Using MRS Namer and co-workers found an association between metabolite concentrations (NAA/ (Cr + Cho)) and T₂ relaxation time and verbal and visual memory tasks but found that the reported seizure frequency correlated only with the ipsilateral value of NAA/ (Cr + Cho))(Namer et al., 1999). Sawrie (Sawrie et al., 2001) and Pauli(Pauli et al., 2000) found that left hippocampal Cr/NAA ratios were a sensitive measure of verbal memory dysfunction in TLE and were more predictive of dysfunction than hippocampal volume measurements(Sawrie et al., 2001).

Burneo and co-workers have sought to correlate NAA/Cr with the extent of metabolic dysfunction or with the duration of epilepsy and found no association(Burneo et al., 2004). Other groups have reported association of NAA with seizure frequency in both the frontal lobe and the temporal lobe(Garcia et al., 1997) and Bernasconi has noted that NAA/Cr may be lower in patients with frequent generalised convulsive seizures(Bernasconi et al., 2002).

1.8.4 MRS findings in extra-temporal lobe focal epilepsy

Fewer studies in patients with extra-temporal lobe epilepsy have been reported. Whilst it is generally accepted that mesial TLE secondary to HS is usually

associated with reduced NAA and that “MR Negative” TLE is associated with reduced NAA in approximately one third of subjects, there is no consensus finding for NAA, Cr and Cho in other regions of the brain.

Stanley(Stanley et al., 1998) performed MRSI in 20 patients with extra-temporal lobe epilepsy and measured the ratios NAA/Cr, NAA/Cho and NAA/(Cr + Cho) in a series of voxels in the frontal lobes and in central / post central regions. A diffuse reduction in all three ratios was reported throughout the spectroscopic image as compared to controls, with greatest reduction in metabolite ratios observed in the region of the seizure focus. Wellard et al studied patients with frontal lobe epilepsy and found that Ins appeared to be lower in the frontal lobe ipsilateral to seizure onset but reduced NAA was not observed(Wellard et al., 2003).

Occipital lobe GABA levels (without concurrent measurement of NAA, Cr or Cho) have been reported by several groups using spectral editing techniques. Typically, the recruited patients had extra-occipital lobe focal onset seizures although some studies have included patients with IGE (Petroff et al., 2000); (Petroff et al., 1996b;Petroff et al., 1999a;Petroff et al., 2001a;Mueller et al., 2001b).

The major contribution in this area has been by Petroff and co-workers. They have reported lower mean occipital GABA levels in patients with focal onset epilepsy when compared to healthy volunteers(Petroff et al., 1996b). They have also shown correlation of GABA concentration with increasing seizure control(Petroff et al., 1996b;Petroff et al., 1999a;Petroff et al., 2001a). In their later work they have reported separate resolution of GABA containing compounds into GABA and homocarnosine. When measured separately Petroff reports that it is homocarnosine levels that are particularly linked to seizure control such that levels of this metabolite increase with increasing duration since last seizure(Petroff et al., 2001a;Petroff et al., 2001b). The role of homocarnosine is not established but it is considered likely that it acts as a “reservoir” for GABA(Henry and Theodore, 2001). Petroff and colleagues have also reported that several antiepileptic drugs including vigabatrin, topiramate and gabapentin can increase measured GABA levels in this region (discussed further below).

1.8.5 MRS findings in IGE

Savic used short TE STEAM localised MRS without correction for tissue composition to measure NAA, Cr, Cho and Ins in prefrontal and occipital cortical regions in 15 subjects with JME(Savic et al., 2000a). Reductions in NAA were observed in the prefrontal region compared to the occipital region and 23 control subjects measured in a matched position. This result was taken to provide supporting evidence for the frontal lobe cognitive abnormalities often displayed by patients with JME. Cendes and co-workers have also studied patients with JME and measured reduced NAA/Cr in the thalami compared to levels in a control population(Mory et al., 2003). Using the technique of spectral editing and examining for GABA levels in the occipital lobe Petroff has described reduced combined GABA and homocarnosine levels in patients with JME with 50% of patients having levels more than 2 SD below the control mean. Homocarnosine levels were higher in the JME subjects compared to a group of patients with focal onset epilepsy(Petroff et al., 2001a).

1.8.5 Findings in malformations of cortical development (MCD)

Several MRS studies have examined for neurochemical abnormality in subjects with MCD(Marsh et al., 1996;Kuzniecky et al., 1997b;Li et al., 1998;Simone et al., 1999b;Woermann et al., 2001b). In general the earlier studies reported metabolite ratios at long TE and made variable correction for voxel tissue content. These methodological factors limit the conclusions that can be drawn from their findings. Correction for voxel tissue content is important because voxels containing MRI visible MCD will usually contain a higher proportion of grey matter to white matter than homologous voxels in the contralateral hemisphere. Since it is known that most metabolites have a higher concentration in grey matter than white matter(Doyle et al., 1995;Pouwels and Frahm, 1998;McLean et al., 2000) the composition of the voxels can be expected to influence the interpretation of findings. For example Marsh reported an MRS examination of a single subject with unilateral heterotopia. A “control” voxel was obtained from the contralateral normal appearing hemisphere and asymmetry ratios were given for NAA, Cr and Cho which showed no asymmetry in NAA but elevation of Cr and Cho levels in the heterotopia. In this study it is likely that the heterotopia voxel grey matter proportion would have been higher than in the normal appearing voxel and that if correction had been made

NAA would have been shown to be low in the region of the heterotopia (Marsh et al., 1996).

Kuzniecky measured 11 subjects with MCD (six with focal cortical dysplasia (FCD), three with heterotopia, and two with polymicrogyria (PMG)) at 4.1T (Kuzniecky et al., 1997b). Spectra were obtained from the MRI visible lesion and surrounding grey matter and white matter. The results were presented in the form of the ratios Cr/NAA and Cho/NAA. The subjects with FCD generally showed high Cr/NAA in the lesional voxels as did two of the three subjects with heterotopia. No abnormalities were observed in the two subjects with PMG. The surrounding grey and white matter generally demonstrated a wide variability in Cr/NAA and Cho/NAA ratios. Three of the subjects with FCD went on to have surgical excision of the lesion. Subsequent histopathological examination showed no correlation between cell loss and the preoperative metabolite ratios (Kuzniecky et al., 1997b). Li and colleagues reported an MRSI study on a similar group of subjects (FCD = 5, heterotopia = 12, PMG = 3, tuberose sclerosis = 2 and one subject with PMG and heterotopia). Voxels were analysed in the lesion, contralateral to the lesion and in similar brain regions in healthy volunteers and the ratio NAA/Cr measured in each area and expressed as a z score with respect to the control population normal range. The authors found that for most of the subjects studied there was reduction in NAA/Cr in the lesional (mean = -2.2 +/- 0.32) and perilesional (mean = -1.01 +/- 0.38) voxels. Reduction was most marked for FCD and Heterotopia compared to the subjects with PMG (Li et al., 1998). Simone and colleagues also studied a mixed group of MCD (PMG = 5, heterotopia = 8, FCD = 4). Single voxels were prescribed in the lesion, in the contralateral hemisphere. Grey matter containing voxels and white matter containing voxels in healthy controls were also studied. Reduction in NAA/Cr and Cho/Cr was observed in the lesional voxels compared to control white and control grey voxels. Reduction in Cho/Cr was also seen in the contralateral voxels. Across the sub-groups, PMG showed lower NAA/Cr and higher Cho/Cr than the other MCD sub-types (Simone et al., 1999b).

Woermann and colleagues (Woermann et al., 2001b) reported a MRSI study performed at short TE allowing metabolite quantification. Volumetric MRI studies were also acquired and segmented into grey matter, white matter and CSF to allow the relative proportions of grey matter and white matter in each voxel to be

calculated. Ten subjects with MCD were studied with a mixture of MCD subtypes (polymicrogyria / macrogyria = 6, heterotopia = 4). Voxels were analysed from the lesion, the perilesional area and contralateral normal appearing tissue. An ANCOVA analysis with grey matter proportion as a covariant was performed to correct for variation in voxel tissue composition. Variable levels of abnormality were observed in all regions. The most consistent abnormality in individual subjects was bilateral reduction in NAA, although some voxels showed elevation in NAA. GLX findings were variable in both lesional, perilesional and contralateral voxels with some subjects showing reduction and others showing elevation. Group analysis showed that NAA, Ins and NAA/Cr were reduced in the lesional voxels.

1.8.6 Association of MRS findings with seizure history

A small number of human in vivo studies have investigated the direct effects of a seizure on metabolite concentrations. Seven subjects with TLE were studied in the inter-ictal and post-ictal (within 24 hours) period by Maton with no observed changes in the metabolite ratios NAA/Cr or NAA/(Cr + Cho) suggesting to the authors that this ratio is insensitive to immediate seizure history (Maton et al., 2001b). Cendes measured NAA/Cr ratios in the temporal lobe in subjects during non-convulsive complex partial seizures and in subjects with IGE during a typical absence. The authors found no change in the ratio NAA/Cr but noted an increase in the ratio Lactate/Cr in the focal group (Cendes et al., 1997c). This finding of elevated lactate is consistent with animal studies that have demonstrated elevated brain lactate levels following multiple epileptic stimuli, exogenous glutamate administration, or chemical convulsant administration (Duffy et al., 1975; Chapman et al., 1977; Petroff et al., 1986; Najm et al., 1997; Nepl et al., 2001). Pfund studied 11 patients with medically intractable partial epilepsy with MRS and FDG-PET in the interictal state (N = 11) and later in the ictal / peri-ictal state (n = 4) and found reduced interictal glucose metabolism and reduced GLX concentration in the epileptic focus compared to the contralateral hemisphere but a correlated increase in glucose metabolism and GLX concentrations in the ictal / peri-ictal state suggesting glutamate – glutamine cycle coupling with glucose metabolism (Pfund et al., 2000). There is also a case report (Fazekas et al., 1995) of elevation of GLX and lactate during focal status epilepticus.

Li assessed the relationship between seizure history and inter-ictal NAA/Cr values and found no relationship between NAA/Cr and; a) seizure duration, b) seizure frequency or c) lifetime estimated seizures. The authors also studied 8 subjects with a recent diagnosis of epilepsy before / shortly after commencing antiepileptic medication and 7 months after treatment had been established in 6. Initial NAA/Cr levels were low in 5 of the 8 subjects at the time of the index study and remained low in the follow up study, despite 5 of the 6 followed up subjects becoming seizure free in the intervening period(Li et al., 2000c).

Neppl and colleagues (2001) performed serial post-ictal MRS studies at 0.5T on four adult dogs following induced status epilepticus (duration 30 minutes). They found that compared with pre-status studies there was a 24.7% reduction in Cr, a 15.4% elevation in GLX, and no significant effect on NAA, but they did not describe the time course of metabolite change in the post-ictal period. Possible mechanisms for the measured increase in GLX were proposed: 1) an increase in the synthesis of glutamate and / or glutamine, 2) an increase in the proportion of the more visible glutamine with reduction of the less visible glutamate, and 3) an increase in the MR visibility of glutamate. No explanation for the reduction in Cr was advanced.

Vermathen and workers performed MRSI (1.5T, TE/TR 135/1800 ms) on 10 patients before and after temporal lobe surgery and found a modest increase in NAA post surgery in the contralateral temporal lobe as well as increase to above normal levels of Cr and Cho(Vermathen et al., 2002). Serles measured NAA/Cr pre and post operatively in 16 patients undergoing temporal lobe surgery for refractory TLE. Post-operatively the subjects who became seizure free showed higher contralateral NAA/Cr ratios than those who did not become seizure free and higher values post operatively than pre-operatively. A nonlinear regression model of recovery of NAA/Cr was formulated on the basis of these findings which predicted reversal of neuronal metabolic dysfunction as an exponential function with half-life of 6 months(Serles et al., 2001).

1.8.7 Effect of antiepileptic drugs on MRS metabolites

Several of the newly licensed antiepileptic drugs are thought to modulate GABA function. Vigabatrin irreversibly inhibits GABA-transaminase, the enzyme responsible for the metabolism of GABA to succinic semialdehyde. Gabapentin is

thought to act by increasing the release of GABA from neurons and glia, perhaps by reversal of the GABA transporter, while one of the several modes of action of topiramate is thought to be via the enhancement of GABA_A receptor function. Several groups have demonstrated that the administration of each of these antiepileptic drugs is associated with a demonstrable elevation in GABA⁺ (the combined signal from GABA + homocarnosine) concentrations (Petroff et al., 1996a; Petroff et al., 1998; Kuzniecky et al., 1998a; Petroff et al., 1999b; Petroff et al., 1999c; Petroff et al., 2001b; Mueller et al., 2001b).

This effect is most clearly demonstrated following the administration of vigabatrin. Petroff reported that epileptic subjects taking vigabatrin have GABA⁺ levels more than double the GABA⁺ levels of epileptic subjects not taking this medication (Petroff et al., 1996a). Glutamine levels were also elevated presumably due to blocked metabolism into GABA via glutamate in GABAergic neurons. Petroff later showed that the increase of GABA⁺ occurs within hours of ingestion of a loading oral dose of vigabatrin and is sustained on continued administration (Petroff et al., 1999b). In this study it was also shown that homocarnosine levels start to rise 2 – 3 days following the commencement of Vigabatrin therapy, which might support the proposal that homocarnosine is a “GABA reservoir”. A similarly rapid effect on GABA⁺ and homocarnosine levels was also reported by this group for topiramate (Petroff et al., 2001b), with elevations in GABA⁺ visible within 1 hour of the administration of the first dose of topiramate, and elevations in homocarnosine visible within the first day. Gabapentin was also shown in a small number of subjects to bring about elevation in GABA⁺ that was more marked at high doses of administered drug (Petroff et al., 2000). Whilst these reports did not contain full information about the efficacy of the newly administered antiepileptic drugs, support for an association between elevation of GABA and improved seizure control was later provided by another group (Mueller et al., 2001b). The authors of this study administered vigabatrin to 14 subjects with refractory epilepsy and measured the GABA⁺ level in the epileptogenic hemisphere before drug administration and a second time 1 month after the introduction of the drug. They were able to separate the subjects into three groups (Responders, Partial Responders and Non-responders) in terms of the efficacy of the drug on seizure control. The Responders showed an increase in the GABA⁺/Cr ratio and a low

initial value. The Non-responders showed no change in the GABA+/Cr ratio while the Partial-responders showed a non-sustained elevation in the GABA+/Cr value.

However if these medications are administered to healthy volunteers elevation of GABA+ levels is also seen(Kuzniecky et al., 1998a;Kuzniecky et al., 2002) suggesting that the drugs also cause alteration in GABA+ levels that is independent of the efficacy of the drug in improving seizure control.

Petroff and colleagues have also measured the effects of some of the more established antiepileptic drugs (carbamazepine, phenytoin and sodium valproate)(Petroff et al., 1999d). In a small number of subjects with epilepsy who were taking carbamazepine, phenytoin or valproate as a mono therapy the authors observed similar GABA+ and glutamate concentrations compared with healthy volunteers. In the subgroup taking sodium valproate 3 of 5 subjects showed high glutamine concentrations. The authors noted that raised plasma ammonia levels are observed in some patients taking sodium valproate and that since ammonia is a precursor for glutamine this might be a mechanism for the observed elevation in glutamine. However no blood levels were available on the studied patients to further investigate this possibility.

No drug effects on measured levels of the commonly measured metabolites NAA, Cr or Cho have been reported. However a study of rats treated with valproate or carbamazepine(van Calker and Belmaker, 2000b) identified that these medications reduce measured Ins concentrations. The mechanism for Ins reduction by valproate may be by action on the phosphoinositide Ca^{2+} second messenger system or via inhibition of a cell membrane sodium/Ins co-transporter and it is possible that these mechanisms are shared by carbamazepine. Whether either of these mechanisms could account for some of the anti-seizure efficacy of these drugs has not yet been formally studied.

1.8.8 ^{31}P and ^{13}C MRS findings in epilepsy

^{31}P MRS has also found widespread application to the investigation of subjects with epilepsy (reviewed by (Duncan, 1996)) particularly in the study of temporal lobe epilepsy (as discussed above). Animal studies have shown the relative preservation of pH and ATP levels at the expense of PCr in the course of prolonged

seizures (Petroff et al., 1984; Young et al., 1985). However the necessity for prescription of relatively large volumes of interest (compared even with ^1H MRS) results in heterogeneity of included tissue which limits the interpretation of obtained results: e.g. studies have shown 50% higher levels of PCr in grey matter than in white (Mason et al., 1998). Consequently ^{31}P MRS remains a research tool.

^{13}C MRS techniques are based upon the observation that endogenous levels of ^{13}C in the brain are low and produce negligible signal. Consequently if a labelled metabolite is introduced, any signal that is observed will have arisen from this source. Since ^{13}C metabolite peaks have a wider range of chemical shifts than is observed for ^1H MRS these peaks are more easily resolved. ^{13}C MRS is therefore an appropriate tool for the measurement of flux through different metabolic cycles or between cellular compartments. Rothman and co workers used ^{13}C to measure the rate of flux through the glutamate – glutamine cycle (Rothman et al., 1999; Rothman, 2001; Rothman et al., 2003) and reported that the rate of glutamate – glutamine cycling between the glial and neuronal compartments is proportional to the total rate of glucose consumption (Sibson et al., 1998a; Sibson et al., 1998b; Sibson et al., 2001)

1.8.9 Correlation of MRS findings with other novel imaging modalities

Kantarci and colleagues compared the sensitivity of diffusion weighted MRI (DWI) and MRS for lateralising seizure onset and predicting postoperative seizure control in patients with temporal lobe epilepsy. They found that the hippocampal and temporal stem apparent diffusion coefficient (ADC) measurements were more concordant with electro-clinical findings (correctly lateralising 32/40 and 26/40 respectively) compared to NAA/Cr (18 of 40). However NAA/Cr ratios were the only measures predictive of good surgical outcome (94%) (Kantarci et al., 2002).

Meyer compared ^{18}F -fluorodeoxyglucose (FDG)-PET, MRS (NAA/Cr) and MRI data in 43 subjects with mesial temporal lobe epilepsy. There were no significant differences between the three modalities and their level of concordance with electro-clinical data. However FDG-PET was more predictive of good post-surgical outcome and MRS was more sensitive for abnormality in MR negative cases (Meyer et al., 2001). Knowlton has also compared MRS with FDG-PET finding that PET was the most sensitive single test for the lateralisation of the seizure focus in temporal lobe epilepsy with and without MRI visible abnormality. However, the

combination of MRSI and hippocampal volumetry was as sensitive as PET alone for lateralisation of the seizure focus(Knowlton et al., 1997).

Cross and colleagues compared MRS with interictal SPECT in 14 children with intractable TLE finding hypo-perfusion in one temporal lobe ipsilateral to seizure focus in 10 subjects and lateralised NAA/Cr in 8 of these 10. Of the remaining 4 subjects that showed no regional perfusion abnormality the MRS examination revealed bilateral abnormalities in 3 that were non-lateralising. The authors concluded that the investigations were complementary and that MRS might be more informative in cases where no regional interictal perfusion abnormalities were detectable(Cross et al., 1997).

Chapter 2: Methods

- 2.1 Introduction
- 2.2 Common Methods
 - 2.2.1 Subject recruitment
 - 2.2.2 Volumetric data acquisition and analysis
 - 2.2.3 MRS data acquisition
 - 2.2.4 MRS data processing
 - 2.2.4.1 LCModel
 - 2.2.5 MRS data analysis
- 2.3 Magnetic Resonance Spectroscopic Imaging (MRSI)
- 2.4 Double Quantum Filter (DQF) measurement of GABA
- 2.5 Metabolite nulled measurement of glutamate and glutamine
- 2.6 Post-ictal MRS

2.1 Introduction

Many of the methods relating to subject recruitment, acquisition and segmentation of conventional MRI data, basic MRS acquisition and processing strategies, and data analysis are common to each of the experiments reported in this thesis. To avoid repetition, they are described in detail in the Common Methods section of this chapter and referred to where appropriate in subsequent chapters.

Each Results chapter also involves the application of more advanced techniques. These more specific methodologies are also described later in this chapter, and again referred to where necessary in later chapters.

2.2 Common Methods

2.2.1 Subject recruitment

The patients studied were recruited from the epilepsy clinics of the National Hospital for Neurology and Neurosurgery, Queen Square, London, UK and the National Society for Epilepsy, Chalfont Centre, Chalfont St Peter, UK. Written informed consent according to the declaration of Helsinki was obtained in all cases.

All performed experiments had the approval of The Joint Research and Ethics Committee of The National Hospital for Neurology and Neurosurgery and The Institute of Neurology.

Clinical data and the results of any previous imaging were obtained from the patient hospital notes. Current seizure frequency and time since last seizure were obtained from patients or carers at the time of scanning.

Normal control subjects were all volunteers recruited from the staff population at The National Society for Epilepsy. All controls were free of any significant medical history and in particular reported no personal history or direct family history of epilepsy or epilepsy related illness. They were taking no regular neuro-active medications.

2.2.2 Image data acquisition and analysis

Patients were scanned on a 1.5 Tesla GE Signa Echospeed scanner at the National Society for Epilepsy. Standard departmental epilepsy protocol sequences were acquired for all patients unless the patient had recently undergone such a study as part of a clinical investigation or as part of a different research project. These studies ensured that each patient was given the correct MRI diagnosis and also that there had been no recent development of a second MRI evident pathology. All controls underwent as a minimum an axial inversion recovery prepared fast spoiled gradient echo (IRP-FSPGR) volumetric sequence. The radiological assessment of all the images was performed by two experienced Neuro-radiologists, Dr John Stevens and Dr Brian Kendall.

The standard epilepsy protocol consisted of:

Sagittal T1 weighted localiser. Conventional spin echo sequence (TE / TR = 14ms / 640ms), NEX = 1, slice thickness = 5mm with 2.5 mm gap, field of view (FOV) 24x24cm with a 256x256 matrix, acquisition time = **2 min 47 s**.

Coronal oblique proton density (PD) and T2 weighted. Conventional spin echo, TE/TR/NEX 30&120/2000/1, 28 slices of 5mm thickness with 0 mm gap, FOV 18x24cm with a 256x192 matrix, acquisition time = **1 min 24 s**.

Coronal T1 weighted 3D volume. Inversion recovery prepared fast spoiled gradient recall (IRPFSPGR), TE/TR/NEX 4.2/15.5/1, time of inversion (TI) 450, flip angle 20°, 124 slices of 1.5mm thickness, FOV 18x24cm with a 192x256 matrix, acquisition time = **6 min 56s**.

Coronal oblique fast fluid attenuation inversion recovery (Fast FLAIR). Fast FLAIR sequence, TE/TR/NEX 144/11000/1, TI 2600, 28 slices of 5mm thickness with 0mm gap, FOV 18x24cm with a 192x256 matrix, and orientated perpendicular to the long axis of the hippocampus, **acquisition time = 3 min 10s**.

To this series was routinely added a further volumetric sequence to allow voxel placement and subsequently for segmentation using SPM99 (Statistical Parametric

Mapping; Wellcome Department of Imaging Neuroscience, Institute of Neurology, University College London).

Axial inversion recovery prepared fast spoiled gradient echo (IRP-FSPGR). Images were 124 * 1.5mm thick with field of view (FOV) = 26 cm, and a matrix of 256*128, TE/TI/TR = 4.2/450/16 ms, flip angle 20°, acquisition time = **5 min 47 s**.

2.2.2.1 Voxel segmentation

The methodology of SPM segmentation is well described [www.fil.ion.ucl.ac.uk,(Ashburner and Friston, 2000)]. For the purposes of this programme the MR image is assumed to consist of a number of distinct tissue types (clusters) from which every voxel has been drawn. The intensities of the voxels belonging to each of these clusters conform to a multivariate normal distribution which can be described by a mean vector, a covariance matrix, and the number of voxels belonging to the distribution. These parameters are estimated through a series of iterative computations by comparison with an a priori approximate knowledge of the spatial distributions of these clusters in the form of probability images which have been derived from MR images of a large number of subjects. These template images were segmented into binary images of grey matter (GM), white matter (WM) and cerebro-spinal fluid (CSF) and all normalised into the same space using a nine parameter affine transformation. The probability images are the means of these binary images so that they contain values in the range of 0 to 1 which represents the probability of a voxel being GM WM or CSF after an image has been normalised to the same space using a nine parameter transformation.

SPM99 was applied in each of the MRS experiments in this thesis. Classification of pixels as CSF, GM or WM was not forced. For example, if a pixel was reported as having a 54% probability of being GM, 10% CSF, and 36% WM, the pixel was assumed to have contained various tissues in approximately these proportions.

MRS experiments examine a localised volume of interest (VOI) from which the concentrations of relevant neuro-metabolites are measured. In order to determine the tissue composition of the prescribed VOI the IRP-FSPGR volumetric whole brain images are first segmented as above. The co-ordinates of the prescribed VOI are then given to a locally developed programme written in SAGE 7.0 (the GE MR

spectroscopy software package, based on the Interactive Data Language (IDL: www.itvis.com/IDL) that averages the estimated content of GM, WM, and CSF from within the VOI.

In the ideal situation a VOI would be sufficiently small to allow for the exclusive measurement of a single tissue type. However VOI are limited by the available signal to noise ratio (SNR) as outlined in Equation 1.7.5. Therefore at present in vivo MRS experiments are limited to a minimum VOI of approximately 5 ml (for $B_0 = 1.5$ T, scan duration = 5 min) and consequently the prescribed volume will usually have a heterogeneous tissue composition. It is important that the effects of this heterogeneity are recognised because metabolite concentrations are different in pure grey matter compared to pure white matter voxels (Hetherington et al., 1996; McLean et al., 2000) and may vary in concentration across brain regions (Pouwels and Frahm, 1998). The major differences are between GM or WM and CSF since CSF has negligible metabolite content (Lynch et al., 1993). Comparison of MRS VOI between regions that contain different amounts of CSF can therefore lead to the introduction of partial volume error.

Because of this potential error it has become a standard practice of the NSE MRS group to correct the obtained metabolite concentrations for the presence of CSF which will not have contributed to the final metabolite signal such that:

$$[\text{Metabolite}]_{\text{corrected}} = [\text{Metabolite}]_{\text{measured}} * 1 / (1 - \text{CSF}_{\text{proportion}}) \quad \text{[Eqn. 2.2.1]}$$

Most metabolites have a higher concentration in grey matter than in white matter (Doyle et al., 1995; McLean et al., 2000). In order to correct for this further source of partial volume error the GM proportion obtained from the segmentation process may be used as a covariant in statistical comparisons that compare subjects or groups with different grey matter proportion estimates

2.2.3 MRS data acquisition

This thesis describes single voxel and multiple voxel MRS acquisitions. All studies measured the concentrations of the main metabolites visible at short TE, i.e. NAA, Cho, Cr, GLX and Ins obtained with standard acquisition parameters (TE/TR =

30/3000 ms). The number of averages varied between studies and depended on the trade off between sequence duration and signal to noise requirements in each case.

Voxel placement was from axial volumetric FSPGR images and magnetic field inhomogeneities were minimised using automated gradient shim procedures.

Water suppression was achieved using a series of 3 chemical shift selective (CHESS) pulses. The CHESS sequence entails the application of a frequency selective excitation of water through 90^0 with subsequent dephasing of the transverse magnetisation with a crusher gradient.

VOI localisation was performed using the standard PRESS sequence as described in chapter 1.7.3.5.

2.2.4 MRS data processing

Following localisation the free induction decay (FID) signal is collected without a readout gradient. There are several methods of analysing the FID to allow visualisation of the metabolite peaks. The data can be analysed in the time or, following Fourier transformation, in the frequency domain, and each technique has its own relative merits. In this work all spectral processing was performed in the frequency domain. The GABA+ signal was analysed by locally written programme in SAGE 7 described in Section 2.4. Processing of all other spectra was by the application of LCModel which is an established MRS software package that allows semi-quantitative estimation of metabolite concentrations(Provencher, 1993;Provencher, 2001).

2.2.4.1 LCModel

The LCModel method analyzes an in vivo spectrum as a linear combination of model in vitro spectra from individual metabolite solutions. Complete model spectra, rather than individual resonances, are used in order to incorporate maximum prior information into the analysis. A nearly model-free constrained regularisation method automatically accounts for the baseline and line shape in vivo without imposing a restrictive parameterized form on them. LCModel is automatic (non-interactive) with no subjective input. Approximate maximum-likelihood estimates of the metabolite concentrations and their uncertainties (Cramer-Rao lower bounds) are

obtained. The method has also been shown to deal robustly with a series of potential causes for quantification failure such as the inclusion of excessive water signal following imperfect water suppression.

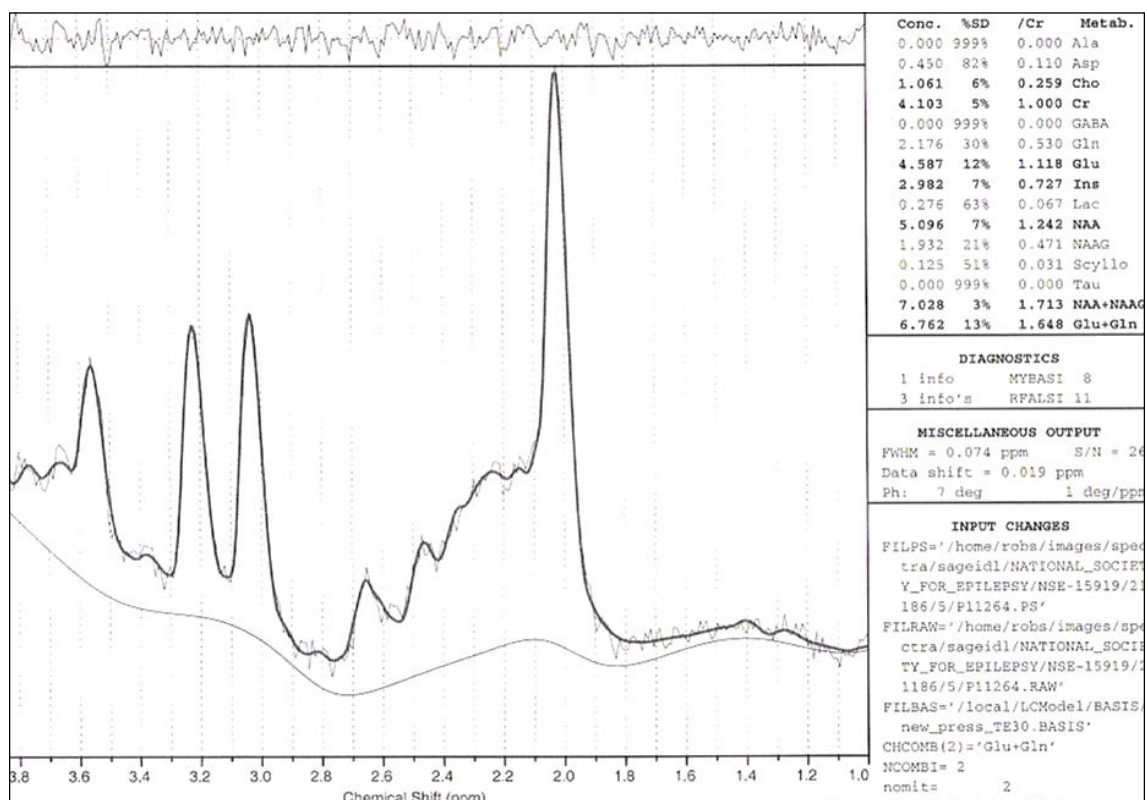


Figure 2.2.2 Typical LCModel output acquired in a patient with IGE examined in the right frontal lobe with TE/TR = 30ms/3000ms and showing LCModel estimates for the obtained metabolite concentrations in the upper right hand section of the output. The estimated baseline is shown below the obtained spectrum as are the residual deviations of the true data from the estimated plot (shown above the spectrum).

In order to calibrate the concentrations for local machine performance, and to monitor any possible fluctuations, an 8 cm diameter spherical phantom containing 50 mM NAA was scanned on a weekly basis. It was kept refrigerated between uses and always scanned directly after removal from the refrigerator to minimise error due to fluctuations in sample temperature. An 8.13 cc PRESS voxel was prescribed graphically in the centre of the sphere, which was positioned in the centre of the head coil. The acquisition (TE/TR/number of averages/scan time = 30ms/3s/256/13 min 46s) reported the obtained NAA concentration with a very high SNR (≥ 100) and a low estimated Cramer-Rao uncertainty ($< 2\%$). This weekly quality assurance measurement was necessary to allow recalibration to correct for any drift in local

machine performance over time and to allow the reliable comparison of results obtained from repeated scans.

2.2.5 MRS data analysis

LCModel reports the concentrations of the modelled metabolites for each studied VOI. Before statistical comparison can be made these concentrations are then corrected for partial volume error due to the inclusion of CSF in the VOI according to equation 2.2. Further metabolite concentration correction was made for the multi-voxel data as described below (Section 2.3).

All statistical comparisons were made using the scientific statistical package SPSS9.0. To account for variation in VOI GM/WM relative content, further analysis was then made using an ANCOVA analysis using GM as a covariant in two of the reported experiments in the next Chapter (Section [3.1] and [3.5]).

2.3 Magnetic Resonance Spectroscopic Imaging (MRSI)

The term MRSI refers to a technique in which spatial information is encoded by magnetic field gradients (phase encoding). The number of encodings required is equal to the desired number of pixels in the spectroscopic image. The data is encoded in k (phase) space. A multi-dimensional Fourier transformation will then return a spectrum for each pixel.

Chapter 3 of this thesis [Section 3.1] reports the findings of an MRSI experiment investigating metabolite variation in the temporal lobes in temporal lobe epilepsy. The methodology for this study is described in more detail elsewhere (McLean et al., 2000; McLean et al., 2001) but the main details are outlined here.

Analysis of regions of interest (ROIs) was performed using LCModel Interactive (McLean et al., 1999; McLean et al., 2000), a locally developed program in Sage/IDL. The program allows the user to define a ROI by drawing with a cursor on a reference image and then extracts voxels that are aligned with the VOI for analysis using LCModel. This allowed the comparison of anatomically matched voxels between hemispheres and between subjects.

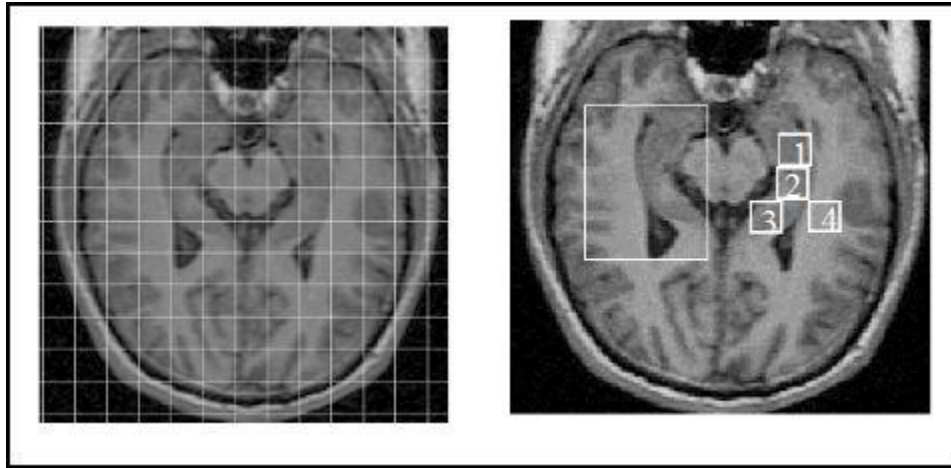


Figure 2.3.1: Axial T1 weighted images of a control patient showing the hippocampal formations bilaterally. The interactive software allowed regions of interest (ROI) to be drawn on the reference image using a cursor. For each ROI, the program then extracted all the spectra within its boundaries after voxel shifting in 2 dimensions to maximise inclusion. The image on the left shows the chemical shift imaging grid at acquisition prior to voxel shifting using LCMoDel Interactive. The right hand image shows the prescribed volume of interest in the right temporal lobe and the final acquired ROIs along the hippocampus and in the adjacent lateral temporal lobe.

Fourier transformation was performed without zero-filling or apodisation. Approximate zero-order phase was applied in order to provide a good starting point for LCMoDel, which optimizes the phase for each individual spectrum. Additionally, to account for frequency shifts across the FOV, peak registration was performed on the singlet peak of NAA. The size and location of the excitation region (ROI) was read from the raw MRSI file header and only spectra within it were extracted for processing and the metabolite concentrations for those voxels outside the ROI were set to zero. A queuing system was established using LSF (Load Sharing Facility: Platform Computing Corporation, <http://www.platform.com>) in order to send LCMoDel jobs to six SUN computers, two of which had dual processors. After completion of peak fitting, another locally developed program was run to read the postscript output and produce Sage/IDL datasets of the metabolite concentrations.

Several further corrections to the data were then made. This was necessary because the volume of interest was comparatively large and any variation in the slice excitation profile across the excitation region could be expected to produce artifactual variation in metabolite concentrations. The data was also corrected for known chemical shift artefact (CSA) across the region. CSA arises from the

differing neuro-metabolite chemical shifts. This causes the excited region of interest for one metabolite, for example NAA, to be slightly shifted with respect to the excited slice for another with a different chemical shift, for example Ins. The amount of this loss of spatial alignment is proportional to the relative difference in their chemical shifts. Therefore comparison of metabolite concentrations from a region must take into account that the regions of interest evaluated for each metabolite are not completely coincident. In most single voxel studies CSA is a small effect and can be ignored. However in MRSI studies where the excitation ROI is subdivided into smaller voxels of interest this effect can become more important and needs to be considered as part of the data interpretation.

To correct for imperfect slice profiles, two images of the MRSI slab were acquired using PRESS localisation: one image with the voxel placed as for MRSI, and one with the voxel the same size as the FOV. Scanning time was 1:20 per image (TE/TR = 35/500, imaging matrix = 256*160, interpolated to 256²). The ROI image was divided by the FOV image to produce a map of the PRESS excitation profile in two dimensions. The average pixel intensity of the excitation profile image over the region corresponding to each MRSI voxel, as a fraction of the theoretical maximum (FPRESS) was used to correct for signal loss:

$$[\text{Metabolite}]_{\text{corrected}} = [\text{Metabolite}]/\text{FPRESS} \quad [\text{Eqn. 2.3.1}]$$

To correct for chemical shift artefact (CSA), this image was translated in both in plane dimensions by a number of pixels for each metabolite calculated from:

$$\text{CSA correction} = (\sigma B_0/G) * (256/\text{FOV}) \quad [\text{Eqn. 2.3.2}]$$

In this equation, B_0 is the field strength (1.5T), G is the calculated gradient amplitude along the axis in mT/m, and the factor 256/FOV converts from metres to pixels.

2.4 Double Quantum Filter (DQF) measurement of GABA

Despite a ¹H MRS visible GABA concentration of approximately 1.5mmol/l, in vivo GABA can at present only be directly measured at very high magnetic field strengths (Tkac et al., 2003). At lower field strengths the three GABA multiplets are

heavily overlapped at 1.9 ppm, 2.3 ppm and 3.0 ppm by other metabolites such as creatine plus phosphocreatine (Creat) at 3.0 ppm, by glutamate and glutamine at 2.3 ppm and by NAA at 2.0 ppm and more generally by the macromolecule baseline in short TE acquisitions. Therefore a number of different MRS techniques have been applied to simplify or edit the spectrum to allow resolution of GABA. The general characteristics of these methods have been described in some detail in Section 1.7. Most studies have been designed to allow measurement of the γCH_2 resonances at 3.0 ppm. This resonance is most amenable to examination because it is overlapped by the singlet Cr resonance which does not exhibit spin-spin (J) coupling. Such techniques then use selective modulation of the J-coupling to suppress or subtract the Cr resonance.

In this thesis I have applied a double quantum filter (DQF) technique to edit the spectrum to measure GABA concentrations in patients with focal epilepsy and idiopathic generalised epilepsy. Several regions of the brain have been studied. The technique allows a “single shot” measurement of GABA and thus reduces the possibility of cancellation errors that may arise following patient movement and other instabilities when using subtraction methods. However a filter efficiency of only ~30% makes SNR calculations an important factor in the design of the experiment.

The resulting “GABA” peak will however include at low intensity other compounds such as homocarnosine, glutathione and some macromolecule signal. The filtered GABA measurements are therefore designated as GABA+. GABA concentrations obtained by spectral editing similarly include homocarnosine and some macromolecule signal.

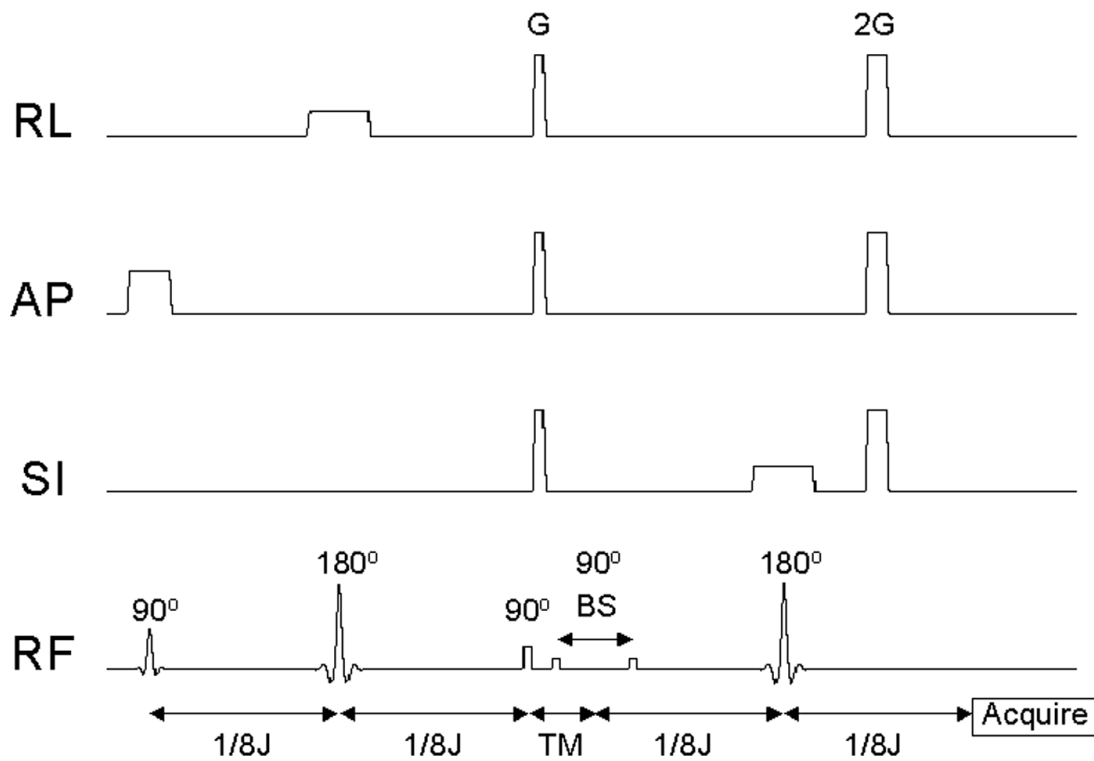


Figure 2.4.1: The Double Quantum Filter GABA+ sequence. For simplicity, the initial water suppression, outer volume suppression, and associated slice-selective crusher gradients are not shown. The total TE was 68 ms ($1/2J$ for $J = 7.35$ Hz). The optimum value for the time TM between the hard 90° pulse and the centre of the binomial read pulse was found to be the minimum obtainable (6 ms). The binomial spacing (BS) was set at 7 ms (McLean et al., 2002).

A simplified version of the DQF pulse sequence is shown above (**Figure 2.4.1**). Multiple quantum coherences are created in the coupled metabolites by the first three pulses (90° , 180° , 90°).

After a period of evolution, TM, these multiple quantum coherences are converted back to observable single quantum coherences by a frequency selective binomial 90° pulse with 7-ms spacing, tuned to the βCH_2 GABA resonance at 1.9 ppm to allow an increase in theoretical efficiency for the γCH_2 by transferring the magnetisation from the βCH_2 to the desired γCH_2 resonance.

The filter gradients, G and 2G, are applied to select only the double quantum coherences. The phase of the double quantum coherence evolves twice as fast as a single quantum coherence therefore only those spins that experienced the first

gradient as double quantum coherences will have zero net phase difference when the signal is acquired.

This DQF sequence is based upon a sequence reported by Keltner and colleagues (Keltner et al., 1997). A full description of the calibration of the filter and evaluation of the filter efficiency can be found elsewhere (McLean et al., 2002). The filter yield of GABA relative to an unfiltered PRESS experiment at a TE of 136 ms was 38.5% with the area of the peak at 2.9 ppm alone estimated to be 16% of the total unfiltered GABA area. The Cr singlet suppression factor was found to be on the order of 1000.

Although, *in vivo*, the 3.1 ppm peak of the γCH_2 multiplet is partially obscured by macromolecular contamination the 2.9 ppm peak is relatively free of macromolecular contamination (forming <10% of the measured area). This degree of contamination is not negligible, but is less than that found in other spectral editing experiments for which macromolecule signal may contribute up to 30% of the resulting “GABA+” peak (Rothman et al., 1993).

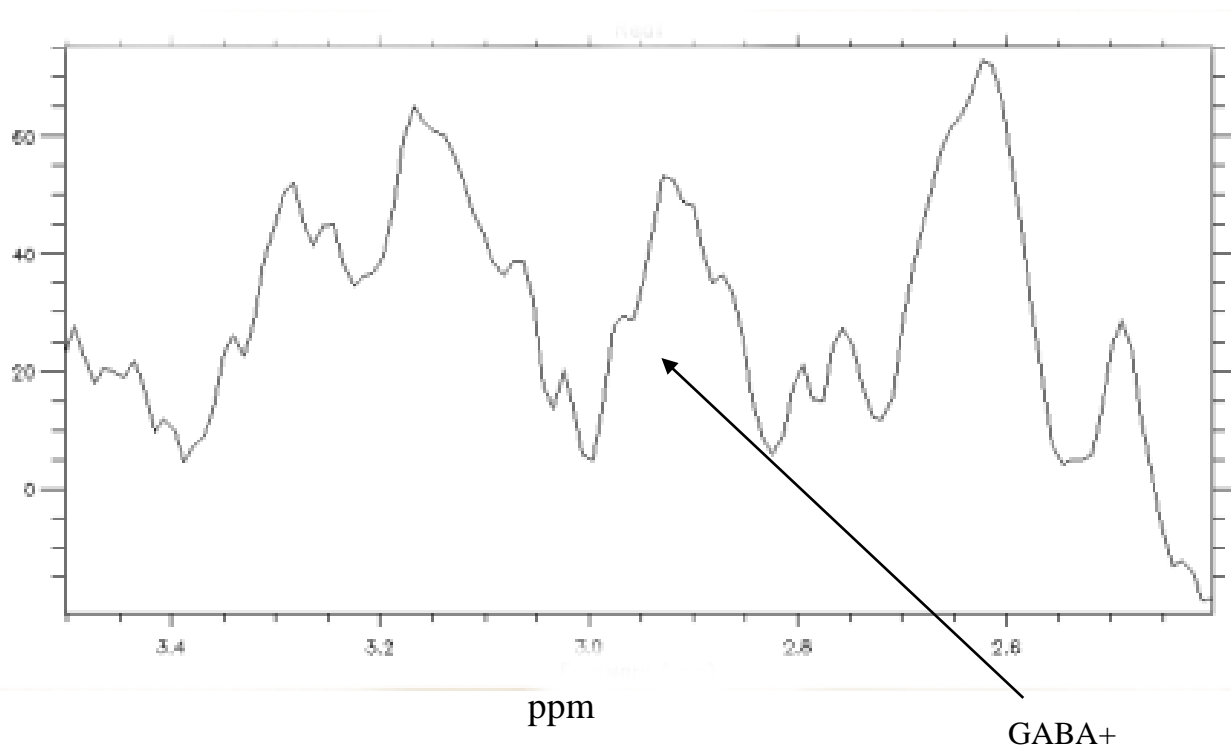


Figure 2.4.2: Typical GABA+ signal following application of DQF sequence

VOI localisation was achieved using slice selective gradients on the first 90° pulse and the two 180° degree pulses. Spectra (TE = 68 ms, TR = 2000ms) were initially acquired with the filter off (1 min) then the DQF filter was applied with the same TE/TR and 512 averages were collected (scan time = 17 min) to measure GABA+. Conventional PRESS localised spectra (TE/TR = 30 / 3000ms) were also acquired during the same examination.

The conventional PRESS spectra at TE =30 ms were analyzed using LCModel. The spectra acquired at TE = 68 ms without the DQF filter were also analyzed using LCModel, in order to obtain a consistent fit to the small baseline still present at this TE. However, the DQF spectra could not be analyzed in this way, so the concentrations of Cr at TE =68ms reported by LCModel were then converted back to peak areas for comparison with DQF spectra.

Since DQF spectra are a mixture of low SNR peaks with varying relative phases it is necessary to ensure that the final spectrum is consistently phased before peak measurement. This is achieved by employing a programme written in General Electric's Sage/IDL processing package to automatically phase the spectra by maximizing the integrated area between 2.4 and 3.8 ppm. The peaks in this region of the DQF spectrum are consistently in phase with the GABA resonance at 3.0 ppm (Figure 2.4.2).

Finally, GABA+ is quantified by taking the ratio of the integrated peak at 2.9 ppm relative to that of Cr without the filter at the same TE (68 ms), correcting for the filter yield and for the number of protons contributing to each resonance (two for GABA, and three for Cr). Conversion to mM concentration is then performed by taking the concentration of Cr from the short TE LCModel analysis and according to:

$$[\text{GABA}^+] = [\text{Cr}] * (\text{AreaGABA}^+ / \text{AreaCr}) * 3/2 * 1/\text{Yield}. \quad [\text{Eqn. 2.4.1}]$$

Where AreaGABA+ = the integrated area of the GABA+ multiplet peak at 2.9 ppm (TE = 68ms), AreaCr = the estimated area of the Cr peak at the same TE and Yield was determined from phantom experiments as 16%.

In some subjects the quality of the DQF spectrum was not sufficient to allow reliable measurement of the GABA+ peak necessitating the development of objective exclusion criteria. In this thesis GABA+ measurements were made in several regions of the brain, producing DQF spectra of differing quality from region to region. Therefore the exact exclusion criteria in each study vary slightly, the details of which are provided in the relevant Results chapters.

2.5 Metabolite nulled measurement of glutamate and glutamine

As described in Chapter 1, performing short TE MRS/MRSI allows the potential measurement of metabolites such as glutamate and glutamine that are of interest to the study of epilepsy, as well as Ins which may be an important marker of glial activity. However as the TE is reduced the macromolecule baseline becomes more difficult to model. There are four broad macromolecule peaks appearing at roughly 0.9, 1.3, 2.4 and 3.2 ppm and at TE = 30ms the macromolecule signal accounts for approximately 30% of the total signal. In particular the 2.4 ppm macromolecule peak underlies the glutamate and glutamine signal which reduces the reliability of estimation of these metabolites, even as the combined peak GLX (Behar et al., 1994; Soher et al., 2001).

Suppression of this macromolecule background has been shown to improve discrimination of the individual metabolites (McLean et al., 2004). This can be particularly useful when VOI are unavoidably placed close to the scalp and the resultant spectra incorporates artifactual macromolecule signal from outside the VOI. In Section 3.5 I describe the results of GABA+ measurement in the temporal lobe of patients with hippocampal sclerosis and TLE. This experiment required prescription of large VOI with outer boundary close to the brain surface and to minimise this potential source of error the study design incorporated the macromolecule suppression sequence (McLean et al., 2004).

This sequence discriminates macromolecule signal from neurochemical signal through their different spin-lattice (T_1) relaxation times. Macromolecules are relatively immobile and consequently their protons have much shorter T_1 . The prescription of an inversion pulse prior to the acquisition sequence can allow either the signal due to the macromolecule baseline or the signal due to the small mobile metabolites to be suppressed.

Practically it is more convenient to suppress the small metabolite signal than the macromolecule signal because an inversion pulse tailored to suppressing the macromolecule signal would also lead to significant loss of signal for the metabolite peaks and the short inversion times needed would be difficult to combine with efficient water suppression.

The basic methodology is as follows. Two spectra are acquired for each VOI. The first is obtained using a standard MRS acquisition (TE/TR = 30/3000 ms) and includes both small metabolites and the broad macromolecular baseline. A second acquisition is then performed that is preceded by an inversion pulse calculated to minimise the metabolite peaks. The final “macromolecule nulled spectrum” is the edited spectrum of the first acquisition minus the second (“macromolecule only”) acquisition. The edited spectrum can then be analysed as previously using LCModel.

The timing of the inversion pulse (TI) was determined from a pilot series of in vivo acquisitions with variable TI times that had been calculated to be close to the theoretical minimum of:

$$S/S_0 = 1 - 2 * \exp(-TI/T_1) + \exp(-TR/T_1) \quad \text{[Eqn. 2.5.1]}$$

Where S/S_0 is the fraction of signal that remains for a given inversion time TI and metabolites with a given T_1 relaxation (McLean et al., 2004).

This method which was validated in 10 healthy volunteers (McLean et al., 2004) has been shown to reduce the LCModel measured Cramer-Rao lower bounds of uncertainty for all the metabolites of interest, including glutamate, glutamine and GLX.

The method of subtracting the macromolecule signal from the standard spectrum does result in loss of SNR. However, in the experiment in which macromolecule suppression was used a large VOI was chosen ensuring sufficient SNR in all cases.

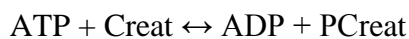
2.6 Post-ictal MRS

The final experiment performed in this thesis was an investigation of transient metabolite disturbance in the immediate post-ictal period [3.7]. A previous in vivo human study had reported that metabolite ratios might show dynamic changes during the post-ictal period (Maton et al., 2001b) and one animal study had noted a change in individual metabolite concentrations in this period (Neppel et al., 2001). For obvious technical reasons only case reports exist of measurement during a seizure and these also have suggested that there is dynamic metabolite change (for example (Fazekas et al., 1995))

In this experiment an additional sequence was added to the basic protocol. This sequence was a standard MRS acquisition performed at longer TE (TE=144ms) than was used for the metabolite nulled experiment (TE = 30ms). The addition of this sequence allowed the examination of post ictal changes in the ratio:

$$[\text{Cr}]_{\text{TE}=30\text{ms}} / [\text{Cr}]_{\text{TE}=144\text{ms}}$$

Recent work had suggested that Creat and PCreat have different T_2 relaxation times with the phosphocreatine signal decaying faster with increasing TE (T_2 for PCreat and Creat = 117 +/- 21 ms and 309 +/- 21 ms respectively) (Ke et al., 2002). Since Creat and PCreat act to buffer ATP according to:



in the immediate post ictal period there is relative shift of this reaction to the left with relative reduction of the contribution that phosphocreatine makes to the combined concentration of Cr which stays relatively constant. At short TE this relative increase in PCreat will make little difference to Cr. However at long TE the increased creatine component of Cr will cause it to decay more slowly and show relatively more signal compared to the resting state where PCreat and Creat will be more evenly balanced. In this circumstance the ratio $[\text{Cr}]_{\text{TE}=144\text{ms}} / [\text{Cr}]_{\text{TE}=30\text{ms}}$ should be increased in the post ictal state compared to the interictal state.

An additional advantage of adding this longer TE sequence was to allow for comparison of any findings in the study with the limited existent literature which used longer TE.

Chapter 3: Results

3.1 Multi-voxel MRSI in TLE

3.2 MRS in the Occipital lobes in IGE and OLE

3.3 MRS in the Frontal lobes in IGE

3.4 MRS in Malformations of Cortical Development

3.5 The effect of Sodium Valproate on MRS Measured Metabolites

3.6 MRS in TLE post Temporal Lobe Surgery

3.7 MRS in the immediate post ictal period

3.1 A Short Echo Time Proton Magnetic Resonance Spectroscopic Imaging Study of Temporal Lobe Epilepsy.

ABSTRACT:

Purpose:

Short echo time proton Magnetic Resonance Spectroscopy Imaging (MRSI) was used to study metabolite concentration variation through the temporal lobe in patients with temporal lobe epilepsy (TLE) with and without abnormal MRI.

Methods:

MRSI was performed at TE=30ms to study 10 control subjects, 10 patients with TLE and unilateral hippocampal sclerosis and 10 patients with TLE and unremarkable magnetic resonance imaging (MRI negative). Concentrations of N-acetyl aspartate + N-acetyl aspartyl-glutamate (NAAt), creatine (Cr), choline (Cho), glutamate + glutamine (GLX), and myo-inositol were measured, in the anterior, middle and posterior medial temporal lobe (MTL), and in the posterior lateral temporal lobe. Segmented volumetric T₁ weighted MR images gave the tissue composition of each MRSI voxel. Normal ranges were defined as the control mean +/-3 SD.

Results:

In the hippocampal sclerosis group seven of 10 had abnormally low NAAt, in the ipsilateral anterior MTL. In the MRI negative group four of 10 had low NAAt in the middle MTL voxel ipsilateral to seizure onset. Metabolite ratios were less sensitive to abnormality than NAAt concentration. Group analysis showed low NAAt, Cr and Cho in the anterior MTL in hippocampal sclerosis. GLX was elevated in the anterior voxel contralateral to seizure onset in the MRI negative group. Metabolite concentrations were influenced by voxel position and tissue composition.

Conclusions:

(1) Low NAAt, Cr and Cho were features of the anterior sclerotic hippocampus whilst low NAAt was observed in the MRI negative group in the middle medial temporal lobe region. The posterior temporal lobe regions were not associated with significant metabolite abnormality. (2) The two patient groups demonstrated

different metabolite profiles across the temporal lobe with elevated GLX a feature of the MRI negative group. (3) Voxel tissue composition and position influenced obtained metabolite concentrations.

Published ref: (Simister et al., *Epilepsia* 2002 **43**, 1031-1041)

3.1.1 Introduction

The value of single voxel proton Magnetic Resonance Spectroscopy (MRS) and Magnetic Resonance Spectroscopy Imaging (MRSI) has been demonstrated in the evaluation of patients with temporal lobe epilepsy (TLE) (Hugg et al., 1993; Cendes et al., 1994; Connelly et al., 1994; Cendes et al., 1995; Hetherington et al., 1995a; Hetherington et al., 1995b; Cross et al., 1996; Vermathen et al., 1997; Achten et al., 1997; Cendes et al., 1997b; Kuzniecky et al., 1998b; Woermann et al., 1999c; Chu et al., 2000; Li et al., 2000b) (Cross et al., 1996; Vermathen et al., 1997; Achten et al., 1997; Kuzniecky et al., 1998b; Woermann et al., 1999c; Chu et al., 2000; Li et al., 2000b) and may identify more abnormalities than magnetic resonance imaging (MRI) volumetry and relaxometry (Cendes et al., 1997b; Kuzniecky et al., 1998b). This could provide important information in the pre-surgical evaluation of patients who have TLE and normal quantitative MRI and those with apparently bilateral pathology (Li et al., 2000b).

The principal advantage of MRSI is that it offers the opportunity to examine regional variation of metabolite concentrations. This may allow improved localisation of the pathological focus and an assessment of the extent of metabolic abnormality outside the clinical and EEG-defined primary epileptogenic area (Li et al., 2000a). There are no other published MRSI studies that report quantification of each of the metabolites (NAA, Cho, Cr, Ins and GLX) through the temporal lobe in controls and patients with TLE. This is because of the technical difficulties of MRSI in this region of the brain, particularly due to the proximity to air spaces, incomplete water suppression and field inhomogeneity. The majority of MRSI studies of the temporal lobes have also used a longer TE (Vermathen et al., 1997; Cendes et al., 1997b) or have only reported ratios of the three main metabolites (Hetherington et al., 1995a; Kuzniecky et al., 1998b).

The aim of this investigation was to apply quantitative MRSI to compare metabolite concentrations at different positions of the temporal lobe for patients with TLE and hippocampal sclerosis (HS) and patients with TLE and normal MRI (MRIN) in comparison with healthy volunteers.

3.1.2.0 Methods

3.1.2.1 Subjects

Ten control subjects and 20 patients with intractable TLE were recruited and investigated as outlined in section 2.2. Ten patients had a MRI diagnosis of unilateral hippocampal sclerosis and 10 had unremarkable MRI scans on visual inspection and according to accepted quantitative criteria (Woermann et al., 1998a). In all patients the localisation and lateralisation of the side of seizure onset was based on a full clinical assessment, interictal and ictal scalp EEG video monitoring and/or intracranial electrodes, neuro-psychometry, MRI and hippocampal volumetry and relaxometry.

3.1.2.2 Magnetic Resonance Spectroscopic Imaging

The subjects were positioned with their necks extended as previously described (Woermann et al., 1999c) to allow the long axis of the hippocampus to be orthogonal to the long axis of the magnet. The two temporal lobes were studied separately to minimise field inhomogeneity effects (Xue et al., 1997) (McLean et al., 2001). On each side a PRESS volume of interest was prescribed of approximate dimension 4.5cm in the Left-Right direction, and 6.5cm in the Anterior-Posterior direction. The acquisition matrix was 20*20 phase encodings over a 26cm FOV. The slice thickness was 12mm, which yielded a nominal voxel volume of approximately 2cc. One excitation was acquired, with TE/TR 30/3000, which gave an acquisition time of 20 minutes for each side, and a total examination time of 75 minutes.

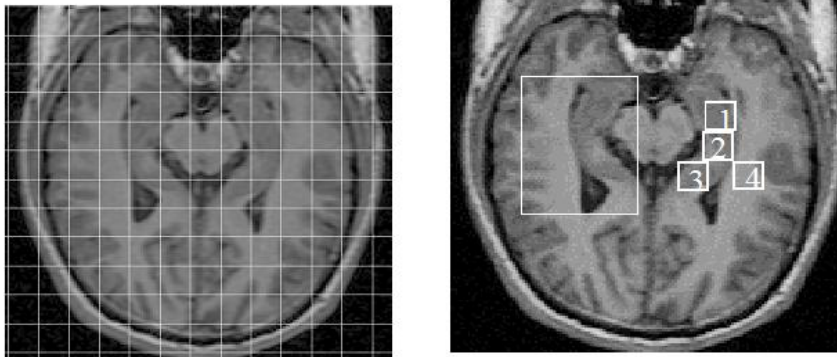
The data was processed using LCModel Interactive (McLean et al., 2001) as outlined in section [2.3]. The program took the user defined hippocampal area and extracted up to three voxels, centred respectively on the head, body and tail of the hippocampus are referred to in this paper as anterior, middle and posterior medial temporal lobe (MTL). If the anterior part of the defined hippocampal region was narrower than the voxel width, only two voxels would be prescribed and would be designated as middle and posterior voxels. Alternatively if the posterior part of the defined region was narrower than the voxel width, two voxels designated anterior and middle would be prescribed. A second region of interest was defined in the lateral temporal lobe (LTL), also resulting in up to three voxels in anterior, middle and posterior LTL positions. This process allowed the selection of up to six voxels in each lobe that were in matched anatomical positions within each subject and between each group.

Figure 3.1.1A) Axial T₁-weighted localising magnetic resonance imaging scans for: (I) a control subject and (II) a patient with left hippocampal sclerosis. In both figures the positions of the prescribed anterior (1); middle (2); and posterior (3) medial temporal lobe voxels are shown in the image on the right. The position of the prescribed posterior lateral temporal lobe voxel (4) is also shown. The prescribed PRESS volume of interest (VOI) is demonstrated in (I). The images on the left show the chemical shift imaging grid at acquisition prior to voxel repositioning using the locally developed software package, LCModel Interactive.

Figure 3.1.1 B) Representative spectra (TE/TR 30/3000ms) are shown from each of the above numbered positions. NAA_t = N-acetyl aspartate plus N-acetyl aspartyl-glutamate; GLX = glutamate plus glutamine; Cho = choline containing compounds; Cr = creatine + phosphocreatine; Ins = myo-inositol.

Figure 1A

I) Control subject



II) Patient with left hippocampal sclerosis

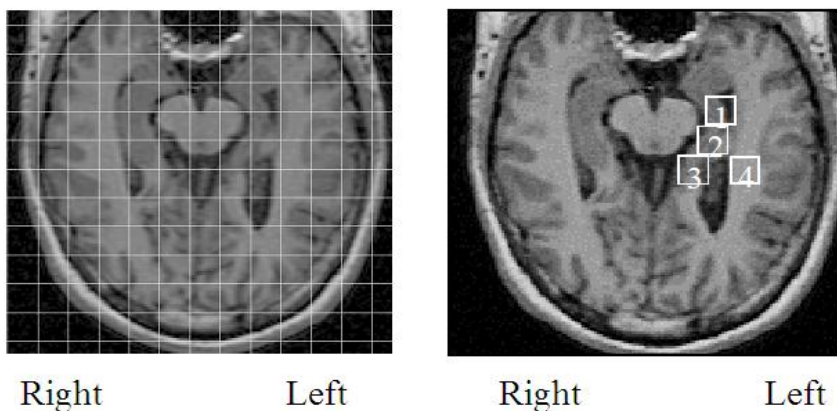
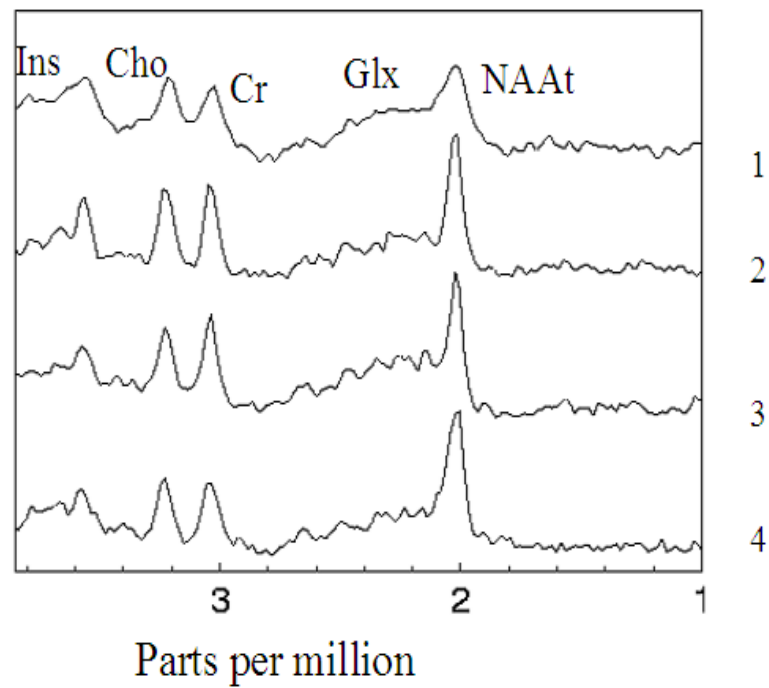
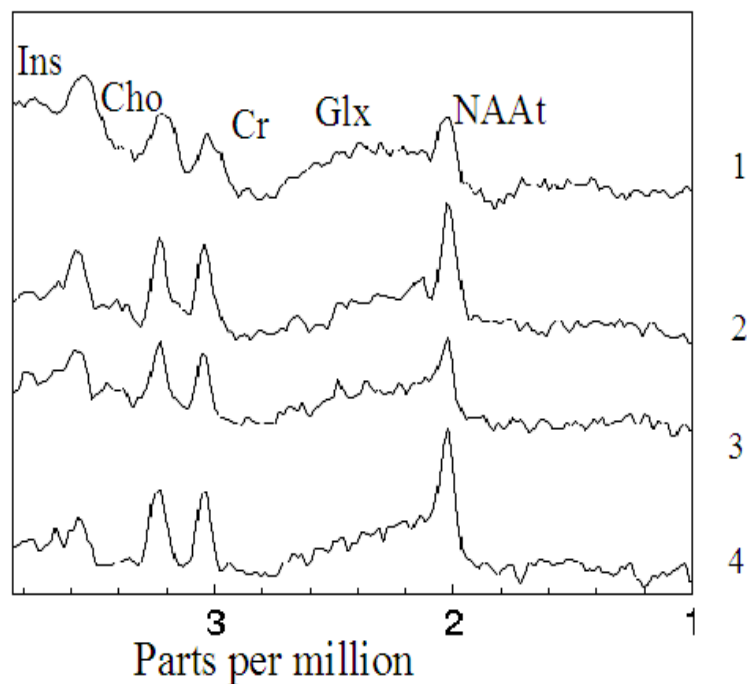


Figure 1B
I) Control subject



II) Patient with left hippocampal sclerosis



LCModel was used to quantify the metabolite concentrations for GLX, Cho, Cr, Ins and NAAt as described in section 2.2.4.1. Data with full width half maximum (FWHM) >0.15 PPM were rejected, which occurred for only 3 of 213 spectra. LCModel reported for each metabolite a mean $SD \leq 15\%$ at every voxel position, which can be considered to indicate reliable determination. The metabolite concentrations were corrected for the cerebro spinal fluid (CSF) partial volume effect and for the PRESS excitation slice profile as described elsewhere (McLean et al., 2000).

3.1.2.3 Statistics

Data were tested for normality with Kolmogorov-Smirnov tests. The control group was investigated for evidence of left versus right temporal lobe asymmetry, using the following function:

$$\text{Asymmetry index (AI)} = [(\text{Right} - \text{Left}) / ((\text{Right} + \text{Left}) / 2)] * 100\% \quad [\text{Eqn. 3.1.1}]$$

which gave a mean range of between 0 and 11% difference between paired voxels

A one-sample t-test was used to determine that there was no significant difference in AI values and zero mean; subsequently mean values of the paired right and left data points were used to calculate a normal range for each metabolite in each position. The normal range was defined as consisting of this control mean ± 3 standard deviations (SD). Individual patient data were compared against the normal range for each metabolite and ratio at each voxel position.

Metabolite concentrations and ratios were individually compared along the MTL in each group using ANOVA and post hoc comparisons were performed using the Least Significant Difference (LSD) test. Similar comparisons were also made across the groups (Control, HS, MRIN) and sides (ipsilateral temporal lobe to seizure onset, contralateral temporal lobe) in the anterior, middle and posterior MTL voxel positions. Due to technical difficulties with data acquisition in the anterior and middle LTL regions, inter-group comparisons in the lateral temporal lobe were made only for the posterior LTL.

3.1.3 Results

3.1.3.1 Subjects

The three subject groups (Control, HS and MRIN) were similar in age and gender distributions. The handedness distribution of the three groups was similarly matched as follows; Control seven right and three left, HS eight right and two left and MRIN eight right and two left. No handedness asymmetry effects were identified in the control group using Mann-Whitney non-parametric testing, but the group sizes were too small for this to be a strong test. No significant differences were noted between the HS group and the MRIN group in terms of seizure frequency, lifetime total number of secondary generalised seizures or time since last seizure (**Table 3.1.1**). For all the patients with HS the affected side was concordant with the side of seizure onset. Six of 10 of the HS group went on to anterior temporal lobe resection. The diagnosis of HS was confirmed histologically in all of these cases. One of the MRI negative TLE subjects had bi-temporal interictal and ictal epileptiform activity. Anti-epileptic drug (AED) therapy was similar in the two patient groups.

3.1.3.2 MRSI in individual patients

Abnormality of a metabolite concentration was defined as a value more than 3 SD distant from the control mean of that variable. The most discriminatory metabolite concentration for detecting abnormality in individual patients was NAA_t.

3.1.3.2.1 MTL data

In the defined MTL regions data were obtained from 168 voxels out of a possible 180. In the HS group nine of 10 patients had abnormally low NAA_t in at least one ipsilateral MTL voxel. In seven of 10 NAA_t was abnormally low anteriorly, in four in the middle voxel and in one NAA_t was low posteriorly. One patient had low NAA_t in all 3 ipsilateral voxels. One patient had bilateral abnormalities in NAA_t. There were no abnormally elevated values for NAA_t in the anterior MTL, but one patient with ipsilateral anterior low NAA_t had bilateral high NAA_t in the posterior MTL voxels.

In the MRIN group four patients had abnormalities ipsilateral to the epileptic focus. All four had low NAA_t in the middle voxel and two of these also had low NAA_t in the anterior voxel. One patient had bilateral low NAA_t. One patient with left TLE

Table 3.1.1: Description of the three groups of subjects. The healthy volunteer group is designated as Control. HS represents the group of patients with temporal lobe epilepsy and hippocampal sclerosis; and MRIN represents the group with temporal lobe epilepsy and unremarkable conventional MRI. Each group has n=10. AED = anti-epileptic drug.

	<u>Control</u>	<u>HS</u>	<u>MRIN</u>
Gender male/female	5/5	4/6	4/6
Age (yrs): median (range)	31 (23-36)	32 (24 – 53)	32 (23- 41)
Duration of epilepsy (yrs): median (range)	Not applicable	23 (11 – 35)	17 (3 – 22)
Time since last seizure (days): median (range)	Not applicable	3 (1 - 14)	5 (1 - 14)
Frequency of complex partial seizures / month: median (range)	Not applicable	13 (2 –60)	15 (2 – 50)
Secondarily generalised seizures	Not applicable	5	6
Past history of prolonged early childhood convulsion.	0	5	0
Family History of epilepsy	0	2	0
Number of AEDs taken: Median (range)	0	2 (2-3)	3 (1-4)

had normal NAA_t in all the voxels on the left side, but a low NAA_t in the middle voxel of the right MTL.

Analysis of the other metabolites using this wide normal range showed no clear patterns of abnormality. Analysis of ratios of metabolites NAA_t/Cr, NAA_t/(Cr+Cho), NAA_t/Ins did not yield any further information over analysis of the individual compounds.

If all the MTL voxels were combined for each subject to form a mean value for each metabolite, two of 10 NAA_t mean values in the HS group were abnormal ipsilaterally, with none abnormal bilaterally. In the MRIN group one of 10 was low ipsilateral to the epileptic focus and there was no contralateral abnormality. No abnormalities were noted with any of the other metabolites.

3.1.3.2.2 Posterior Lateral Temporal Lobe

Due to the constraints of avoiding artifact arising from the auditory canal, satisfactory data was obtained in 27 and 36 voxels from a potential 60 in the anterior and middle voxels of the lateral temporal lobe respectively. In the posterior LTL 56 of the potential 60 were obtained. For this reason only data from the posterior LTL voxel was analysed. In this position one of the HS patients and one of the MRIN patients had low ipsilateral NAA_t. There were no other significant individual metabolite or metabolite ratio abnormalities in this region in either the HS or the MRIN groups.

3.1.3.3 MRSI Group Comparisons

There was significant variation of CSF proportion along the MTL in all groups apart from the contralateral MRIN. The middle voxel contained the smallest proportion of CSF. Across the groups the CSF proportion was generally highest in the HS ipsilateral group, most notably in the middle voxels ($p < 0.01$). The grey matter proportion was higher in the anterior hippocampal voxels in all the groups ($p < 0.01$) and this did not vary significantly between groups (**Table 3.1.2**). As several of the metabolites may have a higher concentration in grey matter than white matter (Pouwels and Frahm, 1998; Noworolski et al., 1999; McLean et al., 2000) each metabolite analysis using ANOVA was repeated by incorporating grey matter proportion as a co-variate.

3.1.3.3.1 Analysis along the MTL

3.1.3.3.1.1 Control Group

In the control group (McLean et al., 2001), concentrations of Cho, GLX and Ins were higher in the anterior hippocampal voxels ($p < 0.01$, $p < 0.05$, $p < 0.01$ respectively). Cho was highest anteriorly (**Fig 3.1.2a**) and lowest in the posterior voxels. NAAAt (**Fig 3.1.2b**) and Cr showed no significant variation. The ratios NAAAt/(Cr+Cho), NAAAt/Ins and NAAAt/Cho were dominated by the changes in the concentrations of Ins and Cho and were lower anteriorly. When grey matter content was incorporated as a co-variate, Cho, Ins, NAAAt/Cho and NAAAt/Ins still varied significantly ($p < 0.05$), but for NAAAt/(Cr+Cho) and GLX there was no longer significant variation.

3.1.3.3.1.2 Patient Groups

Similar patterns of variation to the control group were noted for NAAAt/Cr (**Fig 3.1.2c**), NAAAt/(Cr+Cho) and Ins in the HS ipsilateral MTL. NAAAt was non-significantly lower in the anterior voxel. Cho and Cr were not elevated in the anterior voxel. GLX was higher anteriorly (**Fig 3.1.2d**). Using grey matter as a co-variate, there was no longer significant metabolite variation. In the contralateral MTL a trend for relative reduction in anterior Cr and Cho was observed but was less marked than on the ipsilateral side. There was no significant metabolite variation along the MTL contralateral to HS when grey matter was used as a co-variate.

In the MRIN ipsilateral MTL GLX, Cr, Cho, and Ins followed the pattern of variation noted in the control group. Cr, NAAAt/Cr and NAAAt/(Cr+Cho) all varied significantly in this group and the effect remained after the inclusion of grey matter as a co-variate ($p < 0.05$), all a consequence of low Cr values in the middle voxel.

In the MRIN contralateral MTL GLX was more elevated in the anterior voxel than was observed for the other groups (**figure 3.1.2d**). This variation of GLX along the MRIN contralateral MTL remained significant ($p < 0.01$) despite correction for grey matter. For the other values the pattern of change mirrored that of the control group, with Cho higher anteriorly ($p < 0.01$).

3.1.3.4 Analysis between subject groups

There was no significant variation of grey matter proportion between the groups in any position. NAA_t varied significantly in the anterior MTL position (**Fig 3.1.2b, Table 3.1.2**) ($p < 0.05$). This was due to a lower mean value in the HS ipsilateral side compared with all other groups apart from the MRIN ipsilateral group. Anterior MTL NAA_t values in MRIN ipsilateral were not significantly different from contralaterals and controls. Cr and Cho were lower in HS ipsilateral than all groups ($p < 0.05$) apart from HS contralateral, and were lower in HS contralateral MTL than the control values ($p < 0.05$). These effects remained after grey matter was incorporated as a co-variate. NAA_t/Cr and NAA_t/Cho were higher in HS contralateral MTL anterior voxels ($p < 0.01$ and $p < 0.05$) than in the anterior voxels of any other groups. No significant variation was noted across the middle and posterior MTL or the posterior LTL voxels.

The mean MTL NAA_t was lower in HS ipsilateral than HS contralateral ($p < 0.05$) but not significantly lower than the control population and Cho in the HS ipsilateral group was lower than the control group ($p < 0.05$).

3.1.3.5 Comparison of the posterior MTL and the posterior LTL

For all groups the grey matter proportion was higher in the MTL; Cr was lower and NAA_t/Cr was higher ($p < 0.05$) in the posterior LTL. In the control group ($p < 0.01$) and in both the temporal lobes of the MRIN group ($p < 0.05$), GLX was higher in the MTL. This effect was not seen in the HS groups. In the MRIN group NAA_t was lower in the posterior LTL on the side ipsilateral to the seizure focus ($p < 0.05$).

Table 3.1.2: Metabolite concentrations and ratios in medial temporal (MTL) and posterior lateral temporal (LTL) lobe voxels, expressed as the group mean and standard deviation. The healthy volunteer group is designated as Control. **HSips** refers to the temporal lobe ipsilateral to the side of pathology and seizure onset. **HScont** refers to the contralateral temporal lobe. **MRIN** refers to the MRI negative group and again ips and cont refer to the sides ipsilateral and contralateral to the sides of seizure onset respectively. NAAAt = N-acetyl aspartate plus N-acetyl aspartyl-glutamate; GLX = glutamate plus glutamine; Cr = creatine plus phosphocreatine; Cho = choline containing compounds; Ins = myo-inositol. Mean values and SD are provided for each measurement.

ANTERIOR MTL		<u>Control</u>	<u>HSips</u>	<u>HScont</u>	<u>MRINips</u>	<u>MRINcont</u>
		N=9	N=10	N=9	N=9	N=9
Grey Proportion		0.90(0.07)	0.88(0.06)	0.88(0.06)	0.87(0.08)	0.91(0.03)
Metabolites (mmol/l)	NAAAt	7.8(0.48)	6.4(0.93)	7.6(1.3)	7.1(1.2)	7.7(0.92)
	GLX	13.0(2.6)	13.0(3.3)	13.0(2.5)	13.0(1.2)	15.0(1.9)
	Cho	1.8(0.18)	1.4(0.21)	1.5(0.25)	1.7(0.46)	1.8(0.39)
	Cr	6.3(0.71)	5.1(0.69)	5.4(1.1)	6.3(1.4)	6.2(0.76)
	Ins	6.8(0.81)	6.4(1.6)	5.7(1.1)	6.6(2.3)	6.6(2.1)
Metabolite ratios	NAAAt/Cr	1.2(0.10)	1.3(0.18)	1.4(0.17)	1.2(0.13)	1.3(0.17)
	NAAAt/(Cr+Cho)	0.96(0.07)	0.98(0.12)	1.1(0.12)	0.90(0.11)	0.99(0.14)
	NAAAt/Ins	1.2(0.15)	1.1(0.34)	1.4(0.25)	1.1(0.25)	1.3(0.31)

Table 3.1.2: continued

MIDDLE MTL		<u>Control</u>	<u>HSips</u>	<u>HScont</u>	<u>MRINips</u>	<u>MRINcont</u>
		N=10	N=10	N=10	N=10	N=10
Grey Proportion		0.72(0.10)	0.74(0.07)	0.72(0.10)	0.72(0.10)	0.72(0.11)
Metabolites (mmol/l)	NAAAt	7.9(0.24)	7.4(0.92)	8.0(0.45)	7.6(0.77)	8.0(0.90)
	GLX	10.0(1.2)	11.0(1.7)	9.7(1.8)	9.4(3.1)	10.0(0.91)
	Cho	1.5(0.16)	1.3(0.18)	1.4(0.18)	1.4(0.22)	1.5(0.19)
	Cr	5.8(0.46)	5.6(0.85)	5.7(0.53)	5.3(0.70)	5.6(0.95)
	Ins	5.1(0.66)	4.7(0.81)	4.6(0.56)	4.5(1.42)	4.3(0.90)
Metabolite ratios	NAAAt/Cr	1.4(0.13)	1.4(0.19)	1.4(0.12)	1.5(0.22)	1.5(0.14)
	NAAAt/(Cr+Cho)	1.1(0.10)	1.1(0.14)	1.1(0.08)	1.2(0.17)	1.2(0.10)
	NAAAt/Ins	1.6(0.23)	1.6(0.29)	1.7(0.24)	2.0(0.97)	1.9(0.50)

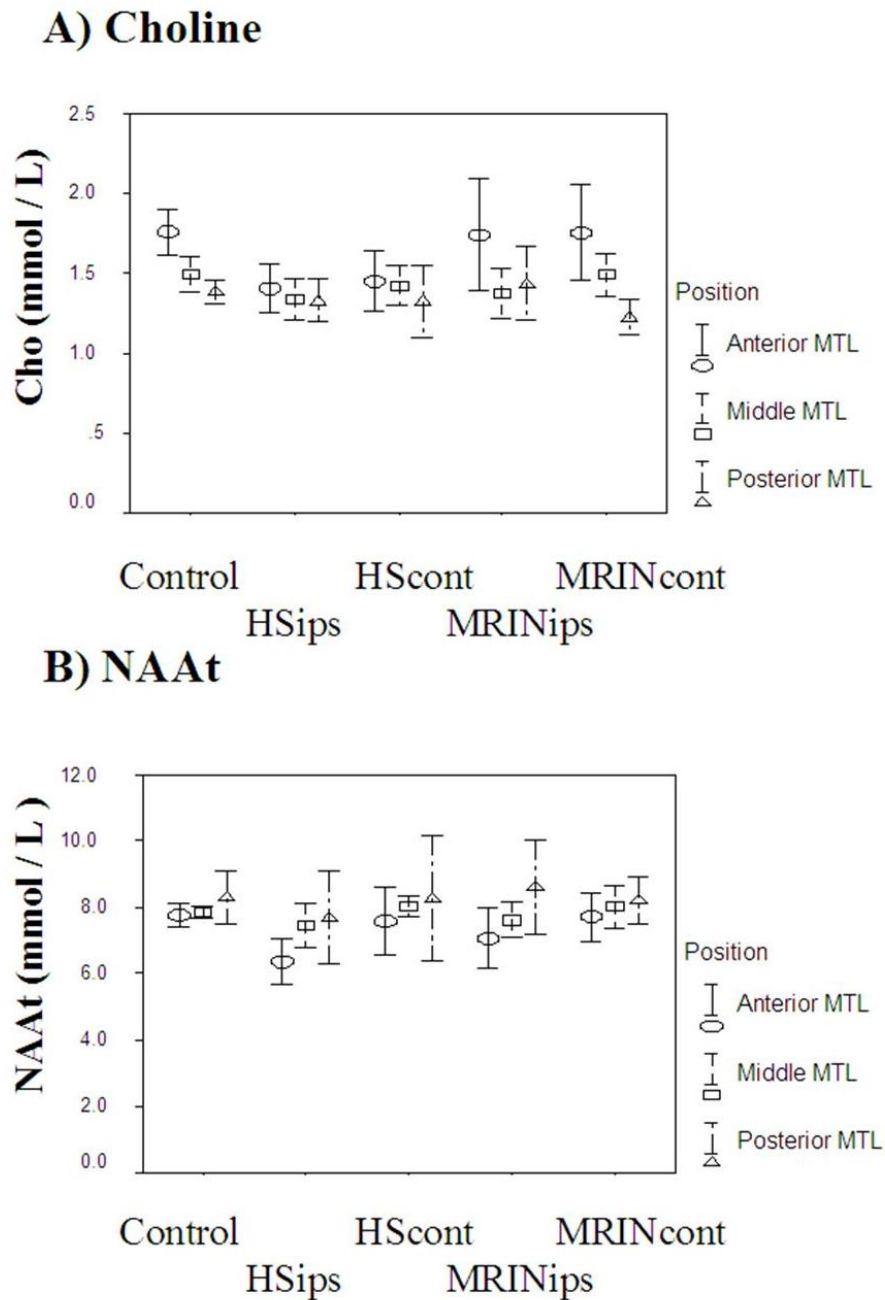
POSTERIOR MTL		<u>Control</u>	<u>HSips</u>	<u>HScont</u>	<u>MRINips</u>	<u>MRINcont</u>
		N=9	N=9	N=8	N=9	N=10
Grey Proportion		0.76(0.10)	0.77(0.10)	0.75(0.09)	0.79(0.06)	0.68(0.18)
Metabolites (mmol/l)	NAAAt	8.3(1.1)	7.7(1.8)	8.3(2.3)	8.6(1.8)	8.2(1.0)
	GLX	12.0(1.4)	9.2(2.0)	10.0(2.3)	11.0(2.3)	11.0(2.1)
	Cho	1.4(0.10)	1.2(0.44)	1.3(0.28)	1.4(0.30)	1.2(0.14)
	Cr	6.4(0.84)	5.9(1.4)	6.4(1.4)	7.0(0.90)	6.0(1.0)
	Ins	5.4(0.59)	4.7(1.03)	5.1(0.54)	4.7(1.5)	4.3(1.2)
Metabolite ratios	NAAAt/Cr	1.3(0.12)	1.3(0.16)	1.3(0.10)	1.2(0.13)	1.4(0.24)
	NAAAt/(Cr+Cho)	1.1(0.09)	1.1(0.13)	1.1(0.10)	1.0(0.10)	1.1(0.18)
	NAAAt/Ins	1.5(0.22)	1.8(0.88)	1.6(0.33)	2.1(1.1)	2.0(0.54)

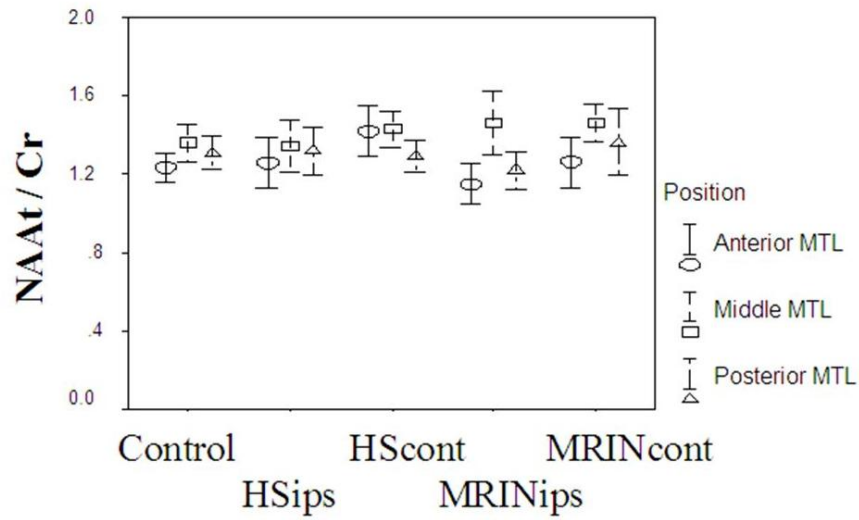
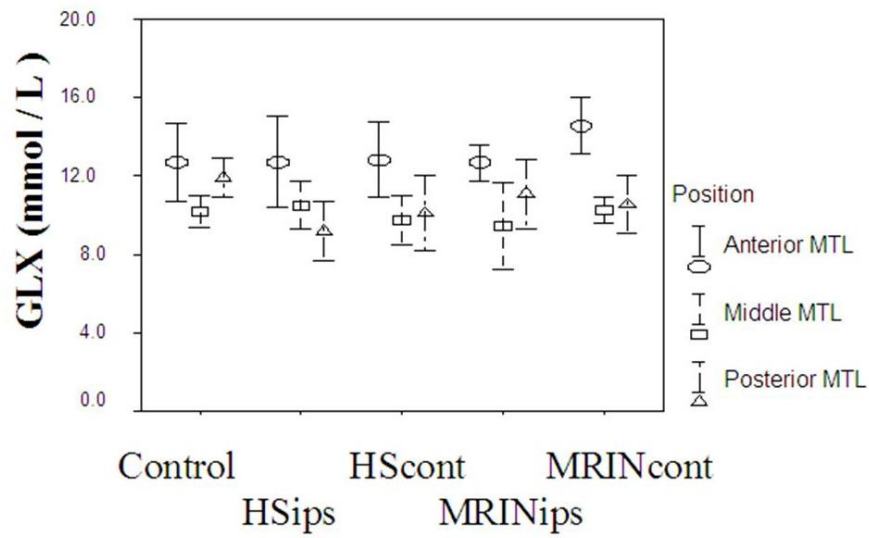
Table 3.1.2: continued

Mean MTL		<u>Control</u>	<u>HSips</u>	<u>HScont</u>	<u>MRINipsi</u>	<u>MRINcont</u>
		N=8	N=9	N=8	N=8	N=9
Grey Proportion		0.78(0.08)	0.80(0.06)	0.79(0.07)	0.80(0.05)	0.76(0.10)
Metabolites (mmol/l)	NAAAt	8.0(0.42)	7.2(1.1)	8.1(1.0)	7.8(1.0)	7.9(0.66)
	GLX	12.0(1.2)	11.0(1.5)	11.0(1.2)	11.0(1.4)	12.0(0.73)
	Cho	1.5(0.10)	1.3(0.2)	1.5(0.18)	1.5(0.22)	1.5(0.19)
	Creat	6.1(0.43)	5.6(0.82)	5.9(0.77)	6.2(0.72)	6.0(0.66)
	Ins	5.8(0.52)	5.4(0.47)	5.3(0.28)	5.5(1.1)	5.2(1.0)
Metabolite ratios	NAAAt/Cr	1.3(0.08)	1.3(0.11)	1.4(0.08)	1.3(0.08)	1.3(0.14)
	NAAAt/(Cr+Cho)	1.0(0.07)	1.0(0.09)	1.1(0.06)	1.0(0.06)	1.1(0.11)
	NAAAt/Ins	1.4(0.15)	1.3(0.20)	1.5(0.17)	1.4(0.19)	1.6(0.31)

POSTERIOR LTL		<u>Control</u>	<u>HSips</u>	<u>HScont</u>	<u>MRINipsi</u>	<u>MRINcont</u>
		N=9	N=9	N=7	N=10	N=10
Grey Proportion		0.26(0.13)	0.32(0.18)	0.18(0.04)	0.28(0.08)	0.24(0.07)
Metabolites (mmol/l)	NAAAt	8.0(0.71)	7.5(1.3)	8.4(1.5)	7.4(1.1)	7.2(1.2)
	GLX	9.0(1.2)	8.4(1.9)	9.1(4.0)	9.4(2.8)	8.4(1.8)
	Cho	1.3(0.21)	1.3(0.28)	1.2(0.33)	1.4(0.31)	1.3(0.29)
	Cr	4.4(0.66)	4.6(1.1)	5.3(1.5)	4.3(0.91)	4.5(0.79)
	Ins	4.8(0.58)	4.3(1.2)	4.0(1.3)	4.1(1.0)	3.8(1.3)
Metabolite ratios	NAAAt/Cr	1.8(0.20)	1.6(0.25)	1.6(0.21)	1.8(0.37)	1.6(0.21)
	NAAAt/(Cr+Cho)	1.4(0.14)	1.3(0.14)	1.3(0.17)	1.3(0.26)	2.1(0.71)
	NAAAt/Ins	1.7(0.27)	1.7(0.30)	2.3(0.63)	1.9(0.67)	1.3(0.16)

Figure 3.1.2: Plots of mean and 95% confidence intervals for: (a) choline containing compounds (Cho); (b) N-acetyl aspartate plus N-acetyl aspartyl-glutamate (NAAt); (c) the ratio NAAt / Creatine (NAAt/Cr) and (d) glutamate plus glutamine (GLX). Metabolites were estimated in the anterior, middle and posterior MTL, in control subjects, patients with hippocampal sclerosis (HS) and temporal lobe epilepsy, and patients with temporal lobe epilepsy and normal magnetic resonance imaging (MRIN). Ips = MTL ipsilateral to HS and/or seizure onset. Cont = MTL contralateral to the side of HS and/or seizure onset.



C) NAAt / Cr**D) GLX**

3.1.4 Discussion

At the time of publication this was the first study to report short TE MRSI measured concentrations of NAA_t, Cr, Cho, GLX, and Ins through the MTL and the posterior LTL in patients with TLE. The study indicated that NAA_t is a marker for abnormality in both HS and MRIN and found that Cr and Cho concentrations follow the NAA_t changes in the anterior hippocampi in HS. The concentration of several metabolites varied significantly through the MTL and lateral neocortex and interpretation must take the grey/white composition and partial volume effects into account.

3.1.4.1 Methodology

MRSI has been considered to be more difficult in the temporal lobe than single voxel spectroscopy, because the anterior hippocampus, where most pathology has been observed in HS (Woermann et al., 1998a), may be less accessible to MRSI studies. Part of this reasoning was based on results obtained by prescription of a single region of interest that included both temporal lobes and resulted in poor field homogeneity in the anterior temporal lobe (Xue et al., 1997; McLean et al., 2001). This is generally resolved by studying each temporal lobe separately with smaller regions of interest localised to the relevant temporal lobe, and also by ensuring that the plane of the MRSI grid is aligned along the long axis of the hippocampus, the anterior MTL is accessible to MRSI (McLean et al., 2001). However, using this technique, quantitative information from the anterior lateral temporal lobe remained inaccessible although other MRS studies have shown that metabolite abnormalities might be observed here (Meiners et al., 2000).

The small size of the hippocampus together with the point spread function of spectroscopic imaging data means that it is currently not feasible to exclusively analyse hippocampal tissue using MRSI on standard 1.5T clinical scanners. In this study the term Medial Temporal Lobe (MTL) was used to indicate that the voxels do not only contain hippocampal tissue, although they can be considered to be predominantly hippocampal tissue particularly in the anterior and middle positions.

The method of voxel analysis (McLean et al., 2001) allowed spectra to be analysed from similar anatomical positions for each group. In common with reports from other

groups this study identified that most metabolite concentrations were higher in neocortical grey matter than white matter(Doyle et al., 1995;Pouwels and Frahm, 1998;Noworolski et al., 1999;McLean et al., 2000).

CSF proportion was highest in the ipsilateral HS group, reflecting the atrophy in this group. CSF is believed to return negligible metabolite signal(Lynch et al., 1993). Consequently without the CSF correction, metabolite concentrations, particularly in the HS ipsilateral group, would be under-estimated, leading to an over interpretation of abnormalities. Correction was also made for potential error due to imperfections in the PRESS slice excitation profile, magnetic field inhomogeneity and chemical shift artifact at the periphery of the PRESS region of interest(McLean et al., 2000). These corrections resulted in Coefficient of Variation (CV) values of mean 13% and range 6-22%, for the five metabolites in the control group across all 4 voxels. These values compare satisfactorily with the CV data that were previously obtained from a hippocampal single voxel study(Woermann et al., 1999c) and hence indicate a similar reproducibility to that study. The values are also similar to data for voxels outside the temporal lobe(McLean et al., 2000).

3.1.4.2 Findings in individual patients

In agreement with most other studies reduction of NAA_t was observed in the region of the sclerotic hippocampi(Hugg et al., 1993;Ende et al., 1997;Woermann et al., 1999c). Bilateral reduction in NAA_t was only observed in 1 HS patient. Several previous studies have reported bilateral abnormalities in 20-54% of subjects(Connelly et al., 1994;Cross et al., 1996;Achten et al., 1997;Cendes et al., 1997b;Woermann et al., 1999c). This variation is partly explained by different definitions of metabolite abnormality. As described above, most groups have discussed changes in metabolite ratios (NAA/Cr, NAA/(Cr +Cho), NAA/Cho) in preference to individual metabolite concentrations or have identified abnormality as the presence of significant ipsilateral - contralateral asymmetry(Achten et al., 1997;Cendes et al., 1997b). Other groups used the individual metabolite concentrations and/or ratios but differed in definition of the normal range as control mean +/- 2 SD(Ng et al., 1994;Hetherington et al., 1995a;Cross et al., 1996). The previous single voxel study undertaken by the NSE

MRS group identified that three of 15 patients with HS and unilateral TLE had bilateral hippocampal NAA lower than 2.5SD of the control mean(Woermann et al., 1999c).

In the MRIN group four of 10 had low MTL NAA_t on the side of seizure onset, and bilateral reductions were found in one of these. These results are consistent with other reports of the frequency of abnormality in the absence of MRI abnormality(Connelly et al., 1998;Woermann et al., 1999c). This compares to the findings in the Single voxel study of four of 15 TLE patients with low NAA_t and with normal MRI(Woermann et al., 1999c).

The pathophysiological explanation for the observed bilateral metabolite changes in TLE patients with normal MR imaging or unilateral MR abnormality remains a subject of discussion. There is evidence from some authors that NAA_t levels do correlate with absolute cell loss in hippocampal sub-fields(Vielhaber et al., 2008;Hammen et al., 2008) whilst others have found no association between neuronal cell counts and NAA(Petroff et al., 2002b). Low NAA_t may represent functional change and / or subtle neuronal loss. Bilateral MRS abnormality may be observed in subjects with either unilateral MRI abnormality(Woermann et al., 1999c) or normal MRI(Connelly et al., 1998;Woermann et al., 1999c) (Connelly et al., 1998;Riederer et al., 2006), and is seen with higher incidence than bilateral EEG abnormality(Matouk et al., 2001a). In the current study conventional investigation suggested bilateral abnormality in only one subject in the MRIN group (bilateral inter-ictal EEG abnormality). MRSI investigation of this subject revealed low NAA_t in the middle MTL region contralateral to the side of seizure onset.

The current study also provided information about the location of maximal metabolite abnormality. In the HS group, low NAA_t was most commonly found in the anterior voxel. In contrast, in the MRIN group the middle voxel was most commonly abnormal. This suggests that studies that concentrate on the anterior position of the MTL may miss abnormalities in the middle or posterior MTL.

In this current study six subjects (one subject with HS, and five subjects with MRI negative TLE), were included who had previously participated in the single voxel

study reported by our group (Woermann et al., 1999c). For the subject with HS, the single voxel study identified ipsilateral reduction in NAA_t. In the current MRSI study bilateral anterior hippocampal reduction in NAA_t was observed. For the five MRI negative subjects, two previously showed unilateral and ipsilateral NAA_t reduction. In the current study both showed ipsilateral reduction in the anterior and middle hippocampal voxels. Of the remaining three overlapping subjects, despite normal single voxel spectroscopy, one showed reduction in NAA_t in the middle hippocampal region ipsilateral to the seizure focus and one was contralateral. Although these numbers are small there is an indication that the multi-voxel study was more sensitive for abnormality and provided spatial information about the position of the region of maximal abnormality.

3.1.4.3 Group comparisons

Variation was observed within both the control and TLE patient MTL and also across these groups in the anterior MTL voxel. Several metabolites co-varied with grey matter content.

In the control group Cho concentrations were higher in the anterior MTL. Cr was non-significantly lower in the middle voxel and NAA_t did not vary significantly. This resulted in lower NAA_t/(Cr+Cho) anteriorly and higher NAA_t/Cr in the middle voxel. GLX and Ins were higher in the anterior voxel. These effects were reduced by the incorporation of grey matter proportion as a co-variate, such that NAA_t/(Cr+Cho) and GLX no longer varied significantly. Other workers have considered metabolite variation in the control temporal lobe. Vermathen et al (Vermathen et al., 2000) used MRSI at TE=135ms, and found lower NAA/(Cr+Cho) and higher Cho in the anterior control MTL although no correction for grey matter proportion was made. Another group has described lower NAA/Cr in the hippocampus than the lateral temporal lobe (Wang et al., 2008). Lower NAA_t/Cr was also seen in the posterior MTL than in the posterior LTL in all the groups, due to a lower Cr in the lateral voxel, without significant variation in NAA_t or Cho. This is consistent with a study of metabolite concentration in grey and white matter in voxels outside the temporal lobe, at the same short echo time (TE=30ms) (McLean et al., 2000). In this study the ratio of Cr concentrations in grey versus white matter was 1.7, compared with 1.16 for NAA_t and

0.9 for Cho. This implies that Cr concentration will be most altered by a reduction in the proportion of grey matter. The concentration of Ins and GLX were lower in the posterior LTL than the posterior MTL in the control group. This would also be in keeping with the observed metabolite ratios for GLX and Ins between grey and white matter of 2.4 and 1.6 respectively (McLean et al., 2000) implying that there would be lower concentrations in regions with lower proportions of grey matter.

In the HS group the anterior ipsilateral voxel showed reduced NAA_t, but also low Cr and Cho (Figure 3.1.2). Other studies have similarly reported reduction in both NAA and Cr in the sclerotic hippocampus (Ende et al., 1997; Duc et al., 1998) and a histological examination in an animal model of temporal lobe epilepsy (Tokumitsu et al., 1997) identified reduced NAA and Cr in the presence of neuronal loss and gliosis. The single voxel study (Woermann et al., 1999c) did not identify significant group effects for Cr or Cho but averaged the entire hippocampus, which could have masked changes confined to the anterior region. It has been held that in the sclerotic anterior hippocampus there is loss of neuronal tissue with consequent loss of NAA_t, because of the localisation of NAA in neurones (Urenjak et al., 1993), and reactive gliosis, with consequent increase in Cr and Cho. This understanding was largely based on single voxel studies or MRSI at longer TE. The finding that all three metabolites were decreased in this region might indicate that Cr and Cho are sufficiently present in neurones to also be affected by the presumed process of neuronal loss/dysfunction (Urenjak et al., 1993).

In agreement with the above trends for NAA_t, Cr and Cho the ratios NAA_t/Cr and NAA_t/(Cr+Cho) were unhelpful in identifying abnormality in the TLE groups. This concurs with the findings of the single voxel study (Woermann et al., 1999c). Other groups, however, and usually with longer TE, have found these ratios to be sensitive (Cendes et al., 1994; Vermathen et al., 1997; Achten et al., 1997). The reason for this difference in findings is not established but these studies were in general performed with different acquisition parameters and utilise different descriptions of abnormality. At short TE there is improved signal to noise which might make quantification more reliable, and although the baseline at short TE is more variable

there are established spectral peak fitting programmes that produce reliable and repeatable estimates of metabolite concentration. It is also possible that metabolite T_2 might be altered in pathological tissue (e.g. hippocampal sclerosis), in which event those studies performed at longer TE would be more likely to introduce metabolite measurement error.

The single voxel study identified elevated GLX in the mesial temporal lobe ipsilateral to seizure onset in the MRIN group. In the current study ipsilateral elevation was not found but elevation of GLX in the anterior voxel of the MRIN contralateral group was observed. It is of interest that both studies identified elevated GLX in patients with TLE and normal MR imaging. However several factors limit the interpretation of these findings. Firstly GLX represents a signal complex of glutamate plus glutamine and it is not currently possible to determine whether elevation in GLX represents change in glutamate, in glutamine or in both metabolites. Also GLX is measured less reliably than NAA_t and in these two studies the number of subjects is relatively small. Furthermore the two studies measured GLX in different volumes (total hippocampal GLX versus anterior MTL GLX in the current study) with a very limited number of subjects participating in both studies.

In the MRIN ipsilateral group NAA_t was significantly lower in the posterior LTL than in the posterior MTL. This finding might indicate involvement of lateral neo-cortex in a pathological process in this group and agrees with a previous MRS study of similarly selected subjects which identified extensive metabolite abnormality in the temporal lobe ipsilateral to seizure onset compared to healthy controls(Connelly et al., 1998).

In this study no relationship between NAA_t and seizure frequency, total lifetime secondary generalised seizures, or time since last seizure was noted. This is consistent with the single voxel findings(Woermann et al., 1999c) and also with a longitudinal study, which did not observe change in the ratio NAA/Cr in patients who had become seizure free on anti-epileptic drug therapy(Li et al., 2000c). Another study(Matton et

al., 2001b) identified no consistent changes in metabolite peak ratios between the inter-ictal and post-ictal state in TLE.

MRSI has a demonstrated role in the study of subjects with epilepsy. The ideal study would provide a full metabolite profile as well as spatial information. This current short TE work is the first MRSI study to quantify Ins and GLX as well as NAA, Cho and Cr at different positions along the MTL and the lateral temporal lobe, in the normal temporal lobe and also in subjects with temporal lobe epilepsy. The study identifies how the obtained concentrations are influenced separately by variation in voxel position and tissue composition and show how such variability might limit the interpretation of metabolite ratios.

3.1.5 Conclusion

The study indicates that low NAA is a marker for abnormality in HS and MRIN TLE, but the location of maximal abnormality appears to be different, with maximal abnormality in the anterior region in HS and in the middle MTL region in MRIN TLE. Low Cr and Cho were also a feature of the anterior sclerotic hippocampus.

3.2 A Proton Magnetic Resonance Spectroscopy Study of Metabolites in the Occipital lobes in Epilepsy.

ABSTRACT:

Purpose:

Gamma amino butyric acid (GABA) and glutamate, respectively the principal inhibitory and excitatory neurochemicals in the brain, are visible to proton Magnetic Resonance Spectroscopy (MRS). In this study GABA+ (GABA plus homocarnosine) and GLX (glutamate plus glutamine) concentrations were measured in the occipital lobes in patients with idiopathic generalised epilepsy (IGE) and in patients with occipital lobe epilepsy (OLE).

Methods:

Fifteen patients with IGE, 15 patients with OLE and 15 healthy volunteers were studied. A single voxel was prescribed in the occipital lobes for each subject. PRESS localised short echo time MRS was performed to measure GLX using LCModel. A double quantum GABA filter was used to measure GABA+. Segmented T₁ weighted images gave the tissue composition of the prescribed voxel.

Results:

Grey matter proportion, GLX and GABA+ were all elevated in IGE. However, analysis using grey matter proportion as a co-variable showed no significant group differences. No correlation was observed between GABA+ concentration and either seizure frequency or time since last seizure.

Conclusions:

GLX and GABA+ were elevated in IGE. Elevated grey matter content in the IGE group despite normal MRI appearance can be expected to account for some or all of this observed elevation of GLX and GABA+. GABA+ concentration did not correlate with seizure control or duration since most recent seizure.

Published ref: Simister et al., *Epilepsia*, 2003 **44**,550–558

3.2.1 Introduction

Proton Magnetic Resonance Spectroscopy (MRS) enables non-invasive in-vivo estimation of brain metabolites relevant to the study of epilepsy. Most MRS studies have typically measured abnormality in the three main visible metabolites; NAA, Cr, Cho expressed as simple ratios, or with careful calibration, as concentrations. Recent methodological advances also allow detection of neurochemicals, such as glutamate plus glutamine (GLX)(Woermann et al., 1999c) (McLean et al., 2000;Woermann et al., 2001b;Simister et al., 2002)and GABA(Petroff et al., 1996a;Petroff et al., 1996b;Petroff et al., 1998;Mescher et al., 1998;Petroff et al., 2000;Petroff et al., 2001a;Petroff et al., 2001b;Mueller et al., 2001b) that are of fundamental importance in the pathophysiology of seizure disorders.

Glutamate is the principal excitatory neuro-transmitter in the mammalian brain. Elevated in-vitro glutamate concentrations have been identified in epileptic tissue(Sherwin et al., 1988;Petroff et al., 1995) whilst in-vivo micro-dialysis studies have shown an increase in extra-cellular glutamate concentration following seizure onset in the epileptogenic temporal lobes of patients with refractory temporal lobe epilepsy (TLE)(During and Spencer, 1993). Glutamate metabolism is tightly coupled with the metabolism of glutamine. Glutamate released from the glutamatergic nerve terminal into the synaptic cleft is taken up by surrounding glial cells and converted to glutamine by glutamine synthetase (an enzyme exclusively localised to the glial cell(Martinez-Hernandez et al., 1977)). Glutamine is subsequently released from the glial cells into the extracellular fluid where it is taken up by neurons. Here it is re-converted into glutamate by the action of phosphate activated glutaminase(Kvamme, 1998). Although direct quantification of glutamate is not yet reliable via proton MRS on clinical scanners, the complex signal GLX (glutamate plus glutamine) is quantified at short echo times(Woermann et al., 1999c;McLean et al., 2000) with repeatability measures approaching those obtained for the main visible metabolites(Woermann et al., 1999c). GLX may be elevated in regions of seizure onset(Woermann et al., 1999c).

GABA is the major inhibitory neurotransmitter in the human brain. Decreases in GABA inhibition may cause seizures(Olsen and Avoli, 1997) whereas several potent anti-epileptic drugs (AED) such as topiramate, gabapentin and vigabatrin are thought to work by enhancement of GABA synthesis or function. Low occipital lobe GABA has been found in patients with partial epilepsy of extra-occipital seizure onset(Petroff et al., 1996b;Petroff et al., 1999a;Petroff et al., 2000) and in these studies is lowest in subjects with poor seizure control(Petroff et al., 1996b). Low occipital GABA is found in subjects with JME(Petroff et al., 2001a). Elevation in observed GABA concentrations is observed following the administration of several AEDs known to modify GABA metabolism or function(Petroff et al., 1996a;Petroff et al., 1998;Kuzniecky et al., 1998a;Petroff et al., 2000;Mueller et al., 2001b). Levels of GABA and homocarnosine, a dipeptide metabolite of GABA and histidine, have been positively correlated with seizure control(Petroff et al., 2001a).

The majority of previous GABA MRS studies have been performed on the occipital lobe in patients with extra-occipital lobe focal epilepsy or in one study JME. The purpose of this current study was to compare the metabolite profiles in the occipital lobes of 15 patients with idiopathic generalised epilepsy (IGE), 15 patients with occipital lobe epilepsy (OLE) and 15 healthy volunteers.

3.2.2 Methods

3.2.2.1 Subjects

15 control subjects and 30 patients with chronic epilepsy were investigated after giving informed consent. This study was approved by the Joint Research Ethics Committee of the National Hospital for Neurology and Neurosurgery. 15 patients had a diagnosis of idiopathic generalised epilepsy (IGE). All fifteen had normal MRI on visual inspection. Thirteen of the 15 had photo-paroxysmal responses on current electro-encephalogram (EEG). Seven of the 15 had IGE syndromes that were sub-classifiable as follows; Juvenile Myoclonic Epilepsy (three), Juvenile Absence Epilepsy (two), Eyelid Myoclonia with Absences (one), Generalised Tonic Clonic Seizures on Awakening (one). In the remaining eight patients sub-syndrome classification was not possible. Fifteen patients had occipital lobe epilepsy (OLE).

Fourteen of this group had normal MRI. The fifteenth had a porencephalic cyst in the right fronto-parietal region and normal occipital lobe appearance. In all patients the diagnosis was based upon full clinical assessment, interictal +/- ictal scalp EEG, neuropsychometry and MRI. Vigabatrin, topiramate and gabapentin, are reported to elevate in vivo GABA levels (Petroff et al., 1996a; Kuzniecky et al., 1998a; Petroff et al., 2000). Only three patients were taking one of these medications. The medications taken by the IGE group were as follows; valproate (six), lamotrigine (five), carbamazepine (two), topiramate (two), clobazam (one), acetazolamide (one). Five patients were taking no regular medications. For the OLE group the medications were: carbamazepine (six); lamotrigine (five); clobazam (two), oxcarbazepine (one), phenytoin (one), gabapentin (one), phenobarbitone (one) and valproate (one). One patient in the OLE group was taking no regular medications. Seizure frequency and the duration in days since the most recent seizure were noted. In the OLE group only those seizures leading to altered level of consciousness were recorded. In the IGE group patients recorded seizure frequency and duration since most recent generalised tonic clonic convulsive seizure. A history of absence seizures was also recorded although this was expected to be less reliably assessed by the subject.

3.2.2.2 Magnetic Resonance Imaging

The study was performed on a 1.5T General Electric SIGNA Horizon Echospeed scanner (Milwaukee, WI) using a standard quadrature head coil for all MRI/MRS studies. Axial T1 weighted inversion-recovery prepared fast spoiled gradient recalled echo (IRP-FSPGR) images were acquired (TE/TI/TR = 4.2/450/16 ms, flip angle 20⁰; matrix 256*128; slice thickness 1.5mm). These images were used both to guide voxel placement and subsequently for segmentation using SPM99 (Statistical Parametric Mapping; Wellcome Department of Imaging Neuroscience, Institute of Neurology, University College London). All the MRI studies were reviewed by two experienced neuro-radiologists.

Locally written software in SAGE 7.0 (General Electric, Milwaukee WI) provided estimates for the resulting grey matter, white matter and cerebro-spinal fluid (CSF) tissue composition of the prescribed MRS volume of interest based on the SPM

segmentations. Metabolite concentrations were then corrected for CSF content, which is considered to provide negligible signal(Lynch et al., 1993). Since most of the observed metabolites have higher concentration in grey matter than white matter voxel grey matter fraction was used as a co-variable in inter-group statistical comparisons.

3.2.2.3 Magnetic Resonance Spectroscopy

3.2.2.3.1 Acquisition

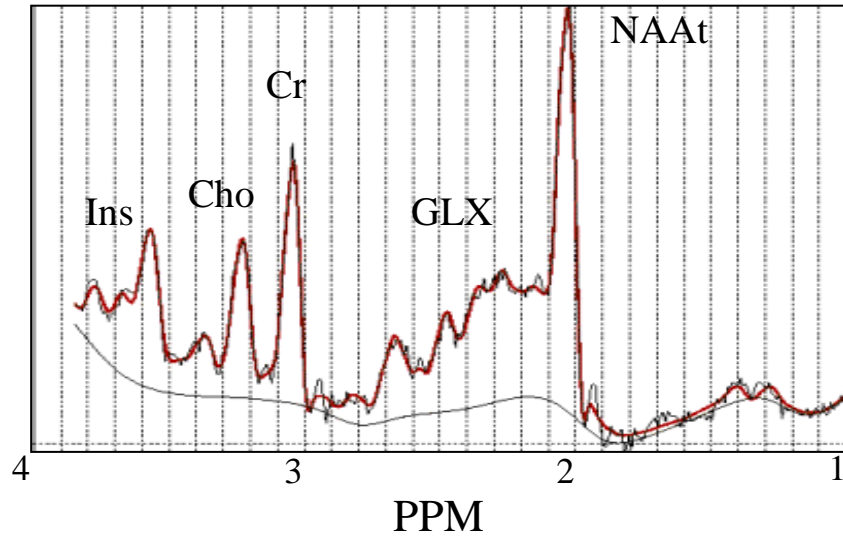
A single voxel was prescribed in the occipital lobe of each subject with approximate dimensions 35 by 40 mm in the Anterior-Posterior and Left-Right directions respectively and thickness 25mm. (**Fig 3.2.1**) Conventional PRESS-localised spectra were obtained initially with the acquisition parameters (TE/TR = 30/3000 ms) matching our previous studies(Woermann et al., 1999c;McLean et al., 2000;McLean et al., 2001), so that LCModel(Provencher, 2001) could be used for quantification of NAAAt, Cr, Cho, myo-inositol (Ins) and GLX. NAAAt is the combined peak of N-acetyl aspartate and N-acetyl aspartyl-glutamate. Ins is considered to be localised to glial cells(Brand et al., 1993). Sixteen averages were performed.

Next the double quantum filter (DQF) sequence was applied to the same PRESS-localised volume(McLean et al., 2002). For the first acquisition the filter was not activated (i.e. normal PRESS, TE/TR = 68/2000 ms), and spectra were acquired with and without applied CHESS water suppression gradients (scan time c. 1 minute each). Subsequently the filter was activated and 512 averages collected (scan time 17:12) to measure GABA+.

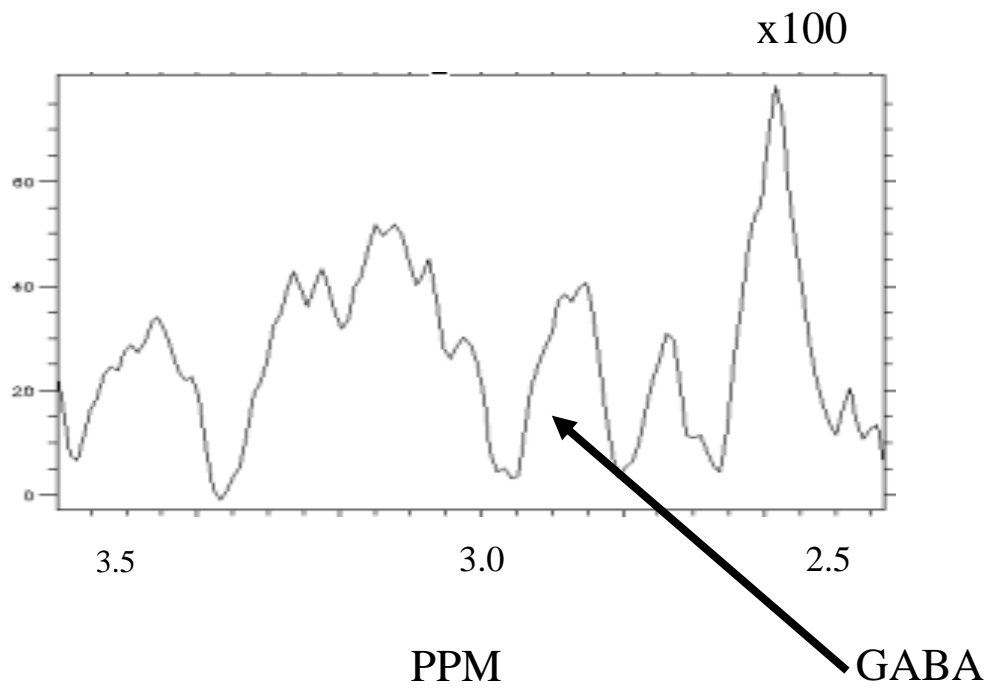
Figure 3.2.1:A) Axial T₁-weighted localising magnetic resonance imaging scan showing the position of the prescribed occipital lobe voxel. B) A representative PRESS localised spectrum (TE/TR 30/3000ms) with superimposed LCModel fit to metabolite concentrations and estimated baseline, and C) a filtered GABA spectrum (TE/TR 68/2000 ms) from the occipital voxel of a control volunteer are shown below. NAA_t = N-acetyl aspartate plus N-acetyl aspartyl-glutamate; GLX = glutamate plus glutamine; Cho = choline containing compounds; Cr = creatine + phosphocreatine; Ins = myo-inositol; GABA₊ = gamma amino butyric acid plus homocarnosine. PPM = chemical shift in parts per million.



B)



C)



3.2.2.3.2 Spectral Processing

The conventional PRESS localised water suppressed spectra (TE/TR = 30 / 3000 ms) were analysed using LCModel. The spectra obtained from the unfiltered DQF sequence (TE/TR = 68 / 2000 ms) were also analysed via LCModel in order to provide a consistent fit to the small baseline still present at this echo time. The LCModel Cr concentration was then converted to a peak area by multiplication with a conversion factor derived from phantom studies. The GABA+ concentration was then obtained according to equation [Eqn. 2.4.1] as described on page 138.

(Fig 3.2.1) includes a typical DQF spectrum and shows a well resolved GABA+ peak with minimal baseline. This allowed for reliable manual integration of the GABA+ peak. Poor quality data was rejected by setting a threshold of 4.5 for the signal to noise ratio (SNR) of the filtered signal (signal taken as the peak height between 3.5 to 2.5 PPM and noise 15 to 20 PPM).

3.2.2.3.3 Statistical Analysis

Statistical analysis was performed with SPSS 9.0. Metabolite concentrations and ratios were individually compared using ANOVA and post hoc comparisons were made using the Least Significant Difference Test (LSD).

3.2.3 Results

3.2.3.1 Subjects

The three subject groups (Control, IGE and OLE) were similar in age and gender distribution (Table 3.2.1). Individual metabolites were correlated against age for each group. No metabolite or metabolite ratio correlated with age or gender for any group. The two patient groups were acceptably matched for seizure control.

The control group was scanned on two occasions and test-retest repeatability scores obtained. The repeatability scores for the individual metabolites were as follows; NAA 16%, Cr 11%, Cho 20%, Ins 18%, GLX 26% and GABA+ 38%. The repeatability measure for the obtained grey matter content was 14%. Repeatability measures are defined as (Bland JM and Altman DG, 1986);

$$[2*SD(\text{scan1} - \text{scan2})/\text{mean}(\text{scan1},\text{scan2})]*100\%$$

[Eqn. 3.2.1]

For the group comparisons the control group data set contemporary in acquisition dates to the acquisition of the patient data sets was used.

Table 3.2.1: Description of the three groups of subjects. The healthy volunteer group is designated as Control. IGE represents the group of patients with idiopathic generalised epilepsy; and OLE represents the group with occipital lobe epilepsy. Each group has n=15.

	<u>Control</u>	<u>IGE</u>	<u>OLE</u>
Gender: Female / Male	7/8	5/10	8/7
Age in years: median (range)	27 (13- 40)	27 (17 – 55)	27 (17- 43)
Duration of epilepsy (years): median (range)	Not applicable	7 (1 - 25)	12 (4 – 31)
Duration in days since last seizure: median (range)	Not applicable	30 (1 - 1200)	75 (1 – 1000)
No. of seizures per year: median (range)	Not applicable	12 (<1 - 300)	5 (<1 – 600)
Duration in days since last convulsive seizure (IGE only):median (range)	Not applicable	45 (2 – 1200)	Not applicable
No. of convulsive seizures per year (IGE only): median (range)	Not applicable	1(1 – 50)	Not applicable
Lifetime convulsive seizures: median (range)	Not applicable	10 (1- 50)	17 (4 – 50)

3.2.3.2 MRS in individual patients

Abnormality of a metabolite concentration was defined as a value more than 3 standard deviations (SD) distant from the control mean of that variable. No significant abnormalities were identified for any single metabolite. Several ratios were also examined; NAAAt/Cr, GLX/Cr, GLX/GABA+, GLX/NAAAt and GLX/Ins. Only the ratio GLX/Ins showed sensitivity for abnormality in individual patients. Elevated GLX/Ins was observed in two of 15 patients in the IGE group and four of 15 in the OLE group. No individuals in the control group had elevated GLX/Ins.

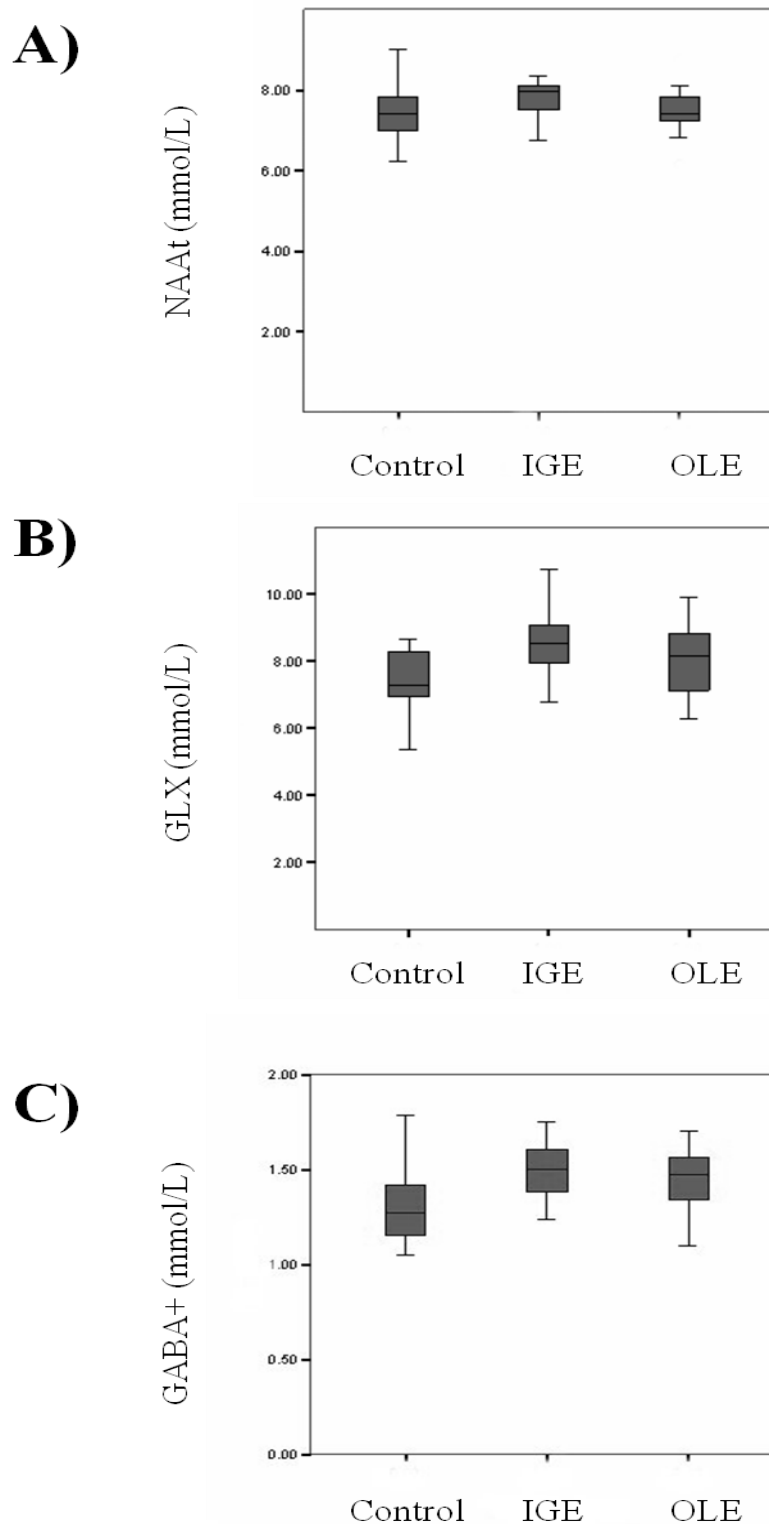
3.2.3.3 Group Results

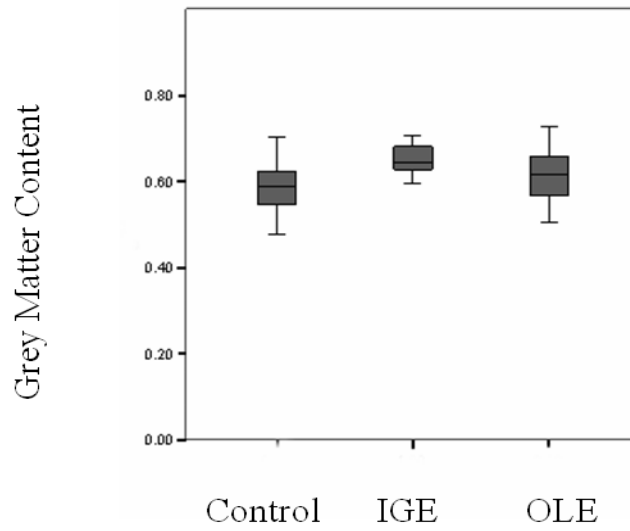
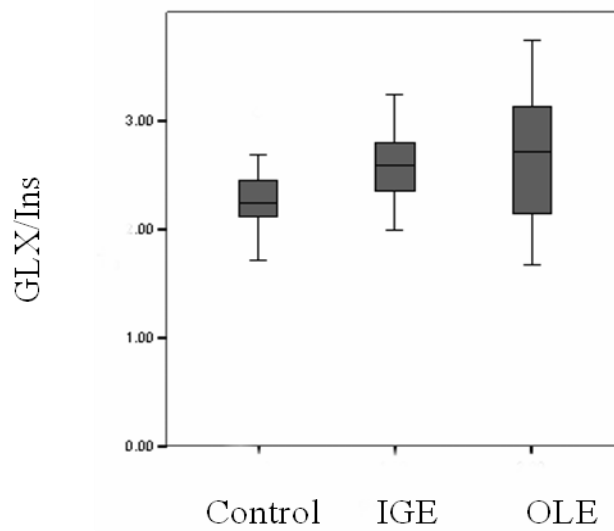
Comparison was made between the three groups (**Table 3.2.2, Fig 3.2.2**). No significant inter-group variation was observed for NAAAt, Cr, Cho or Ins. Significant variation was observed for GLX, Grey matter proportion and GABA+ ($p < 0.05$). Post hoc analysis was made using the LSD test and showed significant elevation of GLX and GABA+ in the IGE group compared to the control population and elevation of grey matter content in the IGE compared to both groups. Following re-analysis with grey matter content as a co-variable, no metabolite showed significant variation, although GLX remained higher in both patient groups than in the control group.

Table 3.2.2: Occipital metabolite concentrations and ratios expressed as the group mean and standard deviation for healthy volunteers (Control), patients with idiopathic generalised epilepsy (IGE) and patients with occipital lobe epilepsy (OLE). NAAAt = N-acetyl aspartate plus N-acetyl aspartyl-glutamate; GLX = glutamate plus glutamine; Cr = creatine plus phosphocreatine; Cho = choline containing compounds; Ins = myo-inositol; GABA+ = gamma amino butyric acid plus homocarnosine. Mean values and SD are provided for each measurement.

		<u>Control</u> N=15	<u>IGE</u> N=15	<u>OLE</u> N=15
Grey matter proportion		0.60(0.06)	0.65(0.04)	0.61(0.07)
Metabolites (mmol/l)	NAAAt	7.43(0.60)	7.74(0.50)	7.48(0.60)
	GLX	7.49(1.21)	8.51(0.90)	8.04(1.12)
	Cho	0.81(0.10)	0.76(0.10)	0.75(0.12)
	Cr	4.66(0.34)	4.85(0.30)	4.71(0.50)
	Ins	3.26(0.30)	3.31(0.40)	3.16(0.61)
	GABA+	1.35(0.21)	1.53(0.17)	1.45(0.17)
Metabolite ratios	NAAAt/Cr	1.61(0.20)	1.60(0.01)	1.59(0.13)
	GLX/Ins	2.30(0.30)	2.58(0.40)	2.64(0.64)

Figure 3.2.2: Box plots for: (A) N-acetyl aspartate plus N-acetyl aspartyl-glutamate (NAAt); (B) glutamate plus glutamine (GLX); (C) gamma-amino butyric acid plus homocarnosine (GABA+); (D) grey matter content and (E) GLX/myo-inositol (Ins) in the prescribed occipital region. The volunteer group is designated Control. IGE = idiopathic generalised epilepsy group and OLE = patients with occipital lobe epilepsy. The ends of the graph boxes fall at the upper and lower quartiles, the solid line within the box represents the median, and the whiskers the range of the data. Significant inter-group variation ($p < 0.05$) was observed for GLX, GABA+ and grey matter content.



D)**E)**

No associations between metabolite concentrations were identified for the control group or the IGE group. However there was a positive association between NAA_t and GLX for the OLE group (**Table 3.2.3**).

Table 3.2.3: Pearman correlation coefficients and levels of significance for metabolites within each group. Levels of significance have been corrected for multiple comparisons within each group. Healthy volunteers = Control; patients with idiopathic generalised epilepsy = IGE; and patients with occipital lobe epilepsy = OLE. NAAAt = N-acetyl aspartate plus N-acetyl aspartyl-glutamate; GLX = glutamate plus glutamine; GABA+ = gamma amino butyric acid plus homocarnosine. A significance level of $p=0.05$ is corrected to 0.015 for 3 comparisons.

	NAAAt	GLX	GABA+
Control:			
NAAAt	-	-	-
GLX	$R^2=0.03$ (not sig)	-	-
GABA+	$R^2=-0.06$ (not sig)	$R^2=0.01$ (not sig)	-
IGE:			
NAAAt	-	-	-
GLX	$R^2=0.33$ (not sig)	-	-
GABA+	$R^2=0.07$ (not sig)	$R^2=0.01$ (not sig)	-
OLE:			
NAAAt	-	-	-
GLX	$R^2=0.49$ (0.002)	-	-
GABA+	$R^2=<0.01$ (not sig)	$R^2=-0.01$ (not sig)	-

The metabolite ratio GLX/Ins showed post-hoc significant variation between the OLE group and the control group only. This was not significant on analysis with grey matter as a covariate analysis. No other ratios showed significant variation between the groups.

3.2.3.4 Relationship to concurrent anti-epileptic therapy

Two patients were taking topiramate in the IGE group. GABA+ values for both these subjects were within 1SD of the control mean. In the OLE group one patient was taking gabapentin. For this patient the GABA+ concentration was also within 1 SD of the control mean. Five patients in the IGE group were taking no medications. Comparison of GABA+ values in those taking AEDs against those on no AEDs showed a trend to lower values in the drug free group however this was not significant.

3.2.3.5 Relationship to seizure frequency and duration since the most recent seizure

A correlation analysis for each patient group for each metabolite against seizure frequency and duration since the most recent seizure was performed. The OLE group showed no correlation with seizure control and GABA+. In the IGE group no correlation was observed between GABA+ and either control of convulsive seizures or control of seizures of any type.

3.2.4 Discussion

At the time of publication this was the first study to apply a double quantum filter in vivo to measure GABA+ concentration in patients with epilepsy. The study was also the first report of in-vivo GABA+ concentrations measured in the region of seizure onset in patients with focal epilepsy. Using this technique GABA+ was measured with repeatability figures approaching those achievable for GLX. In patients with IGE and patients with OLE both GABA+ and GLX were found to be elevated compared to the control population. As noted in earlier studies, inter-group variation in grey matter composition can affect the significance of any observed metabolite differences and

must be taken into account (McLean et al., 2000). However following correction for grey matter content there was still a trend to elevated GLX in IGE albeit not statistically significant.

3.2.4 Methodology

The majority of GABA studies in patients with epilepsy have used spectral editing techniques. Petroff and co-workers have extensive experience of editing GABA in the occipital lobes in patients with partial epilepsy of extra-occipital onset using a 2.1T scanner and a surface coil. However their technique is limited at present to investigation of fairly superficial regions of the occipital lobes.

Double quantum filters have lower theoretical yield than the spectral editing techniques (38% (McLean et al., 2002) versus 100%) but are not prone to subtraction errors. At 1.5T reasonable reliability using a standard quadrature head coil was achieved. This allowed the examination of GABA concentration in other regions of the cerebrum without the limitations of surface coils. However large voxels are required (c. 35ml) that are clearly insensitive to local variation in GABA concentration. The scan time of 17 minutes per filtered acquisition was also a potential cause of patient non-compliance.

The resulting GABA+ signal can be expected to contain some contribution from homocarnosine, glutathione and macromolecules. The role of homocarnosine in vivo is not well understood. Its localisation appears to be the cytosol of a subgroup of GABAergic neurons and it may act as a GABA reservoir (Henry and Theodore, 2001). The contribution to the final signal of glutathione is expected to be small, whilst metabolite nulled studies suggest that there is limited passage of macromolecule through the filter (McLean et al., 2002). Shen and co-workers have reported findings with a doubly selective DQF in healthy volunteers (Shen et al., 2002). Using a 2.1T magnet, similar sized region of interest (30*30*30 mm) and a surface coil they report a slightly lower GABA concentration (1.21 +/- 0.28mmol/L) but similar coefficients of variation (23% versus 15% for the current study). These measures compare with coefficients of variation for GABA of between 5% and 13% reported by Petroff and

co-workers using spectral editing techniques(Petroff et al., 1996b;Petroff et al., 1999b).

In the control and IGE groups there was no correlation between the obtained metabolite concentrations. There was a positive correlation between NAA_t and GLX in the OLE group ($R^2 = 0.49$; $p = 0.002$). This finding agrees with a recent study that identified correlation between NAA and glutamate in specimens of epileptic human hippocampus and which proposed a coupled relationship between glutamate synthesis and NAA synthesis(Petroff et al., 2002b).

3.2.4.2 Findings in individual patients

In the patient groups no metabolite concentration was sensitive for abnormality in individual patients. Reduction in NAA_t is generally considered to reflect neuronal loss/dysfunction and is commonly observed in the temporal lobes in patients with temporal lobe epilepsy. However in this current study the voxel volume of interest is relatively large. Consequently any localised metabolite abnormality at the focus of ictal onset in the OLE group would be diluted by inclusion of surrounding unaffected tissue. This could account for the relative lack of abnormality in this group compared to the control group.

The cerebral concentration of NAA_t in IGE has not been extensively reported. Cendes and co-workers reported normal NAA/Cr in the temporal lobes in patients with absence seizures(Cendes et al., 1997c) whilst published findings in IGE patients measured in the frontal lobes(Savic et al., 2000a;Simister RJ et al., 2003b), [Chapter 3.3] suggest reduced NAA compared to a control population.

The relative sensitivity of the ratio GLX/Ins for abnormality is not simply explained. However, GLX has been found to be elevated in regions of ictal onset(Woermann et al., 1999c;Neppl et al., 2001), whilst Ins is thought to be localised to the glia(Brand et al., 1993). The ratio GLX/Ins may therefore represent the concentration of an excitatory component divided by a term representing glial concentration. There was no correlation observed with either ratio and seizure control or duration since most

recent seizure, so the terms appear to demonstrate no dynamic alteration with seizures. Six patients in the IGE group and one patient in the OLE group were taking VPA which lowers Ins levels [**Chapter 3.5**] and this might be expected to contribute to the elevation in GLX/Ins. However the obtained metabolite concentrations for Ins in IGE and OLE were higher than for the Control group which would argue against a significant effect of concomitant AED usage.

3.2.4.3 Group Comparisons

In the IGE group an increase in voxel grey matter content was observed despite normal MRI appearances. This would be consistent with the presence of microscopic abnormality of grey and/or adjacent white matter structure. Pathological analysis has shown cortical and subcortical dystopic neurons and other microscopic structural abnormalities (“microdysgenesis”) in a large percentage of a limited number of cases with IGE(Meencke and Janz, 1984). Other studies have not identified structural abnormality in IGE(Palmini et al., 1995;Opeskin et al., 2000) although widespread cerebral structural changes have been reported in quantitative MRI examination of patients with IGE leading to an increased mean normalised grey matter volume compared to control subjects(Woermann et al., 1998b).

In the IGE group GLX concentrations were significantly higher than in the control group. Following correction for grey matter content a trend to elevation was still evident in both patient groups. Elevation of GLX in subjects with temporal lobe epilepsy measured in the inter-ictal phase in the region of seizure onset(Woermann et al., 1999c) and in the contralateral temporal lobe(Simister et al., 2002) [**Chapter 3.1**] has been previously reported. Whether increased inter-ictal GLX represents elevation of glutamate and/or glutamine, or an increase in glutamatergic neurons, is not established. Post-ictal measures may also be affected by acute changes in MR “visibility” of these metabolites(Kauppinen et al., 1994). In vitro studies of epileptic tissue have described elevated glutamate(Sherwin et al., 1988) or elevation of glutamate and glutamine(Petroff et al., 1995). One recent animal study reported elevated post-ictal GLX following prolonged generalised seizures(Neppl et al., 2001).

Anticipated progress in separately resolving glutamate and glutamine will help explain these findings further.

AED therapy may also affect the observed concentration of GLX or GABA. Valproate and vigabatrin have both been reported to increase glutamine (Petroff et al., 2000). However in this study six patients in the IGE group were taking valproate, compared to nine patients not taking this medication. Comparison of the two groups did not identify a trend to elevation of GLX or GABA+ in the valproate group, and although a recent study has suggested that lamotrigine may cause elevation in GABA levels (Kuzniecky et al., 2002), a similar comparison showed no effect of lamotrigine on GABA+ or GLX levels.

In this study GABA+ concentrations were not observed to be reduced in our patient groups. This is contrary to earlier in-vivo MRS reports using spectral editing techniques (Petroff et al., 1996b; Woermann et al., 1999c). One study (Petroff et al., 2001a) has reported separate measurement of GABA and homocarnosine in patients with extra-occipital partial epilepsy and in patients with Juvenile Myoclonic Epilepsy (JME), a sub group of IGE. In that study, levels of GABA were generally within the normal range for the partial epilepsy group (three of 11 having GABA levels less than 2SD from the control mean) whilst GABA levels in JME were generally low (seven of 14 below 2SD). Homocarnosine levels were all within the normal range for both groups. These and earlier studies, however, investigated a region that was outside the site of seizure onset in patients with partial epilepsy and it was not known whether or not the JME group were actively photosensitive at the time of the study. Findings might be expected to be different in regions of epileptic neocortex. There was relative inhomogeneity in the IGE group with 8 of the 15 having IGE syndromes that were not sub-classifiable. All the patients with OLE had occipital ictal focal onset and 13 patients in the IGE group had active photo-paroxysmal response on EEG at the time of imaging. Pathological estimates of GABA concentration, although they are interpreted with caution, have not reported low levels of GABA in epileptic neocortex (Perry et al., 1975; Sherwin et al., 1988; Petroff et al., 1995). No variation of

GABA+ concentration was observed in this study with any taken AED therapy. However the numbers taking each medication were small.

There was no correlation between GABA+ and seizure control or interval since most recent seizure in the IGE group or in the OLE group. This is in agreement with the most recent findings of Petroff(Petroff et al., 2001a) who found no correlation between seizure control and GABA levels in patients with JME. That study did also report that seizure control in patients with extra-occipital partial epilepsy correlated with GABA and with homocarnosine concentrations but did not investigate GABA concentration in the region of seizure onset.

3.2.5 Conclusion

Disorders of GABA and Glutamate regulation are closely linked with seizure disorders. Previous work has suggested that MRS detected elevation in GLX is a feature of epileptic tissue whilst GABA levels may be affected by anti-epileptic drug therapy and seizure control. This current study reports reliable measurement of GABA+, by application of a double quantum filter, together with GLX measurement in patients with occipital lobe epilepsy and with IGE. Elevation was observed in both GLX and GABA+ in IGE and a trend to elevation of GLX in occipital lobe epilepsy. However, elevated grey matter content in the IGE group may have been responsible for most of the apparent metabolite abnormalities.

3.3 Proton MRS Reveals Frontal Lobe Metabolite Abnormalities in Idiopathic Generalised Epilepsy.

ABSTRACT

Purpose:

Cortical hyper-excitability may be important in the patho-physiology of idiopathic generalised epilepsy (IGE). In the human brain glutamate is the most important excitatory transmitter and γ -amino butyric acid (GABA) the dominant inhibitory neurotransmitter. This study reports GABA plus homocarnosine (GABA+) and glutamate plus glutamine (GLX) concentrations in the frontal lobes of patients with IGE.

Methods:

Twenty-one patients and 17 healthy volunteers were studied. A single voxel was prescribed in each frontal lobe for each subject. PRESS localised short echo time MRS was performed to measure GLX and the metabolites N-acetyl aspartate plus N-acetyl aspartyl-glutamate (NAAt), creatine and phosphocreatine, choline containing compounds and myo-inositol. A double quantum GABA filter was used to measure GABA+. Segmented T_1 weighted images gave the tissue composition of the prescribed voxel.

Results:

Group comparisons showed elevation of GLX and reduction of NAAt in the patient group ($p < 0.05$). The metabolite ratios GLX/NAAt and GLX/Ins also showed elevation in IGE ($p = 0.01$). No group effect was observed for GABA+, creatine and phosphocreatine, or choline containing compounds. Myo-inositol concentrations were not significantly reduced in the patient group but were less in the sub-group of patients who were taking sodium valproate.

Conclusion:

The results indicate that IGE is associated with frontal lobe metabolite changes that may imply increased excitability or proportion of glutamatergic neurons, and reduced NAAt, implying reduced overall neuronal numbers or neuronal dysfunction.

Published ref: (Simister et al., Neurology 2003 **61**,897-904)

3.3.1 Introduction

Elevated glutamate concentrations have been identified in human epileptic tissue (Sherwin et al., 1988; Petroff et al., 1995), and in vivo microdialysis studies have shown increased extra cellular glutamate in the temporal lobe following a seizure (During and Spencer, 1993). GLX can be estimated using proton MR spectroscopy (MRS) at short echo times (Woermann et al., 1999c; McLean et al., 2000) and may be elevated in regions of seizure onset (Woermann et al., 1999c).

Decreases in GABA inhibition may also cause seizures (Olsen and Avoli, 1997), and several AED enhance GABA function. Low GABA has been measured in patients with focal epilepsy (Petroff et al., 2000). Levels of GABA and homocarnosine, a dipeptide of GABA and histidine, have been shown to increase with improved seizure control (Petroff et al., 1996b; Petroff et al., 2000) or following the administration of AED that modify GABA metabolism or function (Petroff et al., 2000; Mueller et al., 2001b; Kuzniecky et al., 2002).

The purpose of the current study was to investigate GABA+ and GLX concentrations in patients with idiopathic generalised epilepsy (IGE) compared to healthy volunteers measured in the frontal lobes. The frontal lobes were studied because there is evidence for frontal lobe dysfunction (Niedermeyer, 1996; Swartz et al., 1996; Savic et al., 2000a) or subtle structural abnormality (Woermann et al., 1999b) in subjects with IGE.

3.3.2 Methods

3.3.2.1 Subjects

20 control volunteers and 26 patients with IGE were scanned after giving informed consent. Following application of exclusion criteria on the basis of quality of spectroscopic data, 17 controls and 21 patients were included in the study. Ethical approval by the Joint Research Ethics Committee of the National Hospital for Neurology and Neurosurgery was obtained. In all patients the diagnosis was based upon full clinical assessment, interictal +/- ictal scalp EEG, neuropsychometry and

MRI. All subjects had normal MRI on visual inspection. Fifteen of the included patients had IGE syndromes that were sub-classifiable as follows: Juvenile Myoclonic Epilepsy (seven), Juvenile Absence Epilepsy (six), Childhood Absence Epilepsy (one) and Generalised Tonic Clonic Seizures on Awakening (one). In the remaining six patients sub-syndrome classification was not possible. The antiepileptic drugs (AED) taken by the included patients were as follows; valproate (fourteen), lamotrigine (eight), carbamazepine (three), topiramate (two), clobazam (two), phenytoin (two), levetiracetam (two), ethosuximide (one). One patient was taking no regular medications. A full seizure history was obtained and the frequency of both absence and tonic-clonic seizures (GTC) at the time of scanning was recorded. The duration in days since the most recent GTC was also recorded.

3.3.2.2 Magnetic Resonance Imaging

The study was performed on a 1.5T General Electric SIGNA Horizon EchoSpeed scanner (Milwaukee, WI) using a standard quadrature head coil for all MRI/MRS studies. Axial T1 weighted inversion-recovery prepared fast spoiled gradient recalled echo (IRP-FSPGR) images were acquired ($TE/TI/TR = 4.2/450/16$ ms, flip angle 20° ; matrix $256*128$; slice thickness 1.5mm). These images were used both to guide voxel placement and subsequently for segmentation of fractional gray matter, white matter and cerebro-spinal fluid (CSF) content using SPM99 (Statistical Parametric Mapping; Wellcome Department of Imaging Neuroscience, Institute of Neurology, University College London). All the MRI studies were reviewed by two experienced neuro-radiologists.

3.3.2.3 Magnetic Resonance Spectroscopy

A single voxel was prescribed in each frontal lobe of each subject with approximate dimensions 40 by 35 mm in the Anterior-Posterior and Left-Right directions respectively and thickness 25mm (**Fig 3.3.1**). Voxel placement was prescribed from axial images. The voxel was placed with the medial border over the longitudinal fissure and the posterior border at the level of the pre-central sulcus. The most rostral axial slice that could fully contain the in plane dimensions of the voxel was chosen as the superior surface of the voxel. The volume of interest contained pre-motor cortex

including the supplementary motor area, cingulate gyrus and dorsolateral prefrontal cortex.

Conventional PRESS-localised water suppressed spectra were obtained initially with the acquisition parameters (TE/TR = 30/3000 ms) matching previous studies (Woermann et al., 1999c; McLean et al., 2000; McLean et al., 2001; McLean et al., 2002), so that LCModel (Provencher, 1993) could be used for quantification of NAA, Cr, Cho, Ins and GLX. The magnetic field in-homogeneities were successfully compensated for using the provided first order automated gradient shim procedures. Sixteen averages were performed.

Next the double quantum filter (DQF) sequence was applied and the final spectrum consistently phased to allow integration of the GABA+ resonance. The GABA+ concentration was then calculated relative to Cr [Eqn 2.4.1] on page 138. Finally, metabolite concentrations were corrected for CSF content, which is considered to provide negligible signal (Lynch et al., 1993). (This common methodology is fully described in Section 2)

Poor quality data was rejected by setting a threshold of 4.0 for the signal to noise ratio (SNR) of the filtered signal (signal taken as the highest peak between 3.5 to 2.5 PPM and noise 15 to 20 PPM), and rejected data with SNR < 4.0. PRESS localised (TE/TR = 30/3000 ms) datasets were also rejected if the manually measured unsuppressed water full width half maximum (FWHM) > 0.15 PPM. Only two data sets were discarded as a consequence of poor DQF signal to noise, however nine of 92 data sets were discarded with FWHM > 0.15 PPM. Finally, only those subjects with both left and right frontal data fulfilling these criteria were included in order to allow the opportunity to compare right voxel, left voxel and mean concentrations between the two groups. This final restriction resulted in the exclusion of two subjects in the control group and three subjects in the IGE group.

3.3.2.4 Statistics

Statistical analysis was performed with SPSS 9.0. Metabolite concentrations and ratios were individually compared using ANOVA. To investigate for a relationship between seizures and metabolite concentration only patient recorded GTC information was studied with the expectation that this data was the most accurately recorded. IGE subjects with age at the time of the study within the age range for the control group were included. Regression analysis was performed for each metabolite against duration of epilepsy, number of GTC per year, and the duration in days since the most recent GTC.

3.3.3 Results

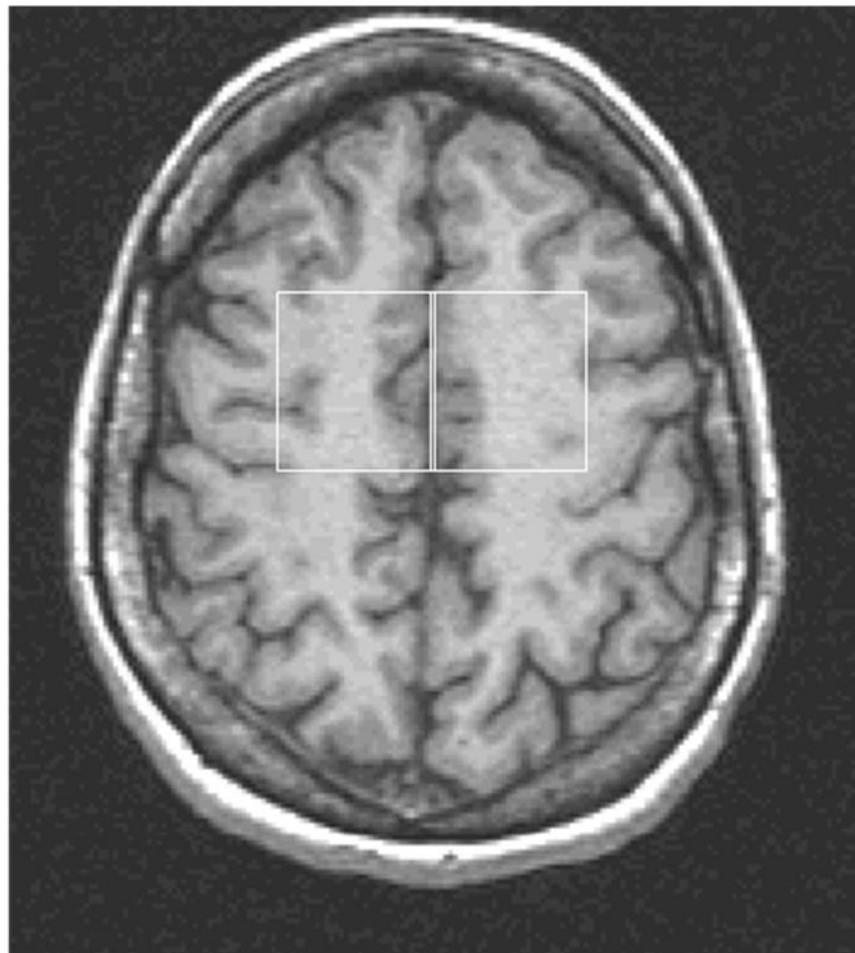
3.3.3.1 Group Results

The SPM estimates of voxel fractional gray matter content were compared between IGE subjects and controls and between right and left voxels, since several metabolites are predominantly concentrated in gray matter. No group differences were observed.

In the IGE group 21 of the 26 subjects met all the criteria for data inclusion. Paired t-tests were applied to examine right-left metabolite symmetry. In the control group right-left asymmetry was identified for NAA_t, Cr, Cho, and GLX. Concentrations in the left frontal voxel were lower than in the right frontal voxel ($p < 0.05$). Consequently inter-group comparisons were performed for right (R) and left (L) voxel concentrations separately as well as for mean (M) metabolite concentration. Two subjects of the Control group were left-handed.

Figure 3.3.1: A) Axial T₁-weighted localizing magnetic resonance imaging scan showing the position of the prescribed frontal lobe voxels. B) A representative PRESS localised spectrum (TE/TR 30/3000ms) with superimposed LCModel fit to metabolite concentrations and estimated baseline, and C) a filtered GABA spectrum (TE/TR 68/2000 ms) from the right frontal voxel of a control volunteer (Vertical scale is increased 100x relative to (B)). NAA_t = N-acetyl aspartate plus N-acetyl aspartyl-glutamate; GLX = glutamate plus glutamine; Cho = choline containing compounds; Cr = creatine + phosphocreatine; Ins = myo-inositol; GABA+ = gamma amino butyric acid plus homocarnosine. PPM = chemical shift in parts per million.

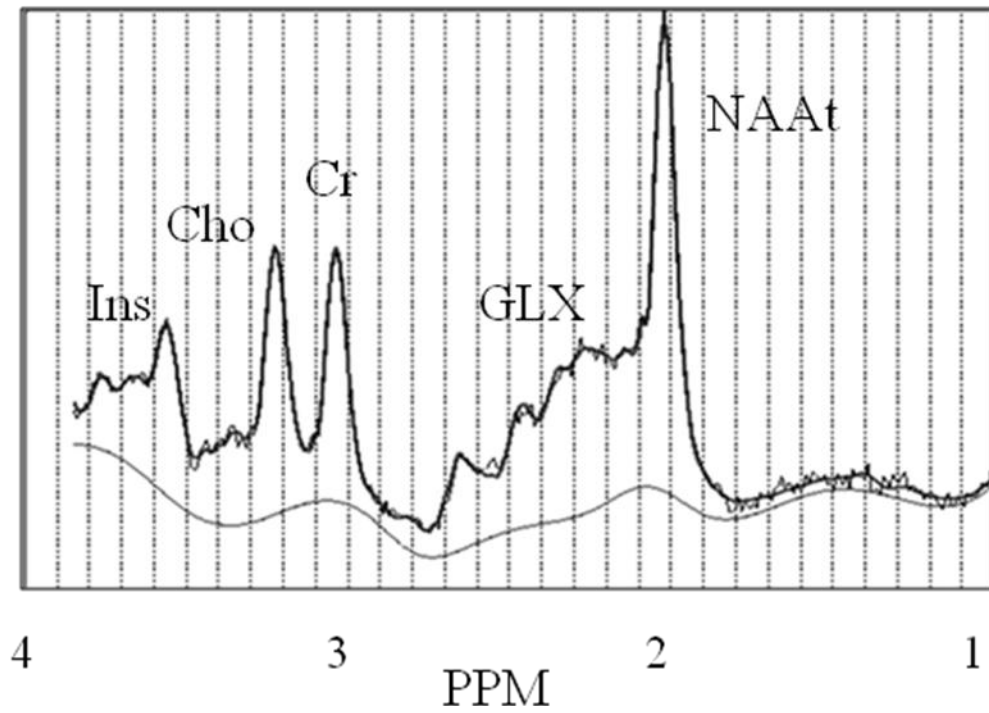
A)



Right

Left

B)



C)

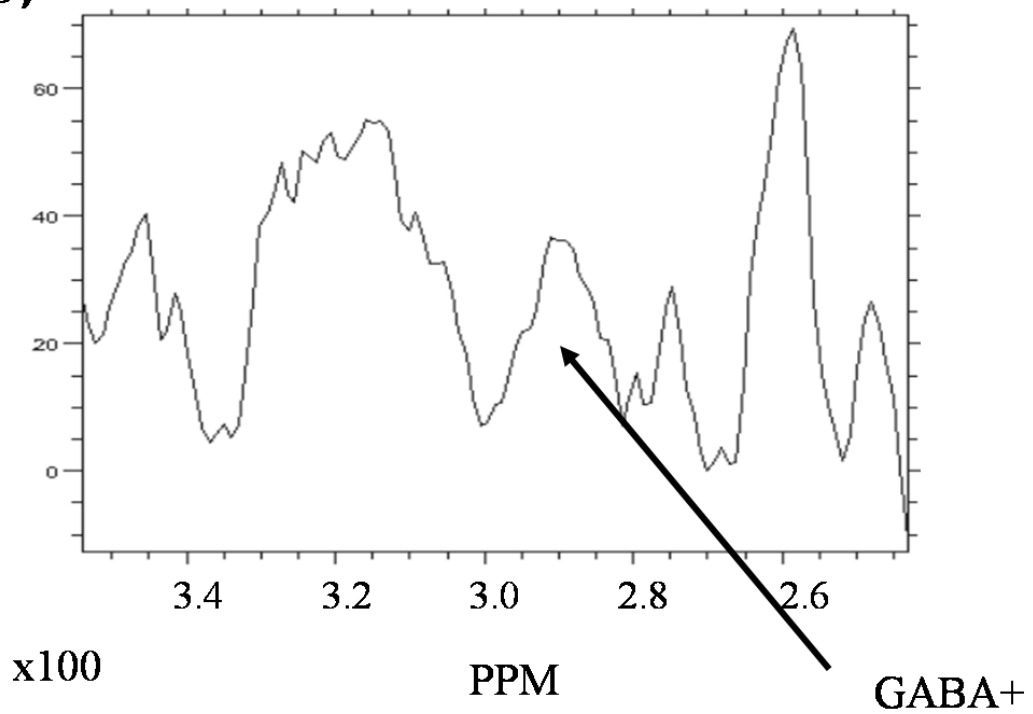


Table 3.3.1: Clinical data for the included IGE subjects. Identified IGE sub-types were juvenile myoclonic epilepsy (JME), juvenile absence epilepsy (JAE), childhood absence epilepsy (CAE) and generalised tonic clonic convulsions on awakening (GTCA). All subjects had normal clinical examination and normal MRI. All had EEG demonstrating generalised spike and wave (SW) discharge. U = unclassified IGE sub-type. GTC = generalised tonic clonic seizure. AED = antiepileptic drug. Cbz = carbamazepine, clb = clobazam, pht = phenytoin, eth = ethosuximide, ltg = lamotrigine, lev = levetiracetam, tpm = topiramate, vpa = sodium valproate, nil = no regular antiepileptic drugs.

Patient No. /Age /gender /handedness	Diagnosis /AEDs	Age of onset / Duration of epilepsy (years)	GTC per year / GTC (lifetime) / Duration since last GTC (days)
1/21/M/R	JME/ ltg	17/4	2/5/6
2/19/M/R	JAE/ ltg	11/8	2/6/30
3/17/M/R	JME/ cbz, clb	10/7	4/17/30
4/19/F/R	JAE/ nil	13/6	0/1/1000
5/23/M/R	JAE/ cbz	13/10	6/40/7
6/19/F/R	JME/ vpa	15/4	4/6/30
7/20/F/R	U/ vpa	14/6	1/5/60
8/19/M/R	JAE/ lev	9/10	12/40/4
9/39/F/R	U/ vpa, ltg	10/29	3/15/60
10/31/F/R	U/ ltg	10/21	6/30/40
11/30/F/R	JME/ vpa	12/18	6/30/30
12/32/M/R	U/ vpa	15/17	0/3/900
13/23/M/R	JAE/ tpm, eth, vpa, ltg	13/10	22/40/2
14/40/M/R	JAE/ vpa, ltg	6/34	0/17/800
15/51/F/R	JME/vpa	11/40	6/100/30
16/43/M/R	CAE/ vpa, clb, ltg	8/35	4/30/9
17/32/M/R	GTCA/ vpa, pht	17/15	15/100/30
18/36/F/R	U/ vpa, cbz	6/30	0/5/800
19/22/M/R	JME/ vpa	18/4	2/5/42
20/44/F/R	U/ vpa, lev	16/28	0/1/1000
21/39/M/R	JME/ vpa, tpm, ltg, pht	7/32	6/18/30

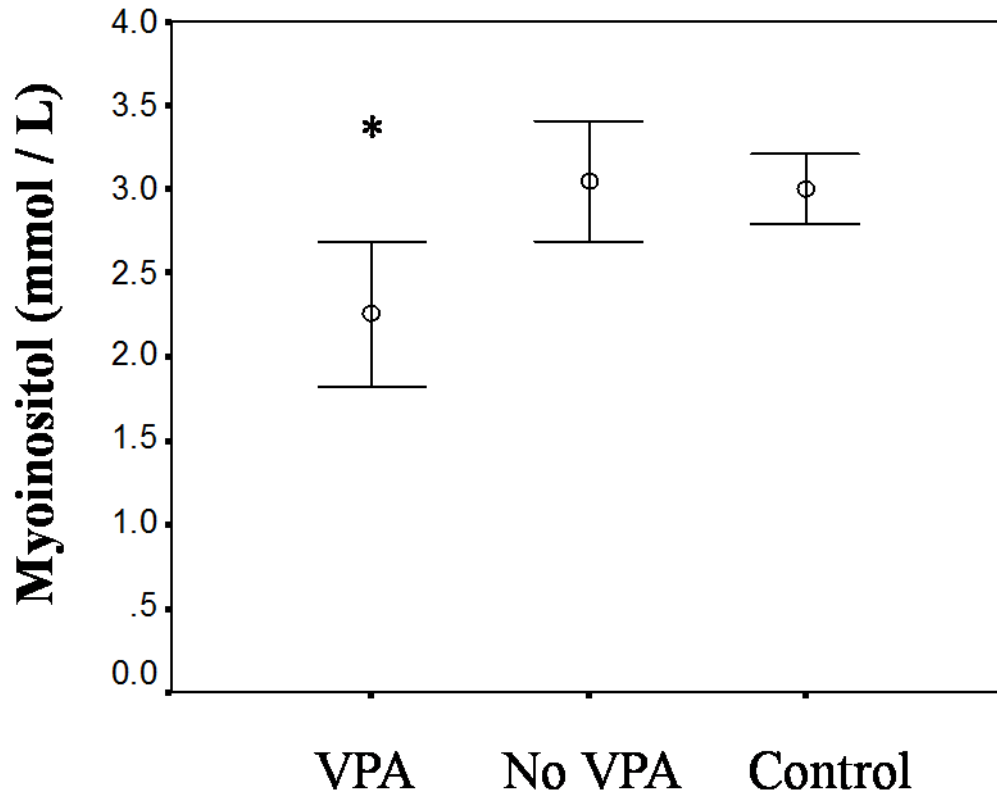
Mean GLX was higher in the IGE group than the controls by 12% (IGEL $p = 0.03$, IGER $p = 0.03$ IGEM $p = 0.04$) (Table 3.3.2). Reduction of NAA_t was observed in IGER by 8% $p = 0.01$ and in IGEM by 7 % $p = 0.01$) as well as a trend to reduction in the IGEL group that was not significant. Ins was reduced in the IGEL and IGEM voxels. No inter-group variation was observed for GABA₊.

Both the ratios GLX/Ins and GLX/NAA_t were higher in all three IGE voxels ($p < 0.01$).

Table 3.3.2: Frontal metabolite concentrations and ratios expressed as the group mean and standard deviation for healthy volunteers (Control) and patients with idiopathic generalised epilepsy (IGE). R = right frontal voxel. L = left frontal voxel. M = mean frontal voxel. NAA_t = N-acetyl aspartate plus N-acetyl aspartyl-glutamate; GLX = glutamate plus glutamine; Cr = creatine plus phosphocreatine; Cho = choline containing compounds; Ins = myo-inositol; GABA₊ = gamma amino butyric acid plus homocarnosine. Variation ($p \leq 0.05$) between IGE and Control is indicated by *. Mean values and SD are provided for each measurement.

		ControlR N=17	ControlL N=17	ControlM N=17	IGER N=21	IGEL N=21	IGEM N=21
Gray matter proportion		0.31(0.03)	0.30(0.04)	0.30(0.03)	0.32(0.05)	0.30(0.04)	0.31(0.04)
Metabolites (mmol/l)	NAA _t	7.4(0.6)	7.0(0.7)	7.2(0.6)	6.8(0.4)*	6.6(0.5)	6.7(0.5)*
	GLX	7.4(0.9)	6.3(1.0)	6.9(0.6)	8.4(1.5)*	7.1(1.1)*	7.7(1.1)*
	Cho	1.1(0.1)	1.0(0.1)	1.0(0.1)	1.1(0.2)	0.9(0.2)	1.0(0.2)
	Cr	4.4(0.4)	4.1(0.5)	4.3(0.4)	4.3(0.4)	4.0(0.5)	4.1(0.4)
	Ins	3.1(0.3)	3.0(0.4)	3.1(0.4)	2.8(0.6)	2.5(0.7)*	2.7(0.6)*
	GABA ₊	1.4(0.3)	1.4(0.2)	1.4(0.3)	1.4(0.3)	1.4(0.3)	1.4(0.3)
Metabolite Ratios	NAA _t /Cr	1.7(0.2)	1.7(0.2)	1.7(0.1)	1.6(0.2)	1.7(0.2)	1.6(0.2)
	GLX/NAA _t	1.0(0.2)	0.9(0.1)	1.0(0.1)	1.2(0.2)*	1.1(0.2)*	1.1(0.2)*
	GLX/Ins	2.4(0.4)	2.1(0.4)	2.3(0.4)	3.1(1.1)*	3.0(1.1)*	3.1(1.0)*

Figure 3.3.2: Error bar plots of mean and 95% confidence intervals for Myo-inositol (Ins) in patients with idiopathic generalised epilepsy (IGE) and in the control group (Control). VPA = subjects taking sodium valproate. No VPA = subjects not taking valproate. Variation ($p \leq 0.05$) between VPA and No VPA in the IGE group is indicated by *.



3.3.3.2 Relationship to current anti-epileptic therapy

In this study only valproate (n = 14) and lamotrigine (n = 8) were AED therapies taken by more than five patients. There was no effect of valproate therapy on GLX or GABA+. Ins was reduced in the valproate taking patients in the mean voxels (p = 0.05) (**Fig 3.3.2**) compared to the non valproate taking IGE subjects and this effect remained after re-analysis using gray matter proportion as a covariable. There was no difference in Ins between the control group and the non valproate taking subjects and no effects were observed for lamotrigine. Topiramate was taken by only two patients. If the topiramate taking patients were removed from the IGE group, GLX was still observed to be elevated in the IGE group.

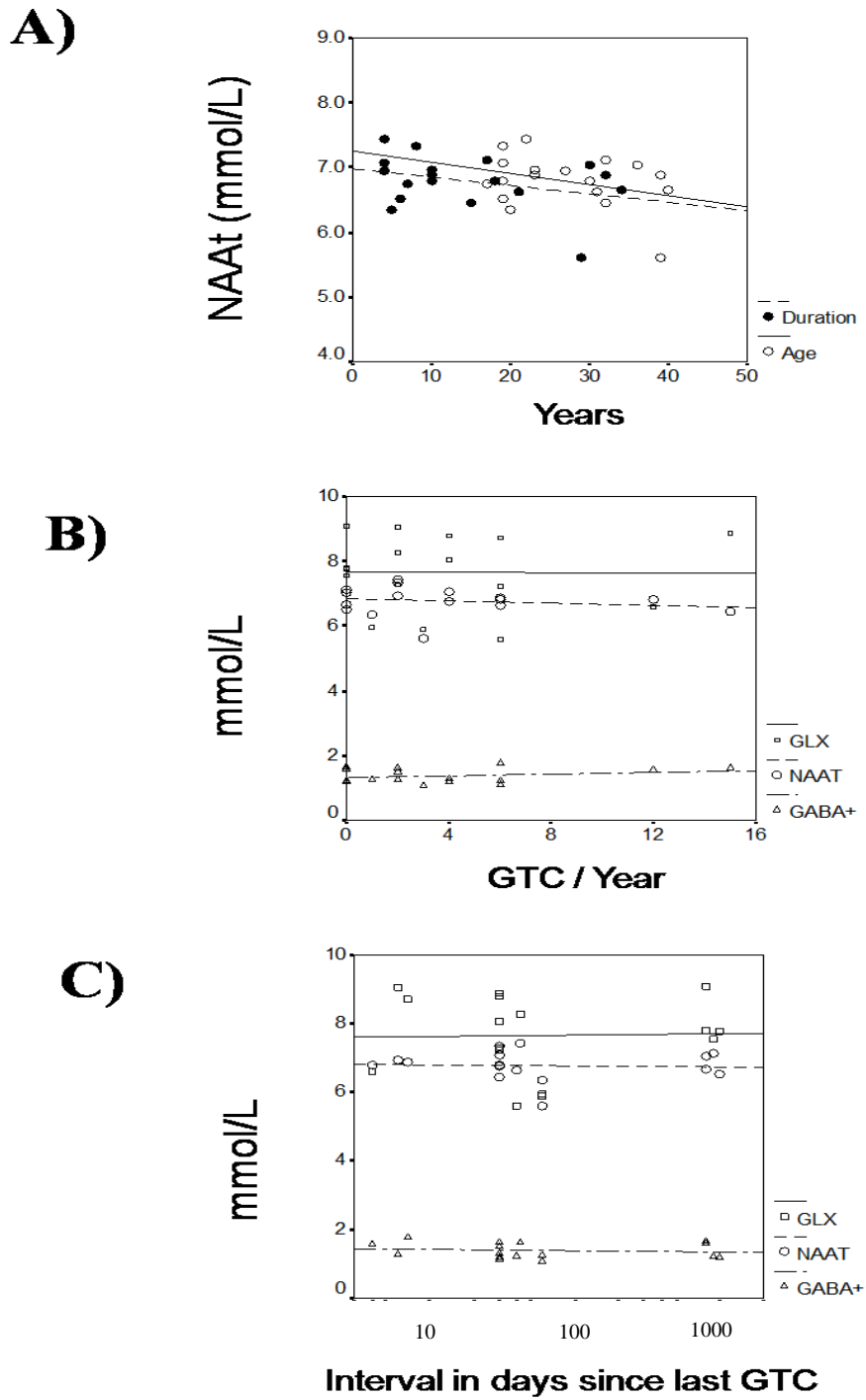
3.3.3.3 Relationship to seizure frequency and duration since the most recent seizure

There were no significant associations for any metabolite or metabolite ratio against tonic-clonic seizure frequency, duration of epilepsy or time since the most recent tonic-clonic convulsive seizure (**Fig 3.3.3**).

3.3.3.4 Relationship to IGE sub-type

Seven subjects in the IGE group had a diagnosis of juvenile myoclonic epilepsy (JME) and six subjects had juvenile absence epilepsy (JAE). Both sub-groups showed elevation in mean GLX and a trend to reduction in mean NAAt compared to the control group. A trend to elevation in mean GABA+ and mean gray proportion was observed in JAE compared to JME and controls.

Figure 3.3.3: Plots of mean GLX, GABA+ and NAAt against (A) age and duration of epilepsy, (B) number of generalised tonic clonic seizures (GTC) in the year preceding the date of the scan and (C) duration in days since the last GTC for the IGE group.



3.3.4 Discussion

The main findings of this study were that GLX was elevated and NAA_t was reduced in patients with IGE. Ins concentrations were lower in patients taking valproate.

Right–left comparison of the metabolite concentrations in the control group revealed lower concentrations of all metabolites in the left frontal voxels. Frontal gray matter volumes have been shown to be higher in the right hemisphere in healthy volunteers (Amunts et al., 2000; Watkins et al., 2001; Rademacher et al., 2001) which would generally be expected to give higher metabolite concentrations (McLean et al., 2000); however, in this study, the gray matter proportions within the prescribed voxels showed no right–left asymmetry. The lateral margins of the prescribed volumes of interest were positioned relatively close to the scalp, allowing some inclusion of signal from scalp lipids, which may differ in the left voxel as compared with the right voxel because of chemical shift artifact and may affect the baseline estimation. Therefore, this side-to-side difference most likely arose as a consequence of methodology rather than true physiologic difference.

Previous volumetric studies have suggested that IGE may be associated with a relative increase in gray matter (Woermann et al., 1998b; Simister RJ et al., 2003a), [Chapter 3.2] possibly due to a subtle abnormality of the cortical layers (Woermann et al., 1998b). In this current frontal lobe study, no gray matter increase was observed in the IGE group compared with the control group, but this was only a small sample of the frontal lobe.

In the IGE group, GLX concentrations were significantly higher than in the control group. This is in agreement with prior studies which have reported elevation of GLX in the region of seizure onset in partial seizures (Woermann et al., 1999c), and a recent animal study has reported elevated post-ictal GLX following prolonged generalized seizures (Neppl et al., 2001). Whether increased GLX directly represents increased glutamatergic neurotransmission is not yet established.

The metabolism of glutamate and glutamine is tightly coupled. After neuronal release of glutamate, glutamate action in the synaptic cleft is terminated by glial uptake mechanisms and the glutamate is subsequently converted within the glia by glutamine synthetase to glutamine. The glutamine is then exported back into the neighbouring neuron, where it is reconverted to glutamate. Astrocytic glutamine synthesis also occurs. Elevation in GLX may therefore be the consequence of a number of processes: increased neuronal glutamate concentrations or glutamatergic neurons; increased astrocytic glutamine content as a consequence of increased glutamate–glutamine flux or increased glial activity of the tricarboxylic acid cycle; increased glial cell numbers; or altered function of glutamine transporters. Post-ictally measures may also be affected by acute changes in MR “visibility” of glutamate (Kauppinen et al., 1994). In vitro studies of epileptic tissue have described elevated glutamate or elevation of glutamate and glutamine (Petroff et al., 1995). Further studies at higher field strengths will help to determine whether GLX elevation in subjects with epilepsy is a consequence of glutamate and/or glutamine elevation and also how the relative proportion of these metabolites changes following epileptic seizures. Elevated GLX would be in keeping with a model of cortical hyperexcitability in IGE but subsequent work by Badawy and colleagues indicates that whilst changes in cortical excitability do occur around the time of a seizure both increased excitability (prior to the seizure) and decreased excitability post seizure are observed (Badawy et al., 2009).

The current study shows reduced NAA in patients with IGE. A similar result was obtained in a study of patients with JME that reported reduction of NAA in the prefrontal cortex (Savic et al., 2000a). In comparison no NAA reduction was observed in patients with IGE when measured in the occipital lobes (Simister RJ et al., 2003a) [Chapter 3.2]. These findings together support the proposal that IGE might be associated with abnormal frontal lobe function. Subsequently published work has added to these observations. Several quantitative MRI studies have reported abnormally increased grey matter content in medial frontal regions (Betting et al., 2006; Kim et al., 2007) whilst Hommet and colleagues have reported frontal cognitive disturbance in IGE patients (Hommet et al., 2006).

In this study, IGE subjects had GABA+ concentrations in the normal range. A similar observation was made when IGE subjects were studied using voxels placed in the occipital lobe (Simister RJ et al., 2003a) [Chapter 3.2]. Few previous MRS studies have included IGE patients, and none has been performed in the frontal lobes. One study reported separate measures of GABA and homocarnosine in the occipital lobes in subjects with JME(Petroff et al., 2001a). GABA levels were generally low, whereas homocarnosine levels were within the normal range. The role of homocarnosine in vivo is not well understood. Its localization appears to be the cytosol of a subgroup of GABAergic neurons, and it may act as a GABA reservoir(Henry and Theodore, 2001).

It is possible that concurrent AED therapy may have affected the concentrations of GLX and GABA+(Petroff et al., 2000). Valproate has been reported to increase glutamine and hence GLX(Petroff et al., 2000), but although 14 of the 21 patients included in the IGE group in the current study were taking valproate, neither GLX or GABA+ concentrations appeared elevated.

Comparison of patients taking valproate with patients not taking valproate revealed lower Ins in the valproate-taking group. Low Ins has been reported in a patient with valproate-associated encephalopathy(Ziyeh et al., 2002). Low Ins and raised inositol monophosphates have also been reported in rats treated with valproate or lithium(O'Donnell et al., 2003). Lithium has no role as an AED, and the relevance of these findings to the anti-seizure activity of valproate is not established. The mechanism for Ins reduction by valproate may be by an unknown action on the phospho-inositide Ca^{2+} second messenger system(O'Donnell et al., 2003) or via inhibition of a cell membrane sodium/Ins co-transporter(van Calker and Belmaker, 2000a). A few studies have reported modulation of the phospho-inositide system in epileptic tissue(Dubeau et al., 1992), but whether this is a cause or a consequence of seizure activity is not established.

There was no correlation between GABA+ and tonic clonic seizure frequency or interval since most recent GTC in the IGE group. This concurs with a recent

study(Petroff et al., 2001a) that found no correlation between seizure control and GABA in JME patients. That study, however, reported that seizure control correlated with homocarnosine concentrations. In the current study DQF measures of GABA+ include GABA and homocarnosine, so a direct comparison cannot be made.

3.3.5 Conclusion

In this study quantitative ¹H MRS demonstrated that IGE is associated with elevated frontal GLX and reduced NAA_t. Sodium valproate appears to be associated with reduction in Ins levels in subjects taking this medication.

3.4 Proton Magnetic Resonance Spectroscopy of Malformations of Cortical Development Causing Epilepsy

ABSTRACT

Purpose:

To use proton Magnetic Resonance Spectroscopy (MRS) to measure concentrations of Gamma-amino butyric acid (GABA) and glutamate plus glutamine (GLX) in adult patients with refractory epilepsy associated with malformations of cortical development (MCD).

Methods:

MRS was used to measure N-acetyl aspartate (NAA), creatine plus phosphocreatine (Cr) and choline containing compounds (Cho), as well as GLX, and GABA. Fifteen patients with epilepsy attributable to MCD and 15 healthy controls were studied. Nine of the MCD group had heterotopia and six had polymicrogyria. Quantitative short echo time MRS [echo time (TE) = 30 ms, repetition time (TR) = 3000 ms] was performed in the MRI evident MCD and in the occipital lobes of the control group and the concentrations of NAA, Cr, Cho, and GLX were measured. GABA plus homocarnosine (GABA+) was measured in the same regions using a double quantum filter.

Results:

The dominant abnormalities in the patient group were elevation of Cho and GLX and reduction in NAA compared to the control group. The ratios GLX/NAA and GABA+/Cr were also increased in the patient group whilst the ratio NAA/Cr was decreased. NAA was significantly lower in polymicrogyria than heterotopia.

Conclusions:

Large cortical malformations had abnormal levels of both GLX and GABA+/Cr. Low NAA and high Cho were also observed. These results indicate that MCD show spectroscopic features of primitive tissue and abnormal metabolism of both inhibitory and excitatory neurotransmitters.

Published ref: (Simister et al., Epilepsy Research 2007 **74**, 107-15)

3.4.1 Introduction

Malformations of cortical development (MCD) are an important cause of refractory focal epilepsy. MCD include a heterogeneous range of conditions that arise at different points along the process of normal cortical development, which have characteristic histopathological features and recognisable appearance on MRI. Microscopic structure of these MCD sub-types can range from heterotopic aggregates of relatively normal neurons to abnormalities of cortical lamination or neuronal differentiation. Invasive EEG studies have demonstrated that MCD are intrinsically epileptogenic (Palmini et al., 1995; Mattia et al., 1995; Kothare et al., 1998) or that surrounding normal appearing tissue is epileptogenic (Jacobs et al., 1999).

Proton Magnetic Resonance Spectroscopy (MRS) is a sensitive measure of neuronal loss or dysfunction (Urenjak et al., 1992; Cendes et al., 1997b; Tasch et al., 1999) or neuronal maturation (Simone et al., 1999b; Kreis et al., 2002; Tkac et al., 2003), and a number of MRS studies have reported the reliable quantification of metabolites relevant to the study of epilepsy (Petroff et al., 2000; McLean et al., 2000; McLean et al., 2002). Most MRS studies in subjects with MCD have used long echo times (TE), and reported only the ratios of the main visible metabolites, NAA, Cr, Cho (Marsh et al., 1996; Kuzniecky et al., 1997b; Li et al., 1998; Simone et al., 1999a; Simone et al., 1999b; Widjaja et al., 2003). These studies have typically shown reduction in NAA/Cr and NAA/Cho in the region of focal cortical dysplasia whilst heterotopia and polymicrogyria may have normal or reduced NAA/Cr (Marsh et al., 1996; Kuzniecky et al., 1997b; Li et al., 1998; Widjaja et al., 2003). There is evidence for metabolic heterogeneity within the visible lesions as well as within normal appearing surrounding tissue (Kuzniecky et al., 1997a). In a quantitative multi voxel MRS study of MCD with correction for tissue composition abnormal metabolite concentrations were found within MCD, within peri-lesional tissue and also in contralateral normal appearing tissue (Woermann et al., 2001b).

Elevation of glutamate is a feature of epileptic tissue (Petroff et al., 1995) and elevations in GLX have been observed in the frontal lobes in subjects with idiopathic

generalised epilepsy (IGE) (Simister RJ et al., 2003b) [Chapter 3.3] and in the temporal lobe in temporal lobe epilepsy (Woermann et al., 1999c).

The role of GABA in the developing brain and in epileptic tissue is the subject of much current research. Reduction in GABA inhibition may cause seizures (Olsen and Avoli, 1997) and several potent anti-epileptic drugs (AED) enhance GABA function. However, in immature or epileptic tissue, activation of GABAergic synapses may be excitatory rather than inhibitory (Ben Ari, 2002; Ben Ari and Holmes, 2005). Animal models of MCD have shown increased GABAergic function associated with impaired GABA transporter function (Calcagnotto et al., 2002), down-regulation of GABA_A receptors (Prince et al., 1997) or decreased neuronal sensitivity to GABA (Benardete and Kriegstein, 2002).

The aim of the current study was to measure the profiles in large MCD of GABA+ and GLX concentrations together with concentrations of the other main MRS visible metabolites.

3.4.2 Methods

3.4.2.1 Subjects

Fifteen controls (seven female, with median age 27 years and range 18 to 40 years) and 15 subjects with MCD (five female, with median age 30 years and range 21 to 51 years) were studied. Ethical approval by the Joint Research Ethics Committee of the Institute of Neurology and the National Hospital for Neurology and Neurosurgery was obtained, and all subjects gave informed consent. All 15 patients had refractory focal epilepsy, and were taking one or more AED. Diagnosis was based upon full clinical assessment, interictal +/- ictal scalp EEG, neuropsychometry and MRI. All control subjects had normal MRI on visual inspection. All patients had a single dominant MRI evident MCD (**Table 3.4.1**). Four had bilateral and symmetrical pathology. In two of these, voxels were placed in homologous regions in both hemispheres and the obtained results averaged. Six subjects had MRI appearance of polymicrogyria (PMG) while nine subjects had MRI appearance of heterotopia (HT).

3.4.2.2 Magnetic Resonance Imaging

A 1.5T SIGNA Horizon Echospeed scanner (General Electric, Milwaukee, WI) with a standard quadrature head coil was used for all studies. Axial T1 weighted inversion-recovery prepared fast spoiled gradient recalled echo (IR-FSPGR) images were acquired (TE/TI/TR = 4.2/450/15.5 ms, flip angle 200; matrix 256*160; FOV 24 cm; slice thickness 1.5mm) to guide voxel placement and for segmentation into fractional grey matter, white matter and cerebro-spinal fluid (CSF) using SPM99 (Statistical Parametric Mapping; Wellcome Department of Imaging Neuroscience, Institute of Neurology, University College London). All MRI studies were reviewed by two experienced neuro-radiologists.

3.4.2.3 Magnetic Resonance Spectroscopy

For each MCD patient a voxel was prescribed from the axial IR-FSPGR images with in plane dimensions 40 by 35 mm and thickness 25mm (**Fig. 3.4.1**). The voxel was centred over the major visible MCD. In the controls a single voxel with dimensions 35 by 40 mm in the Anterior-Posterior and Left-Right directions and thickness 25 mm was prescribed in the occipital lobes as previously described (McLean et al., 2002; Simister RJ et al., 2003a) (Chapter [3.2], [3.3]). This control voxel location was chosen to match the high grey matter proportion seen in MCD.

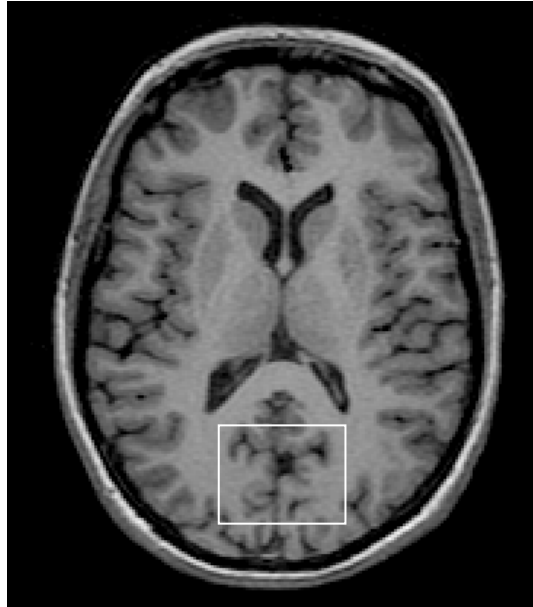
Conventional PRESS-localised water suppressed spectra were obtained with the acquisition parameters (TE/TR = 30/3000 ms) as in previous studies (Woermann et al., 1999c; McLean et al., 2000; McLean et al., 2001; McLean et al., 2002), so that LCModel (Provencher, 2001) could be used for quantification of NAA plus N acetyl aspartyl glutamate (combined as NAAt), Cr, Cho, Ins and GLX. The double quantum filter (DQF) sequence (Keltner et al., 1997; McLean et al., 2002) was used to measure GABA concentration.

Table 3.4.1: Clinical data for the MCD subjects. M = male; F = female; r. = right; l. = left; PMG = polymicrogyria; SCH = sub-cortical heterotopia; SEH = sub-ependymal heterotopia. acetazol = acetazolamide; cbz = carbamazepine; clb = clobazam; gbp = gabapentin; ltg = lamotrigine; lev = levetiracetam; oxc = oxcarbazepine; pht = phenytoin; prm = primidone; tpm = topiramate; vpa = sodium valproate; sec. gen. = secondary generalised. LD = learning disability.

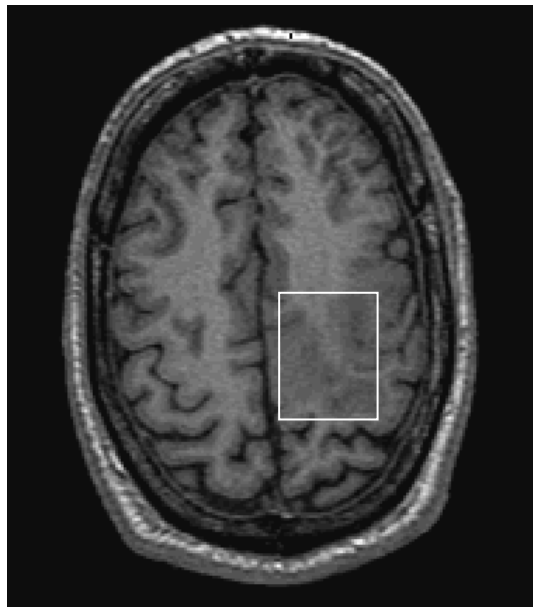
Patient no. /age(years) /gender	Seizure onset (year)	CPS and SGTCS /month	Days since last seizure	Neurology	EEG	MRI	AED
1/45/M	6	30	2	r. hemiparesis	Interictal: l hemisphere	l. frontoparietal PMG	cbz, prm, tpm
2/51/M	7	4	30	l. hemiparesis	Interictal and ictal: r. temporal	r. frontoparietal PMG plus l. occipital PMG	cbz, vpa
3/46/M	8	8	4	r. hemiparesis	Interictal: l. hemisphere	l.parietoccipital PMG and l. HS	cbz, acetazol
4/30/M	7	7	7	Normal	Interictal and ictal:diffuse posterior r. hemisphere	Bilateral r > l occipital PMG	clb, vpa
5/27/F	2	120	3	LD	Interictal: bilateral r.>l.	Diffuse bilateral PMG	tpm, vpa
6/28/M	10	15	1	LD	Interictal: bilateral not localised	Bilateral perisylvian PMG r. > l.	lev, ltg, oxc
7/51/M	28	0	>350	Normal	Interictal:non specific	r. parietal SCH	cbz
8/25/F	2	16	3	LD	Interictal: non localised	Bilateral SCH	cbz, tpm, pht
9/31/M	19	20	6	LD	Interictal: r. temporoparietal	Posterior r. sided SCH	pht
10/25/M	1	4	3	l. hemiparesis	Interictal and ictal: r. frontoparietal	r. frontoparietal SCH	clb, cbz, gbp
11/34/F	4	120	2	Normal	Interictal: bilateral	Diffuse bilateral SCH	clb, cbz, tpm
12/31/M	6	300	1	Normal	Interictal:bilateral diffuse r. > l.	Occipital SCH	cbz, lev, vpa
13/23/F	13	48	2	Normal	Interictal: r. temporal	Occipital SHE	lev, oxc, vpa
14/21/F	15	3	>350	Normal	Interictal:diffuse r. parietotemporal	r. Parietotempero SCH	cbz, ltg
15/25/M	17	40	1	Normal	Interictal: diffuse focus r. hemisphere	Extensive r. temperoparietal SCH	cbz, pht, tpm

Figure 3.4.1: Axial image showing the position of the prescribed voxels A) in the occipital lobes in a control and B) in the MRI visible MCD in patient 1.

A)



B)

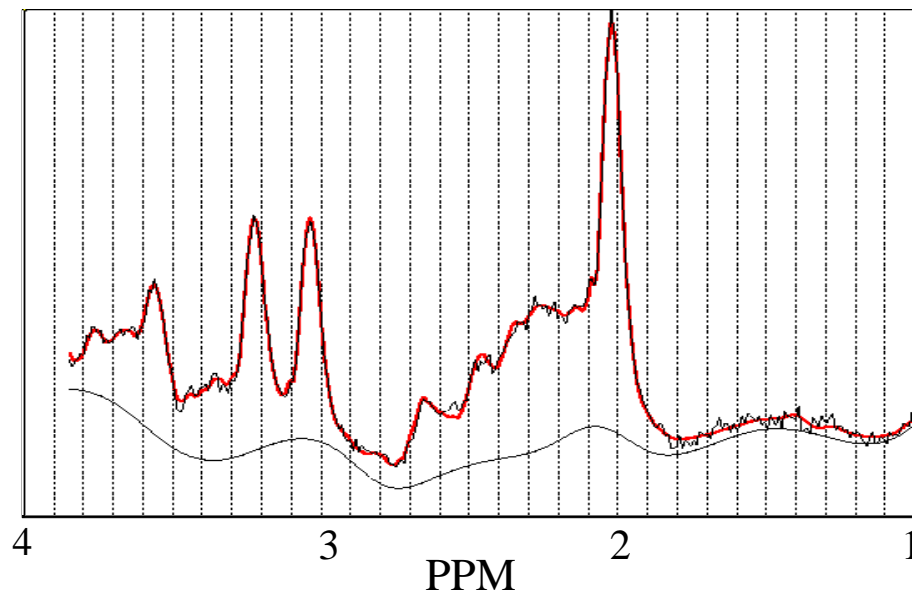


Right

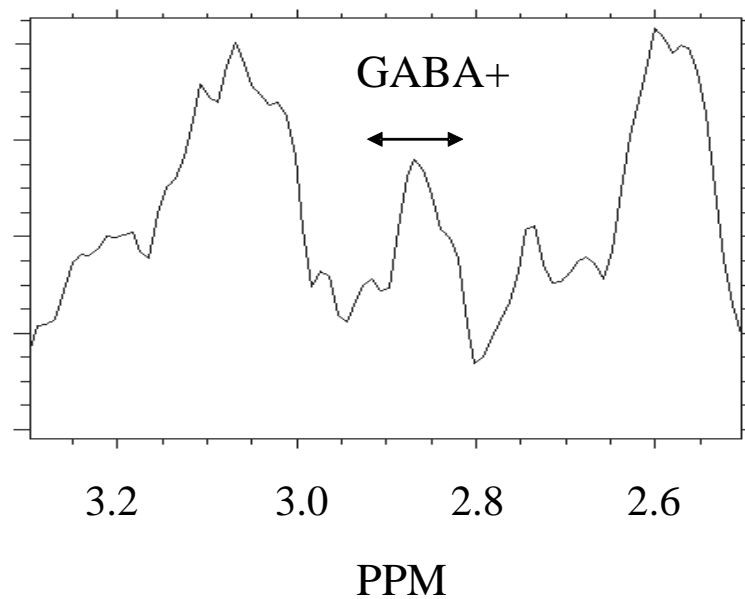
Left

Figure 3.4.2: A) Representative PRESS localised spectrum (TE/TR 30/3000ms) from patient 1 with superimposed LCModel fit to metabolite concentrations and estimated baseline, and B) a filtered GABA spectrum from the same patient. NAA = N-acetyl aspartate plus N-acetyl aspartyl-glutamate; GLX = glutamate plus glutamine; Cho = choline-containing compounds; Cr = creatine + phosphocreatine; Ins = myo inositol; GABA+ = gamma amino butyric acid plus homocarnosine. PPM = chemical shift in parts per million.

A)



B)



All the obtained data achieved the thresholds for data quality of: A) Full width half maximum (FWHM) < 0.15 PPM for PRESS localised (TE/TR = 30/3000 ms) unsuppressed water peaks; and B) DQF signal to noise ratio (SNR) > 4.0 (signal taken as the peak height between 2.5 to 3.5 PPM and noise 15 to 20 PPM). Finally, metabolite concentrations were corrected for CSF content, which is considered to provide negligible signal (Lynch et al., 1993). T₁ and T₂ effects were not corrected for, since they can be considered to be minimal at short TE and long TR.

3.4.2.5 Statistical method

Statistical analysis was performed with SPSS 11.0. Metabolite concentrations and ratios were compared between the patient and control groups using the Mann-Whitney U test. Comparison between the control group and the sub-group of patients with HT was also made for NAA_t, Cho, GLX (and GLX/NAA_t) and GABA₊ (GABA₊/Cr). Comparison between the two MCD sub types was only made for the main metabolites NAA_t and Cho because of the small numbers in each sub group. Individual patient data was compared against a normal range formulated as the control mean +/- 2 SD.

Sodium valproate (VPA) is associated with reduction of Ins (Simister RJ et al., 2003b) [Chapter 3.5] therefore data from the five subjects taking this AED were not included in the analysis of Ins. Elevation in GABA₊ has been consistently reported with Gabapentin and Topiramate (Petroff et al., 2000; Kuzniecky et al., 2002) and therefore data from the six subjects taking these AEDs were similarly not included in the analysis of GABA₊ or GABA₊/Cr.

3.4.3 Results

3.4.3.1 Group Results

The proportion of grey matter in the studied voxels was similar in both groups (Table 3.4.2). Inter-group comparison for the individual metabolites identified significant variation for NAA_t, Cho and GLX. Cho (p < 0.001), GLX (p < 0.05) and GLX/NAA_t (p < 0.001) were all elevated in MCD. NAA_t (p < 0.05) and NAA_t / Cr (p = 0.01) were reduced in the patient group (Fig 3.4.3).

Following removal of patients taking VPA from the Ins analysis and patients taking TPM or GBP from the GABA+ analysis no significant variation in Ins was observed although levels were generally lower in the patient group. GABA+/Cr levels were higher in the patient group ($p < 0.05$) but GABA+ levels showed only a trend to elevation (**Fig 3.4.4**).

Comparison between the control group and patients with HT ($n = 9$) showed elevation in Cho ($p = 0.01$), GLX ($p = 0.05$) and GLX/NAAAt ($p = 0.01$). No difference in NAAAt levels was observed. Comparison of NAAAt and Cho levels between the HT group and the PMG showed lower NAAAt in the PMG group ($p < 0.05$) but similar Cho.

3.4.3.2 Individual patient results

Individual patient metabolite concentrations and ratios were compared against a normal range (**Table 3.4.3**). NAAAt was reduced in four patients, whilst Cho was elevated in seven patients. Four patients showed elevation in GABA+ (all four were taking TPM or GBP). Five patients showed low Ins (two of whom were taking VPA) and one showed elevated Ins. Seven patients showed elevated GLX/NAAAt and six patients showed elevation in GABA+/Cr (five with GBP or TPM).

3.4.3.3 Correlation with seizure control

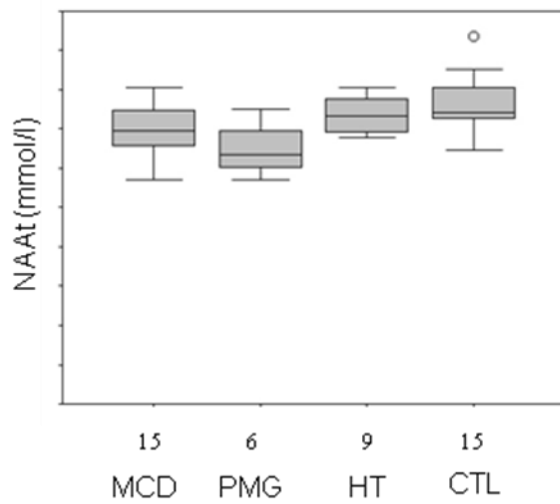
No correlation was observed between the measured metabolite concentrations or ratios and the time since most recent seizure (in days) or seizure frequency (the number of complex partial seizures per month).

Table 3.4.2: Metabolite concentrations (mmol/L) and ratios expressed as the group mean and standard deviation for healthy volunteers (Control) and subjects with malformations of cortical development (MCD). NAAAt = N-acetyl aspartate plus N-acetyl aspartyl-glutamate; GLX = glutamate plus glutamine; Cr = creatine plus phosphocreatine; Cho = choline-containing compounds; Ins = myo-inositol; GABA+ = gamma amino butyric acid plus homocarnosine. *P < 0.05 and ** P < 0.01 between patient group and the control group using Mann-Whitney U test. † patients not taking VPA (N = 10). # patients not taking TPM or GBP (N = 9). GM = voxel grey matter proportion, WM = voxel white matter proportion. Mean values and SD are provided for each measurement.

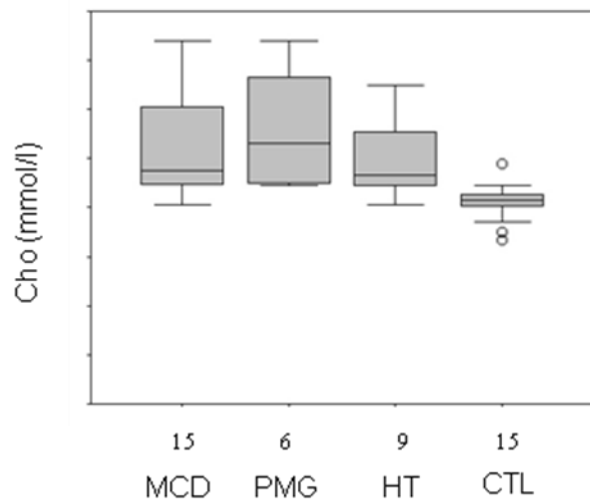
	<u>Control</u> N=15	MCD N=15
GM/(GM+WM)	0.6(0.1)	0.6(0.1)
NAAAt	7.7(0.7)	7.0(0.6)*
GLX	7.7(1.2)	9.0(1.4)*
Cho	0.8(0.1)	1.1(0.2)**
Cr	4.8(0.4)	4.9(0.5)
Ins†	3.4(0.3)	3.2(0.7)
GABA+#	1.3(0.2)	1.5(0.4)
NAAAt/Cr	1.6(0.2)	1.4(0.2)*
GABA+/Cr#	0.27(0.04)	0.32(0.06)*
GLX/NAAAt	1.0(0.2)	1.3(0.2)**

Figure 3.4.3: Box plots for A) NAAc (mmol/l), B) Cho (mmol/l), C) GLX (mmol/l) and D) GLX/NAAc in patients with malformations of cortical development (MCD) and healthy volunteers (CTL). The sub-groups of heterotopia patients (HT) and polymicrogyria patients (PMG) are also shown. The upper and lower edges of the box represents the upper and lower quartile respectively, the thick line within the box the median and the tail and whiskers the extremes of the data. Outliers are indicated. The number of subjects included in each group is indicated.

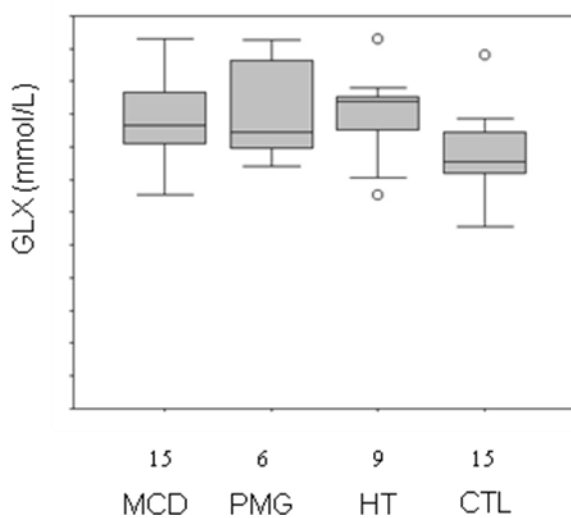
A) NAAc



B) Cho



C) GLX



D) GLX/NAAc

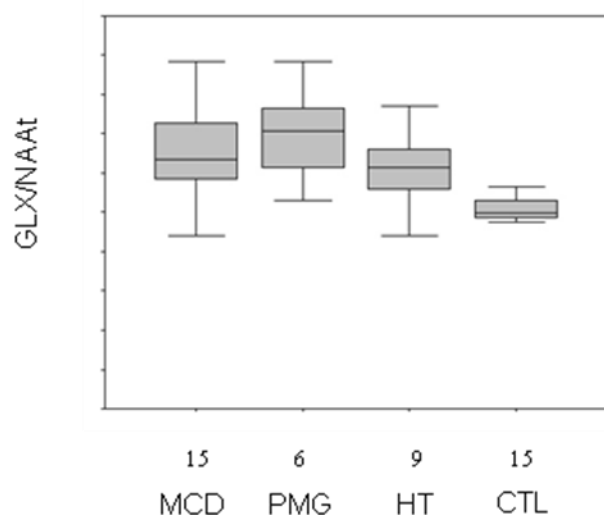
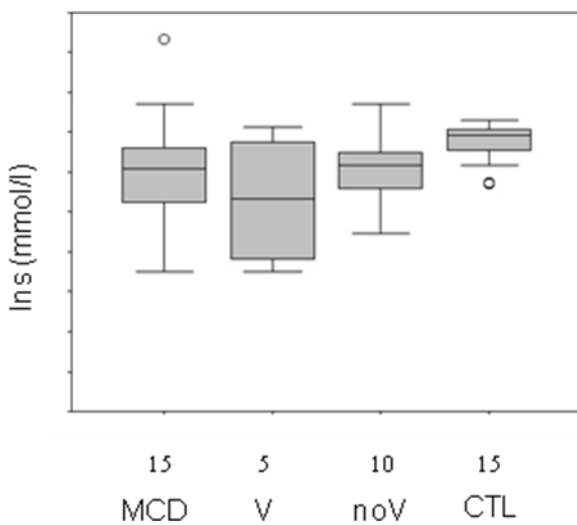


Figure 3.4.4: Box plots for A) Ins (mmol/l) and B) GABA+ (mmol/l) for patients with malformations of cortical development (MCD) and healthy volunteers (CTL). The sub-group levels for those patients taking VPA (V) and those not taking VPA (noV), and for those patients taking TPM or GBP (G) or not taking these medications (noG) are also shown. The upper and lower edges of the box represents the upper and lower quartile respectively, the thick line within the box the median and the tail and whiskers the extremes of the data. Outliers are indicated. * = $P < 0.05$ and ** = $P < 0.01$ between patient group and the control group using Mann-Whitney U test.

A) Ins



B) GABA+

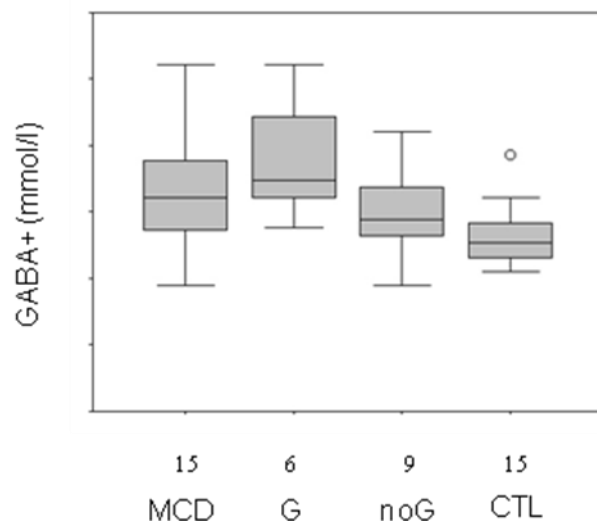


Table 3.4.3: Individual patient data for the MCD subjects. NAA_t = N-acetyl aspartate plus N-acetyl aspartyl-glutamate; GLX = glutamate plus glutamine; Cho = choline-containing compounds; Cr = creatine + phosphocreatine; Ins = myo-inositol; GABA₊ = gamma amino butyric acid plus homocarnosine. ↑/ ↓ = metabolite concentration or ratio more than 2 SD above / below the control mean. † patients taking VPA. # patients taking TPM or GBP. PMG = polymicrogyria and HT = heterotopia.

Patient no.	MCD group	MRS findings
1/45/M [#]	PMG	↑Cho ↑GLX ↑GLX/NAA _t ↓Ins
2/51/M [†]	PMG	↑Cho ↓NAA _t
3/46/M	PMG	↑GLX/NAA _t ↓NAA _t ↓Ins
4/30/M [†]	PMG	↓Ins ↓NAA _t
5/27/F ^{†#}	PMG	↑Cho ↑GLX/NAA _t ↑GABA ₊ ↑GLX ↓Ins ↓NAA _t /Cr ↑GABA ₊ /Cr
6/28/M	PMG	
7/51/M	HT	
8/25/F [#]	HT	↑GABA ₊ ↓Ins ↑GABA ₊ /Cr
9/31/M	HT	↑Cho ↑Ins ↑GLX/NAA _t ↓NAA _t /Cr
10/25/M [#]	HT	↑Cho ↑GLX/NAA _t ↑GABA ₊ ↑GABA ₊ /Cr
11/34/F [#]	HT	↑Cho ↑GABA ₊ /Cr
12/31/M [†]	HT	↑GABA ₊ /Cr
13/23/F [†]	HT	
14/21/F	HT	↑GABA ₊ ↑GABA ₊ /Cr
15/25/M [#]	HT	↑GLX ↑GLX/NAA _t

3.4.4 Discussion

This study was the first MRS study to measure GABA₊ concentrations in MCD in vivo. A modest elevation in GABA₊/Cr was observed together with more marked elevation in GLX, Cho and GLX/NAA_t in large MCD. Low NAA_t was observed but may be a feature of PMG rather than HT. The results indicate highly abnormal metabolism in these lesions.

Quantification of GABA⁺ remains technically difficult and the low sensitivity of the DQF method requires relatively large volumes of interest to be studied. This necessitated recruitment of subjects whose MRI showed extensive MCD. Such a group might be expected to demonstrate a greater level of neurochemical disturbance than would be observed in subjects with less extensive structural abnormalities. The prescribed volumes of interest included both MRI visible lesion and some surrounding normal appearing tissue. Since heterotopia are intrinsically epileptic whilst polymicrogyria lesions show perilesional epileptogenicity (Jacobs et al., 1999) the volume of interest should have included epileptic tissue in all subjects. In eight, the voxels were fronto-parietal and in seven they were parieto-occipital. Findings from earlier studies indicate that there is no large difference in metabolite concentrations between these regions in control subjects (McLean et al., 2000; Simister RJ et al., 2003b) (**Chapter [3.2]** and **[3.3]**) although other groups have reported some regional variation in metabolite concentration (Pouwels and Frahm, 1998). Selection requirements resulted in relatively small numbers of patients, particularly within the PMG sub-type, and this obviously limits inference about sub-type variation in metabolite concentrations.

The majority of previous MRS studies have relied on the use of the ratios NAA/Cr, NAA/Cho or NAA/(Cr and Cho) (Kuzniecky et al., 1997b; Li et al., 1998; Simone et al., 1999b; Widjaja et al., 2003). However, results from studies performed in healthy volunteers indicate that these ratios are sensitive to the tissue composition of the prescribed voxel (McLean et al., 2000). Furthermore, information about the pathological variation in concentration of the individual metabolites is lost. In the current study this possible confounding effect was limited by comparing the individual metabolite concentrations in the patient groups with a control group studied in the occipital lobes where voxel grey matter proportion was similar.

MCD form a heterogeneous group, but they share properties of primitive tissue, and often underlie refractory epilepsy which might well be reflected in discernable abnormalities in GLX and GABA⁺ metabolism. A low NAA_t in MCD probably represents an unchanged density of neurones containing very low NAA_t, a decrease in

the absolute number of neurones which contain normal NAA, or a combination of the two processes.

NAA was lower in polymicrogyria (PMG) than heterotopia (HT) whilst both subtypes showed elevated Cho. The histology of polymicrogyria shows abnormal cortical organisation and abnormal cells, whilst heterotopia are associated with relatively normal neuronal differentiation and organisation. Hence HT NAA might be expected to be less abnormal than in PMG. There is a very limited literature concerning *ex vivo* MRS of MCD (Aasly et al., 1999). In that study histopathological examination identified mild cortical dysplasia in four subjects with associated gliosis in three and MRS examination showed reduced NAA and increased Cho (and GABA) (Aasly et al., 1999). The pattern of reduced NAA and elevated Cho is consistent with immature tissue and concurs with a longitudinal study of neurochemical profiles measured in healthy rats from postnatal day seven to postnatal day 28 (neurodevelopmentally equivalent to the period from 34 weeks gestation to age 2-3 years in the human brain) (Tkac et al., 2003). In that study cortical concentrations of NAA, Ins, Cr and glutamate increased with increasing age, whilst there was no change in GABA concentration and there was reduction in the metabolites making up the Cho signal. Studies of development in the human brain have reported similar neurochemical profiles for NAA, Cr, GABA and glutamate but noted no change (Kok et al., 2002) or reduction of Ins (Kreis et al., 2002) with increasing development, and no change or reduction of Cho.

Glutamate and GABA are predominantly localised to glutamatergic and GABAergic neurones respectively. Following release from the pre-synaptic nerve terminal they are removed from the synaptic cleft by re-uptake into the neurone or transported into neighbouring astrocytes. There they are predominantly metabolised to glutamine which is subsequently returned to the neighbouring neurones. One or more of a number of mechanisms might be responsible for elevation in the concentrations of these compounds. An increase in inter-neuronal connectivity within the neuropil but without increase in absolute neuronal numbers has been suggested to be an underlying mechanism for epileptogenesis in MCD (Sisodiya et al., 1995; Sisodiya, 1995). These

GABA or glutamate containing neuronal projections might add to the total observed concentrations without an associated increase in NAA. Alternatively chronic energy depletion may develop as a consequence of structural changes or the subsequent development of chronic epilepsy, and lead to partial failure of neurotransmitter cycling resulting in neurotransmitter accumulation in the surrounding astrocytes (as glutamine) or within the neuronal cytoplasm as glutamate(Petroff et al., 2002a). Elevation in glial glutamine levels would also lead to increased GLX or, following neuronal metabolism to GABA, an increase in GABA+. Disturbances of uptake could also lead to secondary accumulation or mis-regulation of GABA or glutamate.

In this study elevated GABA+/Cr was noted in MCD, which differs from previous studies which have shown an association between active epilepsy and low GABA+ levels(Petroff et al., 1996b) or unchanged GABA+ levels in IGE or focal epilepsy(Simister RJ et al., 2003b) [Chapter 3.2,3.3] in human adults. The finding in this current study is supported by the identification of reduced expression of GABA transporters in heterotopic neuronal regions in an animal model, suggesting a reduced ability for GABA reuptake(Calcagnotto et al., 2002) and, potentially, abnormal accumulation of GABA. Elevation of GABA+ concentrations is not necessarily associated with reduced epileptogenicity. Ex vivo studies of epileptic tissue not associated with MCD have shown normal or elevated GABA concentrations(Petroff et al., 1995) and several studies have shown reduced GABA receptor function in MCD potentially leading to altered GABAergic inhibition(Redecker et al., 2000). Furthermore, recent animal studies have shown that GABAergic suppression of hippocampal interneurons can enhance seizure activity and spread(Kullmann and Semyanov, 2002).

Ex vivo studies have identified elevated glutamate in resected tissue(Petroff et al., 1995) and in vivo MRS studies have found that NAA_t was reduced and GLX and GLX/NAA_t were elevated in the frontal lobes(Simister RJ et al., 2003b) [**Chapter 3.3**] but not the occipital lobes(Simister RJ et al., 2003a) [**Chapter 3.2**] in subjects with idiopathic generalised epilepsy (IGE). Occipital measurement of subjects with occipital lobe epilepsy showed no significant variation in any metabolite or metabolite

ratio when allowing for variation in voxel grey matter proportion (Simister RJ et al., 2003a) [**Chapter 3.2**].

The effects of concomitant AEDs on metabolite concentrations must be considered. VPA has been associated with increase in glutamine (and by extension GLX) in a proportion of subjects (Petroff et al., 1999d). Previous studies using the same methodology have observed no difference in GLX concentrations between subjects with IGE taking VPA and those not taking this AED (Simister RJ et al., 2003a; Simister RJ et al., 2003b) (**Chapter 3.2** and [**3.3**]) and if this effect is present it is likely to be small. However VPA has previously been associated with reduction in Ins (Simister RJ et al., 2003b) (**Chapter 3.3** and [**3.5**]) and therefore the five subjects taking VPA were not included in the group analyses of Ins. This effect of VPA on Ins levels was again observed in the current study where Ins levels in the excluded patients were generally lower (**Figure 3.4.4**). Similarly the AEDs TPM and GBP have been shown to increase GABA⁺ concentrations (for example (Petroff et al., 2000)) in healthy subjects and this effect appears to be present in the current study where the GABA⁺ levels in the excluded patients were higher than the levels in those patients not taking these medications.

Previous MRS studies have generally reported the ratios NAA/Cr, NAA/Cho or Cho/Cr and have been performed at long TE. These studies have reported that heterotopia and polymicrogyria may be associated with normal Cho/NAA and Cr/NAA ratios (Kuzniecky et al., 1997b; Widjaja et al., 2003), or normal NAA/Cr in polymicrogyria but variable reduction of NAA/Cr in heterotopia (Li et al., 1998). Focal cortical dysplasia has been associated with low NAA/Cr and NAA/Cho (Kuzniecky et al., 1997b; Li et al., 1998). In an earlier MRSI study in a group of subjects with either gyral abnormalities or heterotopia NAA, NAA/Cr and Ins were reduced in the MRI visible MCD (Woermann et al., 2001b). This variability in reported findings may be influenced by differing methodologies but also clearly reflects lesional and perilesional heterogeneity (Woermann et al., 2001a) as well as the relatively small number of subjects studied. Studies at higher field strength, and hence

improved spatial resolution, may allow better characterisation of the MRS appearances of these different MCD sub-types.

In this study no correlation between seizure control and metabolite concentrations or ratios was noted. This agrees with earlier observations in cross sectional studies of patients with epilepsy (Simister et al., 2002; Simister RJ et al., 2003b) (**Chapter [3.1], [3.2] and [3.3]**) but longitudinal studies of GLX and GABA+ are required before any assessment can be made of how sensitive these measurements are to patient seizure control.

3.4.5 Conclusion

In this study quantitative ¹H MRS demonstrated that MCD were associated with abnormal neurochemical profile. Patterns of abnormality were evident with elevated GLX (and GLX/NAA_t) and GABA+ and GABA+/Cr together with previously described reduction in NAA_t and elevation in Cho.

3.5 The Effect of Sodium Valproate on Proton MRS Visible Neurochemical Concentrations

ABSTRACT

Purpose:

Proton Magnetic Resonance Spectroscopy (MRS) measurements in patients with epilepsy may be affected by the use of antiepileptic medications (AEDs). Although sodium valproate (VPA) is a widely used AED no longitudinal MRS study has investigated the effects of VPA administration on MRS measurements in humans.

Methods:

A longitudinal quantitative short echo time Proton Magnetic Resonance Spectroscopy (MRS) study was performed in 10 patients with epilepsy to investigate the effect of the antiepileptic drug (AED), sodium valproate (VPA), on measured metabolite concentrations. The patients were studied on two occasions; whilst taking VPA, and either before commencing or after withdrawing from VPA. Myo-inositol (Ins), N-acetyl aspartate plus N-acetyl aspartyl glutamate (NAA_t), Creatine plus phosphocreatine (Cr) and glutamate plus glutamine (GLX) concentrations were measured.

Results:

Myo-inositol was lower in the VPA taking group, and no significant trends were noted for any other metabolite or ratio. No relationship between the change in metabolite concentration, VPA dose or seizure control was observed.

Conclusions:

The results emphasise importance of interpreting MRS findings in the light of administered medications.

Published ref: (Simister et al., *Epilepsy Research* 2007 **74**, 215—219)

3.5.1 Introduction

Analysis in the frontal lobes in patients with idiopathic generalised epilepsy has reported that sodium valproate (VPA), may be associated with reduced concentrations of Ins in patients compared to subjects not taking VPA (Simister RJ et al., 2003b) [Chapter 3.3]. In rats the introduction of VPA has been associated with reductions in Ins, NAA and Cr (O'Donnell et al., 2003).

No longitudinal study has measured the effect of the introduction or withdrawal of VPA on metabolite concentrations in humans. The aim of the current study was to investigate the effects of VPA administration on MRS measurements in patients with epilepsy.

3.5.2 Methods

3.5.2.1 Subjects

Sixteen healthy controls and 10 patients with epilepsy were included in the study. Ethical approval by the Joint Research Ethics Committee of the Institute of Neurology and the National Hospital for Neurology and Neurosurgery was obtained, and all subjects gave informed consent. All control subjects had normal MRI and were taking no regular medication.

Every subject was scanned twice. For each control subject the data was labelled **CTL1** and **CTL2** dependent on the temporal order of the acquisition. For the patients, the study performed whilst taking VPA was designated **VPA** and that performed either before commencing VPA or four weeks after withdrawing from VPA was designated as **noVPA** (Table 3.5.1). Eight patients were studied before and after commencing VPA and two before and after withdrawing from VPA.

3.5.2.2 Magnetic Resonance Imaging

A 1.5T SIGNA Horizon Echospeed scanner (General Electric, Milwaukee, WI) was used with a standard quadrature head coil. Axial T1 weighted inversion-recovery prepared fast spoiled gradient recalled echo (IR-SPGR) images were acquired

(TE/TI/TR = 4.2/450/15.5 ms, flip angle 200; matrix 256*160; FOV 24 cm; slice thickness 1.5mm) to guide voxel placement and for segmentation into grey matter, white matter and cerebro-spinal fluid (CSF) using SPM99 (Statistical Parametric Mapping; Wellcome Department of Imaging Neuroscience, Institute of Neurology, University College London).

3.5.2.3 Magnetic Resonance Spectroscopy

For all subjects a single voxel was prescribed from the axial IR-SPGR images in the right or the left frontal lobe (40 * 35 * 25 mm)(Simister RJ et al., 2003b) (**Fig 3.5.1**). Care was taken at the time of the second study to assure a comparable spectroscopic acquisition to that of the first study.

Conventional PRESS-localised water suppressed spectra (TE/TR = 30/3000 ms) were obtained(McLean et al., 2000), so that LCModel(Provencher, 1993;Provencher, 2001) could be used for quantification of NAA_t, Cr, Cho, Ins and GLX.

Finally, metabolite concentrations were normalized to 100% brain tissue by correcting for the CSF content estimated from the images by SPM.

Table 3.5.1: Clinical data for the patient group. M = male; F = female; SEH = subependymal heterotopia. Cbz = carbamazepine; dzp = diazepam; lev = levetiracetam; Itg = lamotrigine; pht = phenytoin; vpa = sodium valproate; Sz = generalised tonic-clonic seizures / complex partial seizure. IGE = idiopathic generalised epilepsy, FLE = frontal lobe epilepsy, xTLE = non-localised extra temporal lobe epilepsy.

Patient no. /age (years) /gender	Diagnosis	MRI	Not Taking VPA		Taking VPA	
			Last Sz (days) / Sz frequency (pa)	Concomitant AEDs	Last Sz (days) / Sz frequency (pa)	VPA dose (mg/kg/day)
1/19/M	IGE	Normal	350 / 2	Itg	120 / 1	27.6
2/40/F	IGE	Normal	100 / 1	lev	30 / 1	11.9
3/22/M	IGE	Normal	48 / 4	cbz, dzp	7 / 2	20.7
4/33/F	IGE	Normal	36 / 3	Itg, cbz	6 / 2	7.9
5/17/M	IGE	Normal	45 / 2	nil	30 / 1	8.5
6/35/F	IGE	Normal	6 / 12	pht	15 / 4	14.8
7/25/M	FLE	Normal	4 / 30	Cbz, pht	1 / 36	24.6
8/46/F	xTLE	Bilat Post SEH	280 / 3	cbz, pht	300/2	11.3
9/18/M	IGE	Normal	19 / 9	nil	14 / 4	12.5
10/40/F	IGE	Normal	0 / 0	nil	0 / 0	12.5

Figure 3.5.1: A) Axial image showing the position of the prescribed voxel in the right or left frontal lobe in a patient with idiopathic generalised epilepsy (Patient 3).

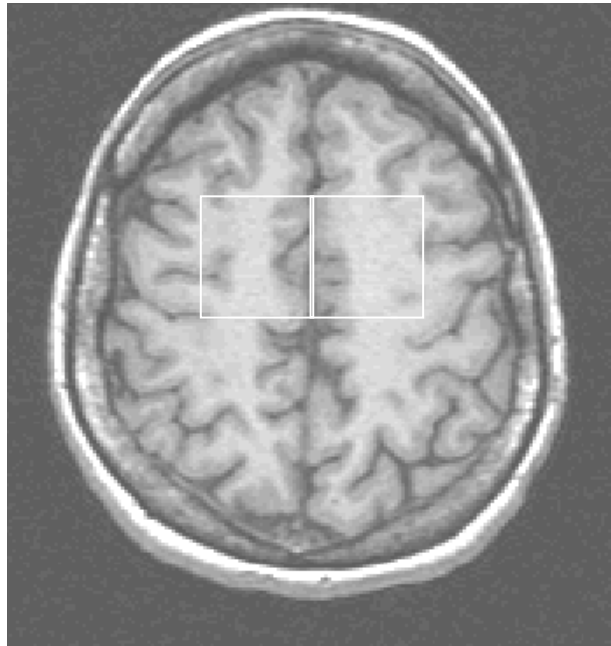
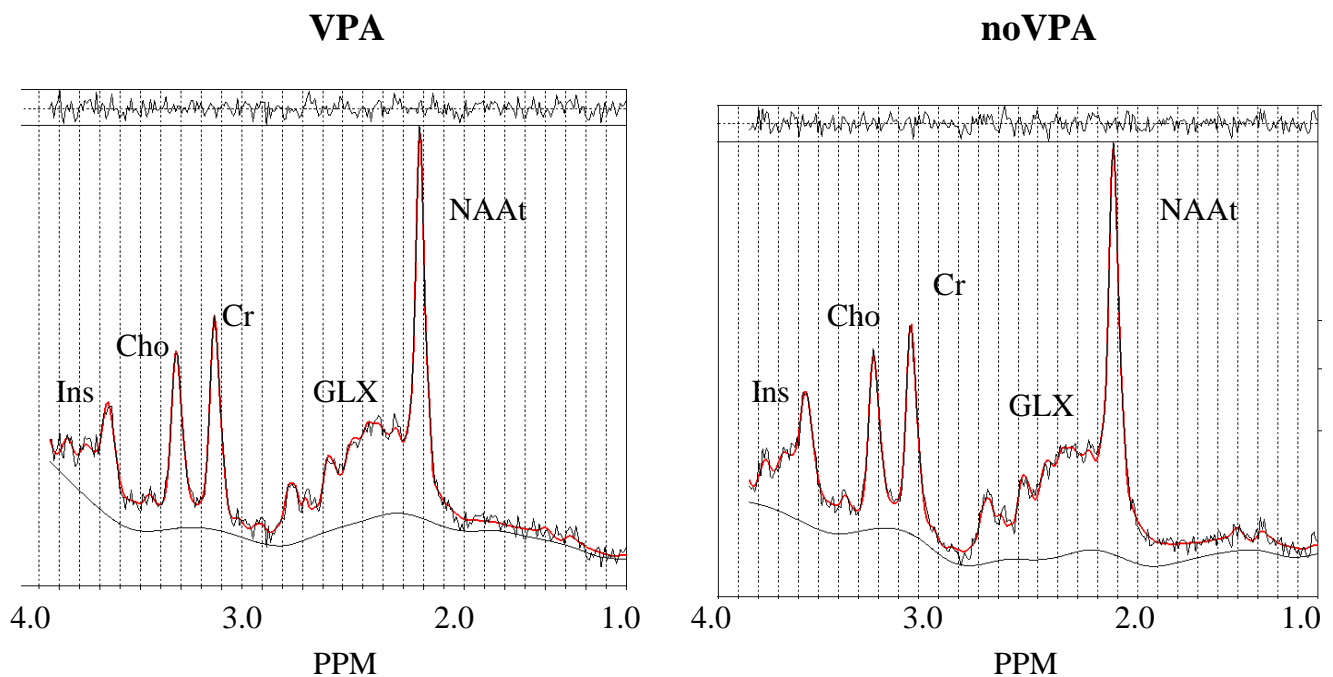


Figure 3.5.1: B) Representative PRESS localised spectra (TE/TR 30/3000ms) for Patient 3 with superimposed LCModel fit to metabolite concentrations and estimated baseline. **VPA** indicates acquisition whilst the patient was taking sodium valproate; and **noVPA** indicates the acquisition performed before commencing this medication. NAAAt = N-acetyl aspartate plus N-acetyl aspartyl-glutamate; GLX = glutamate plus glutamine; Cho = choline-containing compounds; Cr = creatine + phosphocreatine; Ins = myo-inositol.



3.5.2.4 Statistical Analysis

Statistical analysis was performed with SPSS 11.0. Only acquisitions achieving a threshold for data quality of full width half maximum (FWHM) < 0.15 parts per million for PRESS localised (TE/TR = 30/3000 ms) unsuppressed water peaks, were accepted for analysis. The data in the two groups were compared using paired t-tests. Test-retest repeatability measures for the control group were defined as described on page 176 according to [Eqn. 3.2.1](Bland JM and Altman DG, 1986). Change in metabolite concentration (Δ) between the two scans was also calculated and expressed as;

$$\Delta = (\text{noVPA} - \text{VPA}) / \text{mean}(\text{noVPA}, \text{VPA}) \quad [\text{Eqn 3.5.1}]$$

A correlation analysis was performed for VPA dose (mg/Kg), change in seizure control and Δ for each metabolite using Spearman's Rho test. During the course of the study no changes were made to the concomitant AED treatment.

3.5.3. Results

All acquisitions achieved the above quality thresholds and were included for analysis.

3.5.3.1 Group Results

3.5.3.1.1 Control Subjects

In the control group the median age was 32 years (range 20 to 53 years) and 10 of 16 subjects were female. There was no difference in voxel grey matter proportion between CTL1 and CTL2. Repeatability scores were as follows; NAAAt 9%, Cr 10%, Cho 13%, Ins 13%, and GLX 22%. Mean values for CTL1 were NAAAt 7.2 (SD = 0.7) mmol/L, Cr 4.3 (SD = 0.6) mmol/L, Cho 1.1 (SD = 0.1) mmol/L, Ins 3.0 (SD = 0.3) mmol/L, GLX 6.8 (SD = 1.2) mmol/L and grey proportion 0.29 (SD = 0.03).

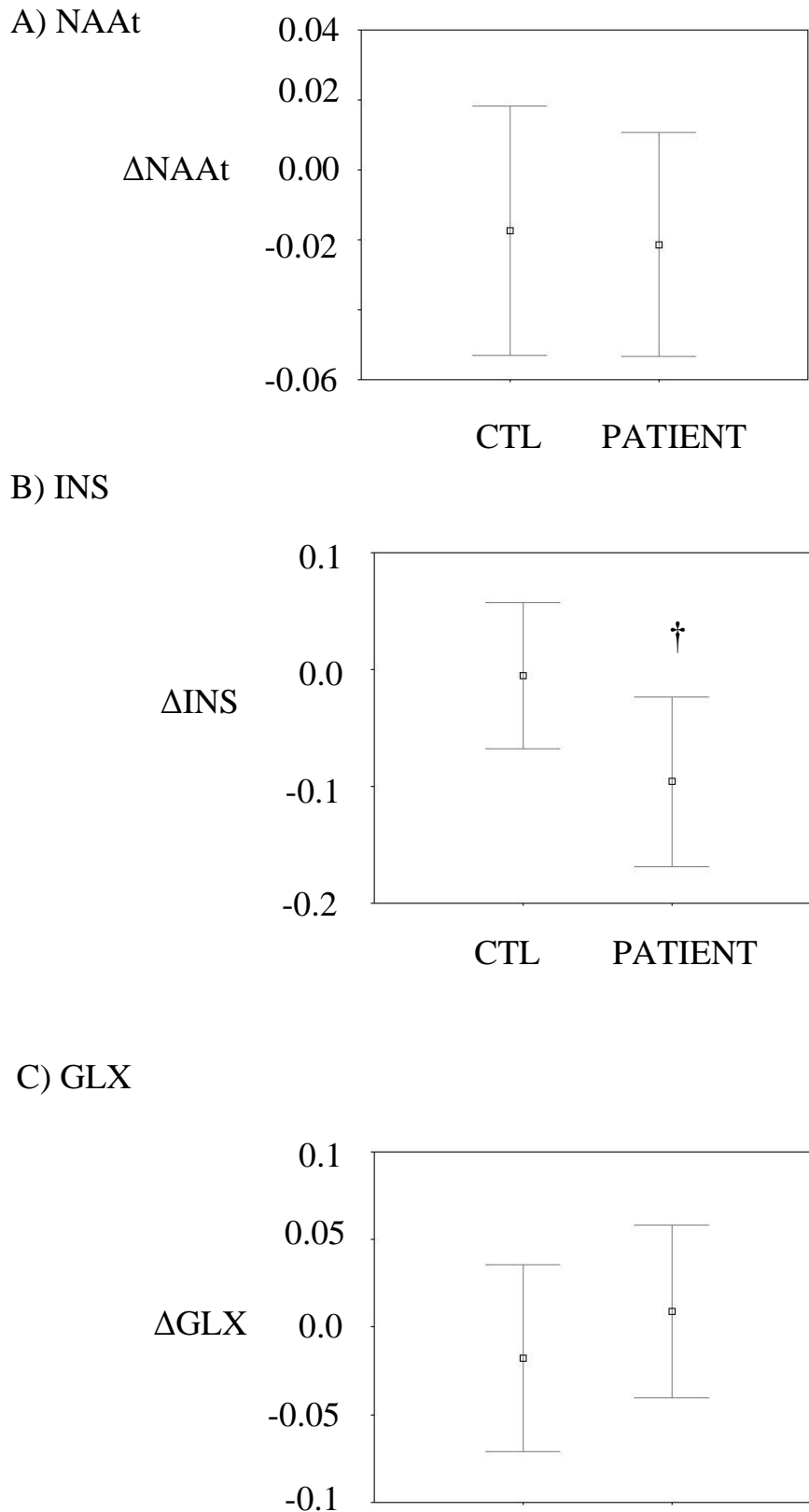
3.5.3.1.2 Patient Group

For the patients the median age was 25 years (range 17 to 46 years) and four subjects were female. In the VPA group, seizure frequency (complex partial seizures or generalised tonic-clonic convulsions) was median six per year (range 0 to 30) and

time since last seizure seven days (range three to 120); whilst the data for the **noVPA** group were eight per year (range 0 to 60) and 20 days (range two to 100). There was no significant difference between seizure control in the two groups. Grey matter proportion was similar in **VPA** (0.29) and **noVPA** (0.30).

Paired analysis showed a 10% lower mean Ins in the **VPA** compared to **noVPA group** ($p = 0.01$). No other metabolite concentration changed by more than 3% between the two scans, and no significant difference was observed in paired analysis for NAA_t, GLX, Cr or the ratios NAA_t/Cr or GLX/NAA_t. Metabolite concentrations for **noVPA** were NAA_t 6.8 (SD = 0.6) mmol/L, Cr 4.2 (SD = 0.6) mmol/L, Cho 1.0 (SD = 0.1) mmol/L, Ins 3.2 (SD = 0.3) mmol/L, GLX 7.0 (SD = 1.2) mmol/L.

Figure 3.5.2: Error bars with 95% confidence limits for proportional difference in metabolite concentration (Δ) between the two scans for A) N-acetyl aspartate plus N-acetyl aspartyl glutamate (NAAt), B) myo-inositol (Ins) and C) glutamate plus glutamine (GLX). **CTL** = control group. **PATIENT** = patient group. $\Delta = (\text{noVPA} - \text{VPA}) / \text{mean}(\text{noVPA}, \text{VPA}), (\text{CTL1-CTL2})/\text{mean}(\text{CTL1,CTL2})$. † = significant to $p < 0.05$.



The inter-scan difference (Δ) in metabolite concentrations did not correlate with the dose of VPA taken and there was no correlation with Δ between the measured metabolites or change in seizure control.

3.5.4 Discussion

In this study relatively large voxels were used to allow for accurate estimation of metabolite concentrations and followed a similar methodology to an earlier study in this thesis (Simister RJ et al., 2003b) [Chapter 3.3]. In that earlier study a difference in the macromolecule baseline fit between the left and right frontal lobe voxels was observed. In the current study patients and controls were not matched for the side examined, precluding a formal cross sectional comparison between patients and controls, although there was an expected trend for reduced mean NAA concentration in the patients.

Ins is predominantly concentrated in glia (Brand et al., 1993), perhaps to store Ins for subsequent transfer to neighbouring neurons and incorporation into the phosphatidylinositol second messenger intracellular signalling system. Ins may also have a significant role as an intracellular osmotic agent via the sodium myo-inositol co-transporter (SMIT) (van Calcar and Belmaker, 2000c). Animal studies (O'Donnell et al., 2003) have shown that both lithium and VPA reduce cellular Ins concentrations. Lithium has no antiepileptic efficacy and the reduction in Ins in itself does not immediately explain the antiepileptic efficacy of VPA. This observation is supported in the current study by lack of correlation between change in Ins concentration and either VPA dose or change in seizure control. MRS measurement of Ins in epilepsy has suggested that Ins might show elevation in epileptogenic tissue either as a consequence of the seizure activity, or secondary to a process of reactive gliosis (Woermann et al., 1999c; Wellard et al., 2003). The current study shows that this effect may be masked if studied patients are taking VPA.

Elevation in GLX has been previously reported with VPA usage in association with hyper-ammonemia (Ziyeh et al., 2002). Increased glutamine concentrations are

thought to result from removal of ammonia in astrocytes by combination with glutamate. Valproate has also been reported to reduce NAA and Cr levels(O'Donnell et al., 2003). In the current study GLX concentrations were not elevated in the **VPA** group and NAA and Cr concentrations were unaffected by VPA usage.

3.5.5 Conclusion

In this MRS study treatment with VPA was associated with a reduction in the concentrations of Ins but unchanged concentrations of NAA, Cr and GLX in a patients with epilepsy. The reduction in Ins was not associated with measured change in seizure control suggesting that Ins reduction is not directly linked with the anti-epileptic properties of VPA.

3.6 Proton MR Spectroscopy of Metabolite Concentrations in Temporal Lobe Epilepsy and Effect of Temporal Lobe Resection

ABSTRACT:

Purpose:

To use proton Magnetic Resonance Spectroscopy (MRS) to measure in vivo temporal lobe GABA and glutamate plus glutamine (GLX) concentrations in patients with temporal lobe epilepsy (TLE) attributable to unilateral hippocampal sclerosis (HS) before and following anterior temporal lobe resection (ATLR).

Methods:

Quantitative short echo time MRS was obtained in both temporal lobes of 15 controls and 16 patients with TLE and HS, and repeat spectra in 10 patients after ATLR. The concentrations of N-acetyl aspartate + N-acetyl aspartyl-glutamate (NAAt), creatine plus phosphocreatine (Cr), and glutamate+glutamine (GLX) were measured using a metabolite-nulled sequence designed to minimize macromolecule artifact. GABA plus homocarnosine (GABA+) concentrations were measured using a previously described double quantum filter.

Results:

In patients with TLE, NAAt/Cr was reduced in ipsilateral and contralateral temporal lobes. No significant variation in GLX/Cr or GABA+/Cr was evident in any group although GABA+/Cr was highest in the ipsilateral temporal lobe in TLE. After ATLR there was a trend to normalization of NAAt/Cr but no change in individual metabolite concentrations, GLX/Cr or GABA+/Cr compared to pre-surgery levels.

Conclusions:

Temporal lobe epilepsy was associated with bilateral reduction in NAAt/Cr but not significant abnormality in GABA+/Cr or GLX/Cr. Normalization of NAAt/Cr in the contralateral temporal lobe was seen following successful ATLR.

Published ref: (Simister et al., Epilepsy Research 2009; 83:168-76.)

3.6.1. Introduction

In the healthy adult hippocampus, GABA pathways tightly control output activity by blocking excitatory input and regulating the synchronous discharge patterns of hippocampal principal cells (dentate granule cells, CA3 and CA1 pyramidal neurons). GABA is the dominant inhibitory neurotransmitter in humans and impairment of GABAergic inhibition may be a feature of epileptic tissue. Compounds that enhance GABA_A receptor mediated inhibition suppress seizures, and epileptiform activity can be triggered when GABA_A receptor mediated inhibition is blocked. Proton Magnetic Resonance Spectroscopy (MRS) experiments in humans with focal onset epilepsy have shown low occipital lobe GABA and increase in GABA levels with the introduction of GABAergic antiepileptic drugs (AED) or improved seizure control (Petroff et al., 1996b; Petroff et al., 1999b; Petroff et al., 2000).

Increased neuronal excitation may be caused by altered glutamatergic function. Glutamate is the dominant excitatory neurotransmitter in the human brain and temporal lobe ECF glutamate levels have been shown to be increased in the interictal period in epileptic temporal lobes (Cavus et al., 2005) and to rise significantly during a temporal lobe onset seizure (During and Spencer, 1993). MRS studies have shown elevation in GLX in patients with TLE but without evidence of HS on MRI (Woermann et al., 1999c; Simister et al., 2002) [**Chapter 3.1**] and in the frontal lobes (Simister RJ et al., 2003b) [**Chapter 3.3**] and thalami in idiopathic generalised epilepsy (Helms et al., 2006).

Recent observations suggest that the concept of a simple balance between excitation and inhibition is inadequate to fully explain epileptic seizures. In particular, GABAergic systems may act as an excitatory neurotransmitter in epileptic tissue, either by altered connectivity of GABAergic interneurons or through changes in GABA_A receptor function (Ben Ari and Holmes, 2005; Cossart et al., 2005). Furthermore, in the developing brain GABA appears to be primarily excitatory and may drive neuronal development and migration (Ben Ari, 2002).

MRS experiments have shown that NAA is reduced in the region of the sclerotic hippocampus (Cendes et al., 1994; Connelly et al., 1994; Kuzniecky et al., 1998b; Woermann et al., 1999c) but also in regions distant from the epileptic focus (Li et al., 2000a) and in particular is often reduced in the contralateral normal appearing hippocampus (Cendes et al., 1995; Woermann et al., 1999c; Simister et al., 2002) [Chapter 3.1]. Contralateral temporal lobe NAA/Cr levels have been shown to normalize following anterior temporal lobe resection (ATLR) for refractory TLE (Hugg et al., 1996; Serles et al., 2001; Vermathen et al., 2002; Cohen-Gadol et al., 2004).

The acquisition of MR spectra in the temporal lobes has typically required long echo times and reporting of the ratios NAA/Cr or NAA/(Cr + Cho) (Connelly et al., 1994; Cendes et al., 1995; Hugg et al., 1996; Cendes et al., 1997b; Kuzniecky et al., 1998b; Vermathen et al., 2000; Serles et al., 2001; Vermathen et al., 2002; Cohen-Gadol et al., 2004). However, short echo time experiments have allowed semi-quantitative measurement of these three main metabolites, as well as glutamate plus glutamine (GLX) (McLean et al., 2000; McLean et al., 2001) and myo-inositol (Ins). Ins is considered to be localised predominantly in glial cells (Brand et al., 1993). GABA+ (GABA plus homocarnosine) measurement has been reported in patients with focal epilepsy with (Simister et al., 2007) [Chapter 3.4] or without (Simister RJ et al., 2003a) [Chapter 3.2] MRI evidence of malformations of cortical development and in patients with idiopathic generalized epilepsy (Simister RJ et al., 2003b) [Chapter 3.2] by application of a double quantum filter in extra-temporal lobe locations.

No previous study has simultaneously measured GABA+ and GLX levels in vivo in TLE. The purpose of this study was to examine these metabolites, and NAA, in the temporal lobes in patients with TLE prior to ATLR and in the contralateral temporal lobe following the surgery.

3.6.2 Methods

3.6.2.1 Subjects

Twenty-eight control subjects and 35 patients with chronic epilepsy secondary to unilateral HS were studied. Twenty three control subjects were scanned twice to assess test-retest repeatability. The study was approved by the Joint Research Ethics Committee of the National Hospital for Neurology and Neurosurgery and all subjects gave informed written consent. All patients had had a comprehensive pre-surgical evaluation including interictal and ictal scalp video-EEG, neuropsychometry and MRI. Thirteen patients underwent ATR and were re-studied post surgery.

MRS data were subject to quality control (see below). Spectra of adequate ipsilateral temporal lobe data quality were obtained in 19 test-retest datasets in the control population. Adequate data in both temporal lobe voxels were obtained in 16 TLE patients with radiological evidence of hippocampal sclerosis (designated as the **HS** group) and 15 control subjects (designated as **CTL**). Temporal lobe voxel data from the non-epileptic temporal lobe were obtained both before and after temporal lobe surgery in 10 patients (designated as **SurgicalHS**). All 10 had HS confirmed histologically, were seizure free following surgery and had no change in medication between the two scans. Six TLE patients were included in both the **HS** and the **SurgicalHS** groups. The frequency of seizures and the duration in days since the most recent seizure were noted for all studies. No patient reported an epileptic seizure within the twenty four hours prior to scanning.

Table 3.6.1: Demographics of the three groups of subjects. The healthy volunteer group is designated as **Control**. **HS** represents the group of patients with temporal lobe epilepsy and hippocampal sclerosis. **Surgical HS** represents the group of patients with HS studied before and after surgical resection. AED = anti-epileptic drug. * indicates data correct at the time of the pre-operative scan.

	<u>Control</u> <u>N =15</u>	<u>HS</u> <u>N=16</u>	<u>SurgicalHS</u> <u>N=10</u>
Gender M/F	8/7	4/12	4/6
Age (yrs): median (range)	31(18-45)	33(20 –48)	33(24-45)
Side of pathology (right / left)	Not applicable	7/9	5/5
Duration of epilepsy (yrs): median (range)	Not applicable	18(7 – 45)	19(8-33)
Time since last seizure (days): median (range)	Not applicable	5(2 - 90)	6(2-10)*
Frequency of complex partial seizures / month: median (range)	Not applicable	50(2 – 300)	50(25-120)*
Past history of prolonged early childhood convulsion.	0	12/16	10/10
Number of AEDs taken: Median (range)	0	2(1-3)	2(1-4)

3.6.2.2 Magnetic Resonance Imaging

The study was performed on a 1.5T General Electric SIGNA Horizon Echospeed scanner (Milwaukee, WI, USA) using a standard quadrature head coil for all MRI/MRS studies. Axial T1 weighted inversion-recovery prepared fast spoiled gradient recalled echo (IRP-FSPGR) images were acquired (TE/TI/TR = 4.2/450/16 ms, flip angle 20°; matrix 256*156; field of view 240x180mm; slice thickness 1.5mm). These images were used both to guide voxel placement and subsequently for segmentation using SPM (Statistical Parametric Mapping; Wellcome Centre for Imaging Neuroscience, Institute of Neurology, University College London). All the MRI studies were reviewed by two experienced neuro-radiologists.

3.6.2.3 Magnetic Resonance Spectroscopy

3.6.2.3.1 Acquisition

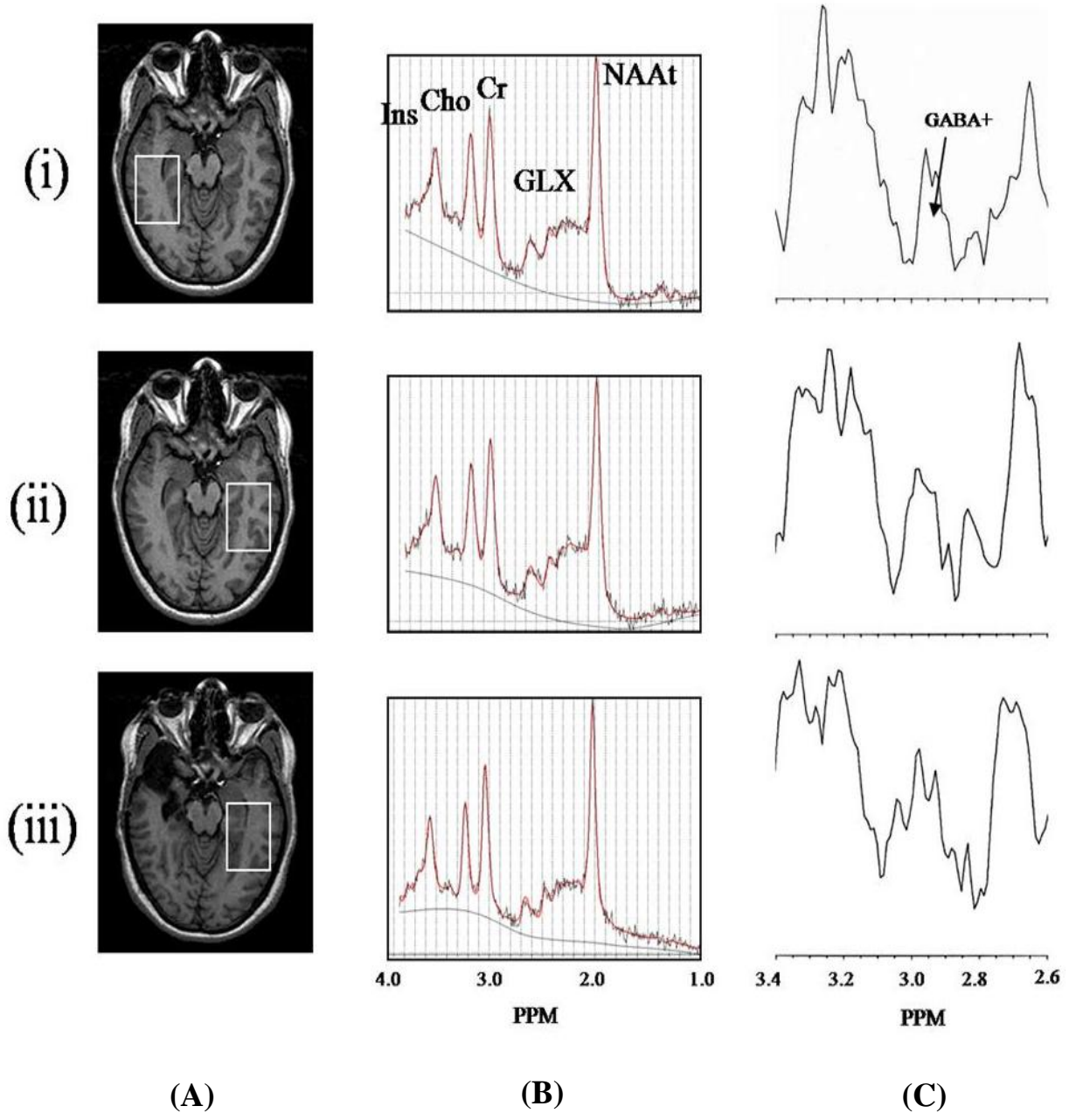
A single voxel was sequentially prescribed in each temporal lobe of each subject with approximate dimensions 40 mm (Anterior-Posterior), 35 mm (Left-Right) 25mm (thickness) (Fig 3.6.1). Two spectra were then acquired for each volume of interest according to our previously reported metabolite nulled protocol (McLean et al., 2004). Point-resolved spectroscopy (PRESS) localization was used to select the spectroscopy volume (TE/TR = 30/3000 ms). Water signal was suppressed using 3 chemical-shift selective (CHESS) pulses in both cases, with the flip angle of the final pulse tailored to ensure slight under-suppression. Thirty-two transients each were collected, with and without an inversion pulse (pulse delay 750ms) along with 16 without water suppression used for phasing of the data. The final “metabolite only spectrum” is the edited spectrum of the first acquisition minus the second metabolite nulled acquisition.

Next the double quantum filter (DQF) sequence was applied to the same PRESS-localised volume (McLean et al., 2002). For the first acquisition the filter was not activated (ie normal PRESS, TE/TR = 68/2000 ms), and spectra were acquired with and without applied CHESS water suppression gradients (scan time c. 1 minute each). Subsequently the filter was activated and 512 transients collected (scan time 17:12) to measure GABA+.

Figure 3.6.1A) Axial T₁-weighted localising MRI scans for a patient with right hippocampal sclerosis examined before and after anterior temporal lobe resection. Prescribed regions of interest are shown in (i) the ipsilateral and (ii) the contralateral temporal lobes prior to surgery and in (iii) the contralateral temporal lobe after surgery.

Figure 3.6.1B) Representative spectra (TE/TR 30/3000ms) following application of the metabolite nulled protocol are shown for the patient above from regions of interest (i) and (ii) prior to surgery and (iii) following surgery as shown. NAA_t = N-acetyl aspartate plus N-acetyl aspartyl-glutamate; GLX = glutamate plus glutamine; Cho = choline containing compounds; Cr = creatine + phosphocreatine; Ins = myo-inositol; and GLX = glutamate plus glutamine. PPM = parts per million.

Figure 3.6.1C) representative filtered GABA⁺ measured in the same patient from regions of interest (i), (ii) and (iii) as indicated. GABA⁺ = GABA plus homocarnosine. PPM = parts per million.



3.6.2.3.2 Spectral Processing

The “metabolite only” spectra (TE/TR = 30 / 3000 ms) were analyzed using LCModel (Provencher, 1993) quantification of NAA_t, Cr, Cho, Ins and GLX. . The spectra obtained from the unfiltered DQF sequence (TE/TR = 68 / 2000 ms) were also analysed via LCModel in order to provide a consistent fit to the baseline. The LCModel Cr concentration obtained was then converted back to a peak area for comparison with the peak area of GABA estimated using SAGE 7.0 (General Electric, Milwaukee WI) as previously described (McLean et al, 2002).

Fig 3.6.1 includes typical DQF spectra and LCModel outputs obtained from a TLE patient. Poor quality data was rejected by application of the following criteria: All PRESS localised (TE/TR = 30/3000 ms) datasets with unsuppressed water full width half maximum (FWHM) > 0.15 ppm were rejected and GABA+ data was rejected if the signal to noise ratio (SNR) of the filtered signal (signal taken as the highest peak between 2.5 to 3.5 ppm and noise 15 to 20 ppm) was less than 4.0. Preoperative patients and controls were only included if there were valid data in both temporal lobes.

Locally written software in SAGE 7.0 provided estimates for the resulting grey matter, white matter and cerebro-spinal fluid (CSF) tissue composition of the prescribed MRS volume of interest based on the SPM segmentations of the IRP-SPGRs. Metabolite concentrations were then corrected for CSF content, which is considered to provide negligible signal.

3.6.2.4 Statistics

Statistical analysis was performed with SPSS 11.0. In the first analysis the ipsilateral temporal lobe (**HSips**) and contralateral temporal lobe (**HScont**) patient data were compared against a control group (**ControlM**) for NAA_t/Cr, GLX/Cr and GABA+/Cr; where **ControlM** represented the mean of the left and right temporal lobe measurements for each control subject. These metabolite ratios were compared using ANCOVA with voxel grey matter content used as a co-variable, and post hoc comparisons were made using the Bonferroni Test. In the analysis of GABA+

concentrations, data from patients taking GABAergic medications known to increase GABA levels were not included.

In the second analysis data from the contralateral temporal lobe in the surgical group, before (**PRE**) and after ATR (**POST**) and from a control group studied in the same temporal lobe on two occasions were analyzed. The change in metabolite concentration or ratio between the two scans was defined as:

$$\Delta = \text{POST} - \text{PRE} / \text{Mean} (\text{PRE}, \text{POST}) \quad \text{[Eqn. 3.6.1]}$$

and for the Control group:

$$\Delta = (\text{SCAN 2} - \text{SCAN1}) / \text{Mean} (\text{SCAN1}, \text{SCAN2}) \quad \text{[Eqn. 3.6.2]}$$

Comparison was made for Δ between the surgical and control groups. The group results for **PRE** and **POST** were also compared against the mean control group **ControlM** for the metabolite ratios NAA_t/Cr, GABA₊/Cr and GLX/Cr (see below).

3.6.3 Results

The demographics of the controls and patients with data of acceptable quality are given in **Table 3.6.1**. The medications taken by the patients were as follows (HS group/surgical group); valproate (3/4), lamotrigine (2/2), carbamazepine (9/6), topiramate (3/1), clobazam (5/2), phenytoin (3/1), Oxcarbazepine (3/1), phenobarbitone (1/0), levetiracetam (6/3).

3.6.3.1 Control Group

Nineteen test-retest studies (11 right TL and 8 left TL) were performed with acceptable data quality to determine repeatability which was calculated according to **[Eqn. 2.4.1]** on page 176 (Bland JM and Altman DG, 1986). Test-retest repeatability scores for the control population were : NAA_t 17%, Cr 23%, Cho 21%, Ins 23%, GLX 32%, GABA₊ 43%, NAA_t/Cr 25%, GLX/Cr 35% and GABA₊/Cr 45%.

Data from the right and left temporal lobes were compared in the Control population. Concentrations of NAA_t, Cr, Cho, GLX, GABA₊ were all lower in the right temporal lobe. NAA_t/Cr, GLX/Cr and GABA₊/Cr values showed no side to side variability, so ratios rather than concentrations were compared between patients and control subjects.

In the group having ATR, both metabolite concentrations and ratios were compared because both measurements for each subject were performed in the same temporal lobe.

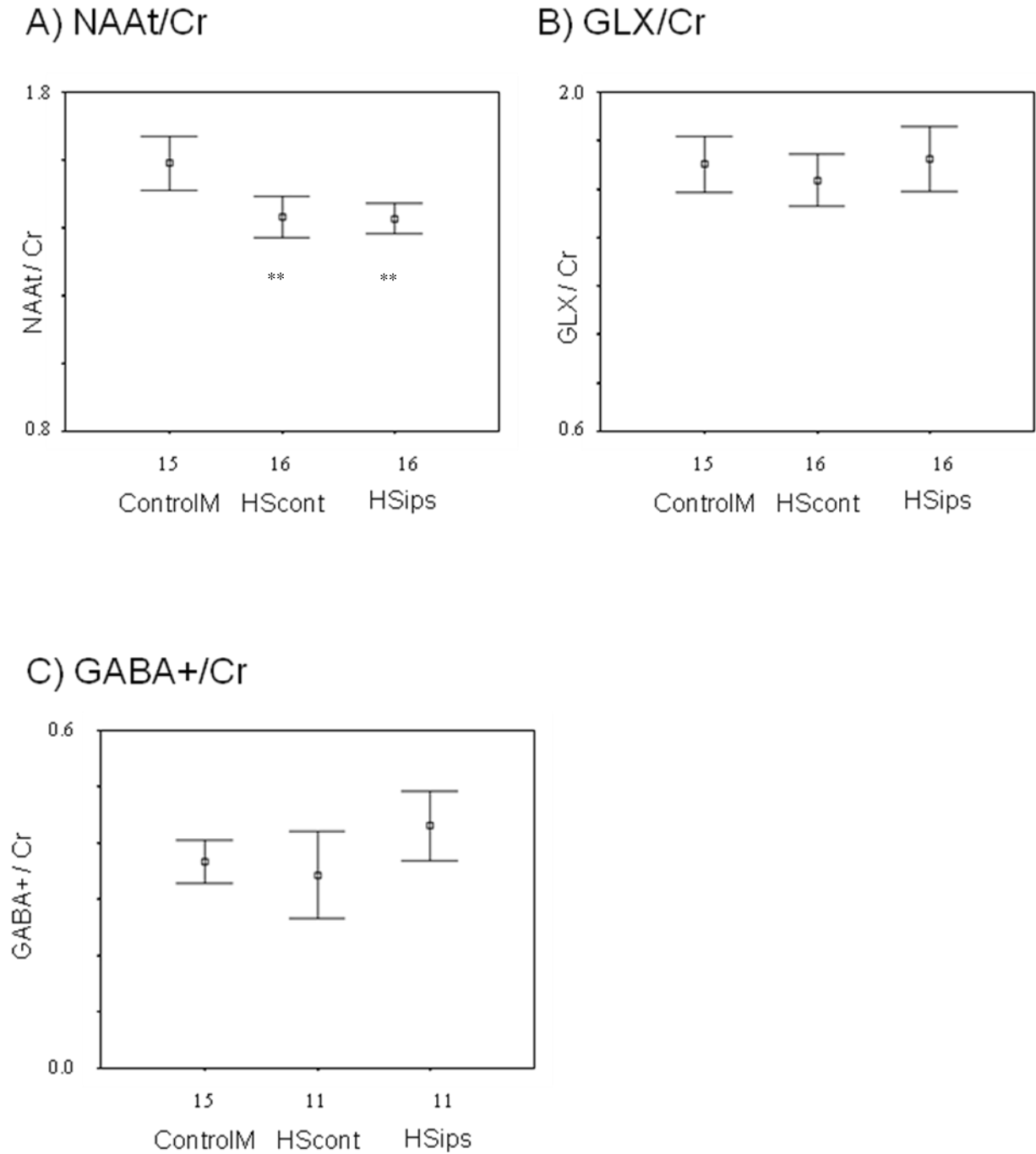
3.6.3.2 Patient Group

NAA_t/Cr was significantly less in the patient than the Control groups (**HSips** $p=0.001$, **HScont** $p=0.002$) and there was no significant difference between patient groups. There was no trend to difference noted with GLX/Cr. ANCOVA analysis showed increased GABA₊/Cr in the **HSips** group compared to Controls, but this did not reach significance ($p = 0.09$).

Table 3.6.2: Metabolite ratios in the temporal lobe ipsilateral to hippocampal sclerosis (**HSips**) and in the contralateral temporal lobe (**HScont**). The healthy volunteer group is designated as Control, measured in the right (R) and left (L) temporal lobes and expressed as a mean value (**ControlM**). NAA_t = N-acetyl aspartate plus N-acetyl aspartyl-glutamate; GLX = glutamate plus glutamine; Cr = creatine plus phosphocreatine; GABA₊ = GABA plus homocarnosine. The grey matter proportion in the analysed voxels is included. [§]Patients not taking GABAergic drugs only (N= 11). (** $p < 0.005$ compared to **ControlM**). Data expressed as mean (standard deviation).

Temporal lobe	<u>Control (R)</u> N=15	<u>Control (L)</u> N = 15	<u>ControlM</u> N=15	<u>HSipsi</u> N=16	<u>HScontra</u> N=16
Grey proportion	0.50(0.03)	0.49(0.03)	0.50(0.03)	0.54(0.11)	0.51(0.04)
NAA _t /Cr	1.6(0.2)	1.6(0.2)	1.6(0.1)	1.4(0.1)**	1.4(0.1)**
GLX/Cr	1.6(0.2)	1.7(0.3)	1.7(0.2)	1.7(0.2)	1.6(0.2)
[§] GABA ₊ /Cr	0.36(0.1)	0.37(0.07)	0.37(0.07)	0.42(0.08)	0.37(0.11)

Figure 3.6.2: Plots of mean and 95% confidence intervals for: (a) NAA_t/Cr; (b) GLX/Cr and (c) GABA⁺/Cr in control subjects (**ControlM**); patients with hippocampal sclerosis measured ipsilateral to the MRI pathology (**HSips**), and in the contralateral temporal lobe pre-surgery (**HScont**). NAA_t = N-acetyl aspartate plus N-acetyl aspartyl-glutamate, Cr = creatine plus phosphocreatine, GABA⁺ = GABA plus homocarnosine, and GLX = glutamate plus glutamine. ** p < 0.005.



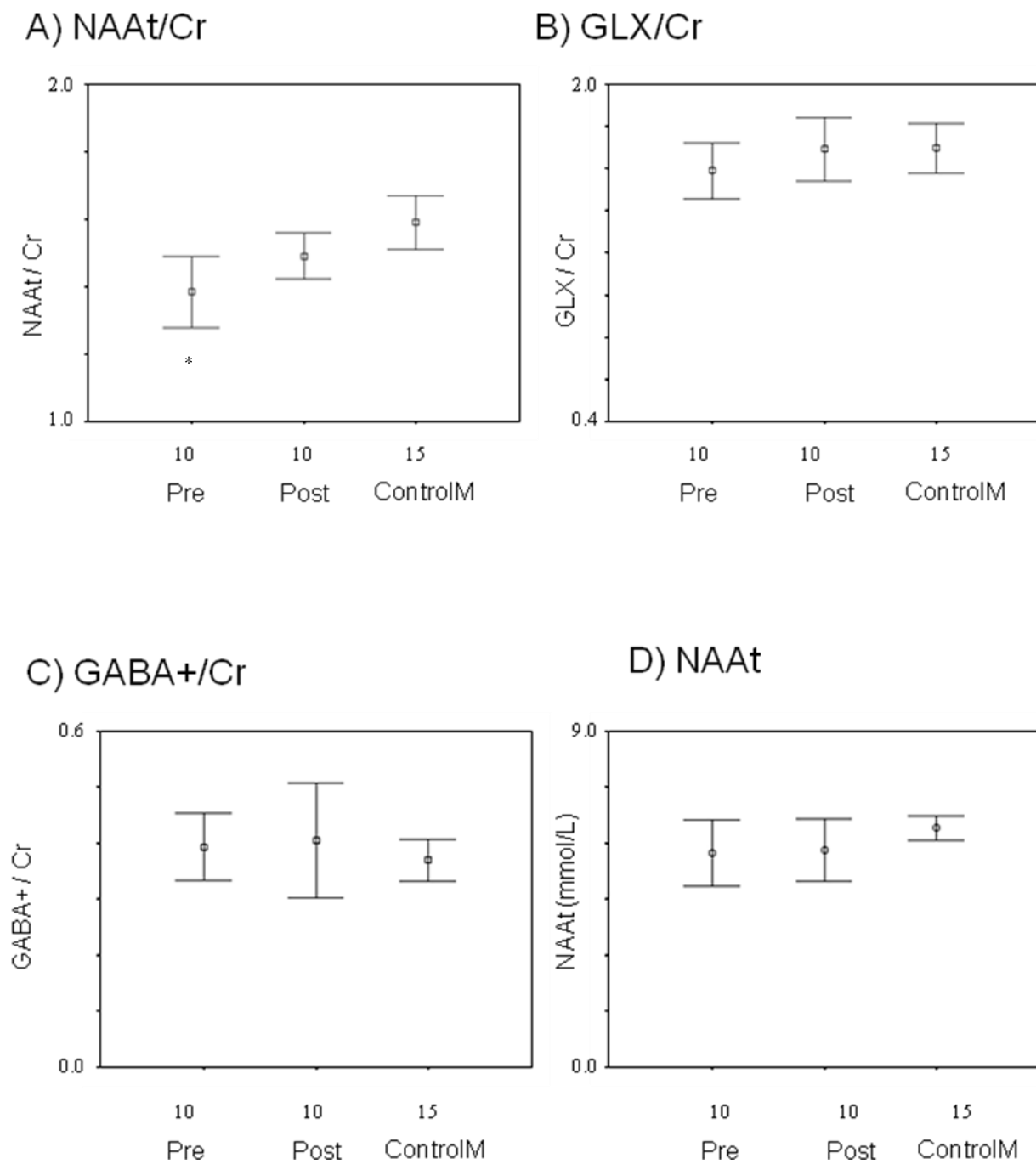
3.6.3.3 Surgical Patient Group

No trend to change in metabolite ratios was noted for GLX/Cr or GABA+/Cr. NAAAt/Cr was significantly higher in the **POST** than the **PRE** group (Δ NAAAt/Cr: mean = 0.08, SD = 0.1) when compared against change in the control group ($p=0.05$). No trend to increase was noted for NAAAt, GLX or GABA+. Cr was lower in the **POST** group (Δ Cr: mean = 0.06, SD = 0.2) but this did not reach significance. NAAAt/Cr was significantly lower in the **PRE** but not in the **POST** group when compared to **ControlM** ($p=0.05$). No correlation was observed between the changes for any metabolite or ratio and prior seizure frequency or interval since the most recent seizure.

Table 3.6.3: Table of the 10 analysed patients undergoing TL surgery to treat medically refractory seizures. Results show **PRE** and **POST** values compared against a mean Control group (**ControlM**). NAAAt = N-acetyl aspartate plus N-acetyl aspartyl-glutamate; GLX = glutamate plus glutamine; Cr = creatine plus phosphocreatine; Cho = choline containing compounds; Ins = myo-inositol; GABA+ = GABA plus homocarnosine. The grey matter proportion in the analysed voxels is included. (* $p = 0.05$). Data are expressed as mean(SD).

Temporal lobe		<u>ControlM</u>	<u>PRE</u>	<u>POST</u>
		<u>N=15</u>	<u>N=10</u>	<u>N=10</u>
Grey proportion		0.50(0.03)	0.50(0.05)	0.50(0.02)
Metabolites (mmol/l)	NAAAt	6.3(0.4)	5.8(0.8)	5.9(0.8)
	GLX	6.7(0.6)	6.7(0.5)	6.5(1.1)
	Cho	0.9(0.1)	0.9(0.2)	0.8(0.2)
	Cr	4.0(0.4)	4.1(0.5)	3.9(0.7)
	Ins	3.0(0.4)	3.1(0.6)	3.0(0.7)
	GABA+	1.5(0.3)	1.6(0.3)	1.5(0.4)
Ratios	NAAAt/Cr	1.6(0.1)	1.4(0.2)*	1.5(0.1)
	GLX/Cr	1.7(0.2)	1.6(0.2)	1.7(0.2)
	GABA+/Cr	0.37(0.07)	0.40(0.09)	0.39(0.07)

Figure 3.6.3: Plots of mean and 95% confidence intervals for: (a) NAA_t/Cr, (b) GLX/Cr, (c) GABA⁺/Cr and (d) NAA_t (mmol/L) for control subjects (**ControlM**); patients with hippocampal sclerosis measured contralateral to the MRI pathology before (**PRE**), and after (**POST**) temporal lobe surgery. NAA_t = N-acetyl aspartate plus N-acetyl aspartyl-glutamate, Cr = creatine plus phosphocreatine, GABA⁺ = GABA plus homocarnosine, and GLX = glutamate plus glutamine. * p = 0.05.



3.6.4.0 Discussion

This was the first MRS study to report in-vivo concentrations of GABA+ in the temporal lobes in TLE. A trend to elevated GABA+/Cr levels was observed in the ipsilateral temporal lobes but normal levels contralaterally. No change was observed in contralateral NAA, GLX or GABA+ concentrations following surgery, but normalization of NAA/Cr levels was seen.

The measurement of metabolite concentrations in the temporal lobes is difficult due to field inhomogeneity and susceptibility artifact. The requirement in the current study for a large volume of interest in which to measure GABA introduced further challenges to data quality. For the acquisition of the main metabolites these difficulties were in part compensated by reporting the metabolite concentrations as ratios with respect to Cr and by using techniques to minimise macromolecule inclusion in the baseline. Compared to previous studies of GABA+ measurement in the occipital and frontal lobes (**Chapter [3.2]** and **[3.3]**) there was reduced signal intensity and increased DQF signal distortion, resulting in the rejection of a larger number of datasets which did not fulfil data quality criteria and potentially poorer quality in the datasets included. These problems, however, will have been similar between both the control and patient groups and in particular between the pre and post operative spectra measured in the same temporal lobe. Despite these technical challenges, the test-retest repeatability for the retained datasets in this study are comparable to earlier studies; NAA 17%, GLX 32%, GABA+ 43% in this study compared with NAA 16%, GLX 26% and GABA+ 38% in the occipital lobes (Simister RJ et al., 2003a) [**Chapter 3.2**].

MRS studies of patients with TLE have generally reported NAA levels expressed with respect to Cr and/or Cho with the expectation that Cr in particular acts as an internal standard (Connelly et al., 1994; Burneo et al., 2004). In earlier work [**Chapters 3.1 – 3.5**] metabolite concentrations as well as ratios were reported (Woermann et al., 1999c; Simister et al., 2002) [**Chapter 3.1**]. However in these previous studies no side to side variability in metabolite concentrations was noted in the control population which allowed the formulation of a normal range for each metabolite that was

independent of the temporal lobe studied. In the current study a side to side difference in all metabolite concentrations for individual metabolites - but not for the ratios NAA_t/Cr, GLX/Cr and GABA₊/Cr - was evident in the control group, probably due to the data quality issues inherent in using larger voxels discussed above. Hence only the ratios have been reported in this study for the comparison between controls and **HSips** and **HScont**. This allows internal adjustment for field inhomogeneity but prohibits assessment of individual metabolite variation.

The field inhomogeneity in the anterior and mesial regions of the temporal lobe meant that the region of interest could not include the anterior hippocampus where metabolite concentrations are most affected in hippocampal sclerosis (Simister et al., 2002) [**Chapter 3.1**]. Despite these limitations low NAA_t/Cr was observed in both the side ipsilateral to the HS and contralaterally. Similar results have been reported by a number of authors and this has been taken to represent evidence for neuronal loss or dysfunction outside the epileptic focus in TLE (Cendes et al., 1995; Hugg et al., 1996; Chu et al., 2000; Li et al., 2000a).

GABA₊/Cr values were highest in the ipsilateral temporal lobe but did not remain significantly increased following correction for voxel grey matter content. Earlier work has previously noted that GABA₊/Cr levels are increased in malformations of cortical development associated with refractory epilepsy (Simister et al., 2007) [**Chapter 3.4**] and these findings would argue against a simple reduction of GABA levels as the cause for epilepsy in these patients. However, sensitivity limitations of the technique at 1.5T preclude measurement of GABA within the hippocampus, where a local effect might be more pronounced and clinically significant.

No abnormality in GLX/Cr was noted in either temporal lobe prior to surgery and no change was apparent following surgery. This is in keeping with previous observations that GLX levels are not elevated in the hippocampus or surrounding temporal lobe in TLE associated with HS (Woermann et al., 1999c; Simister et al., 2002) [**Chapter 3.1**] and also agrees with work performed at higher field strength (Hetherington et al., 2006). Ex-vivo analysis of temporal lobe tissue from TLE patients with HS found

reduced neuronal cell counts and reduced glutamate levels in patients with the most severe pre-operative MRI abnormality, but no correlation between glutamate levels and cell loss (Petroff et al., 2002b). In some samples with the highest amount of cell loss glutamate levels were near normal.

Several studies have measured NAA_t/Cr following surgical treatment and found normalization of levels in those patients with improved seizure control (Hugg et al., 1996; Cendes et al., 1997a; Serles et al., 2001). In this current study normalisation of NAA_t/Cr but no change in NAA_t was found. Cr levels were non-significantly lower after ATR, compared with pre-operatively and this accounted for some of the change in NAA_t/Cr. In previous studies of Cr in TLE a trend to elevation in HS compared to control levels has been observed (Connelly et al., 1994). This elevation in creatine plus phosphocreatine has been attributed to gliosis, which would appear to be unlikely in the current study due to the improved seizure control seen.

As with previous studies no relationship between metabolite concentrations or ratios and seizure frequency was found and there was no correlation between pre-operative seizure frequency and change in NAA_t/Cr or Cr post surgery [**Chapters 3.1-3.3**].

3.6.5 Conclusion

In summary this study again indicates that NAA_t and NAA_t/Cr are sensitive measures of metabolite dysfunction in TLE due to HS. GABA⁺ levels may be elevated in the epileptic temporal lobe but further work is necessary to determine how this might reflect hippocampal GABA metabolism. NAA_t/Cr but not NAA_t appears to normalize in the contralateral temporal lobe after ATL.

3.7 The Effect of Epileptic Seizures on Proton MRS Visible Neurochemical Concentrations

ABSTRACT

Purpose:

To investigate post-ictal changes in cerebral metabolites.

Methods:

We performed a longitudinal quantitative Proton Magnetic Resonance Spectroscopy (MRS) study in 10 patients with epilepsy and 10 control subjects. The patients were studied on two occasions: immediately following a seizure, and on a second occasion at least seven hours after the most recent seizure. Each study measured N-acetyl aspartate plus N-acetyl aspartyl glutamate (NAAt), Creatine plus phosphocreatine (Cr), Choline containing compounds (Cho) and glutamate plus glutamine (GLX) concentrations using a short echo time sequence (TE = 30ms), and NAAt, Cr and lactate using a second sequence with longer echo time (TE = 144ms). The control group was studied on two occasions using the same sequences.

Results:

No inter-scan differences were observed for the control group. NAAt and NAAt/Cr levels were lower in the patient group at both measured TEs but did not change significantly between studies. The ratio of Cr at TE 144ms to TE 30ms (Cr_{144}/Cr_{30}) and GLX/Cr were higher and Cho lower in the post ictal scan compared to the inter-ictal study. Change in Cr_{144}/Cr_{30} and $NAAt_{144}/Cr_{144}$ correlated with the post-ictal interval. Lactate measurement at longer TE was not informative.

Conclusion:

Proton MRS is sensitive to metabolite changes following epileptic seizures within the immediate post-ictal period. The ratio Cr_{144}/Cr_{30} is the most sensitive measure of metabolic disturbance and is highest in the post-ictal period but appears to normalise within two hours of the most recent seizure.

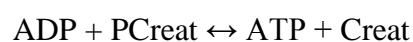
Published ref: (Simister et al., Epilepsy Research 2008 **81**, 36-43)

3.7.1 Introduction

Magnetic Resonance Spectroscopy (MRS) studies performed in human subjects have usually been performed inter-ictally and at least 24 hours after the last seizure. In these patients there appears to be no correlation between NAA, NAA/Cr or GLX and seizure control, or interval since the most recent seizure (Simister et al., 2002; Simister RJ et al., 2003b). GABA levels may rise after administration of several common antiepileptic drugs (AEDs) and with improved seizure control (Petroff et al., 1996b; Petroff et al., 2001a).

The few ictal or post-ictal MRS studies performed in humans have given differing results. Ictal elevation in lactate is the most common observation. NAA may be reduced or unchanged whilst the choline signal may be increased (Lazeyras et al., 2000; Mueller et al., 2001a). Post-ictally dynamic changes may be apparent, with evidence of increased mobility of choline (Maton et al., 2001b; Flugel et al., 2006) or transient generalized reduction in all measured metabolites (Wellard et al., 2004). In animal studies reduction in Cr and elevation in NAA/Cr, GLX and lactate have been reported, shortly following stimulated seizures (Najm et al., 1997; Nepl et al., 2001). Phosphorous MRS has demonstrated acidosis and reduction in phosphocreatine together with stable ATP levels during status epilepticus (Petroff et al., 1984; Young et al., 1985).

The Cr signal visible to proton MRS is the sum of creatine and phosphocreatine. In mammals ATP levels are tightly controlled according to the reaction below using phosphocreatine as an energy store. The relative contributions of creatine and phosphocreatine to the combined Cr signal might therefore be expected to change dependent on the energy demands on the studied system. During periods of high energy demand and increased utilization of ATP the reaction below will be driven to the right to restore ATP levels and reduce PCreat stores.



Phosphocreatine has a shorter T2 relaxation time than Creat (T_2 for PCreat and Creat = 117 +/- 21 ms and 309 +/- 21 ms respectively)(Ke et al., 2002). At short TE any postictal decrease in phosphocreatine will make little difference to the combined signal of Cr. At long TE, however, the increased Creat component of Cr will cause it to decay more slowly and show relatively more signal compared to the resting state where PCreat and Creat are more evenly balanced. This implies that the ratio $[\text{Cr}]_{\text{long TE}} / [\text{Cr}]_{\text{short TE}}$ should be increased in the immediate post-ictal state compared to the inter-ictal state as the equilibrium of the above reaction is driven to the right.

The purpose of our study was to investigate dynamic changes in metabolite concentrations in the brain, particularly changes in the ratio $[\text{Cr}]_{\text{long TE}} / [\text{Cr}]_{\text{short TE}}$, in the immediate post ictal period, using MRS.

3.7.2 Methods

3.7.2.1 Subjects

Ten healthy controls and 10 patients with epilepsy were included in the study. Ethical approval by the Joint Research Ethics Committee of the Institute of Neurology and the National Hospital for Neurology and Neurosurgery was obtained, and all subjects had given prior consent before the onset of the witnessed seizure. All control subjects had normal MRI and were taking no regular medication.

Every subject was scanned twice. For each control subject the data was labelled **CTL1** and **CTL2** dependent on the temporal order of the acquisition. For the patients, the study performed immediately following a complex partial seizure or generalised tonic clonic seizure was designated **POST** and that performed more than seven hours following a witnessed complex partial seizure was designated **INTER** [Table 3.7.1]. During the course of the study no changes were made to patients' AEDs.

Table 3.7.1: Clinical data for the patient group. M = male; F = female; CBZ = carbamazepine; CLB = clobazam; DZP = diazepam; GBP = gabapentin; LEV = levetiracetam; LTG = lamotrigine; PHT = phenytoin; PRM = primidone, VGB = vigabatrin; VPA = sodium valproate; Sz = generalised tonic-clonic seizures or complex partial seizure. FLE = frontal lobe epilepsy, OLE = occipital lobe epilepsy, PLE = parietal lobe epilepsy, TLE = temporal lobe epilepsy, X-TLE = non-localised extra temporal lobe epilepsy. HS = hippocampal sclerosis, MCD = undifferentiated malformation of cortical development and WM = white matter.

Patient no. /age (years) /gender	Diagnosis	AEDs	MRI	Post Ictal Scan		Inter ictal scan	
				Time from end of sz to scan (mins)	Duration of sz (mins)	Time since last clinical seizure (hours)	Time since post ictal scan (hours)
1/28/F	R. TLE	clb, ltg	Normal	60	4	34	34
2/32/F	L. X-TLE	clb, cbz, gbp, ltg, vgb	L.parieto-occipital MCD	60	2	24	24
3/23/F	R. OLE	vpa	Posterior heterotopia	35	2	48	72
4/23/F	L. FLE	cbz, gbp	L.frontal MCD	25	2	9	816
5/63/M	L. TLE	clb, gbp, vpa	L. HS	120	4	72	72
6/45/M	R. TLE	clb,gbp, lev,ltg, prm	R. HS	50	1	24	24
7/33/M	R. FLE	cbz, clb	Normal	120	1	26	26
8/45/F	R. X-TLE	cbz, prm	Multiple WM lesions	120	3	7.5	48
9/32/F	R. TLE	lev, ltg	Normal	70	1	24	24
10/26/M	R. TLE	cbz, lev	R. HS	45	2	48	48

3.7.2.2 Magnetic Resonance Imaging

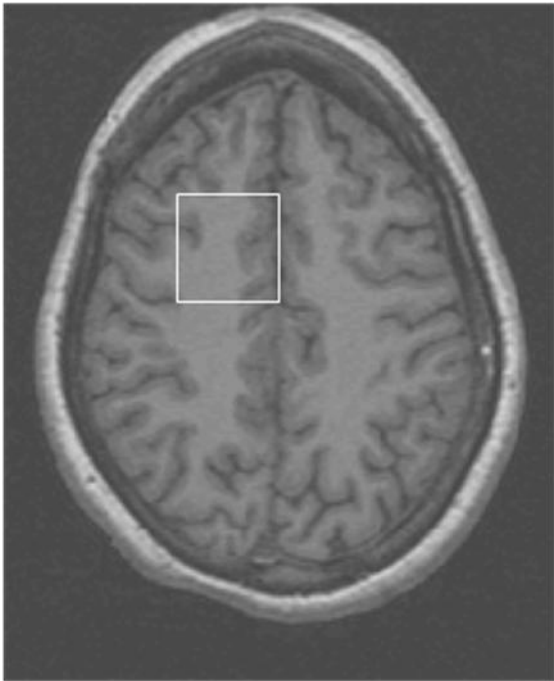
All scanning took place on a 1.5T SIGNA Horizon Echospeed scanner (General Electric, Milwaukee, WI) with a standard quadrature head coil. Axial T1 weighted inversion-recovery prepared fast spoiled gradient recalled echo (IR-SPGR) images were acquired (TE/TI/TR = 4.2/450/15.5 ms, flip angle 200; matrix 256*160; FOV 24 cm; slice thickness 1.5mm) to guide voxel placement and for segmentation into grey matter, white matter and cerebro-spinal fluid (CSF) using SPM (Statistical Parametric Mapping; Wellcome Centre for Imaging Neuroscience, Institute of Neurology, University College London).

For each patient a single region was investigated, in the frontal lobe ipsilateral to the side of seizure onset. A single voxel was prescribed from the axial IR-SPGR images with dimensions (40 * 35 * 25 mm)(Simister RJ et al., 2003b) (**Figure 3.7.1**). For each control subject an otherwise identical acquisition was performed separately in both the right and left frontal lobes. Care was taken at the time of the second study to assure comparable voxel positions to the first study.

Conventional PRESS-localised water suppressed spectra were obtained, so that LCModel(Provencher, 1993) could be used for quantification of metabolite concentrations. In the first sequence (TE/TR 30/3000ms) NAA_t, Cr, Cho, Ins, and GLX were measured and these results are designated by the subscript ₃₀. In the second sequence with longer echo time lactate, NAA_t and Cr were measured and designated with the subscript ₁₄₄.

Figure 3.7.1: A) Axial T1 weighted MR image showing the position of the prescribed voxel in patient 3. **B)** Representative PRESS localised spectra with superimposed LCModel fit to metabolite concentrations and estimated baseline for the same patient in the post ictal period (**POST**) and inter-ictal period (**INTER**). **Top:** (TE/TR 30/3000ms); **bottom:** (TE/TR 144/3000ms). NAA_t = N-acetyl aspartate plus N-acetyl aspartyl-glutamate; GLX = glutamate plus glutamine; Cho = choline-containing compounds; Cr = creatine + phosphocreatine; Ins = myo-inositol, Lac = lactate.

A)

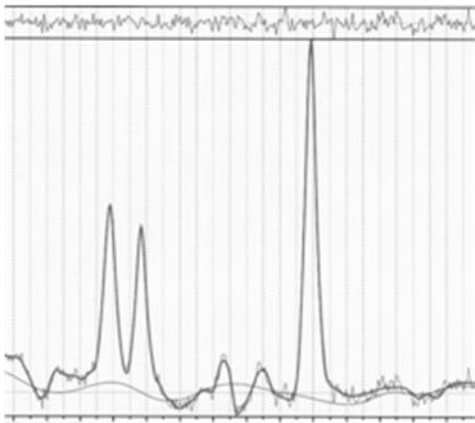
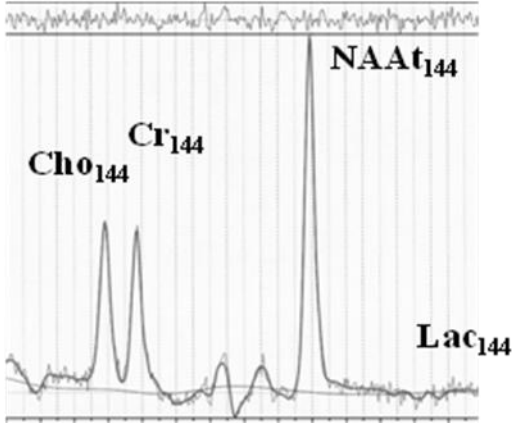
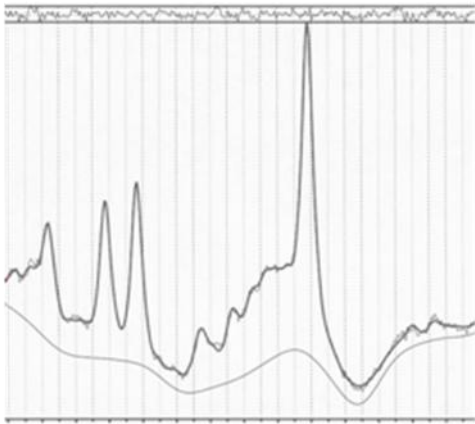
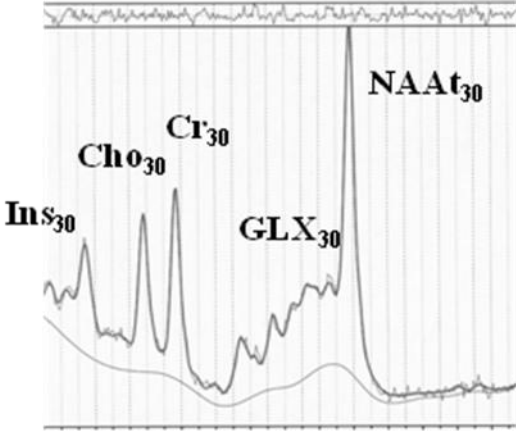


Right

Left

Bi) POST

Bii) INTER



Finally, metabolite concentrations were normalized to 100% brain tissue by correcting for the CSF content within the voxel, estimated from the SPGR images using SPM.

3.7.2.3 Statistical analysis

Statistical analysis was performed with SPSS 11.0. Only acquisitions achieving a threshold for data quality (full width half maximum (FWHM) < 10 Hz for PRESS localised (TE/TR = 30/3000 ms) unsuppressed water peaks) were accepted for analysis. Group changes in the following concentrations were examined: NAA_{t30}, Cr₃₀, Cho₃₀, Ins₃₀, GLX₃₀, NAA_{t144}, Cr₁₄₄, Lac₁₄₄, and the following ratios: NAA_{t30}/Cr₃₀, NAA_{t144}/Cr₁₄₄, GLX₃₀/Cr₃₀ and Cr₁₄₄/Cr₃₀.

Data from the right and left frontal voxels were obtained from each control subject and averaged to give a mean metabolite concentration or ratio for that subject (**CTLM**). An ANOVA comparison was then performed between **CTLM** and the patient **POST** and **INTER** groups. Bonferroni correction was made in each case to allow for multiple comparisons.

Change in metabolite concentration (Δ) between the two scans was calculated for each subject, being defined for each patient as:

$$\Delta = (\text{POST} - \text{INTER}) / \text{mean} (\text{POST}, \text{INTER}) \quad [\text{Eqn. 3.7.1}]$$

and for each control subject as:

$$\Delta = (\text{CTL1} - \text{CTL2}) / \text{mean} (\text{CTL1}, \text{CTL2}) \quad [\text{Eqn. 3.7.2}]$$

Differences were analysed for significance using a one sample t-test.

Finally, we performed a correlation analysis for time since most recent seizure, inter-ictal interval and Δ for each metabolite and ratio using Spearman's Rho test.

3.7.3 Results

All spectra satisfied quality thresholds and were included for analysis. In the control group the median age was 35 years (range 28 to 52 years) and four of the 10 subjects were female. There was no difference in voxel grey matter proportion between **CTL1** and **CTL2** or between right and left frontal lobe voxels. No side to side differences were observed for any metabolite between the left and right frontal voxels. No trend to inter-scan difference (Δ) was noted for any metabolite concentration or ratio.

Metabolite concentrations were lower for patients than controls both in the **POST** and **INTER** scans for $\text{NAA}_{t_{30}}$ and $\text{NAA}_{t_{144}}$ and for $\text{NAA}_{t_{30}}/\text{Cr}_{30}$ and $\text{NAA}_{t_{144}}/\text{Cr}_{144}$ but following Bonferroni correction only **POST** $\text{NAA}_{t_{30}}$ ($p = 0.05$) and **INTER** $\text{NAA}_{t_{30}}/\text{Cr}_{30}$ ($p=0.05$) remained significant compared to the **CTLM**. $\text{Cr}_{144}/\text{Cr}_{30}$ was lower for **INTER** compared to **POST** ($p = 0.05$).

Comparison of inter-scan differences (Δ) revealed that apparent Cho_{30} concentration was 9% lower post ictally ($p = 0.03$). No other significant change in concentrations was noted. The ratio $\text{GLX}_{30}/\text{Cr}_{30}$ was 9% higher ($p=0.02$) and $\text{Cr}_{144}/\text{Cr}_{30}$ 7% higher ($p=0.03$) post-ictally.

There was a correlation between $\Delta(\text{Cr}_{144})$ and post-ictal interval ($R^2 = 0.5$, $p = 0.02$). No other individual metabolite showed an association with post-ictal or inter-ictal intervals. There was a significant correlation between post-ictal interval and $\text{Cr}_{144}/\text{Cr}_{30}$ ($R^2 = 0.74$, $p = 0.001$) and $\text{NAA}_{t_{30}}/\text{Cr}_{30}$ ($R^2 = 0.6$, $p = 0.007$). Regression analysis indicated that these ratios normalised to inter-ictal levels at post-ictal intervals of approximately 105 minutes and 85 minutes respectively.

Table 3.7.2: showing data for the mean control group (CTLM) measured on two occasions (CTL1 and CTL2) and the patient group measured in the post ictal (POST) and inter ictal (INTER) periods. NAA_t = N acetyl aspartate plus N acetyl aspartyl glutamate, Cr = creatine plus phosphocreatine, Lac = lactate, Cho = choline containing compounds, GLX = glutamate plus glutamine. Metabolite concentrations measured in mmol/L. (₁₄₄) TE = 144ms. (₃₀) TE = 30ms. * significant variation (p < 0.05) when compared against CTLM. † significant elevation in POST compared to INTER levels (p < 0.05). Metabolite and ratio data presented as mean (SD).

		CTL1 N = 10	CTL2 N = 10	CTLM N=10	POST N = 10	INTER N = 10	
	Grey Proportion	0.29	0.29	0.29	0.29	0.29	
Metabolites (mmol/L)	NAA _{t144}	4.4(0.4)	4.4(0.4)	4.4(0.4)	4.1(0.3)	4.1(0.4)	
	Cr ₁₄₄	1.9(0.1)	1.9(0.1)	1.9(0.1)	1.9(0.2)	1.9(0.2)	
	Lac ₁₄₄	0.20(0.12)	0.28(0.08)	0.24(0.09)	0.30(0.10)	0.26(0.16)	
	NAA _{t30}	7.0(0.5)	7.1(0.6)	7.1(0.5)	6.5(0.5)*	6.6(0.7)	
	Cr ₃₀	4.3(0.5)	4.4(0.5)	4.3(0.5)	4.2(0.4)	4.5(0.5)	
	Cho ₃₀	1.2(0.2)	1.2(0.1)	1.2(0.2)	1.1(0.2)	1.2(0.1)	
	Ins ₃₀	3.1(0.4)	3.0(0.4)	3.1(0.4)	3.2(0.6)	3.2(0.4)	
	GLX ₃₀	6.3(0.9)	6.7(1.0)	6.5(0.8)	6.5(1.0)	6.4(0.8)	
	Ratios	(NAA _t /Cr) ₁₄₄	2.3(0.2)	2.3(0.1)	2.3(0.1)	2.1(0.3)	2.2(0.3)
		(NAA _t /Cr) ₃₀	1.7(0.2)	1.6(0.2)	1.6(0.1)	1.5(0.2)	1.5(0.2)*
(GLX/Cr) ₃₀		1.5(0.1)	1.6(0.2)	1.5(0.1)	1.5(0.2)	1.4(0.2)	
Cr ₁₄₄ /C ₃₀		0.45(0.05)	0.45(0.04)	0.45(0.04)	0.47(0.04)†	0.43(0.03)	

Figure 3.7.2: Error bars with 95% confidence limits for the change in metabolite concentrations between the two scans (Δ) for each subject [where $\Delta = (\text{POST} - \text{INTER}) / \text{mean}(\text{POST}, \text{INTER})$ for each patient and $(\text{CTL1} - \text{CTL2}) / \text{mean}(\text{CTL1}, \text{CTL2})$ for each control]: **A)** ΔNAA_{30} , **B)** $\Delta(\text{GLX}/\text{Cr})_{30}$, **C)** ΔCho_{30} , and **D)** $\Delta(\text{Cr}_{144}/\text{Cr})_{30}$ where $_{30}$ represents studies performed at TE = 30ms and $_{144}$ represents TE=144ms. **CTL** = control group. **Patients** = patient group. * = significant to $p < 0.05$.

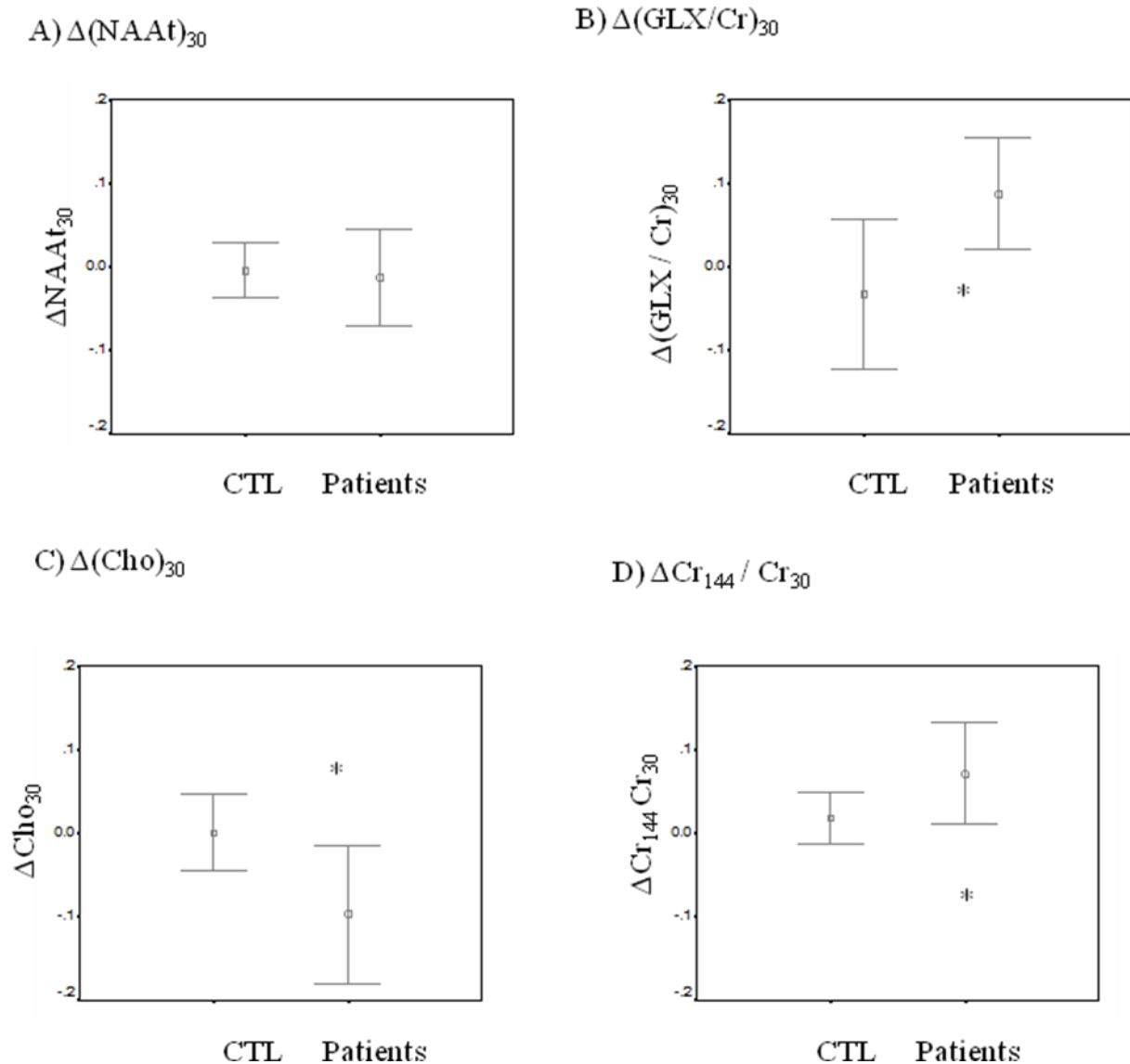
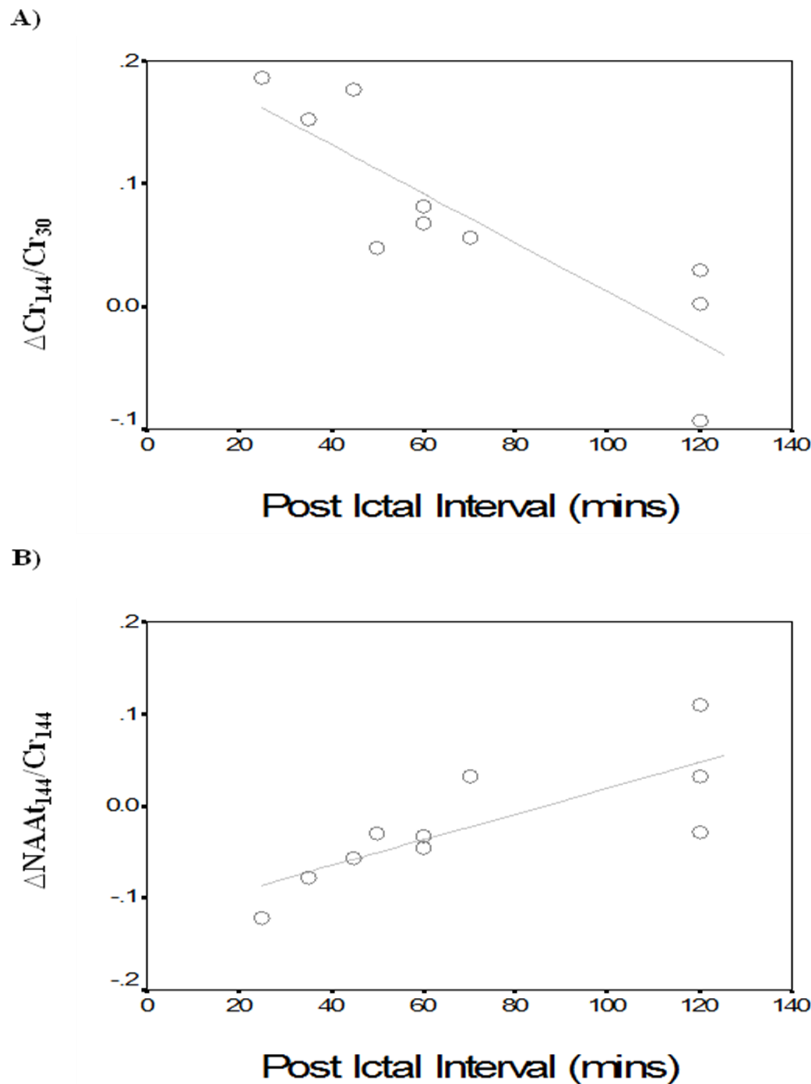


Figure 3.7.3: Scatter plot and regression curve for **A)** $\text{Cr}_{144}/\text{Cr}_{30}$ and **B)** $\text{NAA}_{144}/\text{Cr}_{144}$ against post-ictal interval measured in minutes.



3.7.4 Discussion

This is the first in-vivo proton MRS study to indicate a time line for recovery of metabolite dysfunction following seizures in humans. The results show that metabolite disturbances are apparent in the immediate post-ictal period but normalize within two hours. Changes in the concentration of the combined Cr signal were demonstrated, and were the most sensitive markers for recent seizure activity.

No trend to difference was noted for voxel tissue composition or any metabolite concentration in the control group between scans, or between the right and left frontal lobes. Performing MRS shortly after seizures was challenging, but was possible because of the location of the MR scanner within the Epilepsy Assessment Centre. Additionally, each patient had consented to participation in the study before the day of the seizure. The longer TE sequence was performed second and therefore post ictal intervals were slightly longer for this acquisition. All patients included in the study had had witnessed complex partial or generalized seizures and approximate seizure duration was noted.

As expected, NAA_t and NAA_t/Cr were low in the patient groups, despite prescription of the MRS voxel outside the seizure focus in several cases. Lactate could not reliably be estimated by LCModel and no significant elevation was seen post-ictally compared to the other groups. Previous studies have reported elevated lactate following a prolonged seizure (Petroff et al., 1986; Fazekas et al., 1995; Najm et al., 1997; Neppi et al., 2001), but it is likely in the current study that the seizures witnessed were too short to produce detectable lactate elevation. Similar results were obtained in an earlier study (Flugel et al., 2006).

In the patient group, Cho was lower and GLX/Cr and Cr₁₄₄/Cr₃₀ higher in the post-ictal study. In the earlier study reduction in Cho post-ictally was not seen (Flugel et al., 2006), although reduced Cho MTR was identified, indicating alteration in the interaction of choline containing moieties with the immobile phospholipid pool. Synthesis of phosphatidylcholine is impaired by NMDA receptor overactivity before phospholipid degeneration occurs (Gasull et al., 2003) and impaired formation of phosphocholine from choline is observed during periods of high energy demand and excess glutamatergic activity (Gasull et al., 2002). Since the visible choline signal is mainly made up of phosphocholine and glycerylphosphocholine, both metabolites of phosphatidylcholine, it may not be surprising that there is reduction in this signal following brief epileptic seizures. Prolonged seizures with irreversible cell damage would be more likely to be associated with phospholipid membrane degeneration and release of high concentrations of choline containing metabolites. In the current study

there was no association with the post-ictal interval indicating a slower recovery period of choline metabolism than in the post-ictal monitoring period of the current study.

Elevation of GLX/Cr was seen post-ictally compared to the inter-ictal period but there were no significant changes for GLX itself. Elevated glutamate has been reported in the region of a temporal lobe seizure (During and Spencer, 1993) and in ex-vivo analysis of epileptic cortex (Petroff et al., 1995) and it is possible that a similar effect here could have been masked by the relative insensitivity of our techniques, which cannot distinguish between different metabolite pools within the brain, and the unavoidable postictal interval. Subsequent work by Badawy and colleagues has shown reduced cortical excitability in the immediate post ictal period and this finding would suggest that intracellular glutamate and glutamine levels may well not be elevated post-ictally (Badawy et al., 2009).

NAA concentrations were similar in the post-ictal and inter-ictal studies, concurring with the earlier study (Flugel et al., 2006) and also with post-ictal animal studies (Nepl et al., 2001). Other studies have shown reduced ictal NAA in focal cortical dysplasia (Nepl et al., 2001), reduced post-ictal NAA in Rasmussen's encephalitis (Wellard et al., 2004) or elevated ictal levels in animals (Najm et al., 1997). Ex-vivo findings have shown that NAA levels are not directly correlated with neuronal cell loss (Kuzniecky et al., 2001; Petroff et al., 2002b) and further work is needed to evaluate the patho-physiological correlate of low or high NAA levels. However it may not be surprising that NAA levels were not affected in this study. NAA synthesis appears to be linked with the rate of glucose metabolism (Moreno et al., 2001). Periods of increased glucose metabolism such as occur during seizures may be expected to lead to NAA accumulation whilst periods of neuronal hypo-excitability and consequently reduced glucose metabolism as shown to occur in the immediate post-ictal period (Badawy et al., 2009) will lead to reduced NAA levels. The exact balance between accumulation and reduced synthesis may well vary significantly depending on the intensity of metabolic activity during the seizure, seizure duration and time since seizure cessation.

Cr_{144}/Cr_{30} was elevated post-ictally and Cr_{144} was highest in the immediate post-ictal period. These findings are consistent with the post-ictal phase being marked by a shift of equation (1) to the right and increased proportions of the slower decaying creatine signal. Phosphorus MRS studies (Petroff et al., 1984; Young et al., 1985) have reported lowered post-ictal phosphocreatine, which is consistent with our findings. The advantages of using 1H instead of ^{31}P MRS to monitor this is that proton MRS allows potentially much higher spatial resolution and the hardware needed is more widely available.

Correlation analysis with the post-ictal interval suggests that these changes will only be observed if the patient is scanned within the first 100 minutes following a single complex partial or generalized seizure.

The post-ictal interval at which measurements are made is likely to be critical and may explain the variation in published findings. One previous in-vivo post-ictal study did not find changes in the ratio NAA/Cr post ictally, but generally performed the post ictal study after a longer interval (Maton et al., 2001b). Flugel et al. used a similar methodology and had a median post-ictal interval of 70 mins, compared to 60mins in the current study, and did not use a longer TE acquisition (Flugel et al., 2006). Post-ictal MRS animal studies have previously found elevated lactate and NAA/Cr or reduced Cr (Najm et al., 1997; Neppi et al., 2001) and low phosphocreatine (Petroff et al., 1984; Young et al., 1985) following prolonged stimulated status epilepticus. However the metabolic consequences of prolonged seizures would be expected to be different to those induced by brief self terminating seizures and it is notable that in these studies prolonged elevation in lactate is reported together with histological evidence of neuronal loss (Najm et al., 1997).

3.7.5 Conclusion

In this study MRS demonstrated dynamic disturbances in metabolic function after single seizures. The ratio Cr_{144}/Cr_{30} was the most informative measure and implied a change of energy metabolism in the brain that reverted to normal over one and a half hours.

Chapter 4: Thesis conclusions and Further Work

The work included in this thesis was undertaken with two fundamental aims: The first was to apply a standardised MRS methodology in order to gain reproducible semi-quantitative information about the variation of relevant neurometabolites such as gamma amino butyric acid (GABA), glutamate (as glutamate plus glutamine [GLX]), N acetyl aspartate (NAA), myo-inositol (Ins) and creatine plus phosphocreatine (Cr) within epilepsy syndromes or pathological groups. The second main aim was to test a series of hypotheses relating to the regulation of the concentrations of these metabolites in the region of epileptic seizures, immediately following seizures and associated with particular medical and surgical treatment interventions.

Prior to the period during which this work was undertaken several groups had reported MRS findings in patients with epilepsy. These studies, which had generally reported on only the major visible metabolites and which had used metabolite ratios rather than individual metabolite concentrations, had indicated that MRS may be a sensitive tool for the in vivo assessment of biochemical disturbance associated with epilepsy. This thesis has built on the evidence from these early studies and has taken advantage of the opportunity to measure neurometabolites such as glutamate and γ -amino butyric acid (GABA) that are of fundamental importance to understanding epilepsy.

The thesis was undertaken based upon several hypotheses. Namely that:

Cortical excitability in idiopathic generalised epilepsy (IGE) is associated with reduced concentrations of GABA and / or raised concentrations of glutamate and glutamine in the cerebral cortex. (Hypothesis I)

In patients with focal seizures, there will be a disturbance in GABA and / or glutamate levels in the region of the epileptic focus compared to healthy controls measured in the same anatomical region. (Hypothesis II)

There will be measurable metabolite abnormalities in epileptogenic malformations of cortical development as a consequence of the abnormal development of this tissue. (Hypothesis III)

There will be a measurable disturbance of brain metabolites at the site of interictal epileptiform activity that will help to characterise the epileptic focus. (Hypothesis IV)

Following focal seizures there will be a transient disturbance in those measurable metabolites relevant to cell energetics and neurotransmission such as lactate, GABA, glutamate and glutamine and phosphocreatine. (Hypothesis V)

The thesis findings will now be briefly discussed in the context of these hypotheses.

MRS techniques demonstrate metabolite abnormalities in epileptic patients. NAA is the most commonly observed metabolite marker of chronic pathology but levels are insensitive to recent seizure history. These findings repeat earlier observations of the usefulness of NAA measurement in the assessment of chronic epilepsy whilst illustrating ongoing uncertainty as to the correct pathophysiological interpretation of reduced NAA levels. Low NAA is a feature of 9/10 patients with hippocampal sclerosis and temporal lobe epilepsy and 4/10 with MRI negative temporal lobe epilepsy. NAA levels were otherwise normal in patients with occipital lobe epilepsy. The other measured metabolites are not demonstrated to be sensitive markers for inter-ictal abnormality in the region of the epileptic focus. These findings indicate that characteristic metabolite disturbance in the region of an epileptic focus is not identifiable in occipital lobe epilepsy but that NAA is a good marker of abnormality in temporal lobe epilepsy associated with hippocampal sclerosis (IV).

GLX and GABA⁺ measurement in focal epilepsy did not demonstrate a characteristic pattern of disturbance (II). GLX was elevated in the contralateral hippocampus but not in the epileptogenic hippocampus [3.1]. GABA⁺ levels were not reduced in this region and instead showed a trend to elevated levels compared to the contralateral hemisphere and to the control group [3.6]. In OLE, GLX and GABA⁺ levels were not

altered compared to the control group or to a population with IGE. These findings indicate that *at the resolution of current MRS techniques* GABA and GLX disturbance in epileptic foci is not reliably detectable. A probable explanation for this finding is that several factors have combined to influence the concentrations obtained. Firstly, at the current level of technological development measurement is limited to relatively large volumes of interest, long duration acquisitions, and measurement of combined signals rather than individual metabolites. These factors will become less significant as technology improves. Secondly, the potency of glutamate and GABA molecules at synaptic terminals are such that simple imbalances in the concentrations of these metabolites that remain present over the time span of an MRS acquisition are probably unlikely to be found in patient volunteers well enough to attend for routine research studies. Thirdly, MRS is sensitive to free intracellular GABA and glutamate and relatively insensitive to extracellular signal and signal contained in synaptic vesicles. Consequently, measurement of these signals provides only an indirect measure of the metabolism of these compounds.

In contrast MRS appears to have great promise as an investigatory tool for assessment of malformations of cortical development (MCD) (III). The finding in this thesis that metabolite concentrations demonstrate signal characteristics that show similarities to spectra obtained from immature brain tissue fits well with an understanding that MCD represent abnormal / blocked development. Both GABA⁺ and GLX levels were abnormal in this tissue which may represent abnormal formations of GABAergic and glutamatergic neurons, a highly abnormal metabolic regulation of these compounds, and / or a consequence of epileptogenicity. These results would recommend a role for MRS in the identification of MCD because the examination should be informative both in the region of visible abnormality (to demonstrate the signature of the MCD) and in non-adjacent regions (to assess whether these regions are likely to represent abnormal tissue even if apparently normal at the resolution of today's MRI sequences). Finally, the observation that different sub-types of MCD may show different MRS profiles could recommend a further role for MRS in the sub-classification of MCD.

NAA and GLX/NAA levels were altered in the frontal lobes but not in the occipital lobes in Idiopathic Generalised Epilepsy. This finding provides support for frontal lobe “cortical hyperexcitability” as a cause or consequence of IGE (I). In contrast GABA⁺ levels were not abnormal in either the frontal or occipital lobes in these patients. Reduced frontal NAA would imply abnormal tissue and this finding would support pathological observations of microdysgenesis in patients with IGE. The IGE group studied in the frontal lobes in this thesis was sufficiently heterogeneous in terms of IGE sub-type to preclude any close examination of metabolic profiles within sub-groups but this would be an interesting follow up study.

Inter-ictal MRS measurements do not appear to be sensitive to recent seizure history. In [Chapter 3.3] there was no association between metabolite levels and the time since the previous seizure or with seizure frequency. In [Chapter 3.6] NAA levels were unchanged in the contralateral temporal lobe after successful surgical treatment of mesial temporal lobe epilepsy. However NAA/Cr levels did normalise in this study and this has also been reported by other groups. The results from this thesis and in particular the results of the post-ictal study [Chapter 3.7] would argue that this change may represent alteration in the combined signal of Cr rather than changes in NAA. In [Chapter 3.7] I demonstrated that MRS can detect transient alteration of metabolite concentrations immediately following an epileptic seizure (V). However, rather than GLX, GABA⁺, lactate or NAA disturbance in this period I found alteration of Cr. The finding of high post ictal Cr₁₄₄/Cr₃₀ levels which normalise within minutes appears to fit with our understanding of the role played by the creatine / phosphocreatine buffer system in maintaining ATP levels during periods of brief activation. Since the combined Cr signal is a dominant peak that is easily and reliably determined in 1H MRS experiments, a functional MRSI study in the immediate postictal period would be an interesting follow up of this work. In this study lactate was not shown to be elevated in the post-ictal period whereas there is substantial evidence that lactate is released during prolonged epileptic seizures. In my experiment it is most likely that the ictal events studied were too brief to result in a detectable release of lactate. The further work envisaged would be able to reassess this.

In addition to these tested hypotheses two further observations can be made on the basis of the findings in this thesis.

Firstly, metabolite concentrations are sensitive to the administration of antiepileptic medications. Sodium valproate reduces the levels of MRS visible Ins levels [**Chapter 3.3**] and [**Chapter 3.5**], whilst topiramate and gabapentin appear to be associated with higher GABA+ levels [**Chapter 3.4**]. These findings may find application in the assessment of treatment effect in patients with poor response to initiated treatments and / or in the investigation of patients with suspected drug resistance genes. The obtained Ins signal in 1H MRS experiments is considered to derive from myo-Inositol in the glial pool. Thus, the observation of an effect of valproate on a glial marker may become particularly interesting in the light of a growing understanding of the role of astrocyte dysfunction in a range of neurological conditions which include migraine, epilepsy, Alzheimer's disease, motor neurone disease and stroke.

The second additional observation arising from this work is the difficulty in interpreting the conventionally described ratio NAA/Cr. Whilst it is sometimes necessary to report this ratio (particularly when signal quality is poor (as in [**Chapter 3.6**]) it is now clear that Cr levels do not represent a global "standard" across brain regions and pathologies. Cr levels are affected by recent seizures and inter-ictal levels may be sensitive to variation in seizure control. More importantly there is wide variation in NAA/Cr levels across regions dependent simply on the tissue composition [**Chapter 3.1**]. As long as the majority of papers reporting MRS experiments continue to use this ratio, there will remain uncertainty as to the correct role of MRS in the assessment of epilepsy and other neurological conditions.

Further Work

Further projects suggested by the findings described in this thesis are as follows:

Sub-group analysis of IGE patients to determine whether there is characteristic profile within sub-groups / prominent seizure types.

Sub-group analysis of MCD populations to better characterise the profile of MCD sub-types. Such a work would incorporate assessment of normal appearing tissue and allow correlation with EEG information and / or pathology if available

Functional MRSI assessment could be performed in the immediate post-ictal period to determine if it is possible to map seizure activity across brain regions using the ratio Cr_{144}/Cr_{30} .

High field examination of GABA, glutamate and glutamine to re-examine whether direct observation of these compounds in more localised regions of interest may be more sensitive for abnormality in epileptogenic tissue.

Exploration of the effect of valproate on Ins levels in a group of patients with drug resistant epilepsy may be informative particularly if this group does not show reduction of Ins with administration of valproate

Reference List

- Aasly,J., Silfvenius,H., Aas,T.C., Sonnewald,U., Olivecrona,M., Juul,R., White,L.R., 1999. Proton magnetic resonance spectroscopy of brain biopsies from patients with intractable epilepsy. *Epilepsy Res* 35, 211-217.
- Achten,E., Boon,P., Van De,K.T., Caemaert,J., De Reuck,J., Kunnen,M., 1997. Value of single-voxel proton MR spectroscopy in temporal lobe epilepsy. *AJNR Am J Neuroradiol* 18, 1131-1139.
- Achten,E., Santens,P., Boon,P., De Coo,D., Van De,K.T., De Reuck,J., Caemaert,J., Kunnen,M., 1998. Single-voxel proton MR spectroscopy and positron emission tomography for lateralization of refractory temporal lobe epilepsy. *AJNR Am J Neuroradiol* 19, 1-8.
- Aghakhani,Y., Bagshaw,A.P., Benar,C.G., Hawco,C., Andermann,F., Dubeau,F., Gotman,J., 2004. fMRI activation during spike and wave discharges in idiopathic generalized epilepsy. *Brain* 127, 1127-1144.
- Amunts,K., Jancke,L., Mohlberg,H., Steinmetz,H., Zilles,K., 2000. Interhemispheric asymmetry of the human motor cortex related to handedness and gender. *Neuropsychologia* 38, 304-312.
- Antel,S.B., Li,L.M., Cendes,F., Collins,D.L., Kearney,R.E., Shinghal,R., Arnold,D.L., 2002. Predicting surgical outcome in temporal lobe epilepsy patients using MRI and MRSI. *Neurology* 58, 1505-1512.
- Appleton,R., Beirne,M., Acomb,B., 2000. Photosensitivity in juvenile myoclonic epilepsy. *Seizure* 9, 108-111.
- Arnold,D.L., Matthews,P.M., Francis,G., Antel,J., 1990. Proton magnetic resonance spectroscopy of human brain in vivo in the evaluation of multiple sclerosis: assessment of the load of disease. *Magn Reson Med* 14, 154-159.
- Ashburner,J., Friston,K.J., 2000. Voxel-based morphometry--the methods. *Neuroimage* 11, 805-821.
- Attwell,D., Laughlin,S.B., 2001. An energy budget for signaling in the grey matter of the brain. *J Cereb Blood Flow Metab* 21, 1133-1145.
- Babb,T.L., Pretorius,J.K., Mello,L.E., Mathern,G.W., Levesque,M.F., 1992. Synaptic reorganizations in epileptic human and rat kainate hippocampus may contribute to feedback and feedforward excitation. *Epilepsy Res Suppl* 9, 193-202.

Badawy,R., Macdonell,R., Jackson,G., Berkovic,S., 2009. The peri-ictal state: cortical excitability changes within 24 h of a seizure. *Brain* 132, 1013-1021.

Barker,P.B., 2001. N-acetyl aspartate--a neuronal marker? *Ann Neurol* 49, 423-424.

Barkovich,A.J., Kuzniecky,R.I., Jackson,G.D., Guerrini,R., Dobyns,W.B., 2001. Classification system for malformations of cortical development: update 2001. *Neurology* 57, 2168-2178.

Barnard,E.A., Skolnick,P., Olsen,R.W., Mohler,H., Sieghart,W., Biggio,G., Braestrup,C., Bateson,A.N., Langer,S.Z., 1998. International Union of Pharmacology. XV. Subtypes of gamma-aminobutyric acidA receptors: classification on the basis of subunit structure and receptor function. *Pharmacol Rev* 50, 291-313.

Bartenstein,P.A., Duncan,J.S., Prevett,M.C., Cunningham,V.J., Fish,D.R., Jones,A.K., Luthra,S.K., Sawle,G.V., Brooks,D.J., 1993. Investigation of the opioid system in absence seizures with positron emission tomography. *J Neurol Neurosurg Psychiatry* 56, 1295-1302.

Baslow,M., Suckow,R., Gaynor,K., Bhakoo,K., Marks,N., Saito,M., Saito,M., Duff,K., Matsuoka,Y., Berg,M., 2003. Brain damage results in down-regulation of N-acetylaspartate as a neuronal osmolyte. *Neuromolecular Med* 3, 95-104.

Baslow,M.H., 2000. Functions of N-acetyl-L-aspartate and N-acetyl-L-aspartylglutamate in the vertebrate brain: role in glial cell-specific signaling. *J Neurochem* 75, 453-459.

Baslow,M.H., 2002. Evidence supporting a role for N-acetyl-L-aspartate as a molecular water pump in myelinated neurons in the central nervous system. An analytical review. *Neurochem Int* 40, 295-300.

Baslow,M.H., 2003a. Brain N-acetylaspartate as a molecular water pump and its role in the etiology of Canavan disease: a mechanistic explanation. *J Mol Neurosci* 21, 185-190.

Baslow,M.H., 2003b. N-acetylaspartate in the vertebrate brain: metabolism and function. *Neurochem Res* 28, 941-953.

Baslow,M.H., 2008. The astrocyte surface NAAG receptor and NAAG peptidase signaling complex as a therapeutic target. *Drug News Perspect* 21, 251-257.

Baslow,M.H., 2009. A novel key-lock mechanism for inactivating amino acid neurotransmitters during transit across extracellular space. *Amino Acids*.

Baslow,M.H., Guilfoyle,D.N., 2007. Using proton magnetic resonance imaging and spectroscopy to understand brain "activation". *Brain Lang* 102, 153-164.

Baslow,M.H., Guilfoyle,D.N., 2009. Are astrocytes the missing link between lack of brain aspartoacylase activity and the spongiform leukodystrophy in Canavan disease? *Neurochem Res* 34, 1523-1534.

Baslow,M.H., Hrabe,J., Guilfoyle,D.N., 2007. Dynamic relationship between neurostimulation and N-acetylaspartate metabolism in the human visual cortex: evidence that NAA functions as a molecular water pump during visual stimulation. *J Mol Neurosci* 32, 235-245.

Baslow,M.H., Resnik,T.R., 1997. Canavan disease. Analysis of the nature of the metabolic lesions responsible for development of the observed clinical symptoms. *J Mol Neurosci* 9, 109-125.

Bates,T.E., Strangward,M., Keelan,J., Davey,G.P., Munro,P.M., Clark,J.B., 1996. Inhibition of N-acetylaspartate production: implications for 1H MRS studies in vivo. *Neuroreport* 7, 1397-1400.

Baulac,M., De,G.N., Hasboun,D., Oppenheim,C., Adam,C., Arzimanoglou,A., Semah,F., Lehericy,S., Clemenceau,S., Berger,B., 1998. Hippocampal developmental changes in patients with partial epilepsy: magnetic resonance imaging and clinical aspects. *Ann Neurol* 44, 223-233.

Behar,K.L., Rothman,D.L., Spencer,D.D., Petroff,O.A., 1994. Analysis of macromolecule resonances in 1H NMR spectra of human brain. *Magn Reson Med* 32, 294-302.

Ben Ari,Y., 2001. Developing networks play a similar melody. *Trends Neurosci* 24, 353-360.

Ben Ari,Y., 2002. Excitatory actions of gaba during development: the nature of the nurture. *Nat Rev Neurosci* 3, 728-739.

Ben Ari,Y., Holmes,G.L., 2005. The multiple facets of gamma-aminobutyric acid dysfunction in epilepsy. *Curr Opin Neurol* 18, 141-145.

Ben Ari,Y., Khalilov,I., Represa,A., Gozlan,H., 2004. Interneurons set the tune of developing networks. *Trends Neurosci* 27, 422-427.

Ben-Ari,Y., 2006. Seizures beget seizures: the quest for GABA as a key player. *Crit Rev Neurobiol* 18, 135-144.

Benardete,E.A., Kriegstein,A.R., 2002. Increased excitability and decreased sensitivity to GABA in an animal model of dysplastic cortex. *Epilepsia* 43, 970-982.

Bernasconi,A., Tasch,E., Cendes,F., Li,L.M., Arnold,D.L., 2002. Proton magnetic resonance spectroscopic imaging suggests progressive neuronal damage in human temporal lobe epilepsy. *Prog Brain Res* 135, 297-304.

Berridge,M.J., Downes,C.P., Hanley,M.R., 1982. Lithium amplifies agonist-dependent phosphatidylinositol responses in brain and salivary glands. *Biochem J* 206, 587-595.

Berridge,M.J., Downes,C.P., Hanley,M.R., 1989. Neural and developmental actions of lithium: a unifying hypothesis. *Cell* 59, 411-419.

Berridge,M.J., Irvine,R.F., 1989. Inositol phosphates and cell signalling. *Nature* 341, 197-205.

Bessman,S.P., Geiger,P.J., 1981. Transport of energy in muscle: the phosphorylcreatine shuttle. *Science* 211, 448-452.

Betting,L.E., Mory,S.B., Li,L.M., Lopes-Cendes,I., Guerreiro,M.M., Guerreiro,C.A., Cendes,F., 2006. Voxel-based morphometry in patients with idiopathic generalized epilepsies. *Neuroimage* 32, 498-502.

Bhakoo,K.K., Craig,T.J., Styles,P., 2001. Developmental and regional distribution of aspartoacylase in rat brain tissue. *J Neurochem* 79, 211-220.

Bianchi,M.C., Sgandurra,G., Tosetti,M., Battini,R., Cioni,G., 2007. Brain magnetic resonance in the diagnostic evaluation of mitochondrial encephalopathies. *Biosci Rep* 27, 69-85.

Biden,T.J., Wollheim,C.B., 1986. Active transport of myo-inositol in rat pancreatic islets. *Biochem J* 236, 889-893.

Bland JM, Altman DG, 1986. Statistical methods for assessing agreement between two methods of clinical measurement. *Lancet* February 8, 307-311.

Blumenfeld,H., 2005. Cellular and network mechanisms of spike-wave seizures. *Epilepsia* 46 Suppl 9, 21-33.

Bottomley,P.A., 1987. Spatial localization in NMR spectroscopy in vivo. *Ann N Y Acad Sci* 508, 333-348.

Bottomley,P.A., Charles,H.C., Roemer,P.B., Flamig,D., Engeseth,H., Edelstein,W.A., Mueller,O.M., 1988. Human in vivo phosphate metabolite imaging with ³¹P NMR. *Magn Reson Med* 7, 319-336.

Brand,A., Richter-Landsberg,C., Leibfritz,D., 1993. Multinuclear NMR studies on the energy metabolism of glial and neuronal cells. *Dev Neurosci* 15, 289-298.

Briellmann,R.S., Berkovic,S.F., Syngeniotis,A., King,M.A., Jackson,G.D., 2002. Seizure-associated hippocampal volume loss: a longitudinal magnetic resonance study of temporal lobe epilepsy. *Ann Neurol* 51, 641-644.

Briellmann,R.S., Wellard,R.M., Jackson,G.D., 2005. Seizure-associated abnormalities in epilepsy: evidence from MR imaging. *Epilepsia* 46, 760-766.

Brose,N., Rosenmund,C., 2002. Move over protein kinase C, you've got company: alternative cellular effectors of diacylglycerol and phorbol esters. *J Cell Sci* 115, 4399-4411.

Brustovetsky,N., Brustovetsky,T., Dubinsky,J.M., 2001. On the mechanisms of neuroprotection by creatine and phosphocreatine. *J Neurochem* 76, 425-434.

Burneo,J.G., Knowlton,R.C., Faught,E., Martin,R., Sawrie,S., Kuzniecky,R.I., 2004. Chronic temporal lobe epilepsy: spatial extent and degree of metabolic dysfunction studied with magnetic resonance spectroscopy (MRS). *Epilepsy Res* 62, 119-124.

Buzsaki,G., 1991. The thalamic clock: emergent network properties. *Neuroscience* 41, 351-364.

Calcagnotto,M.E., Paredes,M.F., Baraban,S.C., 2002. Heterotopic neurons with altered inhibitory synaptic function in an animal model of malformation-associated epilepsy. *J Neurosci* 22, 7596-7605.

Cavus,I., Kasoff,W.S., Cassaday,M.P., Jacob,R., Gueorguieva,R., Sherwin,R.S., Krystal,J.H., Spencer,D.D., bi-Saab,W.M., 2005. Extracellular metabolites in the cortex and hippocampus of epileptic patients. *Ann Neurol* 57, 226-235.

Cendes,F., 2004. Febrile seizures and mesial temporal sclerosis. *Curr Opin Neurol* 17, 161-164.

Cendes,F., Andermann,F., Dubeau,F., Arnold,D.L., 1995. Proton magnetic resonance spectroscopic images and MRI volumetric studies for lateralization of temporal lobe epilepsy. *Magn Reson Imaging* 13, 1187-1191.

- Cendes,F., Andermann,F., Dubeau,F., Matthews,P.M., Arnold,D.L., 1997a. Normalization of neuronal metabolic dysfunction after surgery for temporal lobe epilepsy. Evidence from proton MR spectroscopic imaging. *Neurology* 49, 1525-1533.
- Cendes,F., Andermann,F., Gloor,P., Evans,A., Jones-Gotman,M., Watson,C., Melanson,D., Olivier,A., Peters,T., Lopes-Cendes,I., ., 1993. MRI volumetric measurement of amygdala and hippocampus in temporal lobe epilepsy. *Neurology* 43, 719-725.
- Cendes,F., Andermann,F., Preul,M.C., Arnold,D.L., 1994. Lateralization of temporal lobe epilepsy based on regional metabolic abnormalities in proton magnetic resonance spectroscopic images. *Ann Neurol* 35, 211-216.
- Cendes,F., Caramanos,Z., Andermann,F., Dubeau,F., Arnold,D.L., 1997b. Proton magnetic resonance spectroscopic imaging and magnetic resonance imaging volumetry in the lateralization of temporal lobe epilepsy: a series of 100 patients. *Ann Neurol* 42, 737-746.
- Cendes,F., Stanley,J.A., Dubeau,F., Andermann,F., Arnold,D.L., 1997c. Proton magnetic resonance spectroscopic imaging for discrimination of absence and complex partial seizures. *Ann Neurol* 41, 74-81.
- Chan,C.H., Briellmann,R.S., Pell,G.S., Scheffer,I.E., Abbott,D.F., Jackson,G.D., 2006. Thalamic atrophy in childhood absence epilepsy. *Epilepsia* 47, 399-405.
- Chapman,A.G., Meldrum,B.S., Siesjo,B.K., 1977. Cerebral metabolic changes during prolonged epileptic seizures in rats. *J Neurochem* 28, 1025-1035.
- Chen,Y., Lu,J., Pan,H., Zhang,Y., Wu,H., Xu,K., Liu,X., Jiang,Y., Bao,X., Yao,Z., Ding,K., Lo,W.H., Qiang,B., Chan,P., Shen,Y., Wu,X., 2003. Association between genetic variation of CACNA1H and childhood absence epilepsy. *Ann Neurol* 54, 239-243.
- Chih,C.P., Lipton,P., Roberts,E.L., Jr., 2001. Do active cerebral neurons really use lactate rather than glucose? *Trends Neurosci* 24, 573-578.
- Chu,W.J., Hetherington,H.P., Kuzniecky,R.I., Simor,T., Mason,G.F., Elgavish,G.A., 1998. Lateralization of human temporal lobe epilepsy by ³¹P NMR spectroscopic imaging at 4.1 T. *Neurology* 51, 472-479.
- Chu,W.J., Hetherington,H.P., Kuzniecky,R.J., Vaughan,J.T., Twieg,D.B., Faught,R.E., Gilliam,F.G., Hugg,J.W., Elgavish,G.A., 1996. Is the intracellular pH different from normal in the epileptic focus of patients with temporal lobe epilepsy? A ³¹P NMR study. *Neurology* 47, 756-760.

Chu,W.J., Kuzniecky,R.I., Hugg,J.W., Abou-Khalil,B., Gilliam,F., Faught,E., Hetherington,H.P., 2000. Statistically driven identification of focal metabolic abnormalities in temporal lobe epilepsy with corrections for tissue heterogeneity using 1H spectroscopic imaging. *Magn Reson Med* 43, 359-367.

Cohen,A.S., Lin,D.D., Quirk,G.L., Coulter,D.A., 2003. Dentate granule cell GABA(A) receptors in epileptic hippocampus: enhanced synaptic efficacy and altered pharmacology. *Eur J Neurosci* 17, 1607-1616.

Cohen-Gadol,A.A., Pan,J.W., Kim,J.H., Spencer,D.D., Hetherington,H.H., 2004. Mesial temporal lobe epilepsy: a proton magnetic resonance spectroscopy study and a histopathological analysis. *J Neurosurg* 101, 613-620.

Collingridge,G.L., Lester,R.A., 1989. Excitatory amino acid receptors in the vertebrate central nervous system. *Pharmacol Rev* 41, 143-210.

Connelly,A., Jackson,G.D., Duncan,J.S., King,M.D., Gadian,D.G., 1994. Magnetic resonance spectroscopy in temporal lobe epilepsy. *Neurology* 44, 1411-1417.

Connelly,A., Van Paesschen,W., Porter,D.A., Johnson,C.L., Duncan,J.S., Gadian,D.G., 1998. Proton magnetic resonance spectroscopy in MRI-negative temporal lobe epilepsy. *Neurology* 51, 61-66.

Constantinidis,I., Malko,J.A., Peterman,S.B., Long,R.C., Jr., Epstein,C.M., Boor,D., Hoffman,J.C., Jr., Shutter,L., Weissman,J.D., 1996. Evaluation of 1H magnetic resonance spectroscopic imaging as a diagnostic tool for the lateralization of epileptogenic seizure foci. *Br J Radiol* 69, 15-24.

Cook,M.J., Fish,D.R., Shorvon,S.D., Straughan,K., Stevens,J.M., 1992. Hippocampal volumetric and morphometric studies in frontal and temporal lobe epilepsy. *Brain* 115 (Pt 4), 1001-1015.

Cossart,R., Bernard,C., Ben Ari,Y., 2005. Multiple facets of GABAergic neurons and synapses: multiple fates of GABA signalling in epilepsies. *Trends Neurosci* 28, 108-115.

Cossette,P., Liu,L., Brisebois,K., Dong,H., Lortie,A., Vanasse,M., Saint-Hilaire,J.M., Carmant,L., Verner,A., Lu,W.Y., Wang,Y.T., Rouleau,G.A., 2002. Mutation of GABRA1 in an autosomal dominant form of juvenile myoclonic epilepsy. *Nat Genet* 31, 184-189.

Cross,J.H., Connelly,A., Jackson,G.D., Johnson,C.L., Neville,B.G., Gadian,D.G., 1996. Proton magnetic resonance spectroscopy in children with temporal lobe epilepsy. *Ann Neurol* 39, 107-113.

Cross,J.H., Gordon,I., Connelly,A., Jackson,G.D., Johnson,C.L., Neville,B.G., Gadian,D.G., 1997. Interictal ⁹⁹Tc(m) HMPAO SPECT and ¹H MRS in children with temporal lobe epilepsy. *Epilepsia* 38, 338-345.

Davanzo,P., Thomas,M.A., Yue,K., Oshiro,T., Belin,T., Strober,M., McCracken,J., 2001. Decreased anterior cingulate myo-inositol/creatine spectroscopy resonance with lithium treatment in children with bipolar disorder. *Neuropsychopharmacology* 24, 359-369.

Dawson,V.L., Dawson,T.M., 1996. Nitric oxide in neuronal degeneration. *Proc Soc Exp Biol Med* 211, 33-40.

de Barry J., Vincendon,G., Gombos,G., 1983. Uptake and metabolism of L-[³H]glutamate and L-[³H]glutamine in adult rat cerebellar slices. *Neurochem Res* 8, 1321-1335.

De Keyser J., Mostert,J.P., Koch,M.W., 2008. Dysfunctional astrocytes as key players in the pathogenesis of central nervous system disorders. *J Neurol Sci* 267, 3-16.

de Kovel,C.G., Trucks,H., Helbig,I., Mefford,H.C., Baker,C., Leu,C., Kluck,C., Muhle,H., von,S.S., Ostertag,P., Obermeier,T., Kleefuss-Lie,A.A., Hallmann,K., Steffens,M., Gaus,V., Klein,K.M., Hamer,H.M., Rosenow,F., Brilstra,E.H., Trenite,D.K., Swinkels,M.E., Weber,Y.G., Unterberger,I., Zimprich,F., Urak,L., Feucht,M., Fuchs,K., Moller,R.S., Hjalgrim,H., De,J.P., Suls,A., Ruckert,I.M., Wichmann,H.E., Franke,A., Schreiber,S., Nurnberg,P., Elger,C.E., Lerche,H., Stephani,U., Koeleman,B.P., Lindhout,D., Eichler,E.E., Sander,T., 2010. Recurrent microdeletions at 15q11.2 and 16p13.11 predispose to idiopathic generalized epilepsies. *Brain* 133, 23-32.

Delanty,N., Dichter,M.A., 1998. Oxidative injury in the nervous system. *Acta Neurol Scand* 98, 145-153.

Dibbens,L.M., Mullen,S., Helbig,I., Mefford,H.C., Bayly,M.A., Bellows,S., Leu,C., Trucks,H., Obermeier,T., Wittig,M., Franke,A., Caglayan,H., Yapici,Z., Sander,T., Eichler,E.E., Scheffer,I.E., Mulley,J.C., Berkovic,S.F., 2009. Familial and sporadic 15q13.3 microdeletions in idiopathic generalized epilepsy: precedent for disorders with complex inheritance. *Hum Mol Genet* 18, 3626-3631.

Dienel,G.A., Hertz,L., 2001. Glucose and lactate metabolism during brain activation. *J Neurosci Res* 66, 824-838.

Ding,D., Greenberg,M.L., 2003. Lithium and valproate decrease the membrane phosphatidylinositol/phosphatidylcholine ratio. *Mol Microbiol* 47, 373-381.

Doyle, T.J., Bedell, B.J., Narayana, P.A., 1995. Relative concentrations of proton MR visible neurochemicals in gray and white matter in human brain. *Magn Reson Med* 33, 755-759.

Dube, C.M., Brewster, A.L., Baram, T.Z., 2009. Febrile seizures: mechanisms and relationship to epilepsy. *Brain Dev* 31, 366-371.

Dubeau, F., Palmieri, A., Fish, D., Avoli, M., Gambardella, A., Spreafico, R., Andermann, F., 1998. The significance of electrocorticographic findings in focal cortical dysplasia: a review of their clinical, electrophysiological and neurochemical characteristics. *Electroencephalogr Clin Neurophysiol Suppl* 48, 77-96.

Dubeau, F., Sherwin, A., Olivier, A., Villemure, J., Leblanc, R., Quesney, L.F., Andermann, E., Andermann, F., 1992. Excitatory amino acids modulate phosphoinositide signal transduction in human epileptic neocortex. *Epilepsia*.

Duc, C.O., Trabesinger, A.H., Weber, O.M., Meier, D., Walder, M., Wieser, H.G., Boesiger, P., 1998. Quantitative ¹H MRS in the evaluation of mesial temporal lobe epilepsy in vivo. *Magn Reson Imaging* 16, 969-979.

Duffy, T.E., Howse, D.C., Plum, F., 1975. Cerebral energy metabolism during experimental status epilepticus. *J Neurochem* 24, 925-934.

Duncan, J.S., 1996. Magnetic resonance spectroscopy. *Epilepsia* 37, 598-605.

Duncan, J.S., 1997. Imaging and epilepsy. *Brain* 120 (Pt 2), 339-377.

Duncan, J.S., 2005. Brain imaging in idiopathic generalized epilepsies. *Epilepsia* 46 Suppl 9, 108-111.

Duncan, J.S., Bartlett, P., Barker, G.J., 1996. Technique for measuring hippocampal T2 relaxation time. *AJNR Am J Neuroradiol* 17, 1805-1810.

During, M.J., Spencer, D.D., 1993. Extracellular hippocampal glutamate and spontaneous seizure in the conscious human brain. *Lancet* 341, 1607-1610.

Eberhardt, K.E., Stefan, H., Buchfelder, M., Pauli, E., Hopp, P., Huk, W., Tomandl, B.F., 2000. The significance of bilateral CSI changes for the postoperative outcome in temporal lobe epilepsy. *J Comput Assist Tomogr* 24, 919-926.

Eberhardt, K.E., Stefan, H., Grabenbauer, G.G., Schafer, I., Tomandl, B., Huk, W.J., Kreisler, P., Kaferlein, M., 1999. Chemical shift imaging spectroscopy findings before and after stereotactic radiotherapy in temporal lobe epilepsy. *Adv Neurol* 81, 339-345.

Elmslie,F.V., Rees,M., Williamson,M.P., Kerr,M., Kjeldsen,M.J., Pang,K.A., Sundqvist,A., Friis,M.L., Chadwick,D., Richens,A., Covanis,A., Santos,M., Arzimanoglou,A., Panayiotopoulos,C.P., Curtis,D., Whitehouse,W.P., Gardiner,R.M., 1997. Genetic mapping of a major susceptibility locus for juvenile myoclonic epilepsy on chromosome 15q. *Hum Mol Genet* 6, 1329-1334.

Emery,J.A., Roper,S.N., Rojiani,A.M., 1997. White matter neuronal heterotopia in temporal lobe epilepsy: a morphometric and immunohistochemical study. *J Neuropathol Exp Neurol* 56, 1276-1282.

Ende,G.R., Laxer,K.D., Knowlton,R.C., Matson,G.B., Schuff,N., Fein,G., Weiner,M.W., 1997. Temporal lobe epilepsy: bilateral hippocampal metabolite changes revealed at proton MR spectroscopic imaging. *Radiology* 202, 809-817.

Engel,J., Jr., 2001. A proposed diagnostic scheme for people with epileptic seizures and with epilepsy: report of the ILAE Task Force on Classification and Terminology. *Epilepsia* 42, 796-803.

Engel,J., Jr., 2006. ILAE classification of epilepsy syndromes. *Epilepsy Res* 70 Suppl 1, S5-10.

Ercinska,M., Silver,I.A., 1987. Energy relationships between ATP synthesis and K⁺ gradients in cultured glial-derived cell line. *Acta Biochim Pol* 34, 195-203.

Ercinska,M., Silver,I.A., 1990. Metabolism and role of glutamate in mammalian brain. *Prog Neurobiol* 35, 245-296.

Eriksson,S.H., Rugg-Gunn,F.J., Symms,M.R., Barker,G.J., Duncan,J.S., 2001. Diffusion tensor imaging in patients with epilepsy and malformations of cortical development. *Brain* 124, 617-626.

Falconer,M., Serafetinides,E., Corsellis,JA., 1964. Etiology and pathogenesis of temporal lobe epilepsy. *Arch Neurol* 10, 233-248.

Fazekas,F., Kapeller,P., Schmidt,R., Stollberger,R., Varosanec,S., Offenbacher,H., Fazekas,G., Lechner,H., 1995. Magnetic resonance imaging and spectroscopy findings after focal status epilepticus. *Epilepsia* 36, 946-949.

Fedosov,S.N., 1994. Creatine-creatine phosphate shuttle modeled as two-compartment system at different levels of creatine kinase activity. *Biochim Biophys Acta* 1208, 238-246.

Fernandez,G., Effenberger,O., Vinz,B., Steinlein,O., Elger,C.E., Dohring,W., Heinze,H.J., 1998. Hippocampal malformation as a cause of familial febrile convulsions and subsequent hippocampal sclerosis. *Neurology* 50, 909-917.

Fisher,R.S., Harding,G., Erba,G., Barkley,G.L., Wilkins,A., 2005. Photic- and pattern-induced seizures: a review for the Epilepsy Foundation of America Working Group. *Epilepsia* 46, 1426-1441.

Flott,B., Seifert,W., 1991. Characterization of glutamate uptake systems in astrocyte primary cultures from rat brain. *Glia* 4, 293-304.

Flugel,D., McLean,M.A., Simister,R.J., Duncan,J.S., 2006. Magnetisation transfer ratio of choline is reduced following epileptic seizures. *NMR Biomed* 19, 217-222.

Fonnum,F., 1984. Glutamate: a neurotransmitter in mammalian brain. *J Neurochem* 42, 1-11.

Fox,P.T., Raichle,M.E., 1986. Focal physiological uncoupling of cerebral blood flow and oxidative metabolism during somatosensory stimulation in human subjects. *Proc Natl Acad Sci U S A* 83, 1140-1144.

Frahm,J., Bruhn,H., Gyngell,M.L., Merboldt,K.D., Hanicke,W., Sauter,R., 1989. Localized high-resolution proton NMR spectroscopy using stimulated echoes: initial applications to human brain in vivo. *Magn Reson Med* 9, 79-93.

Free,S.L., Bergin,P.S., Fish,D.R., Cook,M.J., Shorvon,S.D., Stevens,J.M., 1995. Methods for normalization of hippocampal volumes measured with MR. *AJNR Am J Neuroradiol* 16, 637-643.

Fridovich,I., 1997. Superoxide anion radical (O₂⁻), superoxide dismutases, and related matters. *J Biol Chem* 272, 18515-18517.

Friedman,D.L., Roberts,R., 1994. Compartmentation of brain-type creatine kinase and ubiquitous mitochondrial creatine kinase in neurons: evidence for a creatine phosphate energy shuttle in adult rat brain. *J Comp Neurol* 343, 500-511.

Fuerst,D., Shah,J., Shah,A., Watson,C., 2003. Hippocampal sclerosis is a progressive disorder: a longitudinal volumetric MRI study. *Ann Neurol* 53, 413-416.

Fujiwara-Tsukamoto,Y., Isomura,Y., Nambu,A., Takada,M., 2003. Excitatory GABA input directly drives seizure-like rhythmic synchronization in mature hippocampal CA1 pyramidal cells. *Neuroscience* 119, 265-275.

Gadian,D.G., Connelly,A., Duncan,J.S., Cross,J.H., Kirkham,F.J., Johnson,C.L., Vargha-Khadem,F., Nevile,B.G., Jackson,G.D., 1994. 1H magnetic resonance spectroscopy in the investigation of intractable epilepsy. *Acta Neurol Scand Suppl* 152, 116-121.

- Garcia,M., Huppertz,H.J., Ziyeh,S., Buechert,M., Schumacher,M., Mader,I., 2009. Valproate-induced metabolic changes in patients with epilepsy: assessment with H-MRS. *Epilepsia* 50, 486-492.
- Garcia,P.A., Laxer,K.D., van der,G.J., Hugg,J.W., Matson,G.B., Weiner,M.W., 1997. Correlation of seizure frequency with N-acetyl-aspartate levels determined by ¹H magnetic resonance spectroscopic imaging. *Magn Reson Imaging* 15, 475-478.
- Gasull,T., DeGregorio-Rocasolano,N., Enguita,M., Hurtan,J.M., Trullas,R., 2002. Inhibition of phosphatidylcholine synthesis is associated with excitotoxic cell death in cerebellar granule cell cultures. *Amino Acids* 23, 19-25.
- Gasull,T., Sarri,E., DeGregorio-Rocasolano,N., Trullas,R., 2003. NMDA receptor overactivation inhibits phospholipid synthesis by decreasing choline-ethanolamine phosphotransferase activity. *J Neurosci* 23, 4100-4107.
- Gegelashvili,G., Schousboe,A., 1998. Cellular distribution and kinetic properties of high-affinity glutamate transporters. *Brain Res Bull* 45, 233-238.
- Girard,N., Fogliarini,C., Viola,A., Confort-Gouny,S., Fur,Y.L., Viout,P., Chapon,F., Levrier,O., Cozzone,P., 2006a. MRS of normal and impaired fetal brain development. *Eur J Radiol* 57, 217-225.
- Girard,N., Gouny,S.C., Viola,A., Le,F.Y., Viout,P., Chaumoitre,K., D'Ercole,C., Gire,C., Figarella-Branger,D., Cozzone,P.J., 2006b. Assessment of normal fetal brain maturation in utero by proton magnetic resonance spectroscopy. *Magn Reson Med* 56, 768-775.
- Gjessing,L.R., Gjesdahl,P., Sjaastad,O., 1972. The free amino acids in human cerebrospinal fluid. *J Neurochem* 19, 1807-1808.
- Gloor,P., 1968. Generalized cortico-reticular epilepsies. Some considerations on the pathophysiology of generalized bilaterally synchronous spike and wave discharge. *Epilepsia* 9, 249-263.
- Gotz,M.E., Kunig,G., Riederer,P., Youdim,M.B., 1994. Oxidative stress: free radical production in neural degeneration. *Pharmacol Ther* 63, 37-122.
- Govindaraju,V., Young,K., Maudsley,A.A., 2000. Proton NMR chemical shifts and coupling constants for brain metabolites. *NMR Biomed* 13, 129-153.
- Gruetter,R., 2002. In vivo ¹³C NMR studies of compartmentalized cerebral carbohydrate metabolism. *Neurochem Int* 41, 143-154.

Gruetter,R., Seaquist,E.R., Kim,S., Ugurbil,K., 1998a. Localized in vivo ¹³C-NMR of glutamate metabolism in the human brain: initial results at 4 tesla. *Dev Neurosci* 20, 380-388.

Gruetter,R., Weisdorf,S.A., Rajanayagan,V., Terpstra,M., Merkle,H., Truwit,C.L., Garwood,M., Nyberg,S.L., Ugurbil,K., 1998b. Resolution improvements in in vivo ¹H NMR spectra with increased magnetic field strength. *J Magn Reson* 135, 260-264.

Guerrini,R., Dravet,C., Genton,P., Bureau,M., Bonanni,P., Ferrari,A.R., Roger,J., 1995. Idiopathic photosensitive occipital lobe epilepsy. *Epilepsia* 36, 883-891.

Hamandi,K., Laufs,H., Noth,U., Carmichael,D.W., Duncan,J.S., Lemieux,L., 2008. BOLD and perfusion changes during epileptic generalised spike wave activity. *Neuroimage* 39, 608-618.

Hamandi,K., Salek-Haddadi,A., Laufs,H., Liston,A., Friston,K., Fish,D.R., Duncan,J.S., Lemieux,L., 2006. EEG-fMRI of idiopathic and secondarily generalized epilepsies. *Neuroimage* 31, 1700-1710.

Hamberger,A., Nystrom,B., 1984. Extra- and intracellular amino acids in the hippocampus during development of hepatic encephalopathy. *Neurochem Res* 9, 1181-1192.

Hammen,T., Hildebrandt M, Stadlbauer,A., Doelken,M., Engelhorn,T., Kerling,F., Kasper,B., Romstoek J, Ganslandt,O., Nimsky,C., Blumcke,I., Doerfler,A., Stefan,H., 2008. Non-invasive detection of hippocampal sclerosis: correlation between metabolite alterations detected by (¹H)-MRS and neuropathology. *NMR Biomed* 21, 545-552.

Hammen,T., Kerling,F., Schwarz,M., Stadlbauer,A., Ganslandt,O., Keck,B., Tomandl,B., Dorfler,A., Stefan,H., 2006. Identifying the affected hemisphere by (¹H)-MR spectroscopy in patients with temporal lobe epilepsy and no pathological findings in high resolution MRI. *Eur J Neurol* 13, 482-490.

Hammers,A., Koepp,M.J., Richardson,M.P., Labbe,C., Brooks,D.J., Cunningham,V.J., Duncan,J.S., 2001. Central benzodiazepine receptors in malformations of cortical development: A quantitative study. *Brain* 124, 1555-1565.

Hammond,G.R., Schiavo,G., 2007. Polyphosphoinositol lipids: under-PPIning synaptic function in health and disease. *Dev Neurobiol* 67, 1232-1247.

Hashemi,M., Buibas,M., Silva,G.A., 2008. Automated detection of intercellular signaling in astrocyte networks using the converging squares algorithm. *J Neurosci Methods* 170, 294-299.

Headley,P.M., Grillner,S., 1990. Excitatory amino acids and synaptic transmission: the evidence for a physiological function. *Trends Pharmacol Sci* 11, 205-211.

Heales,S.J., Davies,S.E., Bates,T.E., Clark,J.B., 1995. Depletion of brain glutathione is accompanied by impaired mitochondrial function and decreased N-acetyl aspartate concentration. *Neurochem Res* 20, 31-38.

Helbig,I., Mefford,H.C., Sharp,A.J., Guipponi,M., Fichera,M., Franke,A., Muhle,H., de,K.C., Baker,C., von,S.S., Kron,K.L., Steinich,I., Kleefuss-Lie,A.A., Leu,C., Gaus,V., Schmitz,B., Klein,K.M., Reif,P.S., Rosenow,F., Weber,Y., Lerche,H., Zimprich,F., Urak,L., Fuchs,K., Feucht,M., Genton,P., Thomas,P., Visscher,F., de Haan,G.J., Moller,R.S., Hjalgrim,H., Luciano,D., Wittig,M., Nothnagel,M., Elger,C.E., Nurnberg,P., Romano,C., Malafosse,A., Koeleman,B.P., Lindhout,D., Stephani,U., Schreiber,S., Eichler,E.E., Sander,T., 2009. 15q13.3 microdeletions increase risk of idiopathic generalized epilepsy. *Nat Genet* 41, 160-162.

Helbig,I., Scheffer,I.E., Mulley,J.C., Berkovic,S.F., 2008. Navigating the channels and beyond: unravelling the genetics of the epilepsies. *Lancet Neurol* 7, 231-245.

Helms,G., Ciumas,C., Kyaga,S., Savic,I., 2006. Increased thalamus levels of glutamate and glutamine (Glx) in patients with idiopathic generalised epilepsy. *J Neurol Neurosurg Psychiatry* 77, 489-494.

Henry,T.R., Theodore,W.H., 2001. Homocarnosine elevations: a cause or a sign of seizure control? *Neurology* 56, 698-699.

Heron,S.E., Khosravani,H., Varela,D., Bladen,C., Williams,T.C., Newman,M.R., Scheffer,I.E., Berkovic,S.F., Mulley,J.C., Zamponi,G.W., 2007. Extended spectrum of idiopathic generalized epilepsies associated with CACNA1H functional variants. *Ann Neurol* 62, 560-568.

Hertz,L., 2004. The astrocyte-neuron lactate shuttle: a challenge of a challenge. *J Cereb Blood Flow Metab* 24, 1241-1248.

Hertz,L., Hertz,E., 2003. Cataplerotic TCA cycle flux determined as glutamate-sustained oxygen consumption in primary cultures of astrocytes. *Neurochem Int* 43, 355-361.

Hetherington,H., Kuzniecky,R., Pan,J., Mason,G., Morawetz,R., Harris,C., Faught,E., Vaughan,T., Pohost,G., 1995a. Proton nuclear magnetic resonance spectroscopic imaging of human temporal lobe epilepsy at 4.1 T. *Ann Neurol* 38, 396-404.

Hetherington, H., Pan, J., Mason, G., Adams D., Vaughn MJ, Twieg, D. B., and Pohost, G. M. Quantitative proton spectroscopic imaging of human brain at 4.1T using image segmentation. *Magn Reson Med* 36, 21-29. 1996.

Hetherington,H.P., Chu,W.J., Gonen,O., Pan,J.W., 2006. Robust fully automated shimming of the human brain for high-field 1H spectroscopic imaging. *Magn Reson Med* 56, 26-33.

Hetherington,H.P., Kuzniecky,R.I., Pan,J.W., Vaughan,J.T., Twieg,D.B., Pohost,G.M., 1995b. Application of high field spectroscopic imaging in the evaluation of temporal lobe epilepsy. *Magn Reson Imaging* 13, 1175-1180.

Hetherington,H.P., Kuzniecky,R.I., Vives,K., Devinsky,O., Pacia,S., Luciano,D., Vasquez,B., Haut,S., Spencer,D.D., Pan,J.W., 2007. A subcortical network of dysfunction in TLE measured by magnetic resonance spectroscopy. *Neurology* 69, 2256-2265.

Hetherington,H.P., Pan,J.W., Spencer,D.D., 2002. 1H and 31P spectroscopy and bioenergetics in the lateralization of seizures in temporal lobe epilepsy. *J Magn Reson Imaging* 16, 477-483.

Hetherington,H.P., Spencer,D.D., Vaughan,J.T., Pan,J.W., 2001. Quantitative (31)P spectroscopic imaging of human brain at 4 Tesla: assessment of gray and white matter differences of phosphocreatine and ATP. *Magn Reson Med* 45, 46-52.

Hilberman,M., Subramanian,V.H., Haselgrove,J., Cone,J.B., Egan,J.W., Gyulai,L., Chance,B., 1984. In vivo time-resolved brain phosphorus nuclear magnetic resonance. *J Cereb Blood Flow Metab* 4, 334-342.

Hirose,S., Mitsudome,A., Okada,M., Kaneko,S., 2005. Genetics of idiopathic epilepsies. *Epilepsia* 46 Suppl 1, 38-43.

Hommet,C., Sauerwein,H.C., De,T.B., Lassonde,M., 2006. Idiopathic epileptic syndromes and cognition. *Neurosci Biobehav Rev* 30, 85-96.

Huang,C.C., Chang,Y.C., 2009. The long-term effects of febrile seizures on the hippocampal neuronal plasticity - clinical and experimental evidence. *Brain Dev* 31, 383-387.

Hugg,J.W., Kuzniecky,R.I., Gilliam,F.G., Morawetz,R.B., Fraught,R.E., Hetherington,H.P., 1996. Normalization of contralateral metabolic function following temporal lobectomy demonstrated by 1H magnetic resonance spectroscopic imaging. *Ann Neurol* 40, 236-239.

Hugg,J.W., Laxer,K.D., Matson,G.B., Maudsley,A.A., Weiner,M.W., 1993. Neuron loss localizes human temporal lobe epilepsy by in vivo proton magnetic resonance spectroscopic imaging. *Ann Neurol* 34, 788-794.

Huijin, H, Tianzhen, S, and Xingrong, C. Comparison of MRI, MRS, PET and EEG in the diagnosis of temporal lobe epilepsy. *Chin.Med.J* 114, 70-79. 2001.

Husted,C.A., Goodin,D.S., Hugg,J.W., Maudsley,A.A., Tsuruda,J.S., de Bie,S.H., Fein,G., Matson,G.B., Weiner,M.W., 1994. Biochemical alterations in multiple sclerosis lesions and normal-appearing white matter detected by in vivo ³¹P and ¹H spectroscopic imaging. *Ann Neurol* 36, 157-165.

Ibsen,L., Strange,K., 1996. In situ localization and osmotic regulation of the Na(+)-myo-inositol cotransporter in rat brain. *Am J Physiol* 271, F877-F885.

ILAE Commission on Classification and Terminology. Revised terminology and concepts for organisatin of the epilepsies: Report of the Commission on Classification and Terminology. 2009. (http://www.ilae-epilepsy.org/ctf/over_frame.html)

Irvine,R.F., 2003. 20 years of Ins(1,4,5)P₃, and 40 years before. *Nat Rev Mol Cell Biol* 4, 586-590.

Jackson,G.D., Berkovic,S.F., Tress,B.M., Kalnins,R.M., Fabinyi,G.C., Bladin,P.F., 1990. Hippocampal sclerosis can be reliably detected by magnetic resonance imaging. *Neurology* 40, 1869-1875.

Jackson,G.D., Connelly,A., 1999. New NMR measurements in epilepsy. T₂ relaxometry and magnetic resonance spectroscopy. *Adv Neurol* 79, 931-937.

Jacobs,K.M., Hwang,B.J., Prince,D.A., 1999. Focal epileptogenesis in a rat model of polymicrogyria. *J Neurophysiol* 81, 159-173.

Jacobus,W.E., Lehninger,A.L., 1973. Creatine kinase of rat heart mitochondria. Coupling of creatine phosphorylation to electron transport. *J Biol Chem* 248, 4803-4810.

Jasper HH, Kershman J, 1941. Electroencephalographic classification of the epilepsies. *Arch Neurol Psychiatry* 45, 903-943.

Kaneko,S., Okada,M., Iwasa,H., Yamakawa,K., Hirose,S., 2002. Genetics of epilepsy: current status and perspectives. *Neurosci Res* 44, 11-30.

Kantarci,K., Shin,C., Britton,J.W., So,E.L., Cascino,G.D., Jack,C.R., Jr., 2002. Comparative diagnostic utility of ¹H MRS and DWI in evaluation of temporal lobe epilepsy. *Neurology* 58, 1745-1753.

- Kapoor,A., Ratnapriya,R., Kuruttukulam,G., Anand,A., 2007. A novel genetic locus for juvenile myoclonic epilepsy at chromosome 5q12-q14. *Hum Genet* 121, 655-662.
- Kauppinen,R.A., Pirttila,T.R., Auriola,S.O., Williams,S.R., 1994. Compartmentation of cerebral glutamate in situ as detected by $^1\text{H}/^{13}\text{C}$ n.m.r. *Biochem J* 298 (Pt 1), 121-127.
- Ke,Y., Cohen,B.M., Lowen,S., Hirashima,F., Nassar,L., Renshaw,P.F., 2002. Biexponential transverse relaxation ($T(2)$) of the proton MRS creatine resonance in human brain. *Magn Reson Med* 47, 232-238.
- Keevil,S.F., 2006. Spatial localization in nuclear magnetic resonance spectroscopy. *Phys Med Biol* 51, R579-R636.
- Keltner,J.R., Wald,L.L., Frederick,B.D., Renshaw,P.F., 1997. In vivo detection of GABA in human brain using a localized double-quantum filter technique. *Magn Reson Med* 37, 366-371.
- Kim,D., Song,I., Keum,S., Lee,T., Jeong,M.J., Kim,S.S., McEnery,M.W., Shin,H.S., 2001. Lack of the burst firing of thalamocortical relay neurons and resistance to absence seizures in mice lacking $\alpha(1\text{G})$ T-type $\text{Ca}(2+)$ channels. *Neuron* 31, 35-45.
- Kim,J.H., Lee,J.K., Koh,S.B., Lee,S.A., Lee,J.M., Kim,S.I., Kang,J.K., 2007. Regional grey matter abnormalities in juvenile myoclonic epilepsy: a voxel-based morphometry study. *Neuroimage* 37, 1132-1137.
- Kimelberg,H.K., Pang,S., Treble,D.H., 1989. Excitatory amino acid-stimulated uptake of $^{22}\text{Na}^+$ in primary astrocyte cultures. *J Neurosci* 9, 1141-1149.
- Kimelberg,H.K., Rutledge,E., Goderie,S., Charniga,C., 1995. Astrocytic swelling due to hypotonic or high K^+ medium causes inhibition of glutamate and aspartate uptake and increases their release. *J Cereb Blood Flow Metab* 15, 409-416.
- Knowlton,R.C., Laxer,K.D., Ende,G., Hawkins,R.A., Wong,S.T., Matson,G.B., Rowley,H.A., Fein,G., Weiner,M.W., 1997. Presurgical multimodality neuroimaging in electroencephalographic lateralized temporal lobe epilepsy. *Ann Neurol* 42, 829-837.
- Kok,R.D., van den Berg,P.P., van den Bergh,A.J., Nijland,R., Heerschap,A., 2002. Maturation of the human fetal brain as observed by ^1H MR spectroscopy. *Magn Reson Med* 48, 611-616.
- Koppenol,W.H., 1998. The basic chemistry of nitrogen monoxide and peroxy nitrite. *Free Radic Biol Med* 25, 385-391.

Kothare,S.V., VanLandingham,K., Armon,C., Luther,J.S., Friedman,A., Radtke,R.A., 1998. Seizure onset from periventricular nodular heterotopias: depth-electrode study. *Neurology* 51, 1723-1727.

Kreis,R., Ernst,T., Ross,B.D., 1993. Development of the human brain: in vivo quantification of metabolite and water content with proton magnetic resonance spectroscopy. *Magn Reson Med* 30, 424-437.

Kreis,R., Hofmann,L., Kuhlmann,B., Boesch,C., Bossi,E., Huppi,P.S., 2002. Brain metabolite composition during early human brain development as measured by quantitative in vivo ¹H magnetic resonance spectroscopy. *Magn Reson Med* 48, 949-958.

Kuks,J.B., Cook,M.J., Fish,D.R., Stevens,J.M., Shorvon,S.D., 1993. Hippocampal sclerosis in epilepsy and childhood febrile seizures. *Lancet* 342, 1391-1394.

Kullmann,D.M., Semyanov,A., 2002. Glutamatergic modulation of GABAergic signaling among hippocampal interneurons: novel mechanisms regulating hippocampal excitability. *Epilepsia* 43 Suppl 5:174-8., 174-178.

Kuzniecky,R., 1999. Magnetic resonance spectroscopy in focal epilepsy: ³¹P and ¹H spectroscopy. *Rev Neurol (Paris)* 155, 495-498.

Kuzniecky,R., Elgavish,G.A., Hetherington,H.P., Evanochko,W.T., Pohost,G.M., 1992. In vivo ³¹P nuclear magnetic resonance spectroscopy of human temporal lobe epilepsy. *Neurology* 42, 1586-1590.

Kuzniecky,R., Hetherington,H., Ho,S., Pan,J., Martin,R., Gilliam,F., Hugg,J., Faught,E., 1998a. Topiramate increases cerebral GABA in healthy humans. *Neurology* 51, 627-629.

Kuzniecky,R., Hetherington,H., Pan,J., Hugg,J., Palmer,C., Gilliam,F., Faught,E., Morawetz,R., 1997a. Proton spectroscopic imaging at 4.1 tesla in patients with malformations of cortical development and epilepsy. *Neurology* 48, 1018-1024.

Kuzniecky,R., Hetherington,H., Pan,J., Hugg,J., Palmer,C., Gilliam,F., Faught,E., Morawetz,R., 1997b. Proton spectroscopic imaging at 4.1 tesla in patients with malformations of cortical development and epilepsy. *Neurology* 48, 1018-1024.

Kuzniecky,R., Ho,S., Pan,J., Martin,R., Gilliam,F., Faught,E., Hetherington,H., 2002. Modulation of cerebral GABA by topiramate, lamotrigine, and gabapentin in healthy adults. *Neurology* 58, 368-372.

Kuzniecky,R., Hugg,J., Hetherington,H., Martin,R., Faught,E., Morawetz,R., Gilliam,F., 1999. Predictive value of 1H MRSI for outcome in temporal lobectomy. *Neurology* 53, 694-698.

Kuzniecky,R., Hugg,J.W., Hetherington,H., Butterworth,E., Bilir,E., Faught,E., Gilliam,F., 1998b. Relative utility of 1H spectroscopic imaging and hippocampal volumetry in the lateralization of mesial temporal lobe epilepsy. *Neurology* 51, 66-71.

Kuzniecky,R., Palmer,C., Hugg,J., Martin,R., Sawrie,S., Morawetz,R., Faught,E., Knowlton,R., 2001. Magnetic resonance spectroscopic imaging in temporal lobe epilepsy: neuronal dysfunction or cell loss? *Arch Neurol* 58, 2048-2053.

Kuzniecky,R.I., Barkovich,A.J., 2001. Malformations of cortical development and epilepsy. *Brain Dev* 23, 2-11.

Kvamme,E., 1998. Synthesis of glutamate and its regulation. *Prog Brain Res* 116, 73-85.

Kwon,H.M., Yamauchi,A., Uchida,S., Preston,A.S., Garcia-Perez,A., Burg,M.B., Handler,J.S., 1992. Cloning of the cDNA for a Na⁺/myo-inositol cotransporter, a hypertonicity stress protein. *J Biol Chem* 267, 6297-6301.

Laxer,K.D., Hubesch,B., Sappey-Mariniere,D., Weiner,M.W., 1992. Increased pH and inorganic phosphate in temporal seizure foci demonstrated by [31P]MRS. *Epilepsia* 33, 618-623.

Lazeyras,F., Blanke,O., Zimine,I., Delavelle,J., Perrig,S.H., Seeck,M., 2000. MRI, (1)H-MRS, and functional MRI during and after prolonged nonconvulsive seizure activity. *Neurology* 55, 1677-1682.

Leblanc,R., Robitaille,Y., Andermann,F., Ptito,A., 1995. Retained language in dysgenic cortex: case report. *Neurosurgery* 37, 992-997.

Lehmann,A., Isacson,H., Hamberger,A., 1983. Effects of in vivo administration of kainic acid on the extracellular amino acid pool in the rabbit hippocampus. *J Neurochem* 40, 1314-1320.

Lehre,K.P., Danbolt,N.C., 1998. The number of glutamate transporter subtype molecules at glutamatergic synapses: chemical and stereological quantification in young adult rat brain. *J Neurosci* 18, 8751-8757.

Leonard,W.R., Snodgrass,J.J., Robertson,M.L., 2007. Effects of brain evolution on human nutrition and metabolism. *Annu Rev Nutr* 27, 311-327.

Levy, L.M., Warr, O., Attwell, D., 1998. Stoichiometry of the glial glutamate transporter GLT-1 expressed inducibly in a Chinese hamster ovary cell line selected for low endogenous Na⁺-dependent glutamate uptake. *J Neurosci* 18, 9620-9628.

Li, L.M., Cendes, F., Andermann, F., Dubeau, F., Arnold, D.L., 2000a. Spatial extent of neuronal metabolic dysfunction measured by proton MR spectroscopic imaging in patients with localization-related epilepsy. *Epilepsia* 41, 666-674.

Li, L.M., Cendes, F., Antel, S.B., Andermann, F., Serles, W., Dubeau, F., Olivier, A., Arnold, D.L., 2000b. Prognostic value of proton magnetic resonance spectroscopic imaging for surgical outcome in patients with intractable temporal lobe epilepsy and bilateral hippocampal atrophy. *Ann Neurol* 47, 195-200.

Li, L.M., Cendes, F., Bastos, A.C., Andermann, F., Dubeau, F., Arnold, D.L., 1998. Neuronal metabolic dysfunction in patients with cortical developmental malformations: a proton magnetic resonance spectroscopic imaging study. *Neurology* 50, 755-759.

Li, L.M., Dubeau, F., Andermann, F., Arnold, D.L., 2000c. Proton magnetic resonance spectroscopic imaging studies in patients with newly diagnosed partial epilepsy. *Epilepsia* 41, 825-831.

Liu, A.W., gado-Escueta, A.V., Serratosa, J.M., Alonso, M.E., Medina, M.T., Gee, M.N., Cordova, S., Zhao, H.Z., Spellman, J.M., Peek, J.R., .., 1995. Juvenile myoclonic epilepsy locus in chromosome 6p21.2-p11: linkage to convulsions and electroencephalography trait. *Am J Hum Genet* 57, 368-381.

Liu, R.S., Lemieux, L., Bell, G.S., Sisodiya, S.M., Bartlett, P.A., Shorvon, S.D., Sander, J.W., Duncan, J.S., 2005. Cerebral damage in epilepsy: a population-based longitudinal quantitative MRI study. *Epilepsia* 46, 1482-1494.

Loiseau, P and Panayiotopoulos, C. P. Childhood Absence Epilepsy. 2005. (http://www.ilae-epilepsy.org/visitors/centre/ctf/childhood_absence.cfm)

Lu, Y., Waltz, S., Stenzel, K., Muhle, H., Stephani, U., 2008. Photosensitivity in epileptic syndromes of childhood and adolescence. *Epileptic Disord* 10, 136-143.

Lynch, J., Peeling, J., Auty, A., Sutherland, G.R., 1993. Nuclear magnetic resonance study of cerebrospinal fluid from patients with multiple sclerosis. *Can J Neurol Sci* 20, 194-198.

Lyon G, Gastaut H, 1985. Considerations on the significance attributed to unusual cerebral histological findings recently described in eight patients with primary generalized epilepsy. *Epilepsia* 26, 365-367.

MacAulay,N., Gether,U., Klaerke,D.A., Zeuthen,T., 2001. Water transport by the human Na⁺-coupled glutamate cotransporter expressed in *Xenopus* oocytes. *J Physiol* 530, 367-378.

Magistretti,P.J., Pellerin,L., 1997. Regulation by neurotransmitters of glial energy metabolism. *Adv Exp Med Biol* 429, 137-143.

Magistretti,P.J., Pellerin,L., 1999. Astrocytes Couple Synaptic Activity to Glucose Utilization in the Brain. *News Physiol Sci* 14, 177-182.

Magistretti,P.J., Pellerin,L., 2000. The astrocyte-mediated coupling between synaptic activity and energy metabolism operates through volume transmission. *Prog Brain Res* 125, 229-240.

Magistretti,P.J., Pellerin,L., Rothman,D.L., Shulman,R.G., 1999. Energy on demand. *Science* 283, 496-497.

Magistretti,P.J., Sorg,O., Yu,N., Martin,J.L., Pellerin,L., 1993. Neurotransmitters regulate energy metabolism in astrocytes: implications for the metabolic trafficking between neural cells. *Dev Neurosci* 15, 306-312.

Maher,F., Vannucci,S.J., Simpson,I.A., 1994. Glucose transporter proteins in brain. *FASEB J* 8, 1003-1011.

Maki,R., Robinson,M.B., Dichter,M.A., 1994. The glutamate uptake inhibitor L-trans-pyrrolidine-2,4-dicarboxylate depresses excitatory synaptic transmission via a presynaptic mechanism in cultured hippocampal neurons. *J Neurosci* 14, 6754-6762.

Mangia,S., Garreffa,G., Bianciardi,M., Giove,F., Di,S.F., Maraviglia,B., 2003a. The aerobic brain: lactate decrease at the onset of neural activity. *Neuroscience* 118, 7-10.

Mangia,S., Giove,F., Bianciardi,M., Di,S.F., Garreffa,G., Maraviglia,B., 2003b. Issues concerning the construction of a metabolic model for neuronal activation. *J Neurosci Res* 71, 463-467.

Mangia,S., Simpson,I.A., Vannucci,S.J., Carruthers,A., 2009. The in vivo neuron-to-astrocyte lactate shuttle in human brain: evidence from modeling of measured lactate levels during visual stimulation. *J Neurochem* 109 Suppl 1, 55-62.

Marsh,L., Lim,K.O., Sullivan,E.V., Lane,B., Spielman,D., 1996. Proton magnetic resonance spectroscopy of a gray matter heterotopia. *Neurology* 47, 1571-1574.

- Martin,E., Capone,A., Schneider,J., Hennig,J., Thiel,T., 2001. Absence of N-acetylaspartate in the human brain: impact on neurospectroscopy? *Ann Neurol* 49, 518-521.
- Martinez-Hernandez,A., Bell,K.P., Norenberg,M.D., 1977. Glutamine synthetase: glial localization in brain. *Science* 195, 1356-1358.
- Mas,C., Taske,N., Deutsch,S., Guipponi,M., Thomas,P., Covanis,A., Friis,M., Kjeldsen,M.J., Pizzolato,G.P., Villemure,J.G., Buresi,C., Rees,M., Malafosse,A., Gardiner,M., Antonarakis,S.E., Meda,P., 2004. Association of the connexin36 gene with juvenile myoclonic epilepsy. *J Med Genet* 41, e93.
- Mathern,G.W., Pretorius,J.K., Babb,T.L., 1995. Quantified patterns of mossy fiber sprouting and neuron densities in hippocampal and lesional seizures. *J Neurosurg* 82, 211-219.
- Maton,B., Gilliam,F., Sawrie,S., Faught,E., Hugg,J., Kuzniecky,R., 2001a. Correlation of scalp EEG and ¹H-MRS metabolic abnormalities in temporal lobe epilepsy. *Epilepsia* 42, 417-422.
- Maton,B., Londono,A., Sawrie,S., Knowlton,R., Martin,R., Kuzniecky,R., 2001b. Postictal stability of proton magnetic resonance spectroscopy imaging (¹H-MRSI) ratios in temporal lobe epilepsy. *Neurology* 56, 251-253.
- Mattia,D., Olivier,A., Avoli,M., 1995. Seizure-like discharges recorded in human dysplastic neocortex maintained in vitro. *Neurology* 45, 1391-1395.
- McKnight,T.R., 2004. Proton magnetic resonance spectroscopic evaluation of brain tumor metabolism. *Semin Oncol* 31, 605-617.
- McLean,M.A., Busza,A.L., Wald,L.L., Simister,R.J., Barker,G.J., Williams,S.R., 2002. In vivo GABA+ measurement at 1.5T using a PRESS-localized double quantum filter. *Magn Reson Med* 48, 233-241.
- McLean,M.A., Simister,R.J., Barker,G.J., Duncan,J.S., 2004. Discrimination between neurochemical and macromolecular signals in human frontal lobes using short echo time proton magnetic resonance spectroscopy. *Faraday Discuss* 126:93-102; discussion 169-83., 93-102.
- McLean,M.A., Woermann,F.G., Barker,G.J., Duncan,J.S., 2000. Quantitative analysis of short echo time (¹H-MRSI) of cerebral gray and white matter. *Magn Reson Med* 44, 401-411.

McLean,M.A., Woermann,F.G., Simister,R.J., Barker,G.J., Duncan,J.S., 2001. In vivo short echo time 1H-magnetic resonance spectroscopic imaging (MRSI) of the temporal lobes. *Neuroimage* 14, 501-509.

McLean,M., Barker,G., Tofts,P., Duncan,J., 1999. Interactive ROI analysis in 1H CSI. *Proc Intl Soc Mag Reson Med* 7, 1562.

Meencke,H.J., Janz,D., 1984. Neuropathological findings in primary generalized epilepsy: a study of eight cases. *Epilepsia* 25, 8-21.

Meencke,H.J., Janz,D., 1985. The significance of microdysgenesis in primary generalized epilepsy: an answer to the considerations of Lyon and Gastaut. *Epilepsia* 26, 368-371.

Meeren,H., van,L.G., Lopes da,S.F., Coenen,A., 2005. Evolving concepts on the pathophysiology of absence seizures: the cortical focus theory. *Arch Neurol* 62, 371-376.

Meeren,H.K., Pijn,J.P., Van Luijtelaar,E.L., Coenen,A.M., Lopes da Silva,F.H., 2002. Cortical focus drives widespread corticothalamic networks during spontaneous absence seizures in rats. *J Neurosci* 22, 1480-1495.

Meiners,L.C., van der,G.J., van Rijen,P.C., Springorum,R., de Kort,G.A., Jansen,G.H., 2000. Proton magnetic resonance spectroscopy of temporal lobe white matter in patients with histologically proven hippocampal sclerosis. *J Magn Reson Imaging* 11, 25-31.

Meinild,A., Klaerke,D.A., Loo,D.D., Wright,E.M., Zeuthen,T., 1998. The human Na⁺-glucose cotransporter is a molecular water pump. *J Physiol* 508 (Pt 1), 15-21.

Meldrum,B.S., 2000. Glutamate as a neurotransmitter in the brain: review of physiology and pathology. *J Nutr* 130, 1007S-1015S.

Meldrum,B.S., Chapman,A.G., 1999. Excitatory amino acid receptors and antiepileptic drug development. *Adv Neurol* 79, 965-978.

Merlis,J.K., 1970. Proposal for an international classification of the epilepsies. *Epilepsia* 11, 114-119.

Mescher,M., Merkle,H., Kirsch,J., Garwood,M., Gruetter,R., 1998. Simultaneous in vivo spectral editing and water suppression. *NMR Biomed* 11, 266-272.

Meyer,P.T., Schreckenberger,M., Spetzger,U., Meyer,G.F., Sabri,O., Setani,K.S., Zeggel,T., Buell,U., 2001. Comparison of visual and ROI-based brain tumour grading using 18F-FDG PET: ROC analyses. *Eur J Nucl Med* 28, 165-174.

Moeller,F., Siebner,H.R., Ahlgrimm,N., Wolff,S., Muhle,H., Granert,O., Boor,R., Jansen,O., Gotman,J., Stephani,U., Siniatchkin,M., 2009. fMRI activation during spike and wave discharges evoked by photic stimulation. *Neuroimage* 48, 682-695.

Moeller,F., Siebner,H.R., Wolff,S., Muhle,H., Boor,R., Granert,O., Jansen,O., Stephani,U., Siniatchkin,M., 2008. Changes in activity of striato-thalamo-cortical network precede generalized spike wave discharges. *Neuroimage* 39, 1839-1849.

Moore,G.J., Bebchuk,J.M., Parrish,J.K., Faulk,M.W., Arfken,C.L., Strahl-Bevacqua,J., Manji,H.K., 1999. Temporal dissociation between lithium-induced changes in frontal lobe myo-inositol and clinical response in manic-depressive illness. *Am J Psychiatry* 156, 1902-1908.

Moreadith,R.W., Jacobus,W.E., 1982. Creatine kinase of heart mitochondria. Functional coupling of ADP transfer to the adenine nucleotide translocase. *J Biol Chem* 257, 899-905.

Moreno,A., Ross,B.D., Bluml,S., 2001. Direct determination of the N-acetyl-L-aspartate synthesis rate in the human brain by (13)C MRS and [1-(13)C]glucose infusion. *J Neurochem* 77, 347-350.

Morgello,S., Uson,R.R., Schwartz,E.J., Haber,R.S., 1995. The human blood-brain barrier glucose transporter (GLUT1) is a glucose transporter of gray matter astrocytes. *Glia* 14, 43-54.

Mory,S.B., Li,L.M., Guerreiro,C.A., Cendes,F., 2003. Thalamic dysfunction in juvenile myoclonic epilepsy: a proton MRS study. *Epilepsia* 44, 1402-1405.

Mueller,S.G., Kollias,S.S., Trabesinger,A.H., Buck,A., Boesiger,P., Wieser,H.G., 2001a. Proton magnetic resonance spectroscopy characteristics of a focal cortical dysgenesis during status epilepticus and in the interictal state. *Seizure* 10, 518-524.

Mueller,S.G., Suhy,J., Laxer,K.D., Flenniken,D.L., Axelrad,J., Capizzano,A.A., Weiner,M.W., 2002. Reduced extrahippocampal NAA in mesial temporal lobe epilepsy. *Epilepsia* 43, 1210-1216.

Mueller,S.G., Weber,O.M., Duc,C.O., Weber,B., Meier,D., Russ,W., Boesiger,P., Wieser,H.G., 2001b. Effects of vigabatrin on brain GABA+/CR signals in patients with epilepsy monitored by 1H-NMR-spectroscopy: responder characteristics. *Epilepsia* 42, 29-40.

Mueller-Lisse,U.G., Scherr,M.K., 2007. Proton MR spectroscopy of the prostate. *Eur J Radiol* 63, 351-360.

Nahorski,S.R., Young,K.W., John Challiss,R.A., Nash,M.S., 2003. Visualizing phosphoinositide signalling in single neurons gets a green light. *Trends Neurosci* 26, 444-452.

Najm,I.M., Wang,Y., Hong,S.C., Luders,H.O., Ng,T.C., Comair,Y.G., 1997. Temporal changes in proton MRS metabolites after kainic acid-induced seizures in rat brain. *Epilepsia* 38, 87-94.

Namer,I.J., Bolo,N.R., Sellal,F., Nguyen,V.H., Nedelec,J.F., Hirsch,E., Marescaux,C., 1999. Combined measurements of hippocampal N-acetyl-aspartate and T2 relaxation time in the evaluation of mesial temporal lobe epilepsy: correlation with clinical severity and memory performances. *Epilepsia* 40, 1424-1432.

Nedergaard,M., Ransom,B., Goldman,S.A., 2003. New roles for astrocytes: redefining the functional architecture of the brain. *Trends Neurosci* 26, 523-530.

Neppl,R., Nguyen,C.M., Bowen,W., Al Saadi,T., Pallagi,J., Morris,G., Mueller,W., Johnson,R., Prost,R., Rand,S.D., 2001. In vivo detection of postictal perturbations of cerebral metabolism by use of proton MR spectroscopy: preliminary results in a canine model of prolonged generalized seizures. *AJNR Am J Neuroradiol* 22, 1933-1943.

Neumann,D., Schlattner,U., Wallimann,T., 2003. A molecular approach to the concerted action of kinases involved in energy homeostasis. *Biochem Soc Trans* 31, 169-174.

Ng,T.C., Comair,Y.G., Xue,M., So,N., Majors,A., Kolem,H., Luders,H., Modic,M., 1994. Temporal lobe epilepsy: presurgical localization with proton chemical shift imaging. *Radiology* 193, 465-472.

Niedermeyer,E., 1996. Primary (idiopathic) generalized epilepsy and underlying mechanisms. *Clin Electroencephalogr* 27, 1-21.

Nohria,V., Lee,N., Tien,R.D., Heinz,E.R., Smith,J.S., DeLong,G.R., Skeen,M.B., Resnick,T.J., Crain,B., Lewis,D.V., 1994. Magnetic resonance imaging evidence of hippocampal sclerosis in progression: a case report. *Epilepsia* 35, 1332-1336.

Noworolski,S.M., Nelson,S.J., Henry,R.G., Day,M.R., Wald,L.L., Star-Lack,J., Vigneron,D.B., 1999. High spatial resolution 1H-MRSI and segmented MRI of cortical gray matter and subcortical white matter in three regions of the human brain. *Magn Reson Med* 41, 21-29.

- O'Donnell,T., Rotzinger,S., Nakashima,T.T., Hanstock,C.C., Ulrich,M., Silverstone,P.H., 2003. Chronic lithium and sodium valproate both decrease the concentration of myoinositol and increase the concentration of inositol monophosphates in rat brain. *Eur Neuropsychopharmacol* 13, 199-207.
- Oberheim,N.A., Wang,X., Goldman,S., Nedergaard,M., 2006. Astrocytic complexity distinguishes the human brain. *Trends Neurosci* 29, 547-553.
- Olsen,R.W., Avoli,M., 1997. GABA and epileptogenesis. *Epilepsia* 38, 399-407.
- Opeskin,K., Kalnins,R.M., Halliday,G., Cartwright,H., Berkovic,S.F., 2000. Idiopathic generalized epilepsy: lack of significant microdysgenesis. *Neurology* 55, 1101-1106.
- Ordidge,R.J., Bowley,R.M., McHale,G., 1988. A general approach to selection of multiple cubic volume elements using the ISIS technique. *Magn Reson Med* 8, 323-331.
- Ottersen,O.P., Zhang,N., Walberg,F., 1992. Metabolic compartmentation of glutamate and glutamine: morphological evidence obtained by quantitative immunocytochemistry in rat cerebellum. *Neuroscience* 46, 519-534.
- Ottman,R., 2005. Analysis of genetically complex epilepsies. *Epilepsia* 46 Suppl 10, 7-14.
- Pal,D.K., Evgrafov,O.V., Tabares,P., Zhang,F., Durner,M., Greenberg,D.A., 2003. BRD2 (RING3) is a probable major susceptibility gene for common juvenile myoclonic epilepsy. *Am J Hum Genet* 73, 261-270.
- Palmini,A., Andermann,F., Olivier,A., Tampieri,D., Robitaille,Y., 1991a. Focal neuronal migration disorders and intractable partial epilepsy: results of surgical treatment. *Ann Neurol* 30, 750-757.
- Palmini,A., Andermann,F., Olivier,A., Tampieri,D., Robitaille,Y., Andermann,E., Wright,G., 1991b. Focal neuronal migration disorders and intractable partial epilepsy: a study of 30 patients. *Ann Neurol* 30, 741-749.
- Palmini,A., Gambardella,A., Andermann,F., Dubeau,F., da Costa,J.C., Olivier,A., Tampieri,D., Gloor,P., Quesney,F., Andermann,E., , 1995. Intrinsic epileptogenicity of human dysplastic cortex as suggested by corticography and surgical results. *Ann Neurol* 37, 476-487.
- Pan,J.W., Venkatraman,T., Vives,K., Spencer,D.D., 2006. Quantitative glutamate spectroscopic imaging of the human hippocampus. *NMR Biomed* 19, 209-216.

Pan,J.W., Williamson,A., Cavus,I., Hetherington,H.P., Zaveri,H., Petroff,O.A., Spencer,D.D., 2008. Neurometabolism in human epilepsy. *Epilepsia* 49 Suppl 3, 31-41.

Papanagiotou,P., Backens,M., Grunwald,I.Q., Farmakis,G., Politi,M., Roth,C., Reith,W., 2007. [MR spectroscopy in brain tumors]. *Radiologe* 47, 520-529.

Park,S.W., Chang,K.H., Kim,H.D., Song,I.C., Lee,D.S., Lee,S.K., Chung,C.K., Yu,I.K., Han,M.H., Park,Y.H., 2001. Lateralizing ability of single-voxel proton mr spectroscopy in hippocampal sclerosis: comparison with mr imaging and positron emission tomography. *AJNR Am J Neuroradiol* 22, 625-631.

Pauli,E., Eberhardt,K.W., Schafer,I., Tomandl,B., Huk,W.J., Stefan,H., 2000. Chemical shift imaging spectroscopy and memory function in temporal lobe epilepsy. *Epilepsia* 41, 282-289.

Peeling,J., Sutherland,G., 1993. ¹H magnetic resonance spectroscopy of extracts of human epileptic neocortex and hippocampus. *Neurology* 43, 589-594.

Pellerin,L., Bouzier-Sore,A.K., Aubert,A., Serres,S., Merle,M., Costalat,R., Magistretti,P.J., 2007. Activity-dependent regulation of energy metabolism by astrocytes: an update. *Glia* 55, 1251-1262.

Pellerin,L., Magistretti,P.J., 2003. How to balance the brain energy budget while spending glucose differently. *J Physiol* 546, 325.

Pellerin,L., Pellegrini,G., Bittar,P.G., Charnay,Y., Bouras,C., Martin,J.L., Stella,N., Magistretti,P.J., 1998. Evidence supporting the existence of an activity-dependent astrocyte-neuron lactate shuttle. *Dev Neurosci* 20, 291-299.

Pellerin,L., Sibson,N.R., Hadjikhani,N., Hyder,F., 2001. What you see is what you think--or is it? *Trends Neurosci* 24, 71-72.

penfield W, 1952. Epileptic automatism and the centrencephalic integrating system. *Res Publ Assoc Res Nerv Ment Dis* 30, 513-528.

Perry,T.L., Hansen,S., Kennedy,J., Wada,J.A., Thompson,G.B., 1975. Amino acids in human epileptogenic foci. *Arch Neurol* 32, 752-754.

Petroff,O.A., Behar,K.L., Rothman,D.L., 1999a. New NMR measurements in epilepsy. Measuring brain GABA in patients with complex partial seizures. *Adv Neurol* 79, 939-945.

Petroff,O.A., Errante,L.D., Kim,J.H., Spencer,D.D., 2003. N-acetyl-aspartate, total creatine, and myo-inositol in the epileptogenic human hippocampus. *Neurology* 60, 1646-1651.

Petroff,O.A., Errante,L.D., Rothman,D.L., Kim,J.H., Spencer,D.D., 2002a. Glutamate-glutamine cycling in the epileptic human hippocampus. *Epilepsia* 43, 703-710.

Petroff,O.A., Errante,L.D., Rothman,D.L., Kim,J.H., Spencer,D.D., 2002b. Neuronal and glial metabolite content of the epileptogenic human hippocampus. *Ann Neurol* 52, 635-642.

Petroff,O.A., Hyder,F., Collins,T., Mattson,R.H., Rothman,D.L., 1999b. Acute effects of vigabatrin on brain GABA and homocarnosine in patients with complex partial seizures. *Epilepsia* 40, 958-964.

Petroff,O.A., Hyder,F., Mattson,R.H., Rothman,D.L., 1999c. Topiramate increases brain GABA, homocarnosine, and pyrrolidinone in patients with epilepsy. *Neurology* 52, 473-478.

Petroff,O.A., Hyder,F., Rothman,D.L., Mattson,R.H., 2001a. Homocarnosine and seizure control in juvenile myoclonic epilepsy and complex partial seizures. *Neurology* 56, 709-715.

Petroff,O.A., Hyder,F., Rothman,D.L., Mattson,R.H., 2001b. Topiramate rapidly raises brain GABA in epilepsy patients. *Epilepsia* 42, 543-548.

Petroff,O.A., Mattson,R.H., Behar,K.L., Hyder,F., Rothman,D.L., 1998. Vigabatrin increases human brain homocarnosine and improves seizure control. *Ann Neurol* 44, 948-952.

Petroff,O.A., Mattson,R.H., Rothman,D.L., 2000. Proton MRS: GABA and glutamate. *Adv Neurol* 83, 261-271.

Petroff,O.A., Pleban,L.A., Spencer,D.D., 1995. Symbiosis between in vivo and in vitro NMR spectroscopy: the creatine, N-acetylaspartate, glutamate, and GABA content of the epileptic human brain. *Magn Reson Imaging* 13, 1197-1211.

Petroff,O.A., Prichard,J.W., Behar,K.L., Alger,J.R., Shulman,R.G., 1984. In vivo phosphorus nuclear magnetic resonance spectroscopy in status epilepticus. *Ann Neurol* 16, 169-177.

Petroff,O.A., Prichard,J.W., Ogino,T., Avison,M., Alger,J.R., Shulman,R.G., 1986. Combined ¹H and ³¹P nuclear magnetic resonance spectroscopic studies of bicuculline-induced seizures in vivo. *Ann Neurol* 20, 185-193.

Petroff,O.A., Rothman,D.L., Behar,K.L., Hyder,F., Mattson,R.H., 1999d. Effects of valproate and other antiepileptic drugs on brain glutamate, glutamine, and GABA in patients with refractory complex partial seizures. *Seizure* 8, 120-127.

Petroff,O.A., Rothman,D.L., Behar,K.L., Mattson,R.H., 1996a. Human brain GABA levels rise after initiation of vigabatrin therapy but fail to rise further with increasing dose. *Neurology* 46, 1459-1463.

Petroff,O.A., Rothman,D.L., Behar,K.L., Mattson,R.H., 1996b. Low brain GABA level is associated with poor seizure control. *Ann Neurol* 40, 908-911.

Petroff,O.A., Spencer,D.D., Alger,J.R., Prichard,J.W., 1989. High-field proton magnetic resonance spectroscopy of human cerebrum obtained during surgery for epilepsy. *Neurology* 39, 1197-1202.

Pfund,Z., Chugani,D.C., Juhasz,C., Muzik,O., Chugani,H.T., Wilds,I.B., Seraji-Bozorgzad,N., Moore,G.J., 2000. Evidence for coupling between glucose metabolism and glutamate cycling using FDG PET and ¹H magnetic resonance spectroscopy in patients with epilepsy. *J Cereb Blood Flow Metab* 20, 871-878.

Pouwels,P.J., Frahm,J., 1998. Regional metabolite concentrations in human brain as determined by quantitative localized proton MRS. *Magn Reson Med* 39, 53-60.

Prevet,M.C., Duncan,J.S., Jones,T., Fish,D.R., Brooks,D.J., 1995a. Demonstration of thalamic activation during typical absence seizures using H₂(¹⁵O) and PET. *Neurology* 45, 1396-1402.

Prevet,M.C., Lammertsma,A.A., Brooks,D.J., Cunningham,V.J., Fish,D.R., Duncan,J.S., 1995b. Benzodiazepine-GABA_A receptor binding during absence seizures. *Epilepsia* 36, 592-599.

Prince,D.A., Jacobs,K.M., Salin,P.A., Hoffman,S., Parada,I., 1997. Chronic focal neocortical epileptogenesis: does disinhibition play a role? *Can J Physiol Pharmacol* 75, 500-507.

Provencher,S.W., 1993. Estimation of metabolite concentrations from localized in vivo proton NMR spectra. *Magn Reson Med* 30, 672-679.

Provencher,S.W., 2001. Automatic quantitation of localized in vivo ¹H spectra with LCModel. *NMR Biomed* 14, 260-264.

Quigg,M., Bertram,E.H., Jackson,T., 1997a. Longitudinal distribution of hippocampal atrophy in mesial temporal lobe epilepsy. *Epilepsy Res* 27, 101-110.

Quigg, M., Bertram, E.H., Jackson, T., Laws, E., 1997b. Volumetric magnetic resonance imaging evidence of bilateral hippocampal atrophy in mesial temporal lobe epilepsy. *Epilepsia* 38, 588-594.

Rademacher, J., Burgel, U., Geyer, S., Schormann, T., Schleicher, A., Freund, H.J., Zilles, K., 2001. Variability and asymmetry in the human precentral motor system. A cytoarchitectonic and myeloarchitectonic brain mapping study. *Brain* 124, 2232-2258.

Raymond, A.A., Fish, D.R., Sisodiya, S.M., Alsanjari, N., Stevens, J.M., Shorvon, S.D., 1995. Abnormalities of gyration, heterotopias, tuberous sclerosis, focal cortical dysplasia, microdysgenesis, dysembryoplastic neuroepithelial tumour and dysgenesis of the archicortex in epilepsy. Clinical, EEG and neuroimaging features in 100 adult patients. *Brain* 118 (Pt 3), 629-660.

Redecker, C., Luhmann, H.J., Hagemann, G., Fritschy, J.M., Witte, O.W., 2000. Differential downregulation of GABA_A receptor subunits in widespread brain regions in the freeze-lesion model of focal cortical malformations. *J Neurosci* 20, 5045-5053.

Reid, C.A., Berkovic, S.F., Petrou, S., 2009. Mechanisms of human inherited epilepsies. *Prog Neurobiol* 87, 41-57.

Richardson, M.P., Friston, K.J., Sisodiya, S.M., Koepp, M.J., Ashburner, J., Free, S.L., Brooks, D.J., Duncan, J.S., 1997. Cortical grey matter and benzodiazepine receptors in malformations of cortical development. A voxel-based comparison of structural and functional imaging data. *Brain* 120 (Pt 11), 1961-1973.

Riederer, F., Bittsansky, M., Schmidt, C., Mlynarik, V., Baumgartner, C., Moser, E., Serles, W., 2006. ¹H magnetic resonance spectroscopy at 3 T in cryptogenic and mesial temporal lobe epilepsy. *NMR Biomed* 19, 544-553.

Rooney, W.D., Goodkin, D.E., Schuff, N., Meyerhoff, D.J., Norman, D., Weiner, M.W., 1997. ¹H MRSI of normal appearing white matter in multiple sclerosis. *Mult Scler* 3, 231-237.

Ross, B., Michaelis, T., 1994. Clinical applications of magnetic resonance spectroscopy. *Magn Reson Q* 10, 191-247.

Rothman, D.L., 2001. Studies of metabolic compartmentation and glucose transport using in vivo MRS. *NMR Biomed* 14, 149-160.

Rothman, D.L., Behar, K.L., Hyder, F., Shulman, R.G., 2003. In vivo NMR studies of the glutamate neurotransmitter flux and neuroenergetics: Implications for Brain Function. *Annu Rev Physiol* 65, 401-427.

- Rothman,D.L., Petroff,O.A., Behar,K.L., Mattson,R.H., 1993. Localized ¹H NMR measurements of gamma-aminobutyric acid in human brain in vivo. *Proc Natl Acad Sci U S A* 90, 5662-5666.
- Rothman,D.L., Sibson,N.R., Hyder,F., Shen,J., Behar,K.L., Shulman,R.G., 1999. In vivo nuclear magnetic resonance spectroscopy studies of the relationship between the glutamate-glutamine neurotransmitter cycle and functional neuroenergetics. *Philos Trans R Soc Lond B Biol Sci* 354, 1165-1177.
- Salek-Haddadi,A., Lemieux,L., Merschhemke,M., Friston,K.J., Duncan,J.S., Fish,D.R., 2003. Functional magnetic resonance imaging of human absence seizures. *Ann Neurol* 53, 663-667.
- Sanchez-Prieto,J., Budd,D.C., Herrero,I., Vazquez,E., Nicholls,D.G., 1996. Presynaptic receptors and the control of glutamate exocytosis. *Trends Neurosci* 19, 235-239.
- Saphey-Marinier,D., Calabrese,G., Fein,G., Hugg,J.W., Biggins,C., Weiner,M.W., 1992. Effect of photic stimulation on human visual cortex lactate and phosphates using ¹H and ³¹P magnetic resonance spectroscopy. *J Cereb Blood Flow Metab* 12, 584-592.
- Saunders,D.E., 2000. MR spectroscopy in stroke. *Br Med Bull* 56, 334-345.
- Savic,I., Lekvall,A., Greitz,D., Helms,G., 2000a. MR spectroscopy shows reduced frontal lobe concentrations of N-acetyl aspartate in patients with juvenile myoclonic epilepsy. *Epilepsia* 41, 290-296.
- Savic,I., Pauli,S., Thorell,J.O., Blomqvist,G., 1994. In vivo demonstration of altered benzodiazepine receptor density in patients with generalised epilepsy. *J Neurol Neurosurg Psychiatry* 57, 797-804.
- Savic,I., Thomas,A.M., Ke,Y., Curran,J., Fried,I., Engel,J., Jr., 2000b. In vivo measurements of glutamine + glutamate (Glx) and N-acetyl aspartate (NAA) levels in human partial epilepsy. *Acta Neurol Scand* 102, 179-188.
- Savic,I., Widen,L., Thorell,J.O., Blomqvist,G., Ericson,K., Roland,P., 1990. Cortical benzodiazepine receptor binding in patients with generalized and partial epilepsy. *Epilepsia* 31, 724-730.
- Sawrie,S.M., Martin,R.C., Knowlton,R., Faught,E., Gilliam,F., Kuzniecky,R., 2001. Relationships among hippocampal volumetry, proton magnetic resonance spectroscopy, and verbal memory in temporal lobe epilepsy. *Epilepsia* 42, 1403-1407.

- Scanziani, M., Salin, P.A., Vogt, K.E., Malenka, R.C., Nicoll, R.A., 1997. Use-dependent increases in glutamate concentration activate presynaptic metabotropic glutamate receptors. *Nature* 385, 630-634.
- Schousboe, A., 1981. Transport and metabolism of glutamate and GABA in neurons are glial cells. *Int Rev Neurobiol* 22, 1-45.
- Schousboe, A., Waagepetersen, H.S., 2007. GABA: homeostatic and pharmacological aspects. *Prog Brain Res* 160, 9-19.
- Semyanov, A., Kullmann, D.M., 2000. Modulation of GABAergic signaling among interneurons by metabotropic glutamate receptors. *Neuron* 25, 663-672.
- Serles, W., Li, L.M., Antel, S.B., Cendes, F., Gotman, J., Olivier, A., Andermann, F., Dubeau, F., Arnold, D.L., 2001. Time course of postoperative recovery of N-acetyl-aspartate in temporal lobe epilepsy. *Epilepsia* 42, 190-197.
- Shen, J., Rothman, D.L., Brown, P., 2002. In vivo GABA editing using a novel doubly selective multiple quantum filter. *Magn Reson Med* 47, 447-454.
- Sherwin, A., Robitaille, Y., Quesney, F., Olivier, A., Villemure, J., Leblanc, R., Feindel, W., Andermann, E., Gotman, J., Andermann, F., .., 1988. Excitatory amino acids are elevated in human epileptic cerebral cortex. *Neurology* 38, 920-923.
- Shmuel, A., Augath, M., Oeltermann, A., Logothetis, N.K., 2006. Negative functional MRI response correlates with decreases in neuronal activity in monkey visual area V1. *Nat Neurosci* 9, 569-577.
- Sibson, N.R., Dhankhar, A., Mason, G.F., Behar, K.L., Rothman, D.L., Shulman, R.G., 1997. In vivo ¹³C NMR measurements of cerebral glutamine synthesis as evidence for glutamate-glutamine cycling. *Proc Natl Acad Sci U S A* 94, 2699-2704.
- Sibson, N.R., Dhankhar, A., Mason, G.F., Rothman, D.L., Behar, K.L., Shulman, R.G., 1998a. Stoichiometric coupling of brain glucose metabolism and glutamatergic neuronal activity. *Proc Natl Acad Sci U S A* 95, 316-321.
- Sibson, N.R., Mason, G.F., Shen, J., Cline, G.W., Herskovits, A.Z., Wall, J.E., Behar, K.L., Rothman, D.L., Shulman, R.G., 2001. In vivo (¹³C) NMR measurement of neurotransmitter glutamate cycling, anaplerosis and TCA cycle flux in rat brain during. *J Neurochem* 76, 975-989.
- Sibson, N.R., Shen, J., Mason, G.F., Rothman, D.L., Behar, K.L., Shulman, R.G., 1998b. Functional energy metabolism: in vivo ¹³C-NMR spectroscopy evidence for coupling of cerebral glucose consumption and glutamatergic neuronal activity. *Dev Neurosci* 20, 321-330.

- Simister RJ, McLean MA, Barker GJ, Duncan JS, 2003a. A proton magnetic resonance spectroscopy study of metabolites in the occipital lobes in epilepsy. *Epilepsia* 44, 550-558.
- Simister RJ, McLean MA, Barker GJ, Duncan JS, 2003b. Proton Magnetic Resonance Spectroscopy Reveals Frontal Lobe Metabolite Abnormalities in Idiopathic Generalised Epilepsy. *Neurology* 61, 897-902.
- Simister,R.J., McLean,M.A., Barker,G.J., Duncan,J.S., 2007. Proton magnetic resonance spectroscopy of malformations of cortical development causing epilepsy. *Epilepsy Res* 74, 107-115.
- Simister,R.J., Woermann,F.G., McLean,M.A., Bartlett,P.A., Barker,G.J., Duncan,J.S., 2002. A short-echo-time proton magnetic resonance spectroscopic imaging study of temporal lobe epilepsy. *Epilepsia* 43, 1021-1031.
- Simone,I.L., Federico,F., Tortorella,C., De Blasi,R., Bellomo,R., Lucivero,V., Carrara,D., Bellacosa,A., Livrea,P., Carella,A., 1999a. Metabolic changes in neuronal migration disorders: evaluation by combined MRI and proton MR spectroscopy. *Epilepsia* 40, 872-879.
- Simone,I.L., Federico,F., Tortorella,C., De Blasi,R., Bellomo,R., Lucivero,V., Carrara,D., Bellacosa,A., Livrea,P., Carella,A., 1999b. Metabolic changes in neuronal migration disorders: evaluation by combined MRI and proton MR spectroscopy. *Epilepsia* 40, 872-879.
- Simor T, Chu WJ, Hetherington HP, Kuzniecky RI, Elgavish GA, 1997. Tailored temporal lobectomy induced improvements in 4.1T 31P NMR SI generated phosphorous metabolite indices in temporal lobe epilepsy. *Proceedings of the 5th Annual Meeting of ISMRM* 33.
- Simpson,I.A., Carruthers,A., Vannucci,S.J., 2007. Supply and demand in cerebral energy metabolism: the role of nutrient transporters. *J Cereb Blood Flow Metab* 27, 1766-1791.
- Simpson, I. A., Vannucci, S. J., and Carruthers, A. Supply and demand in cerebral energy. Siesjo BK. *Brain Energy Metabolism*. 1978. New York: Wiley.
- Sims,K.D., Robinson,M.B., 1999. Expression patterns and regulation of glutamate transporters in the developing and adult nervous system. *Crit Rev Neurobiol* 13, 169-197.
- Sisodiya,S.M., 1995. Wiring, dysmorphogenesis and epilepsy: a hypothesis. *Seizure* 4, 169-185.

Sisodiya,S.M., 2000. Surgery for malformations of cortical development causing epilepsy. *Brain* 123 (Pt 6), 1075-1091.

Sisodiya,S.M., 2004. Malformations of cortical development: burdens and insights from important causes of human epilepsy. *Lancet Neurol* 3, 29-38.

Sisodiya,S.M., Free,S.L., Stevens,J.M., Fish,D.R., Shorvon,S.D., 1995. Widespread cerebral structural changes in patients with cortical dysgenesis and epilepsy. *Brain* 118 (Pt 4), 1039-1050.

Sloviter,R.S., 1996. Hippocampal pathology and pathophysiology in temporal lobe epilepsy. *Neurologia* 11 Suppl 4:29-32., 29-32.

Sloviter,R.S., Dempster,D.W., 1985. "Epileptic" brain damage is replicated qualitatively in the rat hippocampus by central injection of glutamate or aspartate but not by GABA or acetylcholine. *Brain Res Bull* 15, 39-60.

Sloviter,R.S., Sollas,A.L., Barbaro,N.M., Laxer,K.D., 1991. Calcium-binding protein (calbindin-D28K) and parvalbumin immunocytochemistry in the normal and epileptic human hippocampus. *J Comp Neurol* 308, 381-396.

Soher,B.J., Young,K., Maudsley,A.A., 2001. Representation of strong baseline contributions in 1H MR spectra. *Magn Reson Med* 45, 966-972.

Sommer W, 1880. Erkrankung des Ammon's horn als aetiologis ches moment der epilepsien. *Arch Psychiatr Nurs* 10, 631-675.

Spencer,S., Huh,L., 2008. Outcomes of epilepsy surgery in adults and children. *Lancet Neurol* 7, 525-537.

Spielmeyer,W., 1925. Zur Pathogenese Ortlich selektiver Gehirnveränderungen. *Z Ges Neurol Psychiatr* 99, 756-776.

Stanley,J.A., Cendes,F., Dubeau,F., Andermann,F., Arnold,D.L., 1998. Proton magnetic resonance spectroscopic imaging in patients with extratemporal epilepsy. *Epilepsia* 39, 267-273.

Stefan,H., Eberhardt,K.E., Pauli,E., Schafer,I., Paulus,W., Kasper,B., Kerling,F., Hopp,P., Tomandl,B.F., Buchfelder,M., Huk,W.J., 2001a. [Diagnostic imaging in refractory temporal lobe epilepsy. A comparison of MR volumetry and multivoxel-MR-spectroscopy for assessment of postoperative prognosis]. *Nervenarzt* 72, 130-135.

Stefan,H., Feichtinger,M., Pauli,E., Schafer,I., Eberhardt,K.W., Kasper,B.S., Hopp,P., Buchfelder,M., Huk,J., Paulus,W., 2001b. Magnetic resonance spectroscopy and histopathological findings in temporal lobe epilepsy. *Epilepsia* 42, 41-46.

Storm-Mathisen,J., Danbolt,N.C., Rothe,F., Torp,R., Zhang,N., Aas,J.E., Kanner,B.I., Langmoen,I., Ottersen,O.P., 1992. Ultrastructural immunocytochemical observations on the localization, metabolism and transport of glutamate in normal and ischemic brain tissue. *Prog Brain Res* 94, 225-241.

Suhy,J., Laxer,K.D., Capizzano,A.A., Vermathen,P., Matson,G.B., Barbaro,N.M., Weiner,M.W., 2002. 1H MRSI predicts surgical outcome in MRI-negative temporal lobe epilepsy. *Neurology* 58, 821-823.

Suzuki,T., gado-Escueta,A.V., Aguan,K., Alonso,M.E., Shi,J., Hara,Y., Nishida,M., Numata,T., Medina,M.T., Takeuchi,T., Morita,R., Bai,D., Ganesh,S., Sugimoto,Y., Inazawa,J., Bailey,J.N., Ochoa,A., Jara-Prado,A., Rasmussen,A., Ramos-Peek,J., Cordova,S., Rubio-Donnadieu,F., Inoue,Y., Osawa,M., Kaneko,S., Oguni,H., Mori,Y., Yamakawa,K., 2004. Mutations in EFHC1 cause juvenile myoclonic epilepsy. *Nat Genet* 36, 842-849.

Swanson,M.G., Vigneron,D.B., Tran,T.K., Sailasuta,N., Hurd,R.E., Kurhanewicz,J., 2001. Single-voxel oversampled J-resolved spectroscopy of in vivo human prostate tissue. *Magn Reson Med* 45, 973-980.

Swartz,B.E., Simpkins,F., Halgren,E., Mandelkern,M., Brown,C., Krisdakumtorn,T., Gee,M., 1996. Visual working memory in primary generalized epilepsy: an 18FDG-PET study. *Neurology* 47, 1203-1212.

Tasch,E., Cendes,F., Li,L.M., Dubeau,F., Andermann,F., Arnold,D.L., 1999. Neuroimaging evidence of progressive neuronal loss and dysfunction in temporal lobe epilepsy. *Ann Neurol* 45, 568-576.

Taylor,I., Marini,C., Johnson,M.R., Turner,S., Berkovic,S.F., Scheffer,I.E., 2004. Juvenile myoclonic epilepsy and idiopathic photosensitive occipital lobe epilepsy: is there overlap? *Brain* 127, 1878-1886.

The International League Against Epilepsy, 1989. Proposal for revised classification of epilepsies and epileptic syndromes. Commission on Classification and Terminology of the International League Against Epilepsy. *Epilepsia* 30, 389-399.

Thompson,J.E., Castillo,M., Kwock,L., Walters,B., Beach,R., 1998. Usefulness of proton MR spectroscopy in the evaluation of temporal lobe epilepsy. *AJR Am J Roentgenol* 170, 771-776.

Tkac,I., Rao,R., Georgieff,M.K., Gruetter,R., 2003. Developmental and regional changes in the neurochemical profile of the rat brain determined by in vivo ¹H NMR spectroscopy. *Magn Reson Med* 50, 24-32.

Tofts,P.E., 2003. *Quantitative MRI of the Brain: Measuring Changes Caused by Disease*. John Wiley and Sons, Chichester.

Tokumitsu,T., Mancuso,A., Weinstein,P.R., Weiner,M.W., Naruse,S., Maudsley,A.A., 1997. Metabolic and pathological effects of temporal lobe epilepsy in rat brain detected by proton spectroscopy and imaging. *Brain Res* 744, 57-67.

Urenjak,J., Williams,S.R., Gadian,D.G., Noble,M., 1992. Specific expression of N-acetylaspartate in neurons, oligodendrocyte-type-2 astrocyte progenitors, and immature oligodendrocytes in vitro. *J Neurochem* 59, 55-61.

Urenjak,J., Williams,S.R., Gadian,D.G., Noble,M., 1993. Proton nuclear magnetic resonance spectroscopy unambiguously identifies different neural cell types. *J Neurosci* 13, 981-989.

van Calker,D., Belmaker,R.H., 2000c. The high affinity inositol transport system--implications for the pathophysiology and treatment of bipolar disorder. *Bipolar Disord* 2, 102-107.

van Calker,D., Belmaker,R.H., 2000a. The high affinity inositol transport system--implications for the pathophysiology and treatment of bipolar disorder. *Bipolar Disord* 2, 102-107.

van Calker,D., Belmaker,R.H., 2000b. The high affinity inositol transport system--implications for the pathophysiology and treatment of bipolar disorder. *Bipolar Disord* 2, 102-107.

van den Berg,C.J., Garfinkel,D., 1971. A stimulation study of brain compartments. Metabolism of glutamate and related substances in mouse brain. *Biochem J* 123, 211-218.

van Gelder,N.M., Sherwin,A.L., 2003. Metabolic parameters of epilepsy: adjuncts to established antiepileptic drug therapy. *Neurochem Res* 28, 353-365.

van Hall G., 2000. Lactate as a fuel for mitochondrial respiration. *Acta Physiol Scand* 168, 643-656.

Van Paesschen W., Connelly,A., King,M.D., Jackson,G.D., Duncan,J.S., 1997a. The spectrum of hippocampal sclerosis: a quantitative magnetic resonance imaging study. *Ann Neurol* 41, 41-51.

- Van Paesschen W., Revesz, T., Duncan, J.S., King, M.D., Connelly, A., 1997b. Quantitative neuropathology and quantitative magnetic resonance imaging of the hippocampus in temporal lobe epilepsy. *Ann Neurol* 42, 756-766.
- Vanhaesebroeck, B., Leever, S.J., Ahmadi, K., Timms, J., Katso, R., Driscoll, P.C., Woscholski, R., Parker, P.J., Waterfield, M.D., 2001. Synthesis and function of 3-phosphorylated inositol lipids. *Annu Rev Biochem* 70, 535-602.
- Verkman, A.S., Binder, D.K., Bloch, O., Auguste, K., Papadopoulos, M.C., 2006. Three distinct roles of aquaporin-4 in brain function revealed by knockout mice. *Biochim Biophys Acta* 1758, 1085-1093.
- Vermathen, P., Ende, G., Laxer, K.D., Knowlton, R.C., Matson, G.B., Weiner, M.W., 1997. Hippocampal N-acetylaspartate in neocortical epilepsy and mesial temporal lobe epilepsy. *Ann Neurol* 42, 194-199.
- Vermathen, P., Ende, G., Laxer, K.D., Walker, J.A., Knowlton, R.C., Barbaro, N.M., Matson, G.B., Weiner, M.W., 2002. Temporal lobectomy for epilepsy: recovery of the contralateral hippocampus measured by (1)H MRS. *Neurology* 59, 633-636.
- Vermathen, P., Laxer, K.D., Matson, G.B., Weiner, M.W., 2000. Hippocampal structures: anteroposterior N-acetylaspartate differences in patients with epilepsy and control subjects as shown with proton MR spectroscopic imaging. *Radiology* 214, 403-410.
- Vermathen, P., Laxer, K.D., Schuff, N., Matson, G.B., Weiner, M.W., 2003. Evidence of neuronal injury outside the medial temporal lobe in temporal lobe epilepsy: N-acetylaspartate concentration reductions detected with multisection proton MR spectroscopic imaging--initial experience. *Radiology* 226, 195-202.
- Vielhaber, S., Niessen, H.G., bska-Vielhaber, G., Kudin, A.P., Wellmer, J., Kaufmann, J., Schonfeld, M.A., Fendrich, R., Willker, W., Leibfritz, D., Schramm, J., Elger, C.E., Heinze, H.J., Kunz, W.S., 2008. Subfield-specific loss of hippocampal N-acetyl aspartate in temporal lobe epilepsy. *Epilepsia* 49, 40-50.
- Vikhoff-Baaz, B., Malmgren, K., Jonsson, L., Starck, G., Ljungberg, M., Forssell-Aronsson, E., Uvebrant, P., Ekholm, S., 2001. Lateralisation with magnetic resonance spectroscopic imaging in temporal lobe epilepsy: an evaluation of visual and region-of-interest analysis of metabolite concentration images. *Neuroradiology* 43, 721-727.
- Villringer, A., Dirnagl, U., 1995. Coupling of brain activity and cerebral blood flow: basis of functional neuroimaging. *Cerebrovasc Brain Metab Rev* 7, 240-276.

- Vogt, K.E., Nicoll, R.A., 1999. Glutamate and gamma-aminobutyric acid mediate a heterosynaptic depression at mossy fiber synapses in the hippocampus. *Proc Natl Acad Sci U S A* 96, 1118-1122.
- Wallimann, T., Dolder, M., Schlattner, U., Eder, M., Hornemann, T., O'Gorman, E., Ruck, A., Brdiczka, D., 1998. Some new aspects of creatine kinase (CK): compartmentation, structure, function and regulation for cellular and mitochondrial bioenergetics and physiology. *Biofactors* 8, 229-234.
- Wang, Y., Yang, B., Ng, T.C., 2008. Differences in metabolites in the mesial and lateral temporal lobe. *Proc Intl Soc Mag Reson Med* 1429.
- Watkins, K.E., Paus, T., Lerch, J.P., Zijdenbos, A., Collins, D.L., Neelin, P., Taylor, J., Worsley, K.J., Evans, A.C., 2001. Structural asymmetries in the human brain: a voxel-based statistical analysis of 142 MRI scans. *Cereb Cortex* 11, 868-877.
- Wellard, R.M., Briellmann, R.S., Prichard, J.W., Syngeniotes, A., Jackson, G.D., 2003. Myoinositol abnormalities in temporal lobe epilepsy. *Epilepsia* 44, 815-821.
- Wellard, R.M., Briellmann, R.S., Wilson, J.C., Kalnins, R.M., Anderson, D.P., Federico, P., Fabinyi, G.C., Scheffer, I.E., Harvey, A.S., Jackson, G.D., 2004. Longitudinal study of MRS metabolites in Rasmussen encephalitis. *Brain* 127, 1302-1312.
- Westergaard, N., Sonnewald, U., Schousboe, A., 1995. Metabolic trafficking between neurons and astrocytes: the glutamate/glutamine cycle revisited. *Dev Neurosci* 17, 203-211.
- Widjaja, E., Griffiths, P.D., Wilkinson, I.D., 2003. Proton MR spectroscopy of polymicrogyria and heterotopia. *AJNR Am J Neuroradiol* 24, 2077-2081.
- Wieshmann, U.C., Symms, M.R., Shorvon, S.D., 1997. Diffusion changes in status epilepticus. *Lancet* 350, 493-494.
- Williams, R.S., Cheng, L., Mudge, A.W., Harwood, A.J., 2002. A common mechanism of action for three mood-stabilizing drugs. *Nature* 417, 292-295.
- Williamson, A., Patrylo, P.R., Pan, J., Spencer, D.D., Hetherington, H., 2005. Correlations between granule cell physiology and bioenergetics in human temporal lobe epilepsy. *Brain* 128, 1199-1208.
- Williamson, A., Spencer, S.S., Spencer, D.D., 1995. Depth electrode studies and intracellular dentate granule cell recordings in temporal lobe epilepsy. *Ann Neurol* 38, 778-787.

Willmann,O., Wennberg,R., May,T., Woermann,F.G., Pohlmann-Eden,B., 2006. The role of 1H magnetic resonance spectroscopy in pre-operative evaluation for epilepsy surgery. A meta-analysis. *Epilepsy Res* 71, 149-158.

Woermann,F.G., Barker,G.J., Birnie,K.D., Meencke,H.J., Duncan,J.S., 1998a. Regional changes in hippocampal T2 relaxation and volume: a quantitative magnetic resonance imaging study of hippocampal sclerosis. *J Neurol Neurosurg Psychiatry* 65, 656-664.

Woermann,F.G., Free,S.L., Koepp,M.J., Ashburner,J., Duncan,J.S., 1999a. Voxel-by-voxel comparison of automatically segmented cerebral gray matter--A rater-independent comparison of structural MRI in patients with epilepsy. *Neuroimage* 10, 373-384.

Woermann,F.G., Free,S.L., Koepp,M.J., Sisodiya,S.M., Duncan,J.S., 1999b. Abnormal cerebral structure in juvenile myoclonic epilepsy demonstrated with voxel-based analysis of MRI. *Brain* 122 (Pt 11), 2101-2108.

Woermann,F.G., McLean,M.A., Bartlett,P.A., Barker,G.J., Duncan,J.S., 2001a. Quantitative short echo time proton magnetic resonance spectroscopic imaging study of malformations of cortical development causing epilepsy. *Brain* 124, 427-436.

Woermann,F.G., McLean,M.A., Bartlett,P.A., Barker,G.J., Duncan,J.S., 2001b. Quantitative short echo time proton magnetic resonance spectroscopic imaging study of malformations of cortical development causing epilepsy. *Brain* 124, 427-436.

Woermann,F.G., McLean,M.A., Bartlett,P.A., Parker,G.J., Barker,G.J., Duncan,J.S., 1999c. Short echo time single-voxel 1H magnetic resonance spectroscopy in magnetic resonance imaging-negative temporal lobe epilepsy: different biochemical profile compared with hippocampal sclerosis. *Ann Neurol* 45, 369-376.

Woermann,F.G., Sisodiya,S.M., Free,S.L., Duncan,J.S., 1998b. Quantitative MRI in patients with idiopathic generalized epilepsy. Evidence of widespread cerebral structural changes. *Brain* 121 (Pt 9), 1661-1667.

Wolf, P. Juvenile Absence Epilepsy. 1999. (http://www.ilae-epilepsy.org/Visitors/Centre/ctf/juvenile_absence.cfm)

Wolf,P., Goosses,R., 1986. Relation of photosensitivity to epileptic syndromes. *J Neurol Neurosurg Psychiatry* 49, 1386-1391.

Xue,M., Ng,T.C., Majors,A., Modic,M., Kolem,H., 1997. Oblique proton chemical shift imaging for the presurgical localization of mesial temporal epilepsy. *Magn Reson Med* 37, 619-623.

Yalcin,A.D., Kaymaz,A., Forta,H., 2000. Reflex occipital lobe epilepsy. *Seizure* 9, 436-441.

Yeung,D.K., Yang,W.T., Tse,G.M., 2002. Breast cancer: in vivo proton MR spectroscopy in the characterization of histopathologic subtypes and preliminary observations in axillary node metastases. *Radiology* 225, 190-197.

Ying,W., 1998. Deleterious network hypothesis of apoptosis. *Med Hypotheses* 50, 393-398.

Young,R.S., Osbakken,M.D., Briggs,R.W., Yagel,S.K., Rice,D.W., Goldberg,S., 1985. ³¹P NMR study of cerebral metabolism during prolonged seizures in the neonatal dog. *Ann Neurol* 18, 14-20.

Zeuthen,T., 2000. Molecular water pumps. *Rev Physiol Biochem Pharmacol* 141, 97-151.

Ziyeh,S., Thiel,T., Spreer,J., Klisch,J., Schumacher,M., 2002. Valproate-induced encephalopathy: assessment with MR imaging and ¹H MR spectroscopy. *Epilepsia* 43, 1101-1105.